Risk-Based Corrosion and Biofouling Management for Tidal Stream Devices

Eleanor Ramsden-Lister

This thesis is submitted in accordance with the requirements for the degree of Doctor of Philosophy

July 2014

UNIVERSITY OF SHEFFIELD

FACULTY OF ENGINEERING

DEPARTMENT OF CHEMICAL AND BIOLOGICAL ENGINEERING

Declaration

This thesis is an account of the author's own work carried out at the University of Sheffield, and the industrial sponsors' headquarters in Bristol along with field work at the prototype test site in Orkney. This work has not been submitted for any other degree of qualification.

Acknowledgements

Firstly, I would like to thank my supervisors, Professor Catherine Biggs and Dr Robert Edyvean from the University of Sheffield and James Sheppard and Paul Vigars at Alstom Ocean Energy for their guidance throughout the course of this work. Without their continuous support and encouragement it would not have been possible to achieve the results reported here.

I would also express my gratitude to the technicians in the Department of Chemical and Biological Engineering for their help with the development of experimental apparatus. I would also like to thank other members of staff at Alstom Ocean Energy that have been involved in the risk assessment process which has contributed to this thesis, and Bill Sutherland for his help during my site visits to Orkney. I would also like to thank the EPSRC and AOE for financial support for the thesis.

A special thank you must go to the staff and my colleagues at the E-Futures Doctoral Training Centre who have provided much needed support and reassurance throughout the thesis for which I will always be grateful.

Lastly I would like to thank close family and friends for their constant understanding and encouragement from the start of this work, and for keeping me motivated throughout.

Research Outputs

Papers

Ramsden, E., Edyvean, R.G.J, Dürr, S. (2014) 'Biofouling and marine corrosion'. In: LaQue's Handbook on Marine Corrosion, (eds. D. A. Shifler & B. Little). Wiley.

Ramsden. E. Edyvean, R.G.J, Vigars, P., Biggs, C.A. (2014) 'The Development of a Risk-Based Corrosion Management System for a Tidal Stream Energy Converter'. Corrosion. (Submitted).

Ramsden, E. Edyvean, R.G.J, Biggs, C.A. (2014). The Effect of Temperature on the Corrosion of Carbon Steel. Corrosion Science (In prep).

Presentations

'The Development of a Risk-Based Corrosion Management System for a Tidal Stream Energy Converter'. NACE Risk Management of Corrodible Systems Conference, Washington D.C, USA. June 2013.

'Risk-Based Corrosion Management Systems for Tidal Stream Devices'. E-Futures Autumn Conference, Sheffield, UK. September 2013.

'Land-Based Gas Turbine Particulate Emissions: Effects, Regulations and Measurement Methods'. E-Futures Conference, Sheffield, UK. March 2010.

Abstract

The overall aim of this thesis was to use a risk based management approach developed for tidal stream turbines to identify and quantify the potential risks of failure associated with corrosion and biofouling on such devices. In order to enable the development of risk factors and recommendations for optimising management of the devices throughout their lifetime, a seven-step process was used: review of risk management practices to assess suitability for control of corrosion and biofouling; review of corrosion and biofouling; qualitative assessment of an operational device; quantitative assessment of corrosion and biofouling in situ; analysis of the effect of local conditions on corrosion; risk assessment; development of a risk register and data management capabilities.

The risk assessment process carried out as part of this thesis identified a number of threats. These were categorised with respect to consequence and likelihood to establish a structured, easily implemented analysis of criticality. Metals commonly used on tidal stream devices (carbon steel, nickel aluminium bronze and ductile iron) were initially evaluated in situ in terms of the effect of operating within a tidal regime. Further field studies, statistically analysed, identified the type and extent of biofouling present throughout one year. Fouling and corrosion were found to vary seasonally. A comprehensive two factorial laboratory based experimental programme showed that temperature and flow are the most significant factors in determining corrosion rate for the commonly used metals. These factors were investigated further to determine models for corrosion rates under relevant environmental conditions. All metals exhibited an increase in corrosion rate with an increase in temperature, although the trends found differed. Nickel aluminium bronze exhibited the most significant rate of increase in corrosion rate at temperatures above 20^{o}C. The experiments have been used to provide experimental proof of the theoretical relationship between temperature and corrosion rate according to the Arrhenius relationship. A tidal flow rate of 3.39 ms^{-1} increased the corrosion rate of all four metals. However, carbon steel was the most affected by a change in flow regime. From in situ and laboratory based experiments, predicted corrosion rates for the desired lifetime of tidal stream devices were reported. The risk assessments were incorporated into a newly developed database, created as a tool to enable correct management of corrosion and biofouling threats for the lifetime of tidal stream devices.

This thesis has contributed to current literature by quantifying and enhancing understanding of temperature and flow effects, interactions in the environment and seasonality of corrosion and biofouling, and the application of risk management theory to a new system. This study has shown that flow effects and the localised conditions in a tidal regime will affect the corrosion rate and the settlement of biofouling on the surface of these devices. The work was carried out with the support of Alstom Ocean Energy.

Table of Contents

List of Figures

List of Tables

Abbreviations

ADCP	-	Acoustic Doppler current profiler
ALARP	-	As low as reasonably practicable
AOE	-	Alstom Ocean Energy
APEC	-	Asia-Pacific Economic Cooperation
CHP	-	Combined heat and power
CMS	-	Corrosion management system
CP	-	Cathodic protection
DFT	-	Dry film thickness
DLVO	-	Derjaguin-Landau-Verwey-Overbeek
DNV	-	Det Norske Veritas
DTC	-	Doctoral Training Centre
EMEC	-	European Marine Energy Centre
EPS	-	Extracellular polymeric substances
ETI	-	Energy Technologies Institute
FO	-	Fibre optic
FRC	-	Foul release coating
GENI	-	Global Energy Network Institute
GW	-	Giga watts
HAZ	-	Heat affected zone
HV	-	High voltage
IEA	-	International Energy Agency
IMO	-	International Maritime Organisation
IMS	-	Integrity management system
IRB	-	Iron reducing bacteria
IRP	-	Integrity review process
kW	-	Kilowatts
MIC	-	Microbially influenced corrosion
MMO	-	Marine Management Organisation
$MtCO_2$	-	Mega tonnes carbon dioxide
MW	-	Mega watts
NaREC	-	National Renewable Energy Centre
NDT	-	Non-destructive testing
ODV	-	Ocean Data View
OPEX	-	Operational Experience
ORP	-	Oxidation reduction potential
PDMS	-	Polydimethylsiloxane
PML	-	Plymouth Marine Laboratory
PPT	-	Parts per thousand
PTFE	-	Polytetrafluoroethylene
RBI	-	Risk Based Inspection
ROV	-	Remotely operated vehicle
RPM	-	Revolutions per minute
RTT	-	Rotech Tidal Turbine
SCE	-	Saturated calomel electrode
SE	-	Standard error
SEM	-	Scanning electron microscopy
SG	-	Spheroidal graphite
SRB	-	Sulphate Reducing Bacteria
SQEP	-	Suitably Qualified Experienced Personnel
TBT	-	Tributyltin
TGL	-	Tidal Generation Limited
TWh	-	Terawatt hours

Nomenclature

A	-	Area
C_M	-	Inertia Coefficient
C_o^{2-}	-	Oxygen Concentration
C_P	-	Turbine Power Coefficient
CR	-	Corrosion Rate
D	-	Diffusion Coefficient
E_A	-	Activation Energy
E	-	Corrosion Potential
EW	-	Equivalent Weight
F	-	Faraday Constant
I_{corr}	-	Corrosion Current Density
$I\text{-}E$	-	Current-Potential Relationship
I_L	-	Limiting Current Density
M_a	-	Added Mass
n	-	Number of Trials performed in Corrosion Tests
P	-	Power
R	-	Gas Constant
R^2	-	Coefficient of Determination
SS_{err}	-	Sum of Squares of Residuals
SS_{tot}	-	Total Sum of Squares
V	-	Volumetric Displacement of Body
x	-	Value of Corrosion Rate for a particular Trial
$\bar{x}$	-	Mean Value
Z	-	Number of Electrons
β_a	-	Tafel Constant in Anodic Direction
β_c	-	Tafel Constant in Cathodic Direction
δ_N	-	Thickness of the Nernst Diffusion Layer
ΔW	-	Weight Loss
η_a	-	Overpotential in Anodic Direction
η_c	-	Overpotential in Cathodic Direction
ρ	-	Density
σ	-	Standard Deviation

Chapter 1

Introduction

1.1 The Need for Renewable Energy

There are significant global concerns over the climatic and environmental risks associated with the generation of power from conventional fossil fuels. This, coupled with the knowledge that these fuel sources are depleting and will disappear in the next 2-3 centuries, has heightened awareness that alternative methods of power generation are needed. The World Energy Outlook (International Energy Agency (IEA), 2012) predicts that global energy demand is likely to increase by one third from 2010 to 2035, as the world's population rises and demand for technological advances increases.

Anthropogenic influenced global warming with its potential to cause climate change, is now generally accepted to be happening but with differing opinions on its rate of development and effects. These effects have the potential to severely affect the way the world's current population has come to live. There is now considerable international activity and agreements aimed at reducing carbon dioxide levels in the atmosphere. Amongst these is the development of alternative ways to generate power.

Currently the world remains heavily reliant on fossil fuels with only a small proportion of energy generated from renewable sources. However, between 1973 and 2009 there have been changes in the fuel share, with a reduced reliance on oil and increase in gas (Figure 1.1).

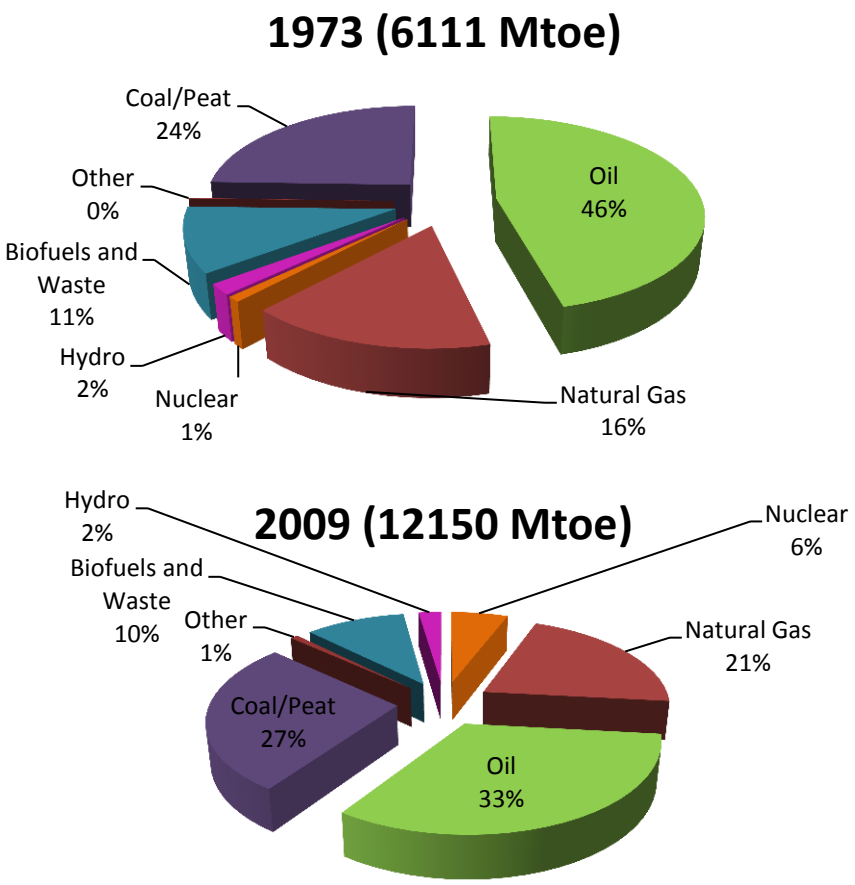

Figure 1.1. Fuel shares of the world Primary Energy Supply in 1973 and 2009 in million tons of oil equivalent (Mtoe). "Other" includes geothermal, solar, wind, and other renewable sources (data obtained from International Energy Agency (IEA), 2011)

In 2009, the UK produced 165 TWh of electricity from gas, with the entire world producing 4301 TWh from gas (International Energy Agency (IEA), 2011). However, the majority of the world's electricity (mainly used for industrial purposes) is still produced from the burning of coal (8119 TWh), resulting in large carbon dioxide and other emissions.

Following significant international meetings (Rio, Kyoto, Copenhagen etc.) commitments have now been made around the world to phase out the use of fossil fuels by removing subsidies (totalling $312 billion in 2009 (International Energy Agency (IEA), 2010)), with the aim of limiting the average global temperature rise to 2 ^{o}C, and to make the transition towards a more sustainable energy system, addressing both climate change and energy security.

This implies a significant shift towards the use of unconventional resources, carbon abatement systems and renewable energy generation instead of conventional fossil fuels.

The speed at which these technologies can contribute to the world energy supply depends heavily on governmental policy and support mechanisms. The term "renewable" defines energy generating technologies which originate from natural replenishing sources, including radiation from the sun, water flow, tidal currents, photosynthesis and geothermal processes, including:

- Solar Photovoltaic cells
- Solar Thermal
- Wind Power
- Geothermal Energy
- Hydroelectric Power
- Tidal Range
- Tidal Stream
- Wave Power
- Ocean Thermal Energy Conversion
- Biomass and Biofuels

1.1.1 Renewable Energy Targets in the UK

As a signatory of the EU Renewable Energy Directive in 2009, the UK is now committed to a legally binding target of 15% of energy from renewable sources by 2020. The Climate Change Act (2008) (HM Government, 2008) states a reduction in emissions by at least 80% of 1990 levels by 2050. In July 2009, the Renewable Energy Strategy was published (Department of Energy and Climate Change, 2009), outlining how the UK government proposes to meet the targets. A recent update in November 2013 to the UK Renewable Energy Roadmap (Department of Energy and Climate Change, 2013) outlines the UK's development and eventual deployment of marine technologies, including tidal stream generation, which it believes is making good progress, moving from individual prototypes to development of arrays and onto commercialisation. In 2012 two UK projects consisting of arrays of tidal stream devices were announced as recipients of the EU New Entrants Reserve 300 competition. Currently the UK Government is focussing on increasing the country's supply of electricity from wind power – increasing the number of both onshore and offshore devices over the next few years. However, it will not be possible to rely solely on wind power to meet the targets as wind power is unreliable and unable to provide "baseline" supplies (Luickx et al., 2008). Due to this, other technologies will have to be used and form part of an 'energy mix'. The Renewable Energy Strategy (Department of Energy and Climate Change, 2009) and the UK Renewable Energy Roadmap (Department of

Energy and Climate Change, 2013) also include information regarding the delivery of the different energy technologies, including marine based devices.

1.2 Tidal Stream Power

Land-based renewable energy technologies face constraints due to conflicts over land use (Fraenkel, 2002) as well as public dissent. Sea-based technologies could offer greater flexibility and less impact. However, marine renewables (including thermal energy, tidal range, tidal stream, wave and offshore wind) are expensive and the energy harder to extract than land-based options, but are necessary to meet future targets with the vast potential energy generating capacity of the oceans. Tidal current devices are hydrokinetic power generators (changing kinetic energy within the current into mechanical energy and finally electrical energy) and use the reliable and predictable nature of the tidal currents. This is an advantage over wind and to a certain extent solar power which are both susceptible to unpredictable weather changes (Nicholls-Lee and Turnock, 2008) and so they potentially provide a less vulnerable option for renewable electricity generation in the future.

Tides are predictable because of the mechanism that causes them. The gravitational field produced from the moon has a small pull effect on the water on Earth, strongest on the side of the Earth facing the moon and weakest on the opposite side. Therefore, the moon causes a slight pull and push of water, hence a rise in water level twice a day due to the orbit of the moon around the Earth (water nearer the moon will experience an upward force towards the moon and water on the other side of the Earth will experience an outward force) (Figure 1.2). The gravitational pull felt on Earth from the sun also has an effect on the water bodies on Earth (the magnitude of the tide generating force is approximately 68% from the moon and 32% from the sun (Ben Elghali et al., 2007)), creating a smaller bulge on the sides in line with the sun. This effect will create overall larger or smaller tides dependent on the alignment of the Earth, Sun and Moon in relationship to each other. Changes in amplitude (or range) follow cycles of approximately 14.5 days duration.

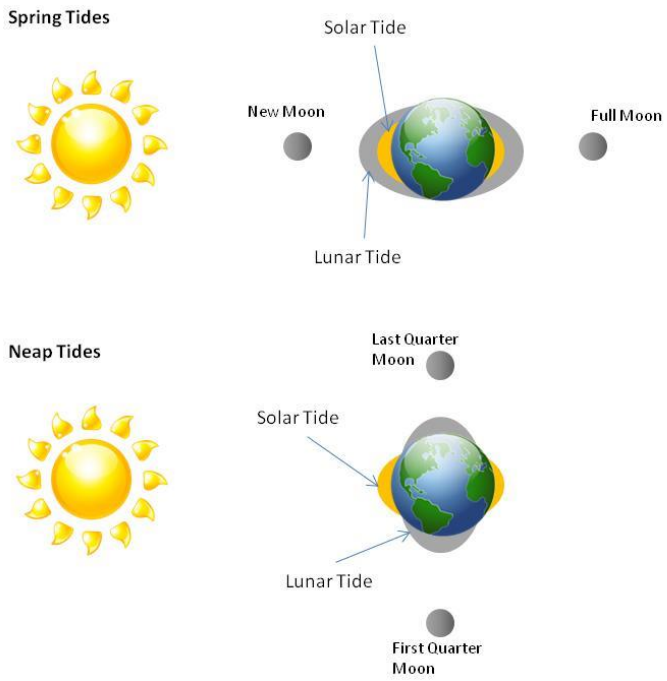

Figure 1.2. Variations in tides with rotation of Earth and Moon (Adapted from Encyclopaedia Britannica, 2006)

The movement of water in response to the influence of the moon and sun results in tidal currents. Due to the underlying topography and geography these tidal currents can be larger in some places than in others. Significant currents can exist where water is channelled through constraining topography or through areas of shallow water between open seas and around headlands (Fraenkel, 2002), where peak velocities can be up to 4 ms^{-1} at spring tide. Using tidal energy converters in areas of large tidal currents is an attractive option since seawater is approximately 800 times denser than air, so more energy can be extracted, even at low rotational speed (Couch and Bryden, 2006). For a free stream turbine a strong spring peak current (in excess of 2 ms^{-1}) is required for economic energy generation from the device (Nicholls-Lee and Turnock, 2008) and the flow needs to be relatively uniform for long periods to maximise power generation. The power available from tidal devices (P) is related to the density of the water (ρ, kgm^{-3}), the sweep area of the turbine (A, m^2), the water velocity (v, ms^{-1}) and the turbine power coefficient (C_p):

$$P = \frac{\rho A v^3}{2} C_p$$

1.2.1 Tidal Resource

Any company developing tidal power devices will aim to deploy them worldwide and maximise return on development investment. Figure 1.3 shows the global tidal energy patterns (Global Energy Network Institute, 2011) and can be used to identify key sites for

exploitation of the resource. The Global Energy Network Institute (GENI) states the strongest tidal resources outside of the UK are offshore north eastern South America, south western Central America, eastern Africa, the Gulf of Alaska and the north and east rims of the north Atlantic. The World Energy Council (2010) published the report, "Survey of Energy Resources", which highlights potential locations for tidal current devices. These include eastern coasts of Russia and several sites along both the east and west coasts of USA, North West New Zealand, Korea, China and India. In European territorial waters alone, there are approximately 106 potential locations for extracting tidal energy.

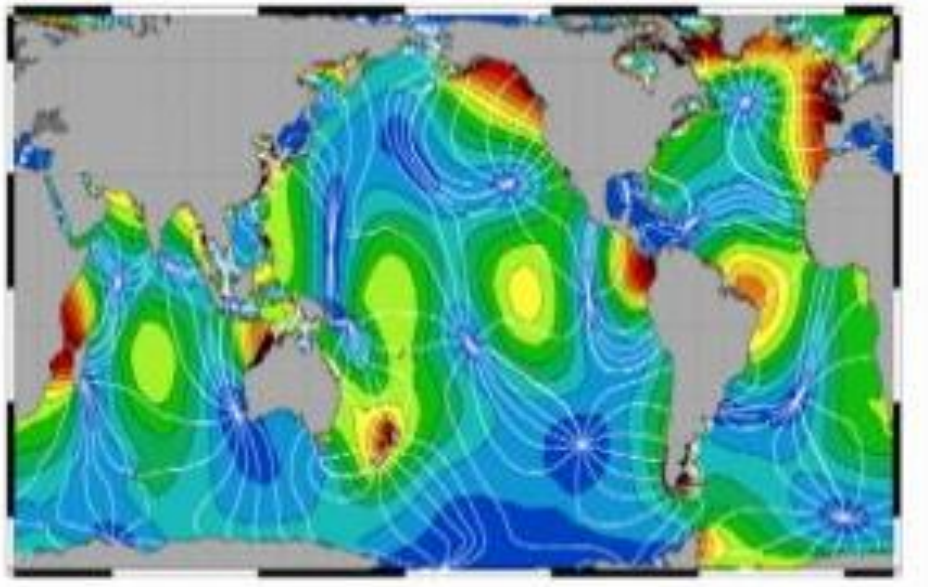

Figure 1.3. Global tidal energy patterns, the strongest tidal flows are represented by red and the weakest by blue (Global Energy Network Institute, 2011)

The UK has an excellent marine energy resource; with some of the largest tidal current potential sites in the world. A report produced for The Carbon Trust by Black and Veatch estimated an exploitable tidal stream resource of approximately 18 TWh/yr (in the order of 50% of the European tidal resource and 10-15% of the global resource (Black and Veatch, 2005)). It is estimated in the report that marine energy as a whole (including wave power) could provide 20% of UK electricity consumption (RenewableUK, 2011). By utilising the potential energy stored in the currents around the coast, the UK would be able to regain some energy self-sufficiency which has been lost as the oil and gas resources in the North Sea are depleted. The UK is currently a global leader in development of tidal stream energy with Europe the leader in all offshore renewable technologies (RenewableUK, 2014). Figure 1.4 indicates the extractable tidal power resources available around the UK (the darker the colour, the greater the available tidal power), and Figure 1.5 shows the likely locations for tidal stream devices. Although the maps from the UK Atlas of Marine Renewables (BERR,

2008) give a good indication of where the potential sites are, they are becoming superseded by more local mapping. The maps are excellent for providing knowledge on open waters but only a coarse representation of the available resource is used around coastlines. There is also no clear distinction between flood and ebb tides contained within the data. More detailed measurements are currently being undertaken to improve and enhance the Atlas lead by APB Marine Environmental Research (ABP Marine Environmental Research, 2014).

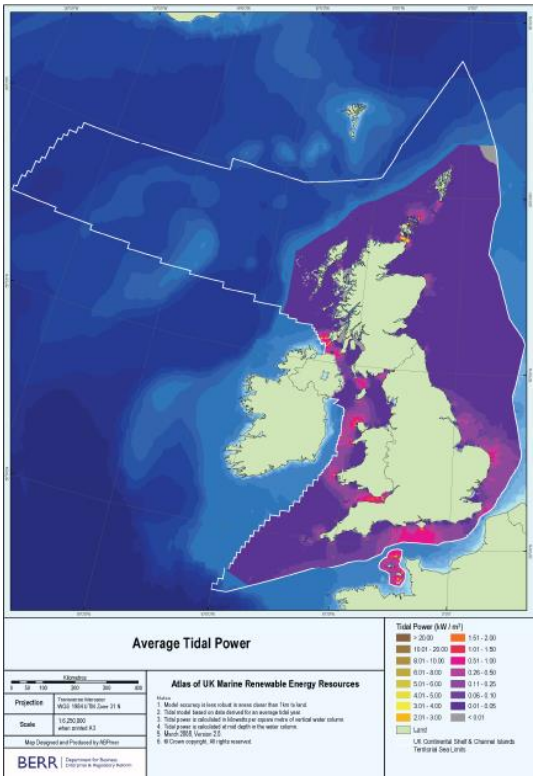

Figure 1.4. Average extractable power around the British Isles obtained from the UK Atlas of Marine Renewables (BERR, 2008)

Figure 1.5. UK Tidal Stream Resource Locations (Metoc PLC, 2007)

Other factors which have to be considered when determining potential sites include water depth, accessibility and ease of maintenance (including amount of shelter from adverse weather), other potential sea users, and the impact on marine flora and fauna.

Although marine technologies (both wave and tidal) will not make a significant contribution to the 2020 target (only estimated at 1-3 GW capacity, equivalent to 2.1% (3 GW capacity would generate approximately 36 GWh per day or 13,000 GWh per year) of UK electricity supply in 2020 (Carbon Trust, 2006; RenewableUK, 2010), it is believed that these technologies will become a large part of the 'energy mix' in the UK between 2020 and 2050 (providing between 15-20% of the current UK demand (Black and Veatch, 2005)). Due to the large offshore oil and gas economy in the North Sea, the UK already has a significant number of skilled operatives working in the conditions associated with offshore and marine environments, with experience in engineering and fabrication of offshore structures; technology deployment; maintenance; and impact assessment of a marine environment on fixed structures (BWEA, 2006), all helping to make tidal power an attractive option for renewable energy generation.

1.3 Tidal Stream Devices

There are six types of tidal energy converters currently under design and construction. All of the devices fundamentally rely on the same conversion of kinetic energy, through

mechanical energy to electrical energy. The device designs are identified as follows (EMEC., 2013):

- Horizontal Axis Turbine
- Vertical Axis Turbine
- Oscillating Hydrofoil
- Venturi
- Archimedes Screw
- Tidal Kite

The most popular design is the horizontal axis device, with several companies currently developing devices of this type (Atlantis Resources Corporation, 2009; Hammerfest Strom, 2011; Marine Current Turbines, 2011; Alstom, 2013).

1.3.1 Potential Problems in the use of Tidal Stream Devices

There are significant challenges before the widespread development of marine renewables can occur (Mueller and Wallace, 2008). Marine renewables are still very much in the prototype and design stage, with the technology 10-15 years behind modern wind technologies (Mueller and Wallace, 2008). Research is being conducted in a variety of areas, including design, operability, maintenance and subsea electrical and grid connection (Batten et al., 2006; Walkington and Burrows, 2009). One major problem, that forms the basis of this research, is that associated with corrosion and biofouling. Corrosion is a common occurrence in the marine environment due to the high conductivity of seawater and its effects can be exacerbated by biofouling. Biofouling itself tends to peak in shallow nutrient rich waters (Dürr and Thomason, 2010) which tend to include the best tidal flow sites.

It has long been recognised that artificial structures and vessels operating in the marine environment will be subject to corrosion and both micro (reducing heat exchange efficiency and accelerating corrosion) and macro (restricting flow, damaging equipment and exacerbating corrosion) levels of biofouling (Institute of Petroleum, 1987; Dürr and Thomason, 2010). It is imperative that any metals used in this environment must have adequate protection against attack and, indeed, formation of fouling.

Although much research has been conducted into biofouling and corrosion of both structures and materials in the marine environment the focus has mainly been on boat

hulls (Larsson et al., 2010; Flemming, 2002) and offshore oil rigs (Houghton, 1978; Edyvean et al., 1985; Edyvean et al., 1988; Yan et al., 2006), and has not yet considered the effects on tidal stream devices. Oil rigs are usually placed in areas of low flow, often far from the shore, and do not experience the flow speeds which are essential to the commercialisation of tidal power devices. Ships on the other hand experience high flow speeds across their hulls as they move through the water. These different flow regimes and locations will mean that a variety of fouling and corrosion will be experienced, but it is not possible to simply rely on previous literature for different applications, to provide information for tidal stream devices.

Tidal stream turbines are also large and complex structures and so the flow regimes around different sections will vary greatly. Enclosed areas will experience low flowing/stagnant water conditions. Blades will be subject to high impingement and could be susceptible to erosion from suspended solids contained in the flowing seawater. They will create variable levels of turbulence in their wake around the main structure causing complex flow patterns with areas of high and low flow close to the metal surface. Turbulence will occur around the support structure which also experiences high flows. The device will also generate a variety of localised surface temperatures above that of the surrounding water. The complex structure means that small crevices may form at joints and corners over the surface area, changing the local flow patterns dramatically. This leads to a complex problem when considering surface effects for corrosion and biofouling.

One solution to minimise problems with corrosion would be to construct the device entirely from metal, such as titanium, which has excellent corrosion resistance to seawater under static, low and high flow conditions (Oldfield, 1996). However, this is not a feasible recommendation due to very high cost. A key requirement for the successful implementation of these types of device is that they are commercially viable. 316L, an austenitic, low carbon grade of stainless steel is often used for seawater applications and does have good corrosion resistance under many environments. However, while much less costly than titanium, there is still a cost penalty both in the material itself and in fabrication and it is not particularly suitable for this application in flowing seawater, (Keane, 2011) as it often exhibits pitting and crevice corrosion. The cost of overcoming problems associated with corrosion and biofouling must be balanced against generation capacity. More research is required in this area is required to fully understand how to minimise the

problems associated with corrosion and biofouling for tidal stream devices and how to implement a successful strategy for this throughout device lifetimes.

1.4 Thesis Aims and Objectives

The overall aim of this thesis is to use a risk based management approach customised for tidal stream turbines to identify and quantify the potential risks of failure associated with corrosion and biofouling on such devices to enable the development of recommendations for mitigation techniques.

Potential failure modes of critical areas of a tidal stream turbine due to corrosion and biofouling will be identified and assessed using a risk-based approach. Through understanding the mechanisms and potential corrosion rates under different environmental conditions, and assessing the biofouling that has settled on a prototype device, this thesis will provide recommendations relating to corrosion and biofouling protection as well as maintenance and operability protocols in different conditions around the world. Suggestions for design alterations to minimise the biofouling and corrosion potential (including anti-fouling protection) and the associated hazards and risks to operation will be made.

The following are key specific objectives of the thesis:

- Review current understanding of risk assessment and risk management in practice (Chapter 2) to aid the development of a methodology for the application of a risk-based management system to tidal stream devices
- Gain a comprehensive understanding of the corrosion and biofouling mechanisms and processes likely to occur on the turbine, through a review of the literature, including review of current global knowledge of marine corrosion and biofouling (Chapter 3)
- Develop an evidence base of corrosion and biofouling that has occurred on a prototype tidal stream device (Chapters 4 and 5) that will provide a basis for assessing threats posed to the operation of the turbine *in situ* including the identification of critical areas and materials used in different locations on the turbine
- Determine the corrosion rates of critical materials used for tidal stream devices under representative environmental conditions at tidal locations around the world

(Chapter 6). Results of this study will be used to identify, quantify and model the effect of the most important environmental factors on rates of corrosion over a device lifetime (Chapter 7 and 8)

- Develop a methodology for the application of a risk-based management system identifying key threats and evaluate the level of risk associated with these, using all evidence gathered (Chapters 3-8) to develop a risk based management system (Chapter 9).
- Form a risk register to provide recommendations and a strategy for the management of corrosion and biofouling on tidal stream devices and develop a methodology for data management which will aid the collection and storage of all evidence gathered (Chapter 10)
- Provide conclusions and a discussion on further development of the thesis (Chapter 11)

Chapter 2

Review of Risk-Based Management

2.1 Introduction

Management of risks should be a central part of any organisation's strategic management (The Institute of Risk Management., 2002). Risk management is the process of methodically addressing risks associated with either the business as a whole or with individual aspects of the undertaking.

The focus of a good risk management process is the identification and treatment of the risks associated with the issue under review. It is the intention of installing such a process that the probability of success is increased, whether that success is measured by safety, operability or profit.

The overall aim of this thesis is to use a risk based management approach. Effective risk-based management provides numerous benefits to the operation and commercial viability of devices and structures. These include compliance with relevant statutory and corporate health, safety and environmental requirements; helping to reduce potential structural failures and other threats to operation of the device; reducing unplanned maintenance and device downtime; increasing operational time; and optimising cost for maintenance, monitoring and repair.

The UK Offshore Installations (Safety Case) Regulations 2005 (HM Government, 2005) which are risk based, require a "whole lifetime" based approach to structural integrity; these, and the financial imperative, mean that there must be emphasis on the design, material selection and fabrication of offshore structures to ensure that structural integrity is maintained throughout the planned lifetime of the device.

The area addressed here is that of externally driven 'hazard risks' - those associated with the environment and the materials used to operate the tidal devices. A risk assessment has a fundamental purpose to answer two questions; what can go wrong, and if something does go wrong, what is the probability of it happening and what are the consequences? The assessment process can be divided into separate milestones to distinguish between the analysis of risk (identification, description and estimation) and the evaluation of risk (The Institute of Risk Management., 2002). Conducting a risk assessment for key 'hazard risks'

associated with tidal turbines will improve decision making for design and operation of the devices; support developers' knowledge base and overall will help to protect the devices and ensure their required design life. This chapter investigates risk-based management in the context of corrosion and biofouling, a key threat in the marine environment (Owen, 2008; O Rourke et al., 2010).

2.2 Risk-Based Management in the context of Corrosion and Biofouling

There are clear areas of tidal stream devices which pose potential hazards with associated risks related to corrosion and biofouling, as well as the environment in which they operate. The corrosion process itself is not necessarily important to operators working in the marine environment. However, the consequences of failure due to corrosion are. To ensure that risk is managed effectively it is imperative to understand how the potential failures due to corrosion and biofouling can be prevented or mitigated to ensure commercial viability in terms of lifetime; energy generation potential, maintenance schedules, efficiency and operability. The first step in corrosion management is a corrosion risk assessment (Ashworth, 1996).

For best practice operation of a system, all business risks should be as low as reasonably practicable (ALARP). In the case of corrosion and biofouling on a device, this can be achieved in a number of ways (Egan, 2007):

- Preventative maintenance
- Up-to-date maintenance
- Regular safety reviews
- Development of understanding of corrosion and biofouling processes likely to manifest on device
- Focus on overall integrity as well as personal safety
- Monitoring of temporary assets and procedures
- Clear, well defined roles and responsibilities

Risk-based corrosion management is a relatively recent technique established to aid the development of a robust framework for managing risks associated with corrosion. It consists of the identification, assessment and prioritisation of risks, followed by coordinated and economical application of resources to minimise, monitor and control the probability and/or impact of unfortunate events or to maximise the realisation of opportunities (Det Norske Veritas, 2012). The management of threats to technical integrity

arising from material deterioration (Energy Institute, 2008) as well as those posed by the settlement of biofouling organisms should be covered. Developing integrity management has become the industry best practice requirement in the offshore oil and gas production industry (ExxonMobil, 2009; International Association of Oil and Gas Producers, 2008; Bea, 2001) and is specifically relevant to the development of marine renewables in terms of corrosion prevention and mitigation.

A structured framework, such as that defined in the Energy Institute Guidance for Corrosion Management in Oil and Gas Production and Processing (Energy Institute, 2008) can be used as a basis for developing risk based management. Although the guidance is aimed at oil and gas production and processing, the generality of the framework makes it suitable for application to other applications in similar environments. The framework is outlined Figure 2.1 (Energy Institute, 2008).

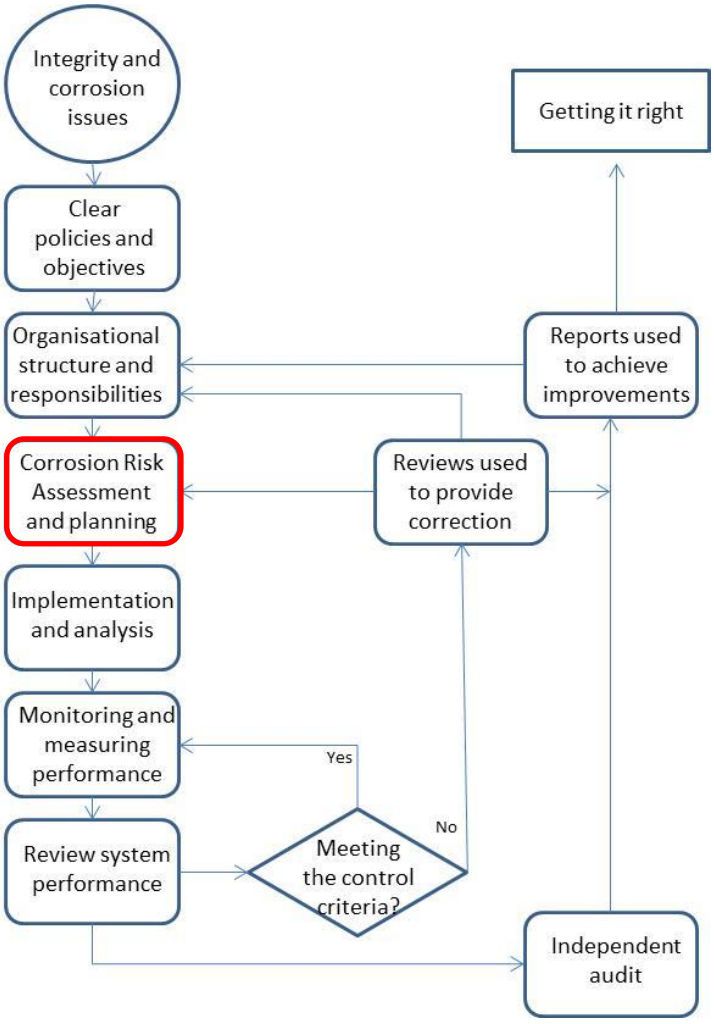

Figure 2.1. Framework for a successful Corrosion Management System (Energy Institute, 2008)

Figure 2.1 shows an iterative method for the management of corrosion and biofouling where evidence should be continuously reviewed to refine the system. The key preliminary stage of the development of risk-based corrosion and biofouling management system falls under the heading of "Corrosion Risk Assessment and Planning", highlighted in red in the flow diagram (Figure 2.1). Further stages involve the development of recommendations on how to implement the system, including monitoring and measuring performance.

A further, well established five step process developed by Det Norske Veritas (DNV) in the Risk Based Corrosion Management Recommended Practice (Det Norske Veritas, 2012) can also be used as the basis of a corrosion and biofouling management system (Figure 2.2), with each stage providing information for the subsequent steps (Det Norske Veritas, 2012). This methodology has been used for structures and vessels operating in the marine environment but has not yet been used for marine renewable technologies.

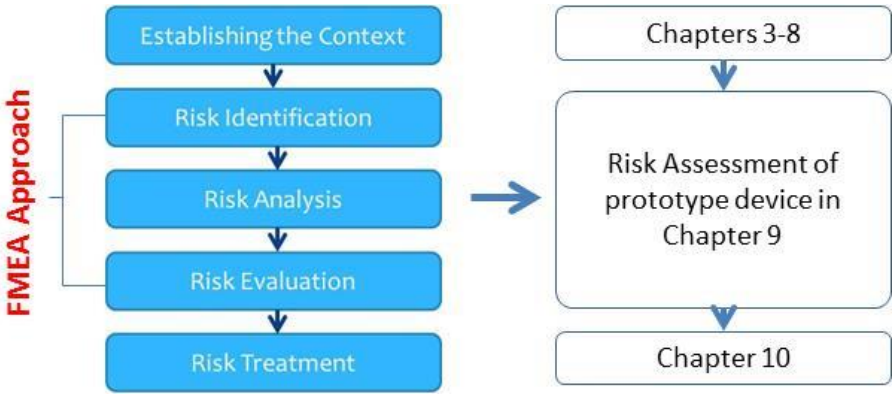

Figure 2.2. Five stage process for risk assessment as established by DNV (Det Norske Veritas, 2012) compared with structure of thesis

This first phase of the process (establishing the context) is the identification and development of corrosion and biofouling management objectives and policy based on evidence collected of the corrosion and biofouling that have occurred on similar structures (see Chapters 3 through to 8 for development of an evidence base). The development of an evidence base is required as a starting point for assessment of risks posed by corrosion and biofouling. This includes observation and interrogation of any devices available (Chapter 4), data gathered from field experiments (Chapter 5) and from laboratory experimentation (Chapter 6-8), all of which are integrated to provide the best possible data available.

Successful corrosion and biofouling management should be based on a risk assessment with three parts - risk identification, identifying potential threats associated with corrosion and biofouling; risk analysis of associated consequences to identify the associated risk; and

risk evaluation to determine high risk threats and critical areas of the device (Chapter 9). Once evaluated, the assessed risks can be used to construct the management strategy, where risk treatment methods are developed in terms of possible preventative measures and methods for mitigation (Chapter 10).

The analysis and evaluation of the risks involves corrosion testing, enabling analysis of potential corrosion rates and the relative performance of different metals with reference to identified high risk areas (Chapters 5-9). The overall risk assessment is a working document and as part of the continual management approach and should be maintained throughout the lifetime of a structure or device (Chapters 9 and 10).

The management planning should be primarily based on the long-term strategies of device deployment. This includes the required device lifetime, inspection schedules, cost efficiency and commercial viability of the device and generation of electricity. Appropriate treatment measures should be chosen so that the risk of failure of the device is reduced to a level that is ALARP. Planning of inspection, monitoring and testing is a continual feedback process with data analysed and stored to enable offsetting of future schedules and inspection requirements. The corrosion and biofouling management strategy could potentially involve lifetime corrosion control for those threats identified as high risk, less rigorous control, but a monitored level of protection, for medium risks, whilst no action may be decided upon for low risks depending on cost (Ashworth, 1996).

2.2.1 Failure Modes and Effects Analysis (FMEA)

Various techniques have been developed and applied to Risk Analysis but one well recognised and industry standard is a Failure Modes and Effects Analysis (FMEA). This is a systematic analysis to allow identification of potential design and process failure modes and their causes and effects and is a method used to identify, analyse and evaluate the risks as shown in phases 2-4 in Figure 2.2 (British Standards Institute, 2006a).

An FMEA can be conducted to assess the potential failure modes associated with corrosion and biofouling, taking into consideration design requirements and the environment in which these devices will be placed. The objective of such an analysis is to determine the criticality and the priority for mitigation of each failure mode with respect to the device's correct design function and performance both at development stage and in the future operation of the devices (British Standards Institute, 2006a). The FMEA process also aids

the development of design and operation improvement plans to mitigate identified failure modes.

The FMEA process has followed the guidelines set out in the British Standard *Analysis techniques for system reliability - Procedure for failure mode and effects analysis (FMEA)* (British Standards Institute, 2006a).

Due to the complex nature of many structures and devices the risk identification often requires sufficient detail to understand the vulnerability of specific areas and components rather than a 'system-based' approach. The risk analysis allows different components to be ranked in relation to the risk and therefore enable evaluation of options to prevent, mitigate or manage the risks (Capcis Limited for the Health and Safety Executive, 2001). This is an identification and analysis not only of the probability (likelihood) of failure but also of the consequences should that failure occur. The consequences relate to the perceived overall cost including loss of business if failure occurs. This can be subjective and emerges from discussions with relevant personnel who are involved in the industry and are deemed as suitably qualified and experienced personnel (SQEP).

To analyse and categorise the risks identified at the first stage of an FMEA, a risk matrix and scoring system can be used (Table 2.1) (British Standards Institute, 2006a). This is semi-quantitative technique that allows risks to be ranked using the consequence and probability identified (Equation 2.1) to define the criticality of the different areas of a device. The spread of numerical risk values amongst all items assessed is discontinuous, and as such it is possible to apply this analysis. This is often the case in risk assessments that use similar data (Ashworth, 1996). The risk is expressed as the product of the probability (likelihood) of the failure and the consequences if such a failure should arise (Energy Institute, 2008).

$$Risk = Probability \times Consequence \quad [2.1]$$

A ranking (high, medium or low) for each risk as set out in the risk matrix can be defined, and can be colour coded for ease of use and communication.

High risk levels are to be seen as unacceptable and require immediate action, medium level risks should be evaluated to determine if any additional control measures are required where feasible and financially practical to ensure that they remain ALARP (Det Norske Veritas, 2012). Low level risks are seen as tolerable and do not need further action.

Table 2.1. Risk Matrix (British Standards Institute, 2006a)

Consequence	Probability of Hazard Occurrence				
	1 (Low)	2	3	4	5 (High)
1 (Low)	1	2	3	4	5
2	2	4	6	8	10
3	3	6	9	12	15
4	4	8	12	16	16
5 (High)	5	10	15	20	25

Operational factors must be taken into consideration during the risk analysis, including the environmental factors as well as the material selection for critical areas (thickness, composition, shape). Competence of personnel and human factors are also key to the risk analysis.

2.2.2 Risk Based Inspection

The final phase of the risk assessment is risk treatment (Figure 2.2) where design, prevention, monitoring and maintenance measures are identified. Once implemented the risk reduction measures must be formally inspected and monitored, through a Risk Based Inspection (RBI) approach. The objective is to maximise the period between inspections and thus reduce costs without compromising on safety and environmental issues (Khan and Haddara, 2003). A RBI regime provides a means for decision making where the probability of failure and its associated consequences can be minimised at an early stage of the process. RBI has become the preferred method for inspection for many industries, (Khan and Haddara, 2003; Khan et al., 2004; Straub and Faber, 2005), and is recommended best practice as part of plant integrity management by the Health and Safety Executive (HSE) (Wintle et al., 2001). Prescriptive inspection has been found to have a number of short-comings, especially associated with the lack of analysis of specific threats posed to the integrity of components, the consequences of failure and the risks created by the component and the environment in which it operates (Wintle et al., 2001).

Using RBI allows the development of an optimum plan for execution of inspection activities (Capcis Limited for the Health and Safety Executive, 2001). RBI involves inspection of a device or structure on the basis of information obtained from a risk assessment of the equipment in question (Wintle et al., 2001). The findings of the risk assessment can be used to plan the emphasis of the inspection procedures and schedule. The RBI approach ensures that risk is reduced to an ALARP level, whilst optimising the inspection schedule and focusing on the most critical areas of the device or structure. It will also provide a means of ensuring the most appropriate methods of inspection are utilised. A simplified

procedure for RBI (including the preliminary risk assessment) is as follows (Straub and Faber, 2005):

1: Identification of critical deterioration mechanisms and potential locations of failure (hazards). All hazards can then be characterised by generic parameters (the respective values of influencing parameter (high flow/low flow/stagnant cavity/open water)

2: Dependencies between the parameters at different hazard levels are estimated. I.e. arrange the device into groups with large interdependencies (location/type of metal, etc.). It is then easier to consider each group separately.

3: Establish a generic database. This should cover relevant deterioration mechanisms and parameter ranges. This database is part of the continual feedback loop and will require additional work to update the data based on inspection results from critical areas throughout the device lifetime.

4: Inspection planning should be carried out for all critical areas taking into account dependency of inspection cost on total number of inspected high risks and accounting for redundancy of the system with respect to critical area failure.

5: The first inspection campaign should be planned for when the first critical areas are due for inspection according to individual inspection plans. Inspections due in ≤ 1 year should also be carried out at the same time to reduce the marginal inspection costs of further retrieval, etc.

6: If the inspection results are better than expected, the required effort for maintenance of critical areas not yet inspected reduces and omitted inspections can be postponed/delayed until the next campaign (semi-quantitative considerations).

7: Update all corrosion factors on database of all critical areas (inspected/not inspected).

8: Recalculate new inspection plans for the critical areas with new data. The cycle should be continued until the end of service life.

As well as RBI, there should also be a procedure documented for opportunity based inspection when a device is retrieved for repair or maintenance for another purpose outside of the corrosion inspection schedule. The reporting of corrosion damage should be a continuous process where deterioration and failures are documented even during periods of unplanned inspection.

Testing is also required on a regular, pre-determined schedule throughout operation. The management system will dictate the frequency of inspection, monitoring and testing depending on the assessed severity and operational requirements. The system allows personnel access to schedules, procedures and policies relating to the risks and how to manage them. The management system produced from this thesis will enable any device operator to manage the inspection, monitoring and testing of the corrosion and the biofouling of the device throughout its lifetime.

RBI is supported by the collection and documentation of operating experience and development of a knowledge base of material degradation mechanisms, corroborating the need to understand tidal devices in more detail, including where they will operate and the materials likely to be used for their construction.

2.3 Feedback and Assessment

Using the results from monitoring and testing of the device, a continual assessment approach should be taken with all data stored in a database for analysis over the operational lifetime. Continual assessment of the device in terms of corrosion damage and biofouling settlement allows hazards to be dealt with prior to significant damage or failure of the particular component. This process also allows the device to be considered as a whole – where certain features may affect others (e.g. galvanic corrosion between dissimilar metals) and provides a method for continual improvement and policy development.

For a subsea device, the assessment process will draw attention to areas where corrosion or biofouling is significant or where it poses higher risk (Det Norske Veritas, 2012). The management system developed will provide recommendations that can be implemented to ensure risks do not become so significant as to pose a severe threat to operation of the device during its lifetime whilst ensuring compatibility with economic and environmental requirements.

The overall system feedback and improvement process should also include review of new monitoring systems and protection techniques. These should be recorded in the management system for reference.

The management system should also be monitored and measured in terms of performance relative to the objectives detailed in the corrosion management policy and to identify if the system is working correctly and effectively at eliminating identified corrosion risks. If the system is not working as required then a review of the strategy and policy should be carried out.

2.4 Conclusions

This chapter has provided an overview of risk management and risk-based inspection processes. These are two processes that are ideal for the management of corrosion and biofouling on tidal devices and will provide many benefits including compliance with relevant statutory and corporate health, safety and environmental requirements; helping to reduce potential structural failures and other threats to operation of the device; reducing unplanned maintenance and device downtime; increasing operational time; and optimising cost for maintenance, monitoring and repair. As such, a risk-based approach has been identified as the most relevant and practicable for tidal stream devices.

By assessing the risks associated with the operation of a turbine in the marine environment and by the development of a risk-based corrosion and biofouling management system, recommendations can be given to aid development and operation of energy generation devices. Recommendations for preventative or mitigation techniques must take into consideration the associated cost implications.

A risk management and risk based inspection approach has been implemented in a wide range of industries. The framework is used here for tidal stream devices, for the first time. From this review of risk management and its applicability to different industries, specifically its wide use in the offshore oil and gas industry, it is believed that this is appropriate with respect to the corrosion and biofouling that will be experienced by the devices. To support the development of a risk based inspection regime and the overall development of a risk based management system, the need to increase understanding of corrosion and biofouling, including the mechanisms; environmental effects and protection methods and how the devices will themselves be affected has been identified. This involves study of

devices already in development and understanding the environment in which they will be placed. This is the focus of future chapters.

Chapter 3

Developing the Evidence Base (i) - A Literature Review of Marine Corrosion and Biofouling

3.1 Introduction

To understand how to prevent and mitigate failure of tidal devices it is essential to understand how different conditions affect the onset and development of corrosion and biofouling in the areas identified as key risk. These conditions include the following:

- Flow patterns, including turbulent flow around the different areas of the turbine; fast flow and areas of stagnant water
- Water conditions, including salinity; dissolved oxygen levels; suspended solid concentration; temperature; light penetration; pH and organic matter concentration
- The metals and materials used in different areas of the device, including how they affect corrosion and settlement of organisms in that particular area and also their interaction with other metals used on the device
- Compatibility of different anti-corrosion and anti-fouling systems
- Surface modification by biofouling and how this will affect corrosion and device operation

By understanding the conditions listed above, and how these vary around the world, evidence can be gathered to establish the context as the first part of the risk assessment process (Figure 2.2 in Chapter 2). This understanding will allow identification of the corrosion and biofouling expected in different conditions and thus assist in development of the risk management strategy.

This chapter provides a detailed review of literature published regarding marine corrosion and biofouling, including the mechanisms for both processes on ships' hulls and on offshore structures; the factors affecting the onset and propagation of corrosion and biofouling and a review of current and past antifouling and anticorrosion systems as the first step in developing an evidence base. Although these regimes are different from that experienced

in a tidal flow, this literature will form part of the evidence base for identifying potential strategies for future device deployment.

Included at the end of this review is a discussion of the literature in terms of tidal stream devices; the forms of corrosion likely to manifest; the consequences of corrosion; methods to assess and monitor corrosion; the known effects of the environment on corrosion; factors affecting the settlement of biofouling; and the effects of biofouling, both on corrosion and on the structure as a whole.

3.2 Marine Corrosion

There is a large amount of literature relating to corrosion spanning many decades, indeed centuries. In the marine environment that relating to modern structures, mostly shipping, dates back to the 1940s with a major output relating to offshore oil and gas platforms in the 1970's. Conventional corrosion theory will be discussed, including the electrochemical principles (Evans, 1960; Tomashov et al., 1966; West, 1980; Melchers, 2003a).

Seawater provides a highly corrosive medium to many materials submerged in it. This is mainly due to the high concentration of chlorides (high salinity - open sea salinity can vary between 33-38 ppt (parts per thousand)). Chloride ions also provide a lower resistivity, allowing anodes and cathodes (the active sites) to form further away from each other. Dissolved oxygen level, carbon dioxide percentage, temperature and electrical conductivity are also important factors affecting corrosion (Chandler, 1985).

There are two main competing processes which occur in seawater; formation and continual repair of a passive film on a metal surface due to the presence of oxygen in the water; and the breakdown of the passive film due to the chloride ion activity (Shifler, 2005a). Both of these processes can be modified by the physico-chemical environment, such as localised changes in pH, temperature, abrasion due to particulates and biofouling. Such modifications can result in one of the processes dominating in a particular area.

Metallic corrosion occurs when a metal is exposed to a reactive environment. The metal contains embodied energy and will preferentially return towards its most stable state (similar to its ore). Corrosion is electrochemical involving anodic and cathodic reactions (oxidation and reduction) (Chandler, 1985; Davis, 2000). At temperatures where water is a liquid, the electrochemical reaction can occur simply due to the water providing a good solvent and the connecting electrolyte needed for corrosion. Thus five key elements are

required for a corrosion cell to be established: the anodic site at which the corrosion takes place (Equation 3.1); the cathode where the protective film is formed and protected from corrosion by the anode (Equation 3.2); the electrolyte which allows ionic contact between the anode and the cathode; electronic contact between the anode and the cathode (either through the metal, or through direct contact of two different metals); and the cathodic reactant, which in seawater is usually dissolved oxygen or the water itself (Chandler, 1985).

$$M \rightarrow M^{n+} + ne^{-} \quad [3.1]$$

$$O_2 + 2H_2O + 4e^{-} \rightarrow 4OH^{-} \quad [3.2]$$

The metal which acts as the anode will pass into the electrolyte (seawater) via anodic dissolution (oxidation reaction). The following reaction shows this process for iron:

$$Fe_{(s)} \rightarrow Fe^{2+}{}_{(aq)} + 2e^{-} \quad [3.3]$$

As can be seen in Equation 3.3, the metal dissolution releases electrons which flow through the metal to the cathode site where they are consumed in a reduction reaction. In seawater the most common cathodic reduction reaction is as follows:

$$O_{2\,(g)} + 2H_2O_{(l)} + 4e^{-} \rightarrow 4OH^{-}{}_{(aq)} \quad [3.4]$$

It is possible for the cathodic reduction reaction to take other forms. In the case of de-aerated water the reduction of hydrogen ions can occur, with the evolution of hydrogen gas, and in the presence of certain bacteria sulphate ions are reduced.

The overall corrosion reaction for iron can be expressed as in Equations 3.5 and 3.6 with the formation of rust in an aqueous environment (hydrated iron oxide):

$$2Fe_{(s)} + O_{2\,(g)} + 2H_2O_{(l)} \rightarrow 2Fe^{2+}{}_{(aq)} + 4OH^{-}{}_{(aq)} \quad [3.5]$$

$$Fe^{2+}{}_{(aq)} + 2OH^{-}{}_{(aq)} \rightarrow Fe(OH)_{2\,(s)} \quad [3.6]$$

If sufficient oxygen is present, a red/brown rust can be formed via the following reactions:

$$Fe(OH)_{2\,(s)} + OH^{-}{}_{(aq)} - e^{-} \rightarrow Fe(OH)_{3\,(s)} \quad [3.7]$$

$$Fe(OH)_{3\,(s)} \rightarrow FeO.OH_{(s)} + H_2O_{(l)} \quad [3.8]$$

The type of rust that forms is determined by pH, rate of oxidation and salinity as well as the dissolved oxygen concentration. If, for example, the oxygen supply is limited (as in stagnant water), magnetite (black in colour) can be formed instead (Fe_3O_4). The type of rust formed can have a subsequent effect on the underlying rate and type of corrosion.

The electrical conductivity of seawater at an average salinity (35 ppt) and a temperature of 10-20 ^{o}C is approximately 4.29 Sm^{-1} (Siemens per meter)(Kaye & Laby, 2005)) and the resistivity of coastal seawater is approximately 30 Ωcm (Chandler, 1985). Electrical conductivity is important when considering the amount of corrosion that occurs under immersed conditions, particularly galvanic couples and at localised situations such as crevices (Chandler, 1985). The low resistivity of seawater allows a greater distance between anode and cathode couples. As the chlorinity, and consequently the salinity, increases, the resistivity decreases further, potentially increasing the rate of corrosion.

In general, electrochemical corrosion is determined by the nature of the oxidising reactants present, but also depends on kinetic factors (bulk diffusion and electron transfer reactions).

Many marine structures and devices are constructed using carbon steel. Carbon steel is not chosen for its corrosion resistance, but its strength and relatively low cost and, in spite of its poor corrosion resistance, is still the most widely used constructional alloy for marine conditions (Chandler, 1985). In clean dry air a protective oxide film will form on the surface of polished mild steel. Unfortunately, it provides almost no protection to carbon steel immersed in seawater (Chandler, 1985). The formation of corrosion products (iron oxides) is an abiotic process involving chemical reactions. However, not only can living organisms influence the corrosion process and rate but microbiologically influenced biomineralisation/transformation of corrosion products may also occur (Duan et al., 2008).

Many different metals are used for structures in the marine environment, including carbon steels, stainless steels and cast irons, chosen due to their specific properties. For example, nickel aluminium bronzes are used in forgings, extrusions and sections and have higher strengths than other copper alloys making them well suited to propellers, fasteners, fixings and pump parts. In addition, they have higher corrosion resistance than many other metals and alloys in the marine environment, including resistance to stress corrosion cracking, corrosion fatigue, and corrosion/erosion.

The corrosion resistance of these alloys is in part due to the aluminium content of the material, and varies depending on the metallurgical structure (including the actual

composition as well as the method of manufacturing the component and treatment prior to use). This allows the material to form an alumina-rich thin, even protective coating, not prone to breakdown or pitting. The alumina layer prevents or significantly slows down the rate of corrosion of the alloy underneath.

However, although proven to withstand most forms of corrosion effectively, there are some situations which will cause crevice corrosion to occur (in areas shielded by fouling, deposits or other components), although this generally results in selective phase dealloying in the area. Nickel aluminium bronzes exhibit a high resistance to mechanical stress.

3.2.1 Forms of Marine Corrosion

General surface corrosion is an issue on metals which are unprotected. Figure 3.1 shows the relative loss of metal thickness in different immersion zones in the marine environment. The zones represent different depth of submersion, from atmospheric corrosion where the device is completely out of, but close to, the water, to subsoil, such as support structures or pipelines that are buried below the surface of the seabed.

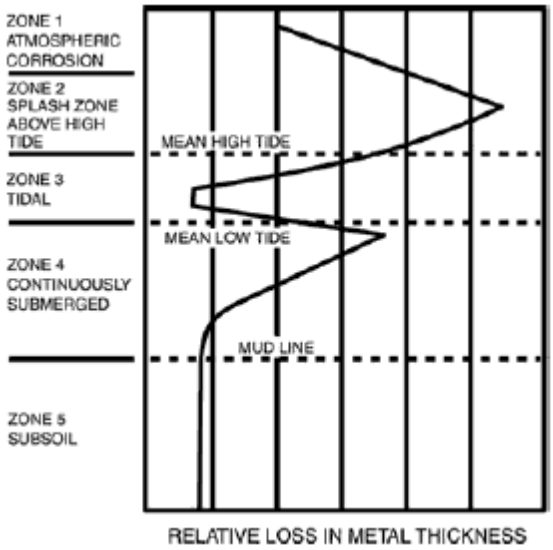

Figure 3.1. Seawater zones and relative loss in steel thickness for unprotected steel structures (Michels and Powell, 2012)

General Corrosion

General (uniform) corrosion is the most common form of corrosion and occurs when all exposed areas corrode at approximately the same rate (Chandler, 1985). It is thus characterised by a progressive uniform thinning across the surface of a metal (West, 1980). The uniformity is due to anodic areas corroding and then becoming stifled by corrosion

products, with new anodic areas corroding next to original ones. The interchange between anodic and cathodic areas leads to an overall approximate uniformity of the corrosion over the exposed surface (Chandler, 1985). However, it is rare for loss of metal to be uniform over the surface.

Galvanic Corrosion

Galvanic corrosion (often called bimetallic corrosion) can occur when dissimilar metals or alloys are in contact with each other (Trethewey and Chamberlain, 1995). The two different metals need to be coupled to form a basic wet corrosion cell. When in electrical contact, the more resistant alloy may aggravate attack on the less resistant alloy adjacent to it. This results in an acceleration of corrosion of the less resistant alloy (Hack, 2010). The galvanic (or electrochemical) series (Figure 3.2) tabulates metals from the most active (anodic) to the most noble (cathodic). The most anodic metal is magnesium, which, in a couple, will corrode preferentially over any other metal. Other anodic metals include zinc, beryllium and aluminium. The least active materials (also the most expensive) include graphite, silver, gold and titanium. Stainless steels are located around the middle of the table with certain types (e.g. 310) more anodic and others (e.g. 202 and 316L) located towards the cathodic end of the scale. If two metals with different corrosion potentials are placed in electrical contact, a driving force for the corrosion reaction exists (Fontana, 1987). This driving force is increased if the surface area of the cathodic metal is significantly greater than that of the anodic metal (for example, all bolts and other fasteners should be made cathodic to the surrounding metal rather than the other way round).

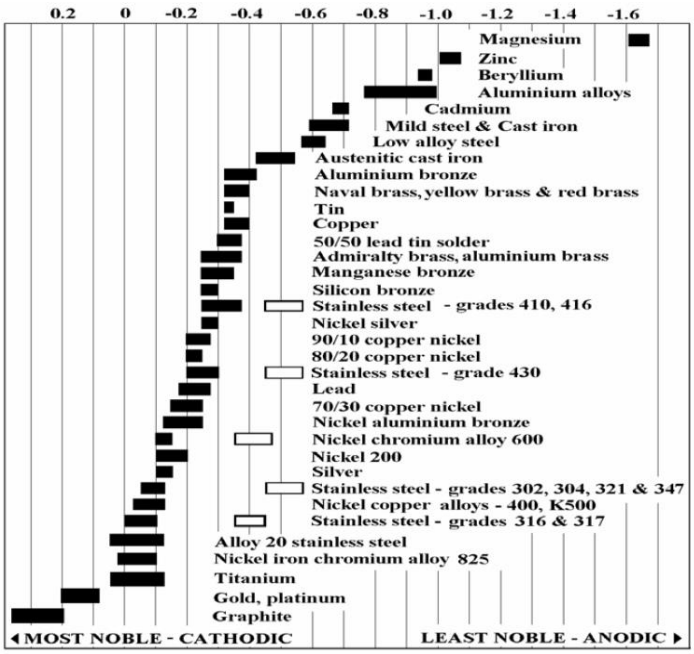

Figure 3.2. The galvanic series which notes the corrosion potentials in flowing seawater (2.4-4.0 ms^{-1}) at ambient temperature (Atlas Steels, 2010)

The unshaded symbols in Figure 3.2 represent the potential range in more acidic locations, such as crevices or stagnant water where there is less oxygen present. These situations are likely to make the material more anodic, and hence more susceptible to corrosion. The most frequently observed form of galvanic corrosion is that between copper/copper-based alloys coupled with iron and steel, mainly due to their extensive use in a wide range of structures because of their low cost and availability (Trethewey and Chamberlain, 1995).

Galvanic corrosion is very common on industrial structures. However, it is possible to prevent this from occurring by making correct decisions at the design stage, including electrical isolation; electrical insulation; exclusion of the electrolyte; controlling the anode-to-cathode area ratio; using corrosion inhibitors for enclosed areas and cathodic protection (Hack, 2010). However, not all of these may be suitable for tidal stream devices.

Pitting

Pitting corrosion is a localised form of corrosion characterised by the development of small cavities on open, exposed surfaces of metals (Yang, 2008), and is one of the most likely forms of localised metal degradation to occur in the marine environment. Generally the pits have a depth of penetration greater than the nominal diameter (Chandler, 1985) and are formed by the aggressive action of anions dissolved in the water on an alloy which is generally passive under conditions ranging from slightly acidic to alkaline. The main problem involving pitting corrosion is where metals that are thought of as passive, such as

aluminium, titanium and stainless steel, are used in environments where they are actually susceptible to pitting attack (Alvarez and Galvele, 2010).

Electrochemical depassivation is the most common type of pitting corrosion and occurs in neutral or alkaline environments. A pitting potential (E_P), above which pitting will occur, and below which the metal will remain passive in the given environment can be defined (Szklarska-Smialowska, 1999; Böhni and Uhlig, 1969; Frankel, 1998). The pitting potential is a function of the composition of the metal/alloy and of the physic-chemical environment in which it is placed. Perhaps the main depassivating agent, hence lowering the pitting potential in seawater is the chloride anion. Pitting corrosion is also characterised by a repassivation potential (Frankel, 1998), which is lower than the pitting potential. Below this potential, pits will cease to grow. Conversely, there exists an inhibition potential, at a potential greater than the pitting potential, above which the pit becomes repassivated (Galvele, 1978).

Pitting results in small areas of the surface corroding with penetration into the bulk metal. This can be a major issue for structural integrity as what may look like only a small area of corrosion may be masking significant deterioration below the surface. The size and depth of the pit is dependent on the reactions that occur and continue inside the pit. Inside the pit, conditions will change from that at the surface, with oxygen depletion, and the formation of acidic conditions.

Any metal that relies upon a passive film for corrosion resistance may be subject to pitting if there is a break in the film, or if the surrounding environmental conditions cause there to be a defect in the protective film. Pitting can occur on carbon steel in seawater, particularly if it remains covered by millscale formed in production. A potential difference between the scale and the metal (the scale is cathodic with respect to the steel) leads to pitting in locations where there is a small break in the scale.

Crevice Corrosion

Crevice corrosion (originally described by Mears and Evans, 1934) is a form of localised attack occurring in occluded regions, crevices or shielded areas. These locations can cause a small stagnant area to be formed, creating differential aeration (a gradient of oxygen) and localised anodic conditions (e.g. a build up in chloride ions) relative to the bulk solution (Corlett et al., 2010; Evans, 1925). On structures in the marine environment, crevices can be both man-made or naturally forming, often around valves, gaskets, flanges and bolt

heads, and also under surface deposits, including sediment, sand, dirt or biofouling (El Din et al., 2003; Shifler, 2005b).

As crevices get smaller, corrosion is more likely to occur due to restricted mass transport (Corlett et al., 2010). In chloride containing solutions such as seawater, a lack of mass transport of metallic ions out of crevices can cause electromigration, where anions migrate into the crevice to preserve electroneutrality (Chandler, 1985; White et al., 2000). This process reduces the pH in the crevice, and the increased acidity can break down the passive film and increase corrosion rate.

Flow Assisted Corrosion

The effect of fluid flow on corrosion can be defined by mass transfer and wall shear stress parameters contacting the solid surface (Efird, 2000). Under flowing conditions, different metals and alloys react in different ways, depending on the type of flow (laminar, turbulent) and the velocity (Wood et al., 1990). The mechanism of failure due to flow requires an understanding of the material, surface structure/roughness and the fluid dynamics of the water in which it is placed (turbulence; one-phase; two-phase; multiphase flow; entrained solid particle concentration and the direction of the flow relative to the material) (Schmitt and Bakalli, 2010; Baboian, 2005; Silverman, 2003). For example, the corrosion of copper increases rapidly above a water velocity of 2 ms^{-1}, with only a low, even rate of corrosion below 1 ms^{-1}. Efird and Anderson (1975) examined corrosion rates over a 14 year period and found varying corrosion rates for 70Cu-30Ni alloy under different flow regimes. The increasing corrosion rates with increasing flow was due to a mechanical stripping of the protective film formed on the surface of the metal. Another study, carried out using jet impingement testing to study the effect of mass transfer and wall shear stress on flow accelerated corrosion (Efird, 2000), showed that corrosion was directly related to the degree of jet impingement testing. Mathematical models have been established for flow induced corrosion in carbon steels, although this work has tended to focus on high velocity seawater (up to 18 ms^{-1} linear velocity) (Jingjun Liu. et al., 2008; Jingjun Liu. et al., 2005). Syrett and Wing (1980) found the flow effect to be related to the electrochemical stability of the film formed as opposed to its mechanical stability.

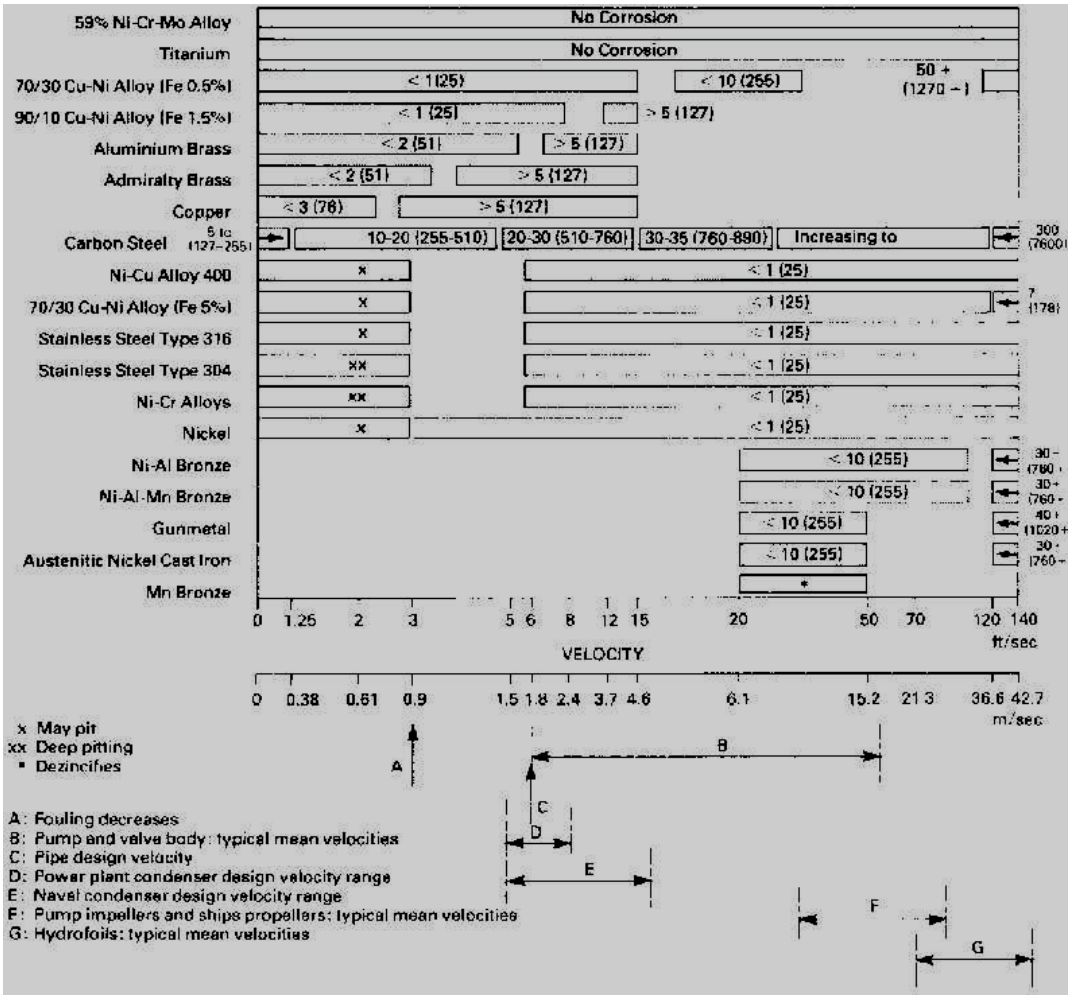

Figure 3.3. Potential corrosion rates of different alloys in flowing seawater. Corrosion rates are shown on the bars, given in units/hr and microns/yr in brackets (Copper Development Association, 1982)

Figure 3.3 shows the potential corrosion rates of various alloys in flowing seawater at a range of flow rates.

Erosion-Corrosion

Erosion is a mechanical process that arises from the flow of seawater over a structure. Depending on the environmental conditions, erosion may mean that protective coatings or passive films are removed from the metal surface. Erosion-corrosion is the simultaneous interactions between erosion and corrosion, including cavitation and liquid erosion with the metal loss rate increasing beyond that due to the combination of the two mechanisms individually (Bermúdez et al., 2005). Impact from solid particles entrained in the flowing seawater can damage a metal surface, removing protective coatings and leaving the exposed metal beneath, activating it for corrosion (Schmitt and Bakalli, 2010). The rate of erosion-corrosion is proportional to the kinetic energy of the impinging particle, and the

frequency of potential impacts. Therefore the velocity of the flowing seawater is an important factor.

Corrosion of Welds

The process of welding metals together can affect the corrosion of the metals used. The heating and cooling cycle affects the microstructure and the surface composition of welds as well as the base surface metal. A heat-affected zone (HAZ) can form that will have a different, often lower corrosion resistance than the rest of the structure.

There are several factors which can affect the corrosion of welds on a structure. These include (Davis, 2006):

- Weldment design including the weld chemical and physical composition
- Fabrication technique
- Welding practice
- Welding sequence
- Contamination of area by moisture
- Presence of organic or inorganic species
- Presence of oxide film and scale on surface
- Porosity
- Cracks and crevices
- Final surface finish

Under Coating Corrosion

Anti-corrosion coatings can delaminate from the underlying metal especially if not applied correctly and corrosion can occur. One such form of under coating corrosion is cathodic delamination (Margarit and Mattos, 1998; Sørensen et al., 2010). This usually propagates from existing breaks or defects in the coating (McMurray and Williams, 2010).

Cathodic delamination can potentially occur whenever the underlying metal is exposed to scratches or other damage either during manufacture or operation (Collazo et al., 2007). This often occurs when a cathodic protection system is used in conjunction with a paint coating anodic dissolution of the underlying metal in defect areas causes electrons to be released to force the cathodic reaction at sites beneath the coating layer. Oxygen, if present, is then reduced to form hydroxide ions, which in turn causes alkalinisation, leading to delamination, and hence failure, of the coating (Khun and Frankel, 2013). In the absence of oxygen, hydrogen reduction can cause hydrogen blistering.

Splash-Zone Corrosion

Corrosion can be very high in the splash zone where there are high levels of oxygen present whilst there is also plenty of seawater available. The splash zone is defined as the zone above the tidal zone, being subject to waves and salt spray (LaQue, 1975). Corrosion rates in this zone are similar to low water levels, and can be significantly higher than the corrosion rates observed in atmospheric environments (see Figure 3.1).

Atmospheric Corrosion

In relation to the marine environment, atmospheric corrosion is the effect of salt laden, often damp, air as experienced on, for example, a quayside. The presence of water dictates the onset and rate of atmospheric corrosion, with mist, marine aerosols and condensation causing the most corrosion risk. It has been found that steel specimens 24.4 m from the shore will corrode at a rate 12 times faster than specimens placed 243.8 m away (Fontana, 1987). Mist and spray allow a thin film of salt laden water to form on the metal surface; this will not drain away as is the case with heavy rain. The size of marine aerosols varies from 0.1 to 400 µm (Blanchard and Woodcock, 1980; Zezza and Macri, 1995), with smaller particles able to travel further than large particles before settlement. The thin film of water can easily be saturated with oxygen from the atmosphere and as such, the rate is no longer determined by the cathodic reaction but by the electrolyte and the amount of dissolved contaminants (chloride ions for the quayside location). The salinity in marine environments will vary with weather conditions (wind speed and direction); proximity to water; water condition (calm or high waves); land topography; exposure angle and altitude (Morcillo et al., 2000; Vera et al., 2003). The annual average wind speed experienced in Orkney, for example, is high at approximately 22 km/h, (Met Office, 2013) and as such the transportation of sea salts on to a device located on the quayside would be very likely. Temperature and it's diurnal variations has indirect effects on atmospheric corrosion, such as the rate of evaporation of moisture from the surface (Chandler, 1985). The presence of chlorides will accelerate the metallic corrosion by raising the conductivity of the electrolyte and forming soluble corrosion products (destroying the formation of a passive film on the metal surface).

Many metals (including iron, steel, copper and zinc) will corrode if the relative humidity exceeds 60%. If it exceeds 80% the rust on iron and steel will become hygroscopic and the rate of corrosion attack will increase further (Trethewey and Chamberlain, 1995). However,

in the presence of chlorides, it has been shown that corrosion can occur at lower relative humidities, even as low as 40% (Chandler, 1966).

Operating in the marine atmosphere also poses risks to protective paint coatings. This is especially important when carrying out maintenance on the coating on the quayside with high levels of soluble salts in the atmosphere. The presence of water soluble contaminants at the metal-paint interface will accelerate corrosion of the metal as well as having a negative effect on the behaviour of the coating applied over substrates that have been contaminated (left exposed to the marine atmosphere) (Morcillo, 1999; Flores and Morcillo, 1999). A protective paint coating on a metal surface will act as an impermeable membrane allowing moisture to penetrate but not salts. If there are soluble salts at the metal-paint interface a process known as osmotic blistering will occur (Funke, 1981). When this occurs, the water will penetrate through the coating due to osmosis (Morcillo, 1999) and will cause blisters to form where salts are present (generally located at metal-corrosion products interface and at the bottom of pits). Where water is present, corrosion can occur and corrosion products are formed between the metal surface and the protective coating.

When a metal that has been in seawater is removed from it, corrosion can continue to occur and even accelerate because the aggressive ions are highly deliquescent, attracting moisture from the air to make the metal surface damp. A highly concentrated salt solution can then form on the surface that is more corrosive than the seawater itself (Valand, 1969; Henriksen, 1969).

3.3 Environmental Effects on the Corrosion of Submerged Structures

Corrosion rate depends both on the metal itself (in terms of alloy composition, alloy surface films, geometry and surface roughness (Shifler, 2005b)) and the environment it is in. The potentially major consequences associated with corrosion of marine based structures mean that prediction of corrosion in a given location prior to deployment is a very useful design tool. Table 3.1 details the effects of various environmental factors studied in a number of tests.

Table 3.1. Environmental factors considered in example corrosion studies (CR is corrosion rate)

Guedes Soares et al (2009)	Relative humidity Chlorides Temperature	CR increase with increase in relative humidity (%) Weight loss increased with increase in chloride concentration CR increase with increase in T
Atashin et al (2011b)	Salinity Velocity Temperature pH	Cumulative effects of these parameters are assessed
Jeffrey and Melchers (2003)	Temperature Dissolved Oxygen Salinity Calcium Carbonate pH Water Velocity Marine Growth	Parameters are assessed with reference to marine growth and corrosion
Al-Malahy and Hodgkiess (2003)	Salinity Temperature Water Flow	Breakdown potential observed at the salinity levels chosen did not show much variation, except in lower alloy steels Breakdown potential lowered at higher temperatures Low flow rates did not cause significant increase in corrosion rates. Jet impingement flow caused large increase in all metals tested
Sridhar (2004)	Temperature Microbial Activity Chlorination Salinity Dissolved Oxygen Water Flow	Cumulative effects of these parameters are assessed for potential for localised corrosion

3.3.1 Temperature

Temperature is a complex external variable in aqueous corrosion, and can affect the corrosion of a metal or alloy in a number of ways (Silverman, 2003). The published literature on investigations of corrosion rate variation with temperature shows significant scatter, but concludes that there is a relationship between temperature and corrosion rate (Evans, 1960; Tomashov et al., 1966; Melchers, 2002). If the corrosion rate is only controlled by the metal oxidation process, the corrosion rate would increase exponentially with an increasing temperature (T), obeying the Arrhenius relationship (West, 1980; Trethewey and Chamberlain, 1995):

$$rate = k[A]^a[B]^b \qquad [3.9]$$

Where $k = Ae^{-\frac{E_A}{RT}}$

E_A is the activation energy (kJ/mol), R is the gas constant ($JK^{-1}mol^{-1}$), A is the frequency factor (s^{-1}), T is the temperature (Kelvin). [A] and [B] are the concentration of species A and B (M) and a and b factors that are determined experimentally. For carbon steel this results in a doubling of corrosion rate for every 10 ^{o}C rise in temperature. In reality this is often not the case, indicating that other factors interact with temperature effects.

Temperature varies with latitude (Figure 3.4), affecting the chemical and physical properties of seawater as well as the electrochemical behaviour of the submerged metal.

As temperature increases, the rate of corrosion generally increases as the breakdown potential lowers (the least noble potential at which pitting or crevice corrosion will initiate and propagate) (Baboian, 2005; Guedes Soares et al., 2009). A change in temperature may also alter the properties of the passive protective film formed on a metal surface during corrosion, with warm seawater depositing a more protective scale on the metal surface than in colder waters (Trethewey and Chamberlain, 1995).

Varying the temperature alters the dissolved oxygen content and biological activity (Shifler, 2005b). The solubility and diffusion of oxygen through an aqueous solution to a metal surface will greatly depend on the temperature of the solution. As temperature increases the solubility of oxygen will decrease which may decrease corrosion rates. However, a temperature increase will also increase the diffusion coefficient of the oxygen, leading to potentially increased corrosion rates (Atashin et al., 2011b). Biological activity tends to increase with increasing temperature (Barchiche et al., 2004).

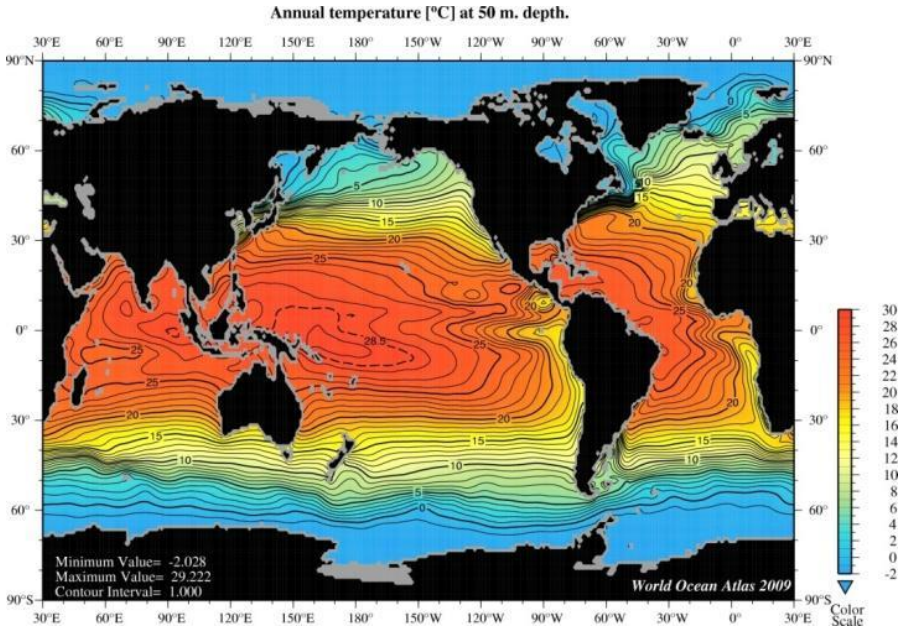

Figure 3.4. Annual temperature (^{o}C) variation with location at 50 m depth (Locarnini et al., 2010)

3.3.2 Dissolved Gases

The amount of dissolved gas in the electrolyte is an important factor (Ailor, 1971). For example, the amount of oxygen present affects the kinetics of the reduction reaction for corrosion (the rate determining step of the process). High oxygen content in seawater will depolarise the cathode and hence increase the activity and rate of attack of the metal surface. When dissolved oxygen is present, this reduction reaction can change from Equation 3.10 to Equation 3.11 which proceeds faster. The dissolved oxygen level varies with temperature; depth; salinity; season and water flow, and is also dependent on the local biological activity (Shifler, 2005b; Ijsseling, 1989). Over the normal range of pH found in natural seawater (normally slightly alkaline), the availability of oxygen has a greater influence on corrosion than that of a change in pH (LaQue, 1975).

$$2H^+ + 2e = H_2 \qquad [3.10]$$

$$2H^+ + \tfrac{1}{2}O_2 + 2e = H_2O \qquad [3.11]$$

The corrosion rate of a metal can be related to the oxygen concentration by the following relationship (Walsh, 1993), which shows that the corrosion current density will increase with an increase in oxygen concentration:

$$I = I_L = \frac{DzFC_o{}^{2-}}{\delta_N} \qquad [3.12]$$

I_{corr} = corrosion current density (Acm^{-2})
I_L = Limiting current density (Acm^{-2})
D = Diffusion coefficient (cm^{2}s^{-1})
F = Faraday constant (96485 Cmol^{-1})
$C_o{}^{2-}$ = oxygen concentration (mol cm^{-3})
Z = number of electrons
δ_N = thickness of the Nernst diffusion layer (cm)

The global variation of dissolved oxygen in seawater can be seen in Figure 3.5.

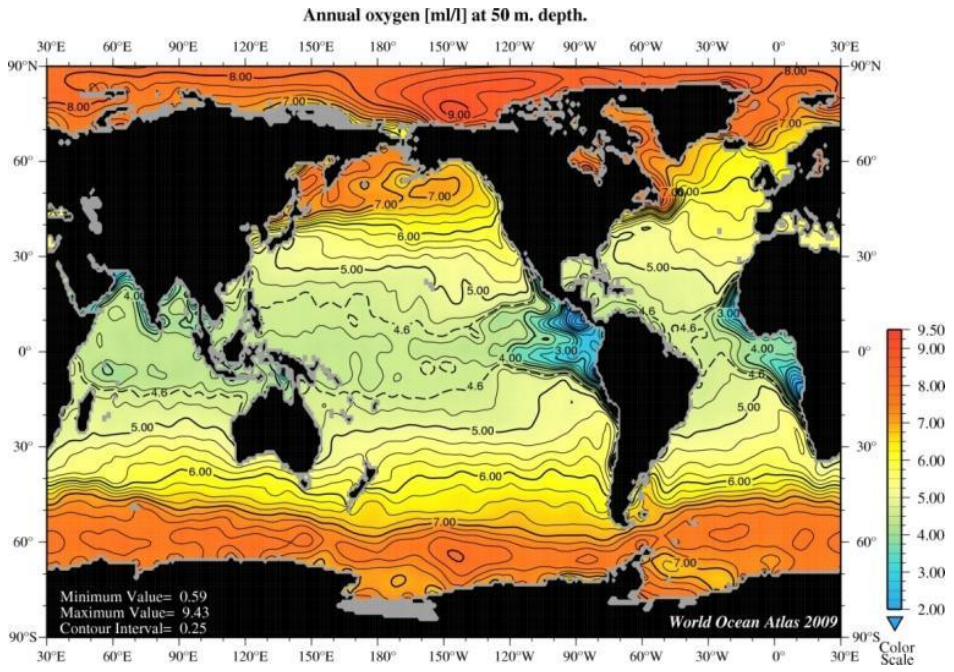

Figure 3.5. Annual dissolved oxygen concentration (ml/l) with location at 50 m depth (Garcia et al., 2010)

3.3.3 Salinity

Salinity is defined as the total weight of salts dissolved in 1000 grams of water. An increase in salinity may decrease the breakdown potential of a metal, providing a more aggressive environment and therefore leading to a higher rate of localised corrosion. However, one laboratory based study has shown that for certain metals, including titanium and superaustentitic stainless steels, an increase in salinity from 35,000 mg/l to 55,000 mg/l in static water conditions at 25^{o}C had no noticeable influence on the localised corrosion behaviour except for lower alloyed steels (e.g. 316L) (Al-Malahy and Hodgkiess, 2003). The variation in the salinity of seawater ranges from approximately 32 to 38 ppt (this approximates to 32-38 grams of dry salts contained in 1000 grams of seawater obtained by titration with silver nitrate (Chandler, 1985)) and varies with geographical location (Figure 3.6), depth and temperature. This variation will not significantly alter corrosion rates. However, for combinations of an increase in salinity and an increase in temperature, or an increase in water flow, a large reduction in breakdown potential for stainless steels has been observed, thus highlighting the need to understand environmental factors both individually and when interacting.

The eleven major, most abundant, ions contained in seawater are shown in Table 3.2. Although the absolute concentrations of these may vary under different factors, their proportions are virtually constant, and so if salinity is known, the concentration of all the major ions can be determined.

Table 3.2. Concentrations of 11 most abundant ions in seawater at a salinity of 35.00 ppt (data obtained from European Federation of Corrosion, 1989)

Ions	Concentration (g/kg) at salinity of 35.00 ppt
Total Salts	35.1
Sodium (Na^{+})	10.77
Magnesium ($Mg^{2+)}$	1.290
Calcium (Ca^{2+})	0.4121
Potassium (K^{+})	0.3990
Strontium (Sr^{2+})	0.0079
Chloride (Cl^{-})	19.354
Sulphate (SO_4^{2-})	2.712
Bicarbonate (HCO_3^{-})	0.140
Bromide (Br^{-})	0.0673
Boric acid ($B(OH)_3$)	0.0257
Fluoride (F^{-})	0.0013

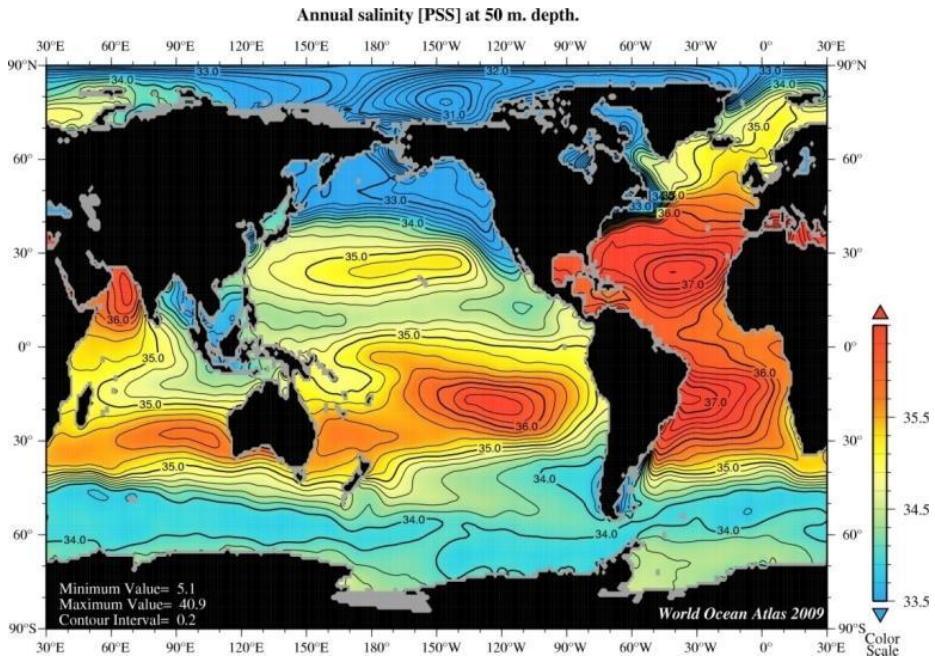

Figure 3.6. Annual salinity (PSS) variation with location at 50 m depth (Antonov et al., 2010)

3.3.4 Water Velocity

Melchers and Jeffrey (2004) observed that a high flow of water contributed to accelerated corrosion. This can be due to either mass transfer effects or mechanical flow effects (Shalaby et al., 1992). If a metal or alloy produces a strongly adhering passivation layer, only very high velocities will cause the layer to breakdown and lead to corrosion. These strongly adhering layers also have a high resistance to erosion corrosion. Al-Malahy and Hodgkiess (2003) found that an increase in flow velocity of 3 ms^{-1} did not result in any significant increase in corrosion. However, an increase to a jet impingement of 95 ms^{-1}

caused significant degradation in stainless steels, and a reduction in the breakdown potential of titanium, nickel-based alloys and a superduplex stainless steel (which are all known to be good performing metals in terms of corrosion resistance).

High flow can also result in an increase in the oxygen availability on a surface altering the corrosion reaction kinetics and potentially causing differential aeration (Trethewey and Chamberlain, 1995). Conversely high flow rates can remove aggressive ions and other species (which may increase corrosion) from a surface and hence decrease the corrosion rate at that point (Heitz et al., 1996). At a sufficiently high water velocity the growth of a biofilm on a metal surface would be retarded so both macrofouling and anaerobic pockets containing sulphate reducing bacteria could not form (Melchers and Jeffrey, 2008). An increasing flow rate may also enhance passivation and hence inhibition of corrosion (Heitz et al., 1996).

3.3.5 Seawater pH

Seawater pH is buffered and only varies a small amount in a range approximately 7.5-8.3 (Shifler, 2005b). A small variation from neutral does not affect the corrosion rate of most metals and alloys. Small variations in pH will, however, affect the formation of calcareous scales on systems with cathodic protection. This may have an indirect effect on the corrosion rate of the alloy. Localised acidic areas are likely to occur in crevices that then become anodic and corrode at a faster rate.

3.3.6 Carbon Dioxide and Calcareous Scales

Carbon dioxide is present in seawater in the form of bicarbonate and carbonate ions (formed on dissolution of the carbon dioxide), in equilibrium with each other and hydrogen ions (Chandler, 1985). The carbon dioxide equilibrium is related to pH and temperature of the seawater and the equilibrium is able to buffer pH.

Seawater contains large amounts of magnesium sulphate and calcium bicarbonate salts. A corrosion reaction will cause the local pH at the cathode to rise which will cause the equilibrium between carbon dioxide and carbonate mentioned above to be altered and will cause the precipitation of calcium carbonate ($CaCO_3$), magnesium sulphate ($Mg(OH)_2$) or mixed scales. These deposit at the cathode and can reduce the corrosion rate and hence protect the metal surface.

3.3.7 Cumulative Effects

Several studies (Sridhar et al., 2004; Atashin et al., 2011b; Malik et al., 1999) have shown that the cumulative effects of temperature, salinity, dissolved oxygen, pH and water velocity result in the degradation and corrosion on metals used in the marine environment as discussed in the sections above.

3.3.8 Biofouling

Marine biofouling is the term given to describe the colonisation and the growth of a community of organisms at the interface of seawater and hard substratum (Wahl, 1989; Dürr and Thomason, 2010) and can have a major effect on the corrosion or indeed, protection, of a structure. The first references to marine biofouling were associated with sea-going vessels over 2000 years ago (Yebra et al., 2004; Finnie and Williams, 2010); when it was discovered that biofouling would not only slow vessels down, but also cause damage to the vessel. However, the effects of fouling on marine renewable technologies are yet to be widely documented in the literature. All inert surfaces in the marine environment foul (Wahl, 1989) and within minutes of immersion in seawater a surface will become colonised. Biofouling has been studied substantially in areas such as the North Sea due to the extensive offshore Oil and Gas production in the area (Edyvean et al., 1983; Heaf, 1981; Picken and Grier, 1984) and offshore platforms in the North Sea are well documented in regards to biofouling and corrosion issues (Forteath et al., 1982; Forteath et al., 1984; Kingsbury, 1981).

The term biofouling encompasses both micro and macro scale fouling; hence it can be further defined as microfouling (for example bacteria) and macrofouling (barnacles, etc.). The latter often occurs on a surface already settled by microfouling and with an established biofilm present. However, this is not always the case and macrofouling organisms can settle if conditions are preferential without a biofilm present (Yebra et al., 2004). Thousands of biological species have now been documented as involved in the fouling of surfaces exposed to water.

The complex process of fouling of a surface immersed in seawater can be simplistically represented by a defined and well researched four stage sequence (Wahl, 1989; Prendergast, 2010), shown in Figure 3.7. Stages 1 to 3 represent microfouling of a surface, and the fourth stage, macrofouling. In this model, each stage occurs at different time periods after submersion of the structure. However, a widely accepted model of fouling is

in fact dynamic, where all fouling stages run continuously throughout immersion (Terlizzi and Faimali, 2010).

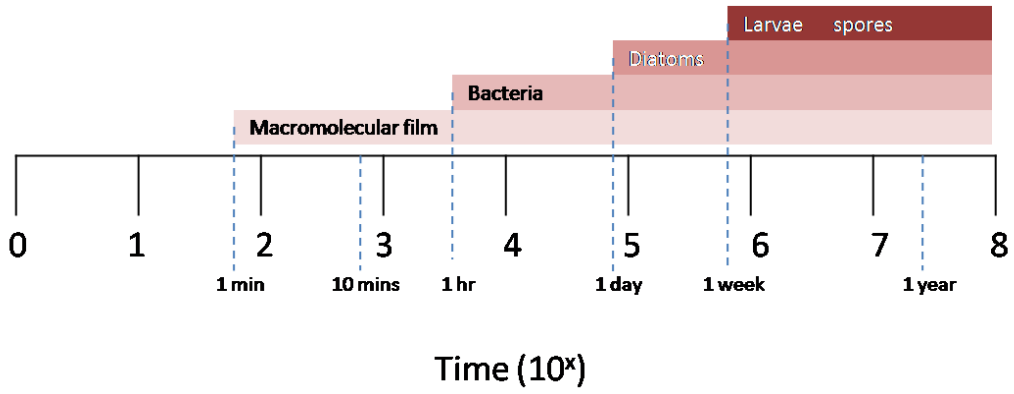

Figure 3.7. Timescales for settlement (reproduced from data in Wahl, 1989)

1. Macromolecules (the conditioning film)

Biofouling begins with a conditioning film of macromolecules (approximately 20-80 nm thick (Videla and Herrera, 2005)) absorbed on to a surface almost instantly after submersion (Callow and Callow, 2002). A dynamic equilibrium is reached within hours (Wahl, 1989). These molecules are generally organic, such as polysaccharides, glycoproteins and proteoglycans with some inorganic compounds. A number of processes govern this first stage, including Brownian motion, electrostatic interaction and van der Waals forces. The adsorption of different molecules will alter the properties of the surface, possibly increasing the nutrient concentration or, conversely, making the surface less inviting to certain organisms (Wahl, 1989).

2. Bacteria

Bacteria grow and colonise preferentially on surfaces modified by the conditioning film to form sessile populations within hours of immersion of a surface into seawater (Videla, 1995). Bacteria are widely dispersed in natural seawater, and can be transported over large distances by natural currents. In turbulent conditions (often formed around a submerged structure), bacteria can be dispersed through eddies, bringing them into close proximity of the viscous boundary layer of a surface. The bacterial cells require an aqueous phase, nutrients and electron acceptors (including oxygen, nitrate, nitrite, sulphate and metal ions such as Fe^{3+} and Mn^{4+}) to survive and grow on a substrate (Little and Lee, 2007). However, different bacteria require different conditions for survival. For example, some survive in anaerobic conditions, whereas others require an aerobic environment.

The small size of bacteria (on the scale of 1 μm) allows these microorganisms to penetrate into small spaces and crevices on a structure. Although the composition varies amongst types of bacteria, the cell wall is always rigid (Madigan et al., 2010). Bacteria also produce extracellular polymeric substances (EPS) that are secreted outside the cell wall, but often remain attached to the outer wall (Flemming and Wingender, 2010). This EPS means that the majority of bacteria are relatively hydrophilic. Adhesion of bacteria is considered in terms of the attractive and repulsive forces between the cell and the substrate as the organism approaches the surface and the free energies of the bacteria, the surface and the liquid medium. Zobell (1943) notes that the attachment of bacteria on to a surface appears not to be influenced by material colour, plane, or angle of immersion, although the types of bacteria species attaching to a surface can be influenced by roughness, wettability and polarisation (Little and Lee, 2007; Characklis and Cooksey, 1983; Wahl, 1989). All bacteria require metal ions for growth and development. The metal species present and their availability are likely to have either a positive or negative impact on the colonisation of a metal surface, with the former leading to microbially influenced corrosion (MIC) and deterioration of the metal through binding of cells with metal ions (Beech, 2004).

The process of adhesion of bacteria on to a surface consists of two steps (Figure 3.8) (Busscher and Weerkamp, 1987). The first step is reversible (adsorption) and is controlled by macroscopic surface properties (surface free energy, hydrophobicity). The second step is irreversible (adhesion) and is governed by microscopic molecular interactions between the bacteria and the surface (Wahl, 1989). When in the region of a surface, the bacteria may respond to nutrient and other gradients on the surface. This is known as chemotaxis and can alter the concentration of bacteria near a surface (Macnab and Koshland, 1972). The bacteria can either have a negative or positive chemotactic response to a gradient (Macnab and Koshland, 1972). When a bacterial cell has a diameter less than 1 μm they will exhibit Brownian motion and can randomly move closer to the surface, with flow also a contributing factor to the movement of the cells (Marshall, 1986; Wahl, 1989). Figure 3.9 is a schematic of bacterial adsorption showing the dominating forces as a function of distance from the surface.

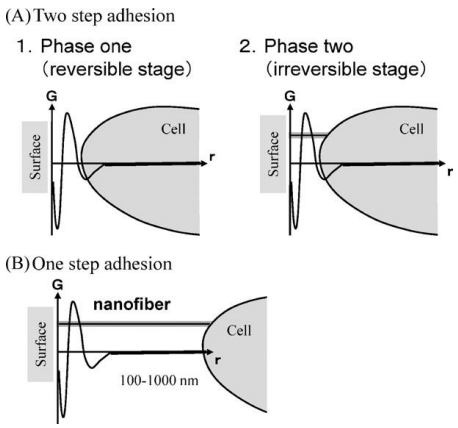

Figure 3.8. Schematics of the two-step process of bacterial adhesion (Hori and Matsumoto, 2010)

The initial attachment and the physical/chemical interactions involved are complex, and have only recently been studied in depth (Ojeda et al., 2008; Geoghegan et al., 2008; Zhang et al., 2010). Approaches to analyse this often rely on polysaccharide chains and proteinous fibres to explain the adhesion between cells and the surface material (Hori and Matsumoto, 2010). Two main theories have been developed to explain the adhesion of bacteria to a surface; the Derjaguin-Landau-Verwey-Overbeek (DLVO) theory (Hermansson, 1999) and the thermodynamic theory (Absolom et al., 1983). The former was originally developed to describe the interaction of a colloidal particle with a surface. However, it has been applied to bacterial adhesion since bacteria can form stable colloidal suspensions due to their small size (0.15-2 µm); a density only slightly greater than that of water; and the possession of a net negative charge (Marshall, 1986). The theory states that the total interaction between a surface and a particle is the summation of the van der Waals interactions and the electrostatic interactions. Far from a surface, the van der Waals forces dominate over any other process (e.g. Brownian motion) to move the cells closer to the surface. Near to the surface, the electrostatic force will dominate, although these are also dependent on the local environment conditions. In contrast, the thermodynamic theory is based on the surface free energies of the surface, the bacterial cell and the suspending liquid medium. Further detail on the DLVO theory and the thermodynamic theory can be obtained from a range of authors (Hermansson, 1999; Busscher and Weerkamp, 1987; Absolom et al., 1983; Neumann et al., 1974).

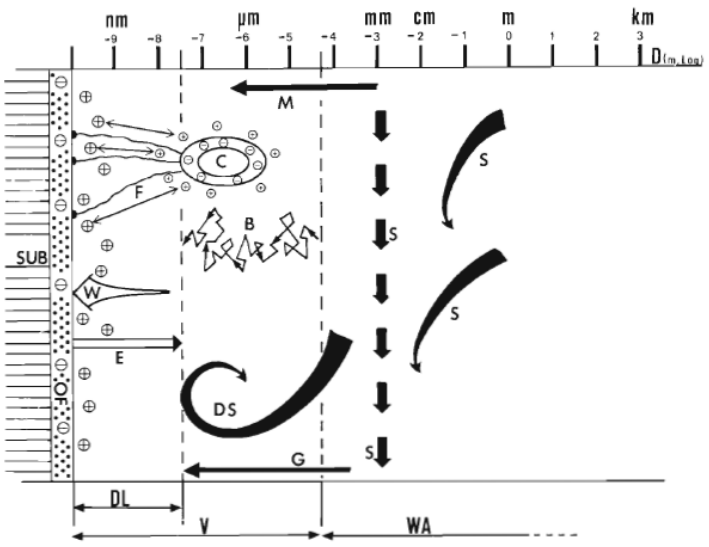

Figure 3.9. Schematic of bacterial adsorption showing the dominating forces as a function of distance from surface (Wahl, 1989)

B is Brownian motion; C is the bacterial cell; DL is the electrostatic double layer; DS is microturbulence (down sweep); E is electrostatic repulsion; F is the bacterial fibrils that attach to the adsorbed macromolecules; G is gravity (for horizontal surfaces); M is the bacterial motility; OF is the organic film of adsorbed macromolecules; S is currents and macroturbulence; SUB is the substratum; V is the viscous boundary layer; W is the Van der Waals forces and WA is the seawater.

An extended DLVO theory was developed by van Oss (1999), taking into consideration the surface tension and interactions between hydrophobic and hydrophilic surfaces that are major factors in thermodynamic theory. Each model developed to explain bacterial adhesion (Hermansson, 1999; Hori and Matsumoto, 2010; Absolom et al., 1983; van Oss et al., 1999) is able to explain certain parts of the process. However, the adhesion process may not proceed as expected or modelled. It is thought that the formation of a macromolecular conditioning film on a surface will alter the properties of the surface dependent on the type of macromolecules deposited and hence experimental results may not predict the real world adhesion process of bacterial cells.

3. Diatoms, Protozoans

After approximately one day of submersion, benthic diatoms and protozoa will settle on the surface (Wahl, 1989). Diatoms are a form of unicellular microalgae encased in a siliceous cell wall or frustules (Lind et al., 1997). Protozoans, such as ciliates and amoebae are unicellular, motile organisms which feed on unicellular algae and bacteria (Matz and Kjelleberg, 2005). Along with bacteria, diatoms and protozoa will form an EPS biofilm matrix on the substratum (Costerton, 1999). The EPS forms a complex matrix around the living cells producing a film layer, which enhances adhesion of cells to the surface (Fletcher

and Floodgate, 1973). These substances also protect the living cells against toxic substances and dehydration. A marine biofilm can be thought of as an organic polymer gel with a mix of species living in it, and water channels to provide nutrients through convective flow (Costerton et al., 1995; Scotto and Lai, 1998). A study carried out by Pedersen (1982) found that the biofilms developed in tests created a transparent layer only a few micrometers thick with numerous filamentous and solitary bacteria along with protozoa and organic debris trapped in and over the layer. Benthic diatoms were also observed here in flow-orientated bands. The main organisms found in marine biofilms include:

- Bacteria (the first colonisers)
- Unicellular algae (only in water depths where there is light present)
- Predator protozoa
- Larvae of benthic macro organisms (serpules, balanus, mussels and macro algae)

The type of biomass in a biofilm can change throughout the year, depending on season, temperature, water flow rate, and presence of light (Pippo et al., 2012; Chiu et al., 2005).

4. Larvae, spores

The fourth stage involves the settlement of macro organisms. This larger scale fouling can be further divided into soft macrofouling (algae and invertebrates including soft corals, sponges and hydroids) and hard macrofouling (invertebrates including barnacles, mussels and tubeworms). Macrofouling begins with the precursor spores of algae and larvae of organisms which are produced and released by adult species. These spores and larvae need to find a suitable surface as soon as possible and will generally attach in a wide range of salinity and temperatures (Callow and Callow, 2002). This occurs over a time frame of days to weeks from release (McQuaid and Miller, 2010), and the distance travelled from release to settlement can vary significantly due to tidal currents and turbulence. Larvae are transported to a surface via natural currents, as well as effects of gravity and swimming. When in the vicinity of a surface the organism will test its suitability for settlement (Rittschof et al., 1984). If the conditions found on the surface are conducive to settlement, then the larvae will permanently adhere (Prendergast, 2010). The larvae and algal spores use a wide variety of ‘glues’ to attach to a surface. The attachment of larvae and spores must be fast, especially in conditions of high current flow, otherwise the organisms may be

swept away from the surface. Ultimately, a position for settlement has to be chosen in terms of survivability.

Factors Affecting Biofouling

There are several factors which affect the overall extent of biofouling on a surface, including geographical location; season; salinity; depth; temperature; topology; surface orientation; water flow; age of larvae/spores; chemical cues; light; interaction between organisms; nutrient availability; predation; local abundance and surface conditioning (Jenkins and Martins, 2010; Rittschof et al., 1984; Kristensen et al., 2008) (Dubost et al., 1996). Experiments have shown that biofilm formation and its viscosity can be higher in regions of dynamic flow rather than in static or turbulent flow conditions (Faille et al., 1999), which may be caused by the structure itself or the surrounding topology. Several studies have been conducted to understand the effect of surface roughness of the substrate on bacterial settlement. These studies appear to be contradictory, with many reporting an increase in settlement (up to 25 times more bacteria in one case (McAllister et al., 1993)) whereas others report no difference in rate or volume of bacterial settlement (An et al., 1995).

Certain organisms have been shown to prefer settlement on new structures, (i.e. those with no previous fouling) and can settle with the range of stresses imposed on an organism by a novel benthic environment. Others, however, prefer surfaces previously colonised but have new unoccupied areas (Jenkins and Martins, 2010).

Past studies that have investigated depth and location in reference to biofouling found that the type of fouling changes with depth down a water column, and many fouling species have been found to naturally occur in distinct zones (Cowie, 2010). It has also been observed that, similar to terrestrial organisms, the diversity of marine biota declines with latitude from the tropics to the poles (Hillebrand, 2004; Tittensor et al., 2010; Canning-Clode and Wahl, 2010), with no significant difference between hemispheres but localised differences depending on location, habitat, the different types of organism, body mass and dispersal methods.

Positive correlations have been observed between settlement on a substrate and wind direction and wave turbulence, showing that spores and larvae are influenced by current direction and flow speeds and pattern (Prendergast, 2010). The settlement of the barnacle

genus, *Balanus* is strongly affected by current flow velocity, and has been reported to not attach at flow rates greater than 5-10 ms^{-1} (Larsson and Jonsson, 2006).

3.4 Effects of Biofouling on Corrosion

There are many reported effects of biofouling on offshore structures. The first of which is an increase in weight of total structure. However, in relation to large structures, such as oil platforms, this is seen as insignificant (Jusoh and Wolfram, 1996) compared to the total weight of the structure itself, due to the low specific gravity of marine growth. An increase in total mass will increase the total displaced volume of the structure and will decrease the natural frequency of the structure.

Biofouling will also alter the surface properties of the structure. An increase in surface roughness can have several effects, the most significant of which is the increase in vortex shedding and cavitation. Cavitation causes erosion at an accelerated rate, and if it occurs can make a surface more prone to corrosion including crevice and stress corrosion. A surface which is rough will increase the drag on a surface as well as the associated inertia coefficient, C_M:

$$C_M = \frac{1 + M_a}{\rho V} \text{ (Rahman and Chakravartty, 1981)} \qquad [3.13]$$

Where M_a is the added mass (kg), ρ is the fluid density (Kgm^{-3}), and V is the volumetric displacement of the body (m^{-3}).

The hydrodynamic load on a structure will be increased by settlement of biofouling. The hydrodynamic load is a key consideration when designing a structure, and increases in the load may incur difficulties in decommissioning.

Both microfouling and macrofouling can have an effect on the corrosion in terms of onset, rate and type and they will interact in many ways, for example macrofouling providing environments at the metal surface for different bacteria to thrive. However, for convenience the different types of fouling and their effect on corrosion are presented separately here.

3.4.1 Microbially Influenced Corrosion (MIC)

The metabolic activity of microorganisms in a biofilm on a surface will have an impact on the electrochemical reactions of the corrosion process (Videla, 1994), and can reduce the lifetime of materials used in the marine environment (Wang et al., 2004). It has been estimated that approximately 20% of the cost of corrosion to marine steel infrastructure is caused by microbial corrosion and degradation (Heitz et al., 1996). Enzyme excretion and extracellular polymeric substances (EPS) have also been associated with potential ennoblement of metals and corrosion (Scotto and Lai, 1998; Mansfeld and Little, 1992b), with the formation of corrosion cells. When a biofilm forms on a metal surface, oxygen reduction (cathodic) reactions (Equation 3.4) are often affected via microbial respiration or organometallic catalysis (Little et al., 1991b) and the corrosion potential can be ennobled, i.e. a noble shift occurs due to the acceleration of the cathodic reduction reactions or the reverse depending on the bacterial metabolism concerned.

Microbiological organisms trapped in the biofilm on the surface of a structure can exclude oxygen from small localised regions creating local differential aeration, resulting in attack of the surface metal. This is of high concern with metals that have a pitting potential only slightly more noble (more anodic) than the corrosion potential. Experiments have shown that the oxygen reduction current can increases significantly over a period of days of exposure to seawater. This increase is related to biofilm development (Busalmen et al., 1998). It has also been demonstrated that ennoblement of the corrosion potential does not occur when the metal/biofilm interface was anaerobic (Little et al., 1991a).

The mechanisms for ennoblement of metals in the marine environment can be grouped into 3 categories; thermodynamic; kinetic and alteration of the nature of the reduction reaction (Little and Mansfield 1994). It is thermodynamically theorised that a pH decrease (causing the pitting potential to become more negative) at the metal/biofilm interface or a localised increased in partial pressure of oxygen raises the potential at the cathode. A pH decrease can be caused by the secretion of organic acids by heterotrophic bacteria trapped in the biofilm matrix. Certain acids that are secreted by these bacteria can accelerate corrosion by preventing the formation of a protective oxide film on the metal surface. Mechanisms related to the enzymes present and catalytic properties of biopolymer metal complexes formed at the interface have also been proposed as potential corrosion accelerators (Little et al., 2008). The polymeric substance that form the biofilm matrix can themselves effect the interfacial processes, including the trapping of water and metal

species at the interface, trapping corrosion products and decreasing the diffusion to and from the metal surface (Kirkpatrick et al., 1980).

As with other forms of marine corrosion, MIC has associated environmental and economic effects including high financial losses associated with device shutdown as well as potential pollution problems and safety hazards (Hamilton, 1985).

3.4.2 Sulphate Reducing Bacteria

An important effect of biofouling on corrosion of a surface is that of sulphate reduction and the production of H_2S by sulphate reducing bacteria (SRB). Because of their importance in the oil industry the effects of these bacteria have been extensively researched (Gouda et al., 1993; Hamilton, 1985; Neville and Hodgkiess, 2000; Barton, 1995), with models produced for predicting corrosion influenced by sulphate reducing bacteria (Melchers and Wells, 2006). SRB are anaerobic and are responsible for most cases of accelerated corrosion on ships and offshore structures in locations where anaerobic conditions are formed.

The anaerobic conditions required for the metabolism of SRB, often occur in localised anaerobic niches in a biofilm on a metal surface that usually forms as a highly non-homogeneous layer (Melchers and Jeffrey, 2008). The metabolites formed by SRB in these locations are in close proximity to the metal surface and it is possible for localised (pitting) corrosion to occur. SRB can cause serious problems for marine industries, the microorganisms use sulphate as an electron acceptor, resulting in the production of sulphide, a reactive, corrosive and toxic product (Muyzer and Stams, 2008). Although, SRB are anaerobic microorganisms, they can survive, but not be active, during periods of exposure to oxygen (Sigalevich and Cohen, 2000). Any sulphate reducing bacteria left undisturbed in the locality of a surface will change the local environmental parameters (Wan et al., 2010) and will produce high concentrations of hydrogen sulphide, aggressive to a number of metals and alloys, including steel and copper based alloys. The hydrogen sulphide will acidify the seawater, and can induce stress corrosion cracking of a structure through hydrogen cracking of the metal. This is a selective form of corrosion and is localised to highly stressed regions of a structure.

3.4.3 Iron Reducing Bacteria

The involvement of iron reducing bacteria (IRB) in the corrosion of steel structures is conflicting in literature. One set of publications discuss the corrosive nature of the organisms, whereas another focusses on the corrosion inhibition properties of the IRB (Herrera and Videla, 2009; Dubiel et al., 2002; Lee and Newman, 2003).

Iron reducing bacteria utilise the reduction of Fe^{3+} for metabolism. This ion acts as the final electron acceptor in a process of anaerobic respiration, allowing growth of the bacteria and corrosion of steel structures (Herrera and Videla, 2009).

Iron oxidising bacteria also exist, which generate energy by the oxidation of ferrous ions to ferric ions. Iron oxidising bacteria are thought to rapidly produce a rusty slime that can then cause crevice corrosion on metals that are susceptible to such corrosion (Starosvetsky et al., 2001). Iron oxidising bacteria can aggravate problems associated with sulphate reducing bacteria by creating an environment that encourages the growth of sulphate reducing bacteria species (Xu et al., 2006; Xu et al., 2008).

3.4.4 Macrofouling

Sneddon (1989) found that corrosion rates reduce with time due to the formation of a partially protective fouling/corrosion composite film. However, deposits of macrofouling that have developed on a surface over a period of time can create localised areas of corrosion by forming crevices on the surface. These become depleted of oxygen, or have varying pH levels, reducing the potentials under the fouling organisms leading to pitting or crevice corrosion. The degradation can go unnoticed for long periods of time due to the macrofouling cover.

De Messano (2009) found that most localised attacks of corrosion on stainless steel samples were associated with barnacle settlement, where Scanning Electron Microscopy (SEM) imaging was used to observe ring marks caused by the barnacles' carapace. This research studied the effect of biofouling on the corrosion of stainless steels over a period of 285 days, allowing sufficient growth of macrofouling species on the surface of the coupons. Open circuit potentials were measured in the absence and presence of biofouling species. Over the first 15 days of the tests diatoms were the most dominant, with barnacles, filamentous macroalgae and encrusting bryozoans from the 22nd day onwards. After 2-3 months the open circuit values in the presence of fouling decreased, signifying the onset of localised corrosion. A negative correlation between the measured potential and the cover

provided by settlement of macrofouling species shows an increase in the number of anodic sites on a surface.

3.5 Marine Corrosion and Biofouling Monitoring and Prevention

There are several techniques that can be used to monitor corrosion and biofouling on structures. These are discussed in this section. The protection of a surface against corrosion and biofouling in a marine environment must not be considered separately, the systems for protection against both must be able to complement each other. It would be ineffective if an anti-fouling coating negatively affected the use of the chosen corrosion protection methods used or vice-versa. As such, it is important that coatings for anti-fouling protection are anticorrosive as well as antifouling and resistant to abrasion, erosion and biodegradation. With surface paint systems, it is often the case that the surface will be coated with an anticorrosive primer and an antifouling topcoat (Almeida et al., 2007).

3.5.1 Laboratory and In Situ Methods to Assess Corrosion

There are several methods that can be used in a laboratory to assess corrosion. Those that are most appropriate to this study and that will be used in corrosion testing (Chapter 5 to 8) are discussed here.

Gravimetric Assessment of Corrosion

Measurements of metal weight can be taken before and after laboratory or field based experimentation to determine how much of the metal has been lost (Ailor, 1971). Weight loss experimental testing takes longer to obtain results than using electrochemical techniques. However, the process is simple and low cost.

The conversion of weight loss measurements into a corrosion rate assumes that general, uniform corrosion has occurred across the exposed surface and does not take into consideration any localised corrosion. The method can be inaccurate when measuring small differences in weight of specimens (Ailor, 1971), so either a longer exposure time or careful procedures must be used to reduce the error.

The corrosion rate (CR) is calculated from the following relationship:

$$CR = \frac{k\Delta W}{\rho A t} \quad [3.14]$$

Where k is a constant that depends on the required units for rate (for a corrosion rate in mmyr^{-1}, k is equal to 87.6). ΔW is the weight loss (mg) for the given time period, t (hours), ρ is the density of the metal or alloy (gcm^{-3}) and A the exposed surface area (cm^2).

Surface Characterisation

The corrosion degradation of a metal can be assessed by observing the surface morphology of the metal or alloy using visual, optical microscopy (for macroscopic surface structure analysis) and SEM (Scanning Electron Microscopy, for microscopic imaging of the surface structure) techniques. These techniques allow surface observation of the type and extent of corrosion across the surface. Although these techniques offer good insight into the nature of the corrosion, the kinetics of the reaction cannot be determined. Surface characterisation can be useful after weight loss experiments to obtain a better representation of the corrosion that has occurred.

Electrochemical Measurements of Corrosion

Wagner and Traud (1938) were the first to suggest the theory of a mixed potential, and were the pioneers of our understanding of the corrosion process today. This 'mixed potential' theory allows the calculation of corrosion rates from relatively simple electrochemical techniques. Electrochemical corrosion testing can be used to characterise the corrosion properties of a metal or alloy when immersed in different electrolyte conditions. These properties will be unique to the metal/electrolyte system that is under consideration and hence will allow determination of specific characteristics relative to other systems. The experiments control and measure the potential and current of the oxidation and reduction reactions to determine corrosion rates.

There are several electrochemical techniques available for the assessment of corrosion. These include measurements of corrosion potentials; redox potentials; polarisation resistance; electrochemical impedance; electrochemical noise; polarisation curves and electrochemical hydrogen permeation techniques (Mansfeld and Little, 1992a). Although electrochemical techniques can be used to give fast results in both field monitoring and laboratory investigations, the results can be difficult to interpret.

Electrochemical polarisation is a popular technique which can be used to determine the corrosion current (I_{corr}) , the corrosion potential (E_{corr}) and the current-potential relationship (I-E) given by Equation 3.15 (Yang, 2008):

$$E - E_{corr} = \eta = \pm\beta \log \frac{I}{I_{corr}} \quad [3.15]$$

Where E is the potential, η the overpotential, β is the Tafel constant and I the rate of oxidation or reduction (current). These techniques use the excitation of an electrode to measure its response to the controlled change. As the electrode is moved away from the steady corrosion potential it is said to be polarised. If the potential of the electrode is varied at a constant rate over time (using a potentiostat) the response of the current can be monitored. This is known as potentiodynamic polarisation (Ailor, 1971).

In potentiodynamic experiments, the current represents the rate at which the anodic or cathodic reactions are taking place on the working electrode (the metal under test) (Enos and Scribner, 1997). The current is usually expressed as current per unit area of the working electrode (current density).

The corrosion potential of a metal cannot be measured individually; a potential can only be measured between two points. A polarisation cell consists of a reference electrode (Commonly used electrodes include the saturated calomel electrode (SCE) and the silver/silver chloride (Ag/AgCl) electrode (Yang, 2008)); a counter electrode (usually made from inert materials, often platinum or graphite) and a working electrode (metal undergoing assessment), all immersed in an electrolyte (Figure 3.10). This configuration is used to ensure that only one overpotential is obtained for the working electrode. The counter electrode is polarised in the opposite direction to the working electrode. The three electrodes are connected to a potentiostat. When immersed in the electrolyte, an electrochemical potential (voltage) is established between the electrodes. By changing and controlling the potential of the metal sample using the potentiostat, a value for the corrosion potential (E_{corr}) can be obtained as an energy difference between the working electrode and the reference SCE electrode. Measuring the potential alone will only provide an indication of the tendency of the metal or alloy to corrode. Determination of the current or current density is also required to assess the rate of corrosion.

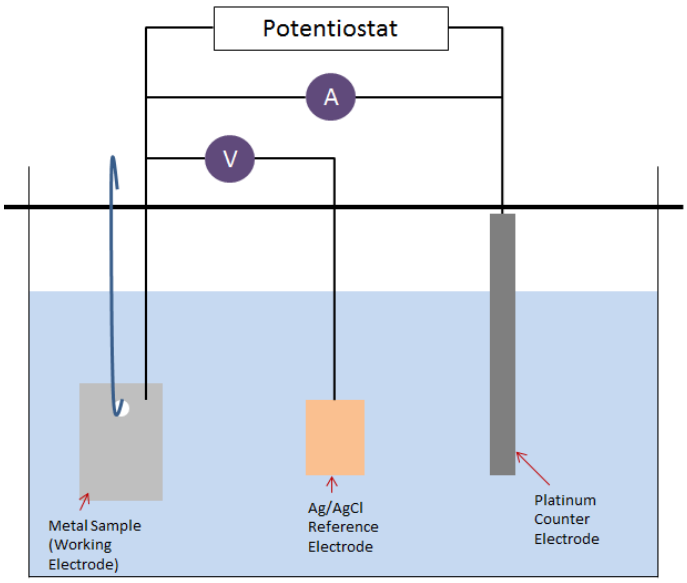

Figure 3.10. Schematic of working electrode, reference electrode and counter electrode and connection to potentiostat

Other methods that can be used instead of potentiodynamic polarisation are potentiostatic polarisation (controlling the potential and measuring the current response but at one fixed potential); galvanodynamic polarisation (varying the current over time, monitoring the potential response); galvanostatic polarisation (similar to potentiostatic polarisation but current is controlled and the potential measured). Potentiodynamic methods are more commonly used than galvanodynamic polarisation methods.

- Tafel Extrapolation

Tafel extrapolation from potentiodynamic polarisation is one of the most popular DC techniques for estimation of corrosion rate (Amin and Ibrahim, 2011) to determine the corrosion rate.

The Tafel Equation defines the relationship between current and potential for an electrochemical reaction under kinetic control and relies on the linear relationship found between potential (*E)* and the log of the current (*logI*) when the electrode is polarised to a sufficiently large potential in both the anodic and cathodic directions (Ailor, 1971; McCafferty, 2005):

$$I = I_0 e^{(2.3(E-E_{corr})/\beta)} \quad [3.16]$$

The Butler-Volmer Equation (3.17), relates the current and the corrosion current and divides the Tafel Equation into respective parts for both the anodic and cathodic reactions (Trethewey and Chamberlain, 1995):

$$I = I_{corr}\left[exp\left\{\frac{2.303(E-E_{corr})}{\beta_a}\right\} - exp\left\{-\frac{2.303(E-E_{corr})}{\beta_c}\right\}\right] \quad [3.17]$$

The difference between the potential and the corrosion potential is known as the overpotential (η).

In the anodic direction: $$\eta_a = \beta_a log\frac{I}{I_{corr}} \quad [3.18]$$

In the cathodic direction: $$\eta_c = -\beta_c log\frac{I}{I_{corr}} \quad [3.19]$$

β_a and β_c are the Tafel constants in the anodic and cathodic direction respectively. These can be obtained from experimental data. The Tafel constants have the units Vdecade^{-1} where a decade of current is one order of magnitude over the Tafel region of the plot, and hence are calculated from the slope of the Tafel region.

Tafel extrapolation uses an overpotential of approximately +500mV from the corrosion potential applied to both the anodic and cathodic directions to obtain Tafel slopes and determine I_{corr}. The corrosion current is determined by extrapolating the Tafel regions on a Tafel plot (Figure 3.11) to the corrosion potential (McIntyre and Mercer, 2010).

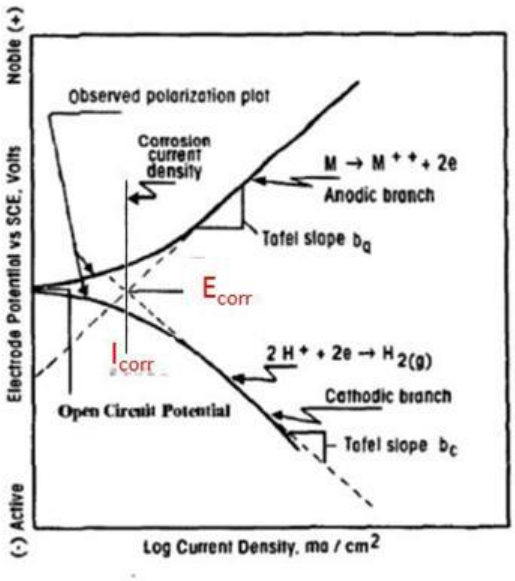

Figure 3.11. Hypothetical cathodic and anodic Tafel polarisation diagram (Obtained from ASTM, 2013 G3)

This method is limited to instantaneous measurements of corrosion and as such represents only a guideline corrosion rate for metals tested. The corrosion rate observed *in situ* will be lower than that obtained in these experiments as the metal will develop corrosion resistance with the development of a corrosion product film. However, controlled

experiments such as these allow comparisons to be made between environmental factors as well as comparisons between different metals. Tafel extrapolation also allows analysis of extremely low corrosion rates and for the experiments to be conducted in relatively short periods of time (especially when compared to weight loss testing).

- Determination of Corrosion Rate from Corrosion Current

The measured corrosion current (I_{corr}) can be converted into a corrosion rate. For this calculation, it is assumed that the current distribution (current density, i_{corr}) is uniform across the entire exposed sample surface:

$$i_{corr} = \frac{I_{corr}}{A} \ (\mu A/cm^2) \qquad [3.20]$$

The corrosion rate can be found using Faraday's law which relates the corrosion current to mass loss ($g/m^2/d$) or corrosion rate (mm/yr) as follows (ASTM, 2010):

$$Mass\ Loss = k_1 i_{corr} EW \qquad [3.21]$$

$$Corrosion\ Rate = \frac{I_{corr} k_2 EW}{\rho A} \qquad [3.22]$$

K_1 = 8.954×10^{-3} $gcm^2/\mu Am^2d$

K_2 = 3272 mm/Acmyr

EW is the equivalent weight, calculated as the mass in grams that will be oxidised by the passage of one Faraday (96489 C) of electric charge (Trethewey and Chamberlain, 1995). For pure metals, this can be calculated from the atomic weight (W) and the number of electrons required to oxidise an atom of the element in the corrosion process (valence, n):

$$EW_{metal} = \frac{W}{n} \qquad [3.23]$$

The equivalent weight of an alloy is calculated taking into consideration the valence of each constituent, the atomic weight of each constituent and the mass fraction (f) of each:

$$EW_{alloy} = \frac{1}{\sum \frac{n_i f_i}{w_i}} \qquad [3.24]$$

3.5.2 In Situ Corrosion Measurement and Monitoring

In situ monitoring can determine the development of corrosion on a system, and can be a cost effective approach if used correctly over the lifetime of the device/structure. Monitoring allows corrosion to be detected and mitigation actions to be put in place prior to severe deterioration as well as providing a basis for predictive maintenance (Rothwell, 1978). The monitoring of corrosion in the field can be segregated into *in-line*, *on-line* and *off-line* techniques (Capcis Limited for the Health and Safety Executive, 2001).

In-line Techniques

In-line techniques involve the use of systems directly attached to the structure, which can then be removed for inspection and analysis.

- Coupon Testing

Using coupons strategically placed in critical locations to monitor corrosion is a relatively simple and low cost method (Chandler, 1985). The coupons can be removed during maintenance or inspection and analysed for weight loss etc. over time.

The method will only provide average corrosion rates. However, coupons can demonstrate any localised effects allowing identification of critical areas of a structure requiring further corrosion protection. Best practice would be to deploy coupons for several years, preferably the lifetime of a structure. The corrosion observed on coupons should not be too readily extrapolated to different areas as this may result in false, inaccurate readings, especially if localised (crevice or pitting) corrosion has occurred.

On-line Techniques

On-line monitoring techniques involve the deployment of specific devices developed to monitor corrosion on the device or structure. Three such techniques are:

- Electrochemical Monitoring

Conventional electrochemical techniques involve either the measurement of potential or galvanic current, newer techniques include Electrical Resistance and Linear Polarisation (Britton, 2010; Chandler, 1985). These techniques use probes to monitor instantaneous changes in electrochemical characteristics and hence determine corrosion rates.

- Fixed Ultra-sonic Probes

Ultra-sonic transducer probes can be permanently installed to monitor corrosion rates, and provide wall thickness measurements on-demand. This technique is one of the most

important for long term corrosion monitoring (Britton, 2010), and can also be used as an off-line technique using portable probes. However, ultra-sonic probes only enable the monitoring of a small surface area, not the whole structure, meaning that localised corrosion may go unnoticed (Rothwell, 1978).

- Acoustic Emission

When defects, such as stress corrosion cracks, form and grow in a structure, acoustic sound waves, emitted during pressure or temperature changes as a consequence of fast energy relaxation at these localised source, can be measured (Kovac et al., 2010) with sensors placed on the structure (Yang, 2008). This method not only detects defects formed through corrosion but also those formed through impact, deformation and load stress.

Off-line Techniques

Off-line monitoring techniques are non-destructive and mainly consist of inspection techniques.

- Visual Inspection

Visual inspection is the simplest, though potentially one of the most valuable, methods for monitoring and evaluating corrosion (Britton, 2010). However, for many marine-based devices this is only a relatively low cost method when carried out during periods of planned maintenance when the device is on the quayside. Visual inspection during normal operation would require expensive diving or ROV (Remotely Operated Vehicle) operations, often requiring camera footage to be interpreted, and both methods are hampered if significant biofouling has settled disguising areas that may be corroded.

Visual inspection and data gathering of deterioration should be conducted at any opportunity. The data from opportunistic inspections can be included in overall monitoring to back up planned corrosion inspections.

- Radiography

This non-destructive technique uses electromagnetic radiation to test for thickness, and is a widely used technique to determine the wall thickness of pipes used for liquid and gas transportation in the petroleum and chemical industries (Edalati et al., 2006).

- Eddy Current Inspection

Pulsed Eddy current inspection of corrosion is a non-destructive technique that uses the principal of electromagnetism. The technique involves the use of a probe coil carrying AC

current which generates a magnetic field. When the probe is brought into close contact with the metal surface to be tested, the magnetic field induces circulating eddy currents on the metal. The strength of the eddy current is affected by changes in thickness and pinholes, and as such corrosion damage can be detected. This system has been used successfully for a number of years (Yang, 2008), especially since it can be interpreted quickly, and can penetrate through any protective coatings or insulating material.

3.5.3 Monitoring of Biofouling

In general, past practice for the monitoring of biofouling on structures in the marine environment has been to measure thickness, distribution and type of marine growth on a structure by divers collecting samples or measuring *in situ* or by using ROVs. Thickness measurements are often averaged using several points to measure. Forteath (1984) monitored the growth of fouling organisms on offshore oil platforms in the North Sea, taking diameters of structural members before and after cleaning to obtain a thickness of deposition. This method is not particularly accurate but provides a good insight into the amount of fouling on a structure. Other studies have been conducted by interpretation of photographs or films (Forteath et al., 1982), although this method is less precise. The determination of species using photographs and films when *in situ* depends significantly on the water clarity and quality of the photography. It is ideal to note the type, density, thickness, pattern of deposition and extent as well as noting any overlap and the order of the fouling layers.

It is often found that fouling abundance differs significantly between surfaces of different orientation (with horizontal surface fouling more significantly than vertical) (Forteath et al., 1984). Many *in situ* studies are purely qualitative and do not provide measurements of growth and development of the fouling organisms present. However, these studies are of equal importance as they provide identification of species present and can aid in determining the possible fouling species which may be expected on new substrates.

3.5.4 Marine Antifouling Systems

Traditional methods of antifouling protection use coatings which released toxins/biocides to kill organisms (Finnie and Williams, 2010). However, highly toxic materials, such as tri-butyl tin, are now subject to international bans and new coatings are being developed using less harmful techniques.

- Copper

Copper sheathing has been used on marine structures for thousands of years, though the first record of it being used as an antifoulant was in 1625 in the British patent of William Beale (Yebra et al., 2004). The paint used was composed of iron powder, copper and cement. Copper deters fouling organisms by the dissolution of copper ions in seawater.

Copper based biocidal paints can be defined as contact leaching (of which there are several examples), and are active against most fouling organisms. However, they are most active against sessile invertebrates (e.g. barnacles), and a higher leaching rate is required for other fouling organisms (macroalgae and bacterial biofilms) (Finnie and Williams, 2010). The majority of copper based anti-fouling paints use cuprous oxide (Cu_2O) mixed with an inert polymer, and they often use a co-biocide to aid in the control of macroalgae and bacterial biofilms (Finnie and Williams, 2010). Copper based paints are less common due to the increase in price of copper in recent years and the concerns over the environmental effects of such paints (Ten Hallers-Tjabbes and Walmsley, 2010; Howell and Behrends, 2010).

- TBT Self-polishing Copolymer Paints

TBT-based (tri-butyltin) self-polishing paints were developed for anti-fouling purposes in the 1970s (Howell and Behrends, 2010; Almeida et al., 2007). The coating contained a copolymer with tributyltin carboxylate groups. These groups are able to undergo hydrolysis and ion-exchange when in contact with seawater (Finnie and Williams, 2010). By allowing the surface to hydrolyse and dissolve into the seawater, a renewed surface is left behind (Ralston and Swain, 2009). The leaching rate is constant for the lifetime of the paint unlike that of copper based paints, allowing a lifetime of approximately five years.

The reactions involving the TBT-copolymer were found to be environmentally unsafe, liberating TBT species into the seawater. Although TBT is an effective biocide, it is also persistent and bio-accumulative as well as toxic to a range of organisms causing imposex, deformation and infertility (Finnie and Williams, 2010; Evans et al., 2000). The use of TBT based coatings is now banned as consequence of a convention imposed by the International Maritime Organisation (IMO) (Cheyne, 2010; Chambers et al., 2006). In the 2010 Quality Status Report by OSPAR, it was reported that the adverse effects of TBT are still seen in four of the five OSPAR Regions (Arctic Waters; Greater North Sea; Celtic Seas; Bay of Biscay and Iberian Coast; Wider Atlantic), but are decreasing in response to the global ban (OSPAR Commission, 2010).

- Tin-free Self-polishing Copolymer Paints

These self-polishing paints contain a biocide bound in an acrylic matrix. There are two main types of tin-free self-polishing copolymer paints; metal acrylate copolymers (copper or zinc) and silyl acrylate copolymers (Almeida et al., 2007). These have been extensively used after the ban on TBT-based self-polishing paints (Omae, 2003). The coatings work in the same way as the TBT-based coatings, releasing the bound active ingredient from the leached layer and renewing the coating surface slowly over time (Finnie and Williams, 2010).

- TBT-free Controlled Depletion Polymers (CDPs)

TBT-free CDPs were first produced globally in the 1980s as the first generation of tin-free antifouling paint coatings. Controlled depletion polymers consist of a high concentration of rosin, a natural product harvested from pine trees, alongside an insoluble, inert polymer (used to provide the paint film with sufficient mechanical strength). The paint coating slowly dissolves into the seawater, allowing biocide release to be controlled over time, with a lifetime of up to 36 months dependent on the leaching behaviour (International Paints, 2010). A problem with these coatings is the biocide release is not constant, with only minor activity during idle times when settlement might be greatest (Chambers et al., 2006). Also, a large proportion of rosin will make the coating susceptible to wear and abrasion. They are expensive due to requiring the application of a sealer coat during recoating, and the need for copper and a co-biocide content (Yebra et al., 2004). The coatings also degrade over time when left out of water (International Paints, 2010).

- Foul Release Coatings (FRCs)

FRCs are a relatively recent development. These do not prevent settlement of fouling organisms; instead they provide a low surface energy and low friction surface coating to prevent their permanent adhesion. The coating exhibits extreme smoothness at the molecular level, reducing friction significantly. Due to the low surface energy of the coating, organisms are not able to develop a strong interfacial bond with the surface (Chambers et al., 2006). These coatings work at a critical velocity, above which organisms will be dislodged as the hydrodynamic shear forces become too great for adhesion (Candries et al., 2000). The critical velocity will depend on the fouling organism. If the water velocity is large enough, then these coatings can be used on static structures. In areas of low water velocity, the coatings are only suitable for moving vessels/parts. The

coatings are also usable where mechanical cleaning will be used. This simple operation is sufficient to remove the attached organisms from a coated surface.

There are two main types of foul release coating. These are based on fluoropolymers, such as Teflon® (low surface free energy), and those based on silicone based polymers (high surface free energy) (Finnie and Williams, 2010). The former has an application thickness of 75 µm whereas the latter has a thickness of approximately 150 µm. Fluoropolymer coatings tend to be harder and utilise shearing effects to dislodge fouling organisms as opposed to a lower energy peeling fracture mechanism used by the thicker silicon based polymers (Larsson et al., 2010).

Although effective at the removal of larger fouling organisms, FRCs are not as effective at removal of small fouling, such as diatoms and biofilms (Anderson et al., 2003; Chambers et al., 2006). Much greater speeds are required to ensure that these organisms are removed from a surface (flow speeds greater than 5 ms^{-1}). Larsson et al (2010) conducted tests using silicon-based foul release coatings measuring the release of barnacles at different stages of life on ships hulls. These experiments found the removal of permanently attached cyprids was efficient. However, the removal of new metamorphosed barnacles was low. The experiments also found a positive relationship between the size of barnacles dislodged and the frequency of fouling release from test plates.

Foul release coatings have a lifetime of 2 - 5 years (Chambers et al., 2006). Therefore, a surface will require multiple repainting within its operational lifetime. As FRCs are based on purely physical effects to prevent the adhesion of fouling organisms they are an alternative to methods based on biocides, with no associated legislation. This method poses interesting possibilities for the future, and it has been noted that they have the potential to be beneficial to operations by increasing the efficiency of surface by reducing drag (Candries et al, 2000).

It must be noted that these forms of coating do not provide any form of protection whilst an object is stationary, for example during periods of maintenance. If left for too long, this fouling may become too significant to be removed when once again in action. Schultz (2003) and Candries and Atlar (2000) have found that low surface energy FRCs performed worse and suffered greater increases in the frictional resistance coefficient with respect to static exposure time in the marine environment than did self-polishing copolymer paints.

Some issues exist with FRCs with regards to the toxicity of silicone oils in the dockyard, as well as the use of dibutyltin laureate as a curing agent for silicon based paints (Chambers et al., 2006; Watermann et al., 2005). The coating will have a soft, rubbery finish, and is resistant to direct impact. However, mechanical impact, such as scratching and scraping, likely to occur in a tidal flow regime, may affect the integrity of the coating, and as such, an anticorrosive primer should always be used with these.

- Electrochemical Control

In the past two decades research has been conducted into the use of the electrochemical effect to prevent and remove biofouling from a surface. Electrochemical control is based on the direct transfer of an electron between a bacterial cell and an electrode. The electrode can be made from a variety of materials including carbon-chloroprene (Nakasono et al., 1993), carbon-urethane and a mix of graphite and carbon black (Matsunaga et al., 1998). The former two materials have been used for sheet coatings and are not suitable for complex surfaces. The latter, however, has been added to urethane resin paint by Matsunaga et al (1998) to produce a coating which can be applied to a variety of surfaces exposed to the marine environment. The application of an alternating potential to the electrode is effective for removal of bacteria. In experiments conducted by Nakasono (1993) and Matsunaga (1998) a potential of 1.2 V vs SCE was sufficient to kill 67% of cells which had adsorbed on to the surface prior to application of the potential.

- Electrochlorination

Electrochlorination uses electrodes to produce sodium hypochlorite from the sodium chloride in seawater via hydrolysis (Omae, 2003). Sodium hypochlorite is an effective anti-fouling chemical (Goodman, 1987). When a direct current is passed through a titanium electrode sodium chloride will disassociate to form chlorine via oxidation of chloride ions at the anode (Broekman et al., 2010). At the cathode, seawater is reduced to form caustic soda and hydrogen. The chlorine produced reacts with the caustic soda to form sodium hypochlorite.

Electrochlorination is effective against the majority of fouling organisms and is environmentally sound since it only uses seawater. The dosing can be monitored and kept at the minimum level required to deter settlement of fouling. Systems can either work in a continual manner or as shock dosing depending on the situation. Continuous dosing maintains a low level of chlorine. Macrofouling species can become resistant to this level and a higher level of chlorine may be necessary over time to ensure no settlement. Shock

dosing uses high levels of chlorine but for short periods of time. Chlorination of seawater may leave some residual chlorine present which may influence the corrosion behaviour of materials present (Malik et al., 1999; Wallén and Henrikson, 1989; Goodman, 1987).

Although this method is environmentally safe (the chlorine will revert back to salt), it is used for enclosed spaces such as sea chests, pipe work for cooling systems and therefore would not be suitable for the exterior of a tidal device.

- Ultrasonics

Ultrasonics use a short high electrical power pulse to prevent biofouling (Broekman et al., 2010). It is potentially useful for enclosed areas including pipe work and heat exchangers. Bott (2001) investigated the effects of ultrasound on the accumulation of biofilms inside vertical glass tubes, using an ultrasound processor to create mechanical vibrations and pressure waves within the test vessels. This process forms small, highly agitated bubbles that, when impinging on surfaces, create a scouring action removing any settled biofilm. This work, based on the results of Mott (1998) found that only small, short bursts of ultrasound were required to clean a surface.

- Surface Flocking

Surface flocking involves the adherence of electrostatically charged fibres on to an originally smooth coating perpendicular to the surface. The fibres can be made from polyester, polyamide, nylon or polyacryl to create a complex surface structure unattractive for settlement of certain fouling species. Fibres are applied densely to the surface (200-500 fibres/mm^{-2}) (Watermann et al., 2005). Changing the surface texture and topology to dissuade fouling organisms has been the subject of research for several decades (Pomerat and Weiss, 1946; Chabot and Bourget, 1988; Barnes and Powell, 1950), although an all-encompassing technique which is unattractive to all types of fouling species has not, to date, been developed.

Phillippi (2001) found during tests that flocking of a surface limited the attachment of green and brown algae, but had no effect on red algae. During this research it was also found that surface flocking was a reasonably effective treatment against the settlement of some encrusting species including barnacles, agreeing with results obtained by Watermann (2005). However, the foul-release properties of this coating are doubtful and the rough surface may contribute to further drag across a surface (Yebra et al., 2004).

- Biomimetics and Bioinspiration

Biomimetics is the design of coatings and anti-fouling methods which are inspired by natural biological functions (Ralston and Swain, 2009). Recent reviews of natural antifouling techniques are provided by Ralston and Swain (2009) and Maréchal and Hellio (2009).

Biomimetics is the use of several diverse mechanisms which have been observed in the marine organisms. Many marine organisms (both sessile and non-sessile) protect themselves from being fouled by other organisms. The methods are both physical and chemical and include the production of deterrent secondary metabolites. Several organisms have been investigated, from bacteria to algae, tunicates and sponges, and natural products from these have been incorporated into commercial paint systems (Armstrong et al., 2000). A natural product which has been used in commercial coatings is tannin, developing a cupric tannate pigment which has a narcotic effect on fouling organisms.

Physical methods, such as spicules (spines) and ridges covering surfaces, both on a macro and micro scale can be used to form an undesirable surface for settlement. Research into the rejection of surfaces by bacteria and larvae has found that surface topography and microtexture are of significant importance (Knoell et al., 1999). Berntsson et al., (2000) found that the barnacle *Balanus improvisus* is more likely to settle on smooth surfaces rather than those with a microtexture. This has led to the development of silicone and polydimethylsiloxane (PDMS) elastomers with tailored surface architecture to deter fouling (Fang et al., 2010).

The main disadvantage and the reason these coatings may never become commercial is their short lifetimes. Most of these coatings last only days or months (de Nys and Steinberg, 2002). The efficiency is limited to specific species, and cannot be used as a broad-spectrum antifouling technology. However, there is scope in immobilising and growing specific bacteria in coatings to produce localised antifouling compounds. An example of this is the development of a hybrid functional sol-gel coating which encapsulates a suitable non-pathogenic biological compound (Akid et al., 2008; Gittens et al., 2010).

- Cleaning

Cleaning a surface is simple and effective. However, for open sea locations, it does require deployment of machinery and divers. It can be expensive and could potentially damage a surface, or release harmful biocides if an antifouling paint is used on the surface being cleaned.

Cleaning will not be as effective on the most stubborn fouling, such as tubeworms and barnacles. Cleaning the surface may also be detrimental in attracting further, new organisms to the cleaned surface as certain organisms are known to prefer secondary succession of a surface (Jenkins and Martins, 2010).

A possible method is to use a high velocity/pressure water jet to remove fouling organisms. The effectiveness of this method may be controlled by primary surface preparation - it has been found that *Ulva linza* zoospores were successfully removed from smooth and very rough surfaces using a water jet, but this method was less successful in removing the spores from surfaces with a roughness in the middle of these (Granhag et al., 2004). Using a high velocity pressure jet will also not be as effective at removing hard marine growth such as tubeworms.

Another method of surface cleaning is to use devices powered by wave action or currents. One such device has been developed by a company named IEV Group, which uses waves (for splash zone control) or currents for underwater control of biofouling to move the device (brush-bearing ring) across a surface (IEV Group, 2011).

3.5.5 Marine Corrosion Prevention

There are five main methods for controlling marine corrosion:

1. Isolation of the metal surface from sea water either by coating or painting
2. Changing the corrosion potential of the metal to a value where corrosion is not preferred. This can be achieved either by impressing a voltage on the metal or coupling to a sacrificial anode
3. Making the metal more passive using corrosion inhibitors
4. Changing the local pH in the environment surrounding the metal by chemical dosing
5. Changing the material used in the structure for a more resistant one

Coatings

Coating a metal surface is a common method of corrosion control (Shifler, 2005b). Ultimately the coating provides a barrier between the material and the electrolyte and therefore prevents corrosion, preventing either oxygen diffusion or providing a high electrical resistance to stop the corrosion reactions from occurring. Both organic and metallic coatings can be used.

1. Organic Coatings

Organic coatings (polymers) provide good protection if applied correctly; this includes preliminary surface preparation, application of a primer layer and the method of application.

Fluoropolymer coatings have become an extremely important type of coating for a range of applications due to their exceptional resistance to a range of temperature, chemical attack and organic solvents (Deflorian et al., 1993). Fluoropolymer coatings have a low surface energy which allows the coating to be water-repellent, low friction and antifouling. An example of such a system is Enviropeel (A&E Systems, 2009) which acts as an impermeable barrier coating containing corrosion inhibitors. This is a solid at room temperature, but can be heated to become a sprayable liquid, allowing coating of different shaped devices.

2. Metallic Coatings

Coating a surface using a metal or alloy provides a new surface layer which will have new properties. Two forms of metal coatings are available – those which use active corrosion protection (zinc or aluminium anodes which corrode preferentially over the metal underneath) and those which work as a protective layer (stainless steels or other alloys with high corrosion resistance). Metallic coatings can be applied using electrodeposition techniques as well as cladding, hot dipping, spraying and chemical conversion.

3. Cladding of Surfaces

Systems have been designed that use a cladding system to provide corrosion protection by isolating the metal from the electrolyte. One such system is Armawrap© from NICC Systems (2005) which is made from neoprene.

Cathodic Protection

Cathodic protection is often used to control marine corrosion. It is effective against the majority of corrosion, including microbiologically influenced corrosion. The method works

by applying a direct current to the structure requiring protection to oppose the natural corrosion current occurring on the metal. The high conductivity of seawater makes the technology very useful by providing a fairly uniform current distribution over the surface of the metal structure (Dexter and Lin, 1992).

There are two types of cathodic protection, sacrificial (using another, more reactive metal) and impressed current (using an external power source). Cathodic protection systems are most commonly used alongside protective coatings which reduce the surface area exposed to the seawater and the total required current for protection as well as reducing the overall cost of the system.

In seawater environments, especially those at shallow depths (where waters are mostly supersaturated in calcium carbonates), a beneficial calcareous scale is formed on the surface of the protected metal due to the interaction between the high mineral content of the water and the high interface pH produced by the cathodic protection (Neville and Morizot, 2002; Möller, 2007). These deposits increase the life of sacrificial anodes and reduce the current requirements for protection.

1. Sacrificial Anodes

Sacrificial anodes use galvanic control and the principle of bimetallic corrosion. By making the structure the cathode and introducing small sacrificial anodes, the anodes will corrode preferentially over the structure. The sacrificial anodes, usually made of aluminium, zinc or magnesium alloys (although the latter has a relatively short lifetime in seawater), are attached directly to the surface of the metal requiring protection. These metals are chosen due to their position in the galvanic series of metals (at the less noble end), ensuring that they will corrode in preference to the metal structure. The life of the anode is governed by three main factors, the weight of the anode, the current output and the efficiency of the system. The distribution of anodes on a structure is dependent on the current distribution requirements, the materials used and the size of the surface requiring protection.

This system has several advantages over impressed current cathodic protection including no requirements for an external power source; easy installation and maintenance; no source for stray interference currents; possibility to achieve uniform distribution of protection current and low costs. Disadvantages include limited and fixed driving potential; and many anodes may be required for large structures or those which are poorly coated. With a sacrificial anode system it is not possible to provide over-protection; the anodes will

only corrode as fast as the current demand (so they counteract the corrosion current but do not "overshoot" as can happen with an impressed current system).

2. Impressed Current Cathodic Protection (ICCP)

Impressed current systems use inert anodes to impose a direct current on to a metal, producing electrochemical changes on the surface of the metal and establishing a condition where the metallic state is more stable than the ionic state. The application of a direct current using an external DC power source will force electrons to the surface of the metal, allowing only a cathodic oxygen reduction reaction to occur. No anodic metal ion dissolution is possible and hence corrosion is prevented (Edyvean et al., 1992). While not preventing fouling, these changes influence the chemistry of the surrounding seawater and hence the settlement of fouling organisms, tending to reduce bacterial adhesion to a metal surface and reproduction during the first stages of biofouling and biofilm development.

The presence of any organic material will affect the amount of current required to maintain the protection of the metal surface and will also alter the nature of any calcareous deposits which are formed. Calcareous deposits are formed on metals in seawater due to the introduction of hydroxyl ions (OH^-). These form a high localised pH and the solubility product of calcium and magnesium compounds in the seawater is exceeded, hence precipitating a scale. The calcareous scales play an important part of the protection of the metal as they reduce the current requirement for protection. However, they can also be detrimental as they can cause a reduction in heat exchange efficiency and can cause disbondment of protective paints/coatings.

Corrosion Inhibition

Inhibitors involve a change in the local environment itself by the addition of certain chemicals, by removal of dissolved oxygen or alteration of the pH (Mercer, 1976). This type of corrosion protection is limited in practice to enclosed spaces or systems to ensure that the application is economically viable (Chandler, 1985).

Inhibitors are used to produce a film which is adsorbed on to the metal surface to reduce the overall corrosion rate of the material. Inhibitors can reduce the cathodic reaction rate, the anodic reaction rate or both. An example of a chemical inorganic inhibitor is sodium nitrate, although there are many more organic and inorganic compounds which work as effective inhibitors of corrosion (including chromates, nitrites, benzoates and silicates),

those used need to be chosen with regard to the metal to be protected, environmental conditions and system size (Chandler, 1985).

Metals and Alloys

The final option for corrosion protection of structures is replacement of the material used for a more resistant metal or alloy. Often these are more expensive options and therefore are only used when the conditions are highly corrosive or the parts are important to the operation of the structure and corrosion has to be prevented for long durations. Carbon steel is usually the alloy chosen for the majority of a tidal device. This alloy is durable and strong as well as cost effective. However, it does not have good corrosion resistant properties and it may be that certain, critical parts, such as connector pins should be made out of a metal such as titanium which exhibits high resistance to corrosion and the cost outweighs the consequences of corrosion.

3.5.6 Examples of Antifouling and Anticorrosion Systems

It is usual that an anticorrosion primer is applied first to a surface to protect against corrosion. One of the antifouling coatings is then applied to protect the surface against fouling settlement, all antifouling coatings ideally should provide good protection against corrosion, but if different systems are used together, it is important to ensure that they are compatible. This section highlights two examples of technologies which have been developed to specifically ensure both corrosion and biofouling protection.

- Cathelco

Cathelco (2010), a UK based company has manufactured a system that uses the electrolytic principle to protect against biofouling as well as providing a coating which protects against corrosion. A transformer provides an electric current to anodes made from copper and aluminium. When fed a current, the anodes produce ions which are free to move through the water. The presence of these ions will deter settlement of barnacles and mussels. The aluminium anodes produce aluminium hydroxide which flocculates copper released from the copper anodes and a film is formed on surfaces deterring the settlement of larvae. The cupro-aluminium film also helps to stop corrosion of these surfaces. This system is often used in pipes, enclosed spaces or regions where there are low flow speeds.

- Subsea Industries' Ecospeed

Ecospeed (Subsea Industries, 2008) uses glass flake technology with large glass platelets to create a homogeneous coating often used for ship hulls. The glass platelets are suspended

in a vinyl ester resin base and provide a barrier to water as well as a smooth, non-stick finish which deters marine settlement. This type of marine antifoulant relies on relative movement to remove the fouling species from the surface, and hence would not provide as good protection for stationary parts. However, the glass technology is strong enough to provide good erosion resistance even in very abrasive uses.

3.5.7 Antifouling Regulation

The Council Directive 76/769/EC of 27 July 1976 relating to restrictions on the marketing and use of certain dangerous substances and preparations was in force in 1976 and bans the placement of organotin compounds in free association antifouling paints on to the market in any member states. The regulation was originally intended for ships used in lakes and inland waterways. However, it has now been extended and is applicable to ships and structures used in any marine environment.

Regulation (EC) No 782/2003 of the European Parliament and of the Council of 14 April 2003 on the prohibition of organotin compounds on ships has brought into force the ICAFS in the European Union. The same limits were set in this regulation and applied to all member states.

The EU Biocidal Products Directive 98/8/EC came into force on 14 May 2000. This directive lists the acceptable biocides which are available for use. Member states have the authority under this act to allow these products which will be used to destroy, deter, render harmless, and prevent action of, on harmful organisms by chemically or biological means (Cheyne, 2010). The list of allowed products does not contain any which are designated as carcinogenic, mutagenic, toxic for reproduction, sensitising or bioaccumulative.

Antifouling specific legislation is comparatively new. The legislation is mainly centered around the International Convention on Control of Harmful Antifouling Systems on Ships (ICAFS), 2001, which came into force on 17 September 2008. The convention is regulated by the International Maritime Organisation (IMO).

Cheyne (2010) provides an excellent review of the impending regulatory strategies, including the potential benefits and costs. The convention prohibits the use of organotin compounds in antifouling systems. An antifouling system is defined in Article 2(2) of the convention as “a coating, paint, surface treatment, surface, or device that is used on a ship to control or prevent attachment of unwanted species.” Although mainly based on the use

of antifouling systems on ships, the convention does also apply to other structures used in the marine environment including offshore stationary and floating structures. The convention stated that any organotin biocide must not be applied or reapplied to a surface after 1st January 2003 and must not be found on any surface operating in the marine environment after 1st January 2008.

3.6 Conclusions and Application to Tidal Stream Devices

Seawater is a hostile environment in which to operate. It provides an excellent electrolyte for corrosion, and also provides an unlimited supply of biofouling, in the form of both micro and macro fouling species. It has been observed that these two phenomenon are closely related in the marine environment and as such require successful management if devices are to operate effectively for the desired lifetime.

The flow regimes in which offshore platforms and ships operate are different from those in which tidal energy devices will be deployed. The literature relating to ships and offshore platforms provides good general knowledge of the mechanisms of corrosion in seawater, but the relevance to tidal energy converters has to be investigated.

Tidal stream devices are likely to be constructed largely from carbon steel, commonly used for structures in the marine environment. A tidal device is designed to be situated in a high tidal flow regime. From this literature review, tidal regime velocities may affect corrosion rate. However, this depends on the metals used and their overall corrosion resistance. The tidal flow regime could also result in significant impact with suspended solids which may lead to localised erosion corrosion on areas of the device subject to the highest flow rates. Suspended solid concentration is likely to increase in periods of storm weather. It is interesting to note the velocity at which fouling decreases in flowing seawater. This velocity (Point A on Figure 3.3, 0.9 ms^{-1}) is low in comparison to the tidal flow regimes which are considered acceptable for commercial exploitation. However, due to the likely complex nature of the design of these devices, there are many areas which will experience lower flow rates and are therefore likely to foul. The continual movement of the seawater, especially in tidal locations not only allows the suspended particles to move freely, it also allows continual oxygenation, which may increase the likelihood of erosion-corrosion occurring.

The relationship between corrosion rate and temperature is a worthwhile correlation to investigate in relation to tidal devices due to the likely range of water temperatures in which they will operate and that their operation can generate a variety of surface temperatures in different parts of the structure.

The majority of a tidal device is likely to be painted to provide protection against corrosion along with cathodic protection. Therefore, there is the potential for under coating corrosion to occur if coatings are not applied or maintained correctly.

Tidal devices are likely to be maintained uncovered on the quayside. There is a high potential for atmospheric corrosion to occur in such a location. The relative humidity at the Orkney national trial site for tidal devices is approximately 75% in April and 86% in November-December (Met Office, 2013).

With respect to tidal devices, Foul Release Coatings would be ideal for the blades as when they reach a critical velocity, any fouling which has accumulated (most likely during stationary periods) will be dislodged. However, there will be periods of inactivity or maintenance when the blades will be stationary with a build-up of biofouling on the blades.

Understanding the effects of physical, chemical and biological factors in tidal environments on the deterioration of metals used in the construction of tidal devices will lead to the development of improved techniques for the protection of the different parts of the structure. This study will investigate how changes in these environmental parameters affect the corrosion of critical areas on tidal devices (Chapters 5-8).

A risk-based management approach as discussed in Chapter 2 can be successful for the management of corrosion, and these systems have been applied in the oil and gas offshore industry for some time. However, for the development of a risk-based management system to be used in practice, the theory only provides an overview, and it is difficult to find information that specifically provides the practical aspect of the corrosion process that will be applicable to tidal devices, hence experiments are conducted as detailed in Chapters 5-8.

The information in this literature review will be the basis for understanding of the processes that are occurring on the device throughout operation, and will also act as a point of reference for the risk analysis and recommendations for protection methods and maintenance procedures. The information discussed in this chapter has been taken

forward to inform the development of a risk management system and specific risk factors drawn from this literature are detailed in Chapter 10.

Chapter 4

Developing the Evidence Base (ii) - Investigation of Prototype Devices

Tidal Stream Energy Devices and the Typical Corrosion and Biofouling effects on them

4.1 Introduction

Ideally, the first stage of the risk assessment process is to establish the context through documentation of preliminary observations of the unit under examination (see Figure 2.2 in Chapter 2). As tidal stream devices are in the early stages of development there is little, if any, directly relevant published work, and therefore inference has to be made from other marine structures such as offshore oil and gas platforms (Chapter 3) in the first instance. However, the author has had access to two devices developed and tested by Alstom Ocean Energy (AOE) (formerly Tidal Generation Ltd) which has permitted qualitative and quantitative assessment of corrosion and biofouling, which are presented here and in Chapter 5 with further qualitative and quantitative assessment of panels immersed in Orkney. The two devices were a 500 kW tidal turbine ("DeepGen III") and associated equipment deployed between 2010 and 2012 and a full scale (1 MW) prototype, "DeepGen IV" deployed in February 2013. Both devices have fed electricity into the grid and are based at the designated test site, the European Marine Energy Centre (EMEC) in Orkney.

4.2 The DeepGen III and IV Prototypes

DeepGen III is a prototype tidal stream energy converter ("tidal turbine") capable of producing electrical power using tidal currents as the primary source of energy. It has a capacity of 500 kW (sufficient to supply power to 300 homes).

The device consists of a buoyant nacelle (housing the main generation equipment), a tripod support structure and electrical cable connections to shore (Figure 4.1).

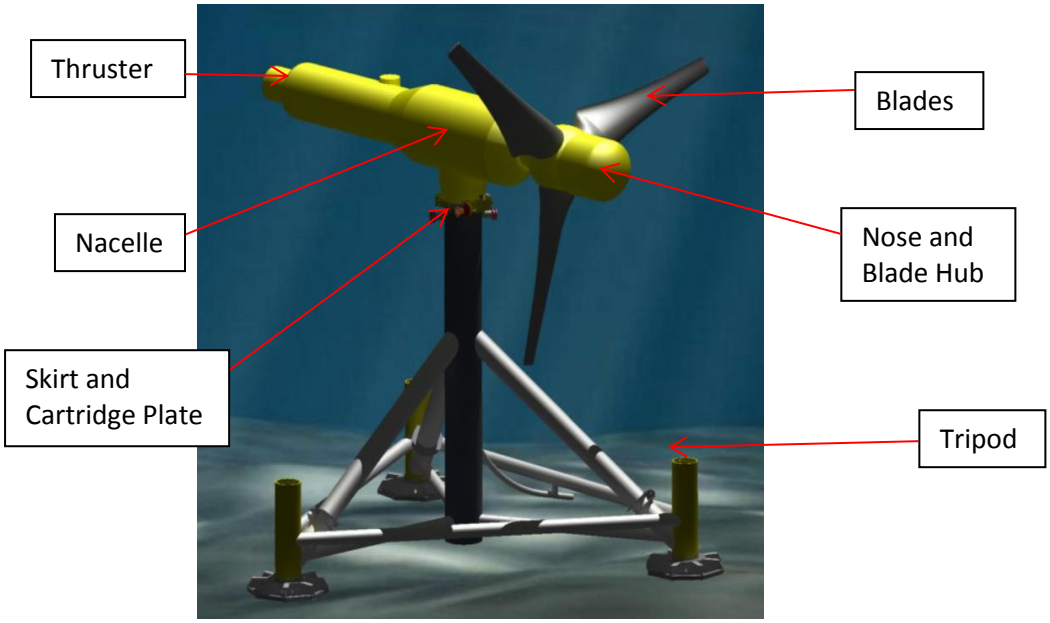

Figure 4.1. Schematic of the Alstom Ocean Energy tidal stream device (Alstom, 2013)

Development and demonstration of the two devices is supported by the ReDAPT project using funding for marine energy research (Energy Technolgies Institute (ETI), 2014).

The tripod (Figure 4.2) remains attached to the seabed for the duration of the turbine lifetime (expected to be in the order of 25-30 years) and has a sea-bed footprint of 129.6 m^2.

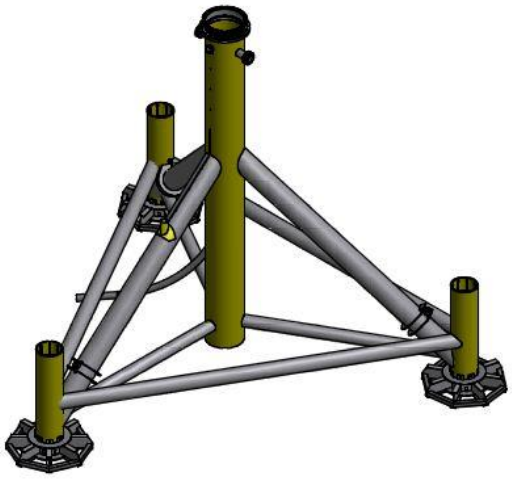

Figure 4.2. Schematic of the DeepGen tripod

Mounted on top of the tripod via a skirt and clamp structure, is a detachable nacelle (length 21 m, width 2.6-3.5 m) weighing 135 tonnes. A tri-blade variable pitch rotor is located at one end coupled to a gearbox situated inside the nacelle body. The semi-enclosed skirt

houses the “cartridge plate” which holds the electrical connectors to export the generated electricity (at 6.5 kV) to grid via seabed cables.

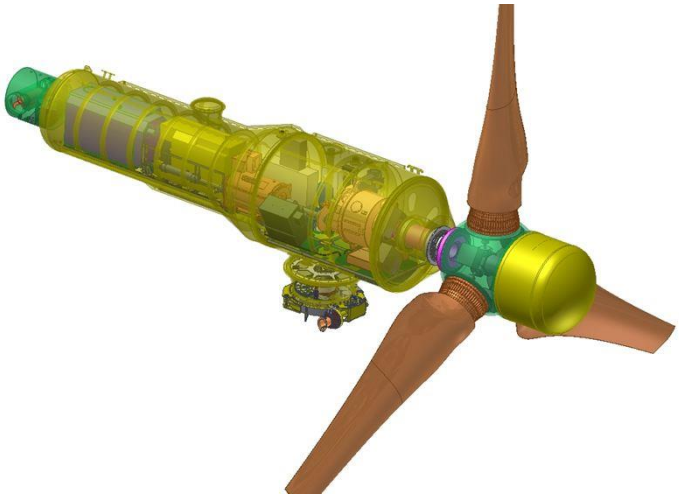

Figure 4.3. Schematic of the AOE nacelle including the three blades, blade hub and buoyant nose

The three blades (rotor diameter 18 m) are each attached to the rotor using 60 bolts. A buoyant nose (see Figures 4.1 and 4.3) is used to ensure that the nacelle remains level during deployment and retrieval. The blades have a copper fibre spar sealed from seawater by glass fibre skins. These materials are used to ensure that the blades are sufficiently strong but also light. All electrical equipment is housed in the water-tight nacelle. The entire nacelle rotates (yaws) during slack tides every 6-7 hours to face oncoming tides via a thruster located at the back of the nacelle, thus optimising the potential power extraction. The thruster has a diameter of 600-700 mm and is enclosed in a steel structure whilst the thruster blades are open to seawater. The thruster blades are made from 316L stainless steel and rotate at approximately 10 rpm.

DeepGen IV is the Alstom Ocean Energy’s fourth stage (commercial size) prototype. The device is the same in principle to the DeepGen III device and uses the same tripod as the DeepGen III device. However, this new device has a greater generation capacity of 1 MW. The device was deployed at EMEC from January 2013. The rated water velocity of the device will be approximately 2.7 ms^{-1} with a maximum operating velocity of 3.4 ms^{-1}. The cut-in velocity, above which electricity is generated, is estimated at 1 ms^{-1}. These values will vary when the devices are deployed on a commercial scale at different global locations depending on local conditions. Due to lack of deployment prior to the end of this work, no evidence has yet been collected from this device. Evidence has been gathered from the longer deployment of the DeepGen III device.

4.3 Location and Deployment

The Fall of Warness in Orkney is located in the North Sea (Figure 4.4). The current flow in the area is complex due to the incoming waters from the Atlantic Ocean and the English Channel.

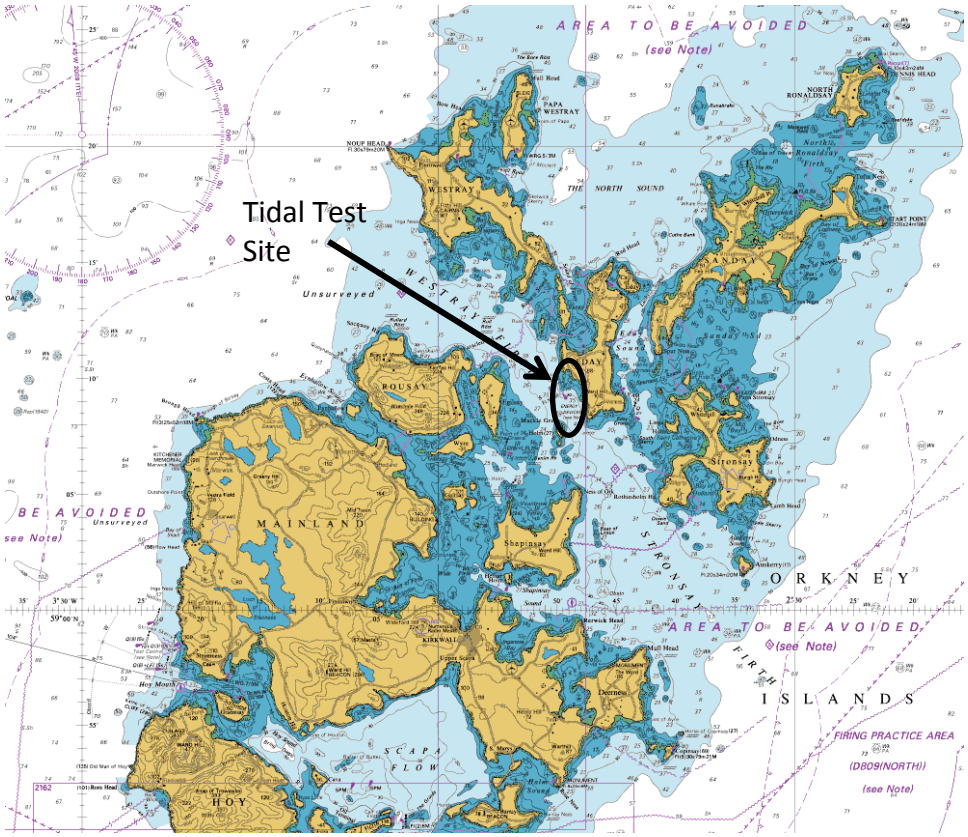

Figure 4.4. Tidal test site location (Harland, 2013)

4.3.1 European Marine Energy Centre (EMEC)

EMEC in Orkney, UK is the world's first purpose built test centre for marine renewable technologies. The centre was established in 2004, providing test berths for both wave power and tidal stream devices across two locations. The tidal power test centre is located in the Fall of Warness, south-west of Eday and to the north of the Orkney mainland.

The Fall of Warness was chosen for its strong tidal energy, with peak tidal flows up to 7 knots (approximately 3.6 ms^{-1}). The tidal pattern is complex, sheltered from oceanic conditions but experiencing waves propagating from both the north-west and south-east, and hence experiencing notable wave-current interaction at certain times, dependent on metocean conditions (Lawrence et al., 2009). The flood tide in the Fall of Warness is towards the south-east and the ebb tide goes towards the north-west.

The sea surface temperatures around Orkney are mainly influenced by the North Atlantic Drift Current which carries water into the North Sea. The net effect of this movement is a warming of sea temperatures allowing them to remain on average at 6-7 ^{o}C during winter and to rise to 12-13 ^{o}C during the summer months. The salinity of the seawater around Orkney remains almost constant throughout the year, averaging between 34.75 and 35 ppt (generally considered normal for seawater). The water in the Fall of Warness is clear with little suspended solids. The channel seabed is flat and consists of smooth scoured bedrock due to the tidal flow speed through the area with a small amount of loose particles (EMEC, 2008). Various models of the tides in the area have been developed as part of the on-going research at EMEC, to enable understanding of regional tidal flow patterns (EMEC, 2013).

4.3.2 DeepGen III Operational Deployments

DeepGen III was deployed several times after fabrication in 2009 and removed from the water on occasions for maintenance and repair. Table 4.1 shows the dates for five deployments and retrievals during the period between September 2010 and October 2011 when the device was generating electricity. These dates of deployment are key to the preliminary investigation as they aid the analysis of seasonal biofouling for settlements.

Table 4.1. 500 kW Turbine Deployments between September 2010 and October 2011

Task Name	Start	Finish	Duration (days)
Deployment a	Sun 19/09/10	Wed 29/09/10	10
Deployment b	Fri 15/10/10	Wed 15/12/10	61
Deployment c	Fri 24/06/11	Mon 25/07/11	62
Deployment d	Wed 24/08/11	Wed 21/09/11	28
Deployment e	Thu 06/10/11	Wed 19/10/11	13

Prior to the first deployment in 2010, the turbine was in the water for two weeks during immersion tests. When out of the water, the device remained in a seawater influenced environment either on a barge or on a quayside.

4.4 Documentation of Corrosion and Biofouling on DeepGen III

Data was collected through inspection of the corrosion and biofouling that occurred on the device and associated equipment. This was either gathered by direct observation or by analysis of remotely operated vehicle (ROV) video surveys and photographs provided by Alstom Ocean Energy.

4.4.1 Tripod Main Structure

Preliminary observations of the tripod using a ROV were obtained in August 2010. An acoustic Doppler current profiler (ADCP) was located on one of the diagonal members of the tripod during this period and was removed in August 2010. The cartridge plate was retrieved in April 2009, redeployed in November 2009 and retrieved again in September 2010. A further ROV survey was carried out in May 2011. It should be noted that the limits of air-diving are around 50-60 m, placing tidal power turbines at the limits of using this form of inspection and maintenance. To go deeper using specialist diving equipment and remotely operated vehicles (ROVs) is expensive and hence every effort must be made to prevent failure of any part of the device between scheduled quayside maintenance periods.

The tripod, made from carbon steel (S355), was fixed in place (in August 2008) using three cylindrical piles grouted to piles drilled into the seabed, with 16 m between the three legs. The structure is 16 m tall and has a mass of 110 tonnes (in air). All surfaces are painted black in 2-pack epoxy glass flake paint (Jotamastic 87 coating for marine structures) apart from the top of the central member which is painted yellow.

At the first ROV survey inspection, (after 24 months exposure, August 2008 - August 2010) the majority of the tripod structure was covered by barnacles (*Balanus crenatus*), although there were small patches on the structure where barnacles had not settled or had settled and then come off. Where this had occurred, small circular marks were left on the surface by the substance used by the barnacles to attach to the surface. Fouling had mostly occurred in the main flow, not in areas of shadow. Interestingly, although the majority of the tripod was covered with marine growth, the area at the top of the central column which was painted yellow had no observed fouling. There was a loose rope here, left from deployment, which may have been cleaning the surface as it moved with the flow and rubbed against the structure.

Soft marine growth was observed on the back frame of the cartridge plate and down the inside of the hollow main column where there is minimal flow (Figure 4.5). This column houses the umbilical used to attach the device to the seabed cables. The fouling shows clear evidence of sea squirts (*Ciona intestinalis*) in this area. Sea squirts are common fouling organisms; the larvae only have a short time to find suitable conditions for settlement during the dispersal stage and hence settle under a variety of conditions.

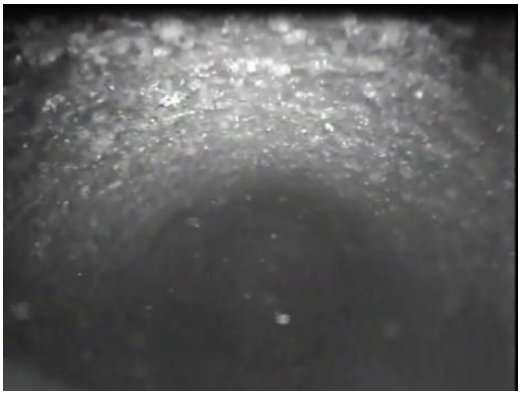

Figure 4.5. Extensive soft growth (sea squirts) inside one of the tripod legs observed during ROV survey

At the top of the tripod central column is a recessed (300 mm deep) cartridge plate. This houses connectors for the high voltage supply and fibre optics. The critical metal components of the connectors sit in oil baths to reduce the likelihood of corrosion. The cartridge plate is made from carbon steel grade S355 and the back frame is made from carbon steel grade S275, a structural steel. A hole which forms a hold for the winch rope is located in the centre of the cartridge plate. This allows ingress of water and organisms into the skirt area since the central member of the tripod is not enclosed. A 2-pack epoxy paint system is used on the cartridge plate for strength and moisture resistance. Around the plate is a bearing surface which allows movement of the turbine in between tides every 6-7 hours.

The tripod with the cartridge plate deployed remained on the seabed without the nacelle for 10 months between November 2009 and September 2010 prior to the device generating electricity. During this time fouling organisms settled underneath caps fitted over connectors (Figure 4.6). Dead sea squirts were observed underneath the caps when removed. It is likely that the conditions underneath the caps become anaerobic due to lack of oxygen. Although this environment is unattractive to many organisms, there are certain bacteria that thrive in anaerobic conditions. The cartridge plate was retrieved after this 9 month period prior to deployment (a) of the nacelle and extensive barnacle growth was observed on the front of the cartridge plate (Figure 4.7).

Figure 4.6. Fouling on cartridge plate after 6 month exposure

Figure 4.7. Cartridge plate on the quayside in September 2010 showing barnacle and soft growth

The tripod was originally deployed with 39 sacrificial anodes located around the structure. During the ROV survey in August 2010 five of these were no longer attached after a much shorter period than expected. The anodes should ideally remain effective for at least 2 years to allow two year maintenance intervals. It is uncertain whether they were already spent or had fallen on to the seabed due to fixings being unsuitable for the high tidal flow regime.

During the second deployment in 2010 significant corrosion occurred on the nickel aluminium bronze fibre optic connector bolt (Figure 4.8). This is discussed in more detail in Chapter 9. The high voltage (HV) supply connector above the cartridge plate is manufactured from uncoated titanium and showed no signs of corrosion or fouling. Titanium is already recognised as a corrosion resistant material. However, the lack of fouling observed under these conditions, especially in a location whether fouling has been observed is notable as it provides a suitable option for manufacture of critical turbine components, especially those which require opening/closing after long periods of immersion.

Figure 4.8. Corrosion of fibre optic connector

A ROV survey in May 2011, after almost three years of submersion, shows clear evidence of mussels settling on the tripod. This is consistent with the literature (Forteath et al., 1982) that found mussels settling on structures after primary colonisation by barnacles in the first 1-2 years. It is also interesting to observe areas found to be free of biofouling. On the supporting diagonal members there are clear areas around the bases of the anode support structure.

4.4.2 Acoustic Doppler Current Profiler (ADCP)

The ADCP was attached to the tripod during the first deployment of the DeepGen III device to monitor local flow speeds. The device was submerged for approximately 18 months and removed in August 2010.

The device was located on one of the diagonal struts of the tripod, with the back of the device sheltered from the flow by the strut and the sensors pointing in the direction of the flood tide. The ADCP consists of a cartridge mounting plate (painted yellow, see Figure 4.9) with a white plastic housing for all electronic equipment. A protective structure can be seen painted orange.

Figure 4.9. The ADCP in Orkney on removal from seabed

The device was removed mid-summer, and so the seaweed observed (Figure 4.9) was more significant than it would be in winter. The seaweed was brown/red in colour, likely to be *Polysiphonia urceolata* or *Polysiphonia byssoides*, important fouling species on central and northern sea oil platforms and identified as present all around the British Isles (Gibbons, 2008).

Figure 4.10. The ADCP on arrival in Sheffield - Front view

The ADCP was extensively fouled (Figure 4.9 and 4.10). Considerable growth had occurred on the front horizontal ledge of the mounting plate and the sensors (Figure 4.10 and 4.11). The only vertical surfaces that were fouled were those directly exposed to flow.

Figure 4.11. Extent of front and back fouling

Only minimal fouling had occurred at the rear of the device where a small number of barnacles had settled. These were mainly found in sheltered areas, behind bolt heads or in crevices (Figures 4.12 and 4.17). These areas provide ideal locations for settlement. The front fouling extended to approximately 25% of the sides in each direction from the front of the device.

Figure 4.12. Extent of fouling at the rear of device (facing ebb tide)

Figure 4.13. Fouling on the front sensors of the device

The Perspex sensor covers showed extensive fouling by hydroids and barnacles (Figure 4.13). The volume and location of the fouling may be influenced by the direction from which the majority of the fouling spores arrive, (Atlantic/North Sea direction). The marine growth on the ADCP is likely to inhibit the sensors on the device and stop it from working effectively.

Figure 4.14. Fouling on the underside of the cartridge plate

The underside of the ADCP cartridge plate showed extensive fouling (Figure 4.14). Fouling was also observed in the ADCP attachment when the device was removed from the tripod.

Two clear generations of barnacle (indicated by size) were found on the ADCP (Figure 4.15). In the British Isles barnacles normally attach in early spring with limited attachment throughout the summer months. The observation of two generations of barnacles on the ADCP correlates to this having been submerged in the sea for 18 months including two springs. The barnacles, identified as *Balanus crenatus,* had 6 plates and diamond shaped apertures. Their size ranged from 2.5 cm in length for the initial settlement to only a few millimetres for the second settlement. These barnacles were also observed in other locations on the tripod and nacelle. The fouling is consistent with that previously found during a seabed survey of the area carried out between 17th and 21st March 2005 (Aurora Environmental, 2005).

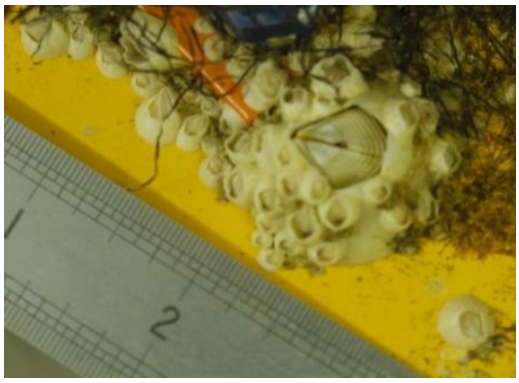

Figure 4.15. Two generations of *Balanus crenatus* found on the ADCP

A single mussel was observed on the front of the ADCP (Figure 4.16).

Figure 4.16. Location of single mussel

Fouling was observed in small crevices either side of the plastic housing. The crevice to the right of the sensors (Figure 4.17) had a greater amount of fouling than the crevice to the left of the sensors. These crevices provide good conditions for growth and settlement, giving reasonable shelter for organisms and a good location to adhere to the surface, as well as ideal flow patterns and velocity.

It is interesting to note that no fouling was observed on the white plastic housing. It is likely that this material is not ideal for settlement as adherence of species is difficult due to its smoothness and the flow pattern over the surface. It is also possible that seaweed attached to the ADCP may provide a certain amount of cleaning of fouling when it first attaches to the surface.

Figure 4.17. Fouling observed in crevices either side of the main device housing

4.4.3 Nacelle Main Body

The main structure of the nacelle (housing the powertrain) is constructed from carbon steel (S355) for reasons of strength and cost. All bearing surfaces have a welded overlay of stainless steel. It is possible that fouling may cause wear of bearing surfaces. All bolts on the nacelle are coated with Xylan (a PTFE based coating). This should provide long lasting protection for the bolts, and is beneficial for maintaining the internal thread on bolts. However, the coating used on external bolts of the DeepGen III device was found to have been removed from the bolts due to the high flow conditions and the associated abrasion. On the nacelle are 15-20 aluminium anodes, each weighing between 5 and 10 kg. The nacelle joins to the tripod central member and rotates during slack tides to face the next oncoming tide by releasing the clamp.

Paint was observed to be flaking off around the external flanges on the nacelle (Figure 4.18) and also on the join between the nacelle and blade hub (Figure 4.19). This will lead to localised corrosion of the exposed metal surface where this becomes anodic relative to the rest of the coated metal.

Figure 4.18. Paint flaking around flanges on Nacelle

Figure 4.19. Paint flaking around join between main nacelle body and blade hub

Several areas of the nacelle have been repainted. The paint (Interzone 505 Glass Flake from International Paint Ltd) should be applied using the manufacturer's guidelines to ensure correct application and maximum protection. The guidelines include specification of paint application method (airless spray), thickness of coats (2 coats, 300 µm DFT per coat) and surface finish prior to application (removal of dust, debris salt, oil and other potential contaminants).

Figure 4.20. Repainting on Nacelle

Towards the rear of the nacelle there is significant coating loss and the exposed metal exhibited corrosion. The coating had been lost during deployment or retrieval where the nacelle had come into contact with the deployment vessel. Coating had also been lost by contact with the support structure on the quayside (Figure 4.21). These supports cause areas to be hidden from view during maintenance and such areas could not be fully assessed for damage and corrosion. The support structure design also means that it is not possible to easily recoat these areas.

Figure 4.21. Significant coating removal from nacelle

In normal operation such nacelles will be removed from the sea regularly for inspection and maintenance on the quayside. However, exposure to air will damage the coatings and the sacrificial anode system only protects the metal from corrosion in water and atmospheric corrosion will occur, so it is imperative that maintenance work is planned properly to ensure the nacelle is exposed to air for the minimum amount of time necessary.

Currently there is no set procedure in place for the cleaning of the nacelle on removal from the sea.

During the period of operation between September 2010 and October 2011 no biofouling was observed on nacelle surfaces. The nacelle is exposed to flowing seawater. Therefore it is likely that the surfaces under higher flow conditions were not as attractive for settlement of biofouling.

4.4.4 Buoyant Nose

The nose cone faces the full oncoming current flow. In April 2011 there was some damage to the paint coating on the front of the nose due to impact with debris in the current. There is a ring around the nose where the coating had been lost and corrosion had occurred associated with a weld.

Figure 4.22. Buoyant nose showing signs of corrosion around the circumference

4.4.5 Blades and Blade Hub

The blades on the DeepGen III device were coated with "Coppercoat" paint (Figure 4.22). This is an epoxy resin densely filled with copper (Aquarius Marine Coatings Ltd, 2011) that uses the production of cuprous oxide (Copper(I) oxide, Cu_2O) to protect against fouling settlement. The coating is anti-leaching and can theoretically provide fouling protection for over 10 years. Coppercoat also protects against osmotic attack of the blades due to the inherently waterproof epoxy resin, but is only effective in situations where there is relative movement (blades or the hulls of ships) to wash away the final product (cupric hydrochloride) and thus allow a fresh surface to be exposed to the seawater.

The rotor height above the seabed is 19 m nominal. The blades rotate at a speed of 10 rpm in a tidal regime of 4-8 knots (2.06-4.12 ms^{-1}). During periods of slack water biofouling may occur on the blades whilst stationary although it is during these times that the nacelle is rotated. Galvanic corrosion may occur on the blades, with cast iron next to nickel aluminium bronze at the interface between the blades and the hub. The horizontal axis design used is less dependent on having a smooth surface finish on the rotor than a vertical axis design so any surface roughness caused by biofouling may not be as significant a problem in terms of maintaining a high lift:drag ratio (Fraenkel, 2002) (the ratio between the amount of lift created by the turbine blade and the drag created from the movement of the blade through the water).

Figure 4.23. Coppercoat coating on blades

Some damage to the blades was observed during inspection in April 2011 (Figure 4.24). This could have been due to impact with debris in the fast flowing water. The damage could also have occurred during deployment or retrieval operations via impact with the boat or the quayside.

Figure 4.24. Damage to blades observed in April 2011

Sixty bolts, with plastic covers and grease to protect against water ingress, attach each blade to the turbine (via the spheroidal graphite iron blade hub). However, water was observed in these areas and this may lead to corrosion. The area around the stud holes had already corroded significantly (Figure 4.25). During the lifetime of these devices the blades will require maintenance, and may even require replacement if they are damaged. In this case, these bolts would be required to be fully operational so that they can be removed. If they are corroded, it may not be possible to remove the bolts from their fixings.

Figure 4.25. Corrosion observed around blade fixings

4.4.6 Stab Mechanism and Connectors

During the second deployment of DeepGen III, corrosion and biofouling were observed on three connectors situated on the stab mechanism (located within the skirt). These are the high voltage (HV) cable connector; the fibre optic connector (for the communication system) and the ADCP connector. The HV connector (Figure 4.26) is finished with uncoated titanium. No corrosion or biofouling was observed on the titanium during the period of deployment.

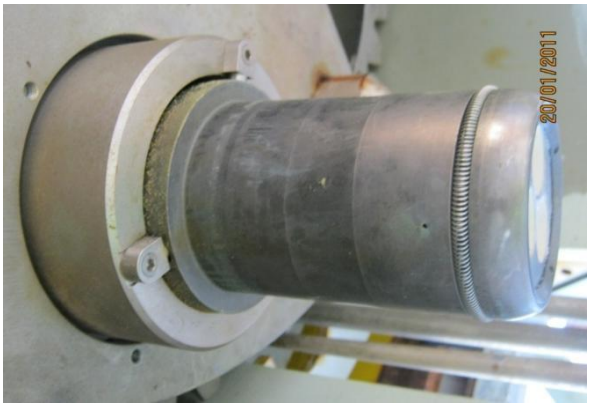

Figure 4.26. High voltage connector on stab mechanism after second deployment

The fibre optic connector is manufactured by Seacon (Hydralight). The outer shell of the connector on the stab mechanism exhibited some sparse settlement of soft hydroids (Figure 4.27). The deployment was relatively short and carried out during autumn/winter when settlement is low and this fouling would not be representative of the coverage expected if the device was deployed in spring or summer months. Corrosion was also observed around the base of the connector outer shell (Figure 4.27).

Figure 4.27. Corrosion and biofouling of the Seacon Hydralight fibre optic connector on the stab mechanism

A connector for the ADCP is also located on the stab mechanism (Figure 4.28). During second deployment this was not used and there was no associated connector located on the cartridge plate so the pins were open to seawater. No biofouling was observed on this connector. However, significant corrosion product was observed on the ends of the connector pins and around the base of the connector on the fixing nut (Figure 4.28).

Figure 4.28. ADCP connector location on stab mechanism. Severe corrosion observed on the connector pins and around the base of the connector at the nut fixing

4.4.7 Skirt

The skirt is located on the underneath of the nacelle and fits to the top of the central tripod column, enclosing the cartridge plate on deployment (Figure 4.1). It is constructed from painted carbon steel, but also contains unpainted stainless steel, nylon and proprietary components and is currently protected cathodically by anodes located around the structure (Figure 4.29). It houses electrical connectors (connecting the device to shore via seabed cables). A chain which houses a centrifugal clutch is used for movement of the nacelle between tides. There is approximately 10 mm clearance between the chain and the plastic

protective housing around it. To allow correct movement of the nacelle, sensors are used to monitor how far the chain is moving.

Once attached to the tripod, the semi-enclosed area houses an almost stagnant volume of water with any flow through the central tripod and the winch rope tube, possibly caused by a venturi effect from the seawater flow across the top of the nacelle. A small volume of water can enter the skirt during yawing when the clamp releases, opening a gap a few millimetres wide. The internal capacity of the skirt is 3000-3500 litres with approximately 100-200 litres of water exchanged per day. Therefore the flow in the cavity is minimal.

Figure 4.29. Anodic protection in the skirt area of the device

When the nacelle was deployed, using an integral camera, fish were observed in the skirt. The camera was used to monitor cable movement in the skirt. The camera had a light, although artificial, which may have had an impact on the type and extent of the corrosion and biofouling observed in this area. The anodes located in the skirt area were seen to be significantly spent after three weeks submersion. Corrosion was observed in multiple locations in the skirt region.

The low flow conditions in the skirt lead to flocculation of sediments and deposits of silt forming on surfaces in this area. These may not be significant, but could cause wear, abrasion and possibly enhance corrosion. Conversely, the deposits may deter or discourage fouling on these surfaces due to unsuitable surface conditions for attachment. Also, silt may harbour (anaerobic) bacteria causing a more aggressive environment for corrosion to occur. The degree of enclosure and the presence of light will influence the type and extent of fouling which occurs.

4.4.8 Clamp

The clamp (Figure 4.30) is made from uncoated carbon steel with some external sections painted. No fouling was observed after three weeks submersion. The high friction surfaces are zinc coated carbon steel with bronze alloy (DEVA) bearings. The clamp is tightened when the nacelle is facing the oncoming tide. To allow the device to yaw between tides, the clamp is loosened, the nacelle floats upwards a bit exposing a gap of approximately 3mm this allows a small flow of water into the skirt during yawing operations.

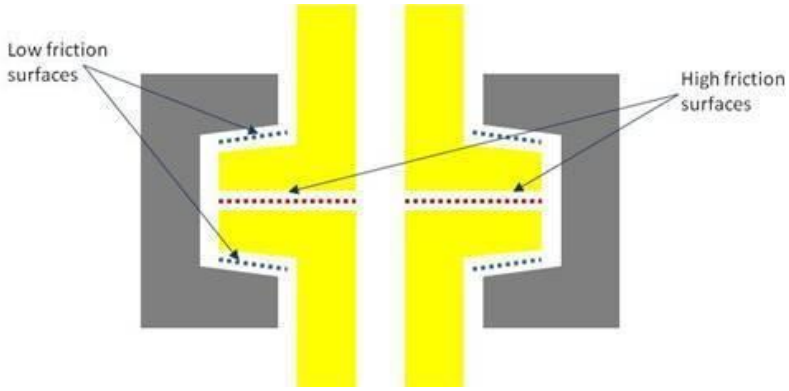

Figure 4.30. Basic schematic of clamp design

To ensure correct movement, no fouling must occur on the high friction surfaces. Any fouling may stop the clamp from working correctly which may result in turbine failure by over-twisting of cables.

Figure 4.31. Painted steel on clamp

The main clamp construction was seen to exhibit corrosion in April 2011, especially on bolts and fixings (Figure 4.31 and 4.32).

Figure 4.32. Corrosion on clamp construction

4.4.9 Thruster

The thruster (diameter 600-700 mm) is located at the back of the nacelle and is open to seawater. The blades are made from stainless steel and the outer case from carbon steel. Although the thruster is open to seawater, no fouling has been observed in this area. This could be because of the regular operation of this device to move the turbine to face the tide cleans away any deposits. However, on inspection in April 2011, corrosion was observed on the flange between the thruster housing and the main nacelle (Figure 4.33) indicating that water has entered the crevice formed between the two surfaces. Any fouling which may occur on or around the thruster will reduce the efficiency and increase the power required to move the nacelle. Sacrificial anodes are located in the thruster housing to protect against corrosion. One anode located in the thruster housing showed signs of corrosion and had provided protection of the metal in this area. Corrosion was also observed around the outer rim of the thruster opening due to coating loss (Figure 4.34).

Figure 4.33. Corrosion of surface between thruster housing and main nacelle

Figure 4.34. Corrosion due to coating removal around rim of thruster opening

4.5 Dummy Foundation

A dummy foundation, used to practice deployment and retrieval of the nacelle was deployed in 2009. In May 2012 this was retrieved from the seabed for maintenance and modification for the DeepGen IV device.

Figure 4.35. Flange at top of dummy foundation prior to cleaning

The dummy foundation had been extensively fouled by a number of species, both hard and soft, including barnacles (Figure 4.35); Larger grazing organisms such as sea urchins (Figure 4.36); common sunstar (Figure 4.37); and painted topshell (Figure 4.38). The Common Sunstar (*Crossaster papposus*) is a circular starfish with 13 arms. It inhabits tidal streams and is found in exposed locations at depths below 15 m (Wood, 2008). The Painted Topshell (*Calliostoma zizyphinium*) is found in water below 9 m depth, and prefers tidal locations where it can feed on algae and bryozoans. It is identified by its conical shape with the pointed apex, and the colours shown in Figure 4.38 (Wood, 2008). In fact, the dummy

foundation had begun to act as an artificial reef, providing a site for the settlement and development of fouling organisms in the area.

Figure 4.36. Common Sea Urchin on flange

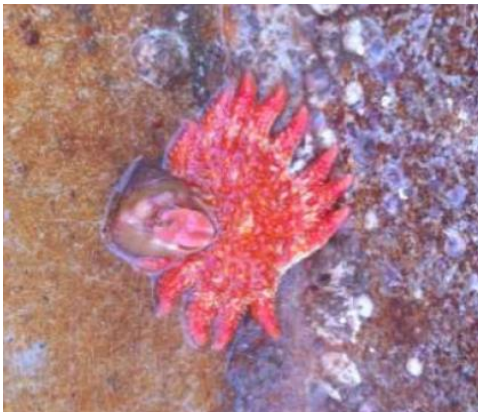

Figure 4.37. Common Sunstar

Figure 4.38. Painted Topshell

Figure 4.39. Flange after cleaning and removal of biofouling

Once the flange had been cleaned of fouling, the extent of the damage to the metal surface beneath could be seen (Figure 4.39). The location of barnacles could be seen where the natural adhesive that attached them still remained on the surface. There was also evidence of localised corrosion around locations where the fouling organisms settled.

Localised corrosion can occur on surfaces that have been settled by macrofouling as crevices are formed close to the fouling causing differential aeration and hence anodic areas can be created on the metal surface.

4.6 Final Observations of the DeepGen III Device

In August 2012, the 500 kW device was out of the water in preparation for deployment of the 1 MW prototype. The opportunity was taken to inspect the device for any further corrosion that had taken place. At this time, the device had been out of the water for several months and had suffered from degradation in various areas due to atmospheric corrosion. The following images were taken on 20th August 2012.

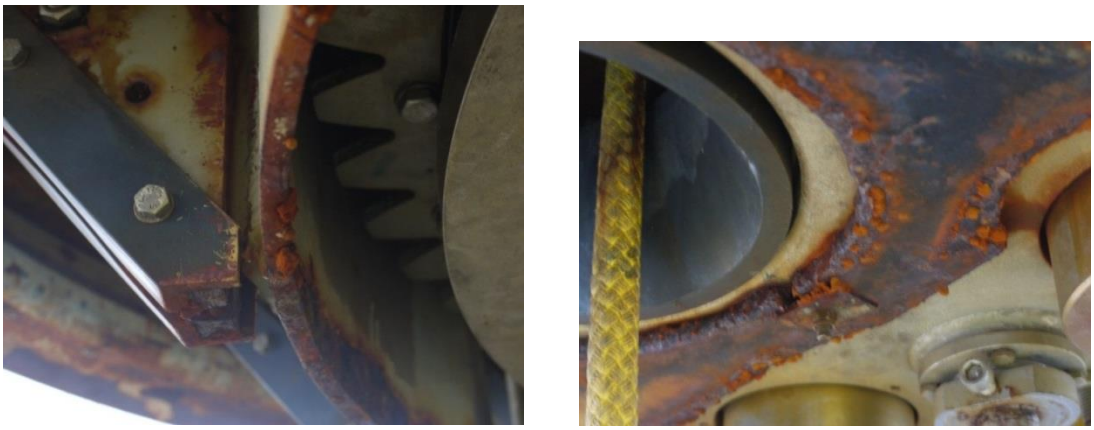

Figure 4.40 (a) and (b). Build-up of corrosion product in skirt

Figure 4.41 (a) and (b). Corrosion in skirt area and blistering of protective paint around fixings

Figure 4.42. Corrosion on clamp equipment

Figure 4.43. Corrosion on nacelle in small areas where protective paint has been removed

Figure 4.43 shows the anode located towards the front of the nacelle. This had corroded and therefore it had provided corrosion protection to the device whilst it was underwater. The anode had not completely corroded and so sufficient protection had been provided throughout the duration of deployment. However, it may be the case that further anodes are required in other locations where corrosion is more prolific. Corrosion of small areas on the nacelle was also evident, where impact has caused the protective paint coating to be lost. This had occurred significantly on all flanges. The majority of fixings on the nacelle also exhibited corrosion (Figures 4.44 and 4.45), which may cause problems in the future if these need to be removed.

Figure 4.44. Corrosion and paint removal around fixings

Figure 4.45. Corrosion around blade root fixings

4.7 Relevance to Risk Management Development

The estimated design life requirement of tidal stream turbines is 25-30 years. Planned maintenance schedules are required to be every 2 years for minor maintenance and every 10 years for major maintenance to fit in with their economic forecasts. The tripod will remain on the seabed for the entire lifetime of the device. No maintenance is scheduled for the tripod during this period. The turbine design allows for easy (although fairly costly) deployment and retrieval. Due to this, maintenance is expected to be carried out on the

quayside, reducing the costs associated with *in situ* maintenance which would require deployment of divers and Remotely Operated Vehicles (ROVs).

This investigation has highlighted the extent and type of fouling and corrosion which can occur on a real structure, allowing correlation to the literature and with further studies as well as identifying areas with high potential for fouling and corrosion in the future. It has also identified the requirement for on-going evidence gathering and documentation to ensure that sufficient longer term data is obtained throughout the device lifetime to ensure correct management of risks.

4.8 Conclusions

The observations presented in this chapter form the basis of the development of a risk based management system (Chapter 9) for corrosion and biofouling, including development of risk based inspection. A number of areas on the DeepGen III device exhibit extensive corrosion and settlement of biofouling during short deployment periods and so have provided valuable input to the risk analysis and future developments and modifications. The extent of corrosion and biofouling that has already occurred highlights how this may become a significant issue for the turbine over the design life if not effectively managed. The tripod remains on the seabed and it was difficult to observe in detail any corrosion that may have occurred by reviewing the ROV footage due to insufficient resolution. However, corrosion could be seen on various parts of the device.

Key findings for the risk assessment are as follows:

- External and internal surfaces on the tripod have been fouled along with the cartridge plate and ADCP (all remaining in the water for extended periods). Many external surfaces had been fouled by barnacles. In past studies in the North Sea (Forteath et al., 1982) it was observed that mussels are often found on surfaces at depths between 30-70 m. It was also found that structures submerged in seawater are primarily colonised by barnacles in the first 1-2 years. After this period, mussels will tend to become dominant. The mussel *Modiolus modiolus* has been identified in the area around Orkney at depths of between 5 and 70 m in fully saline conditions (Bennett and Covey, 1998). It is also thought that the inflow of Atlantic water southwards into the north region of the North Sea in late summer/autumn may

introduce further oceanic species including zooplankton *Salpa fusiformis* (Reid et al., 2003).

- Sheltered regions (seen in the crevices on the ADCP and also on cartridge plate) had fouled extensively.
- Considerable soft fouling had occurred in pipes and the skirt region (dark and little flow).
- No hard fouling was observed in regions of low flow (pipes and skirt region).
- More fouling could be seen on horizontal surfaces than on vertical surfaces which, due to period of immersion, agrees with past research (Forteath et al., 1984). Research conducted on the Montrose Alpha platform in the late 1970s when first constructed has shown that the type of marine growth on a structure is related to depth, and hence light (Forteath et al., 1982). The work found that seaweeds dominate from MLW (mean low water) to a depth of 10 m due to sunlight conditions. The seaweeds were replaced by arborescent bryozoans (small colonial organisms) down to a depth of 31 m. Below this depth calcareous and encrusting bryozoans dominated until below a depth of 71 m where aggregate tubeworms *Filograna implexa* and deep-water barnacles *Balanus hameri* were prominent.
- No biofouling settlement had occurred on the white plastic housing of the ADCP. This could have been due to the surface smoothness or the flow pattern around the device. The latter is a more likely explanation due to the observation of settlement in crevices.
- Man-made structures below the surface of the sea, in any location, act as artificial reefs for a plethora of marine life (Langhamer et al., 2009; Guerin et al., 2007) as well as being subjected to corrosion related issues at all depths of immersion. It is thought that when these devices have been deployed for longer periods when fully operational the majority of surfaces will eventually foul as the device becomes more of an artificial reef. Located on the nacelle are areas of complexity such as the access hatch located on the top of the structure and flanges. These areas are required to be fully operational after deployment for maintenance or access. Therefore, it would be desirable for these not to become fouled or corroded.

- Localised corrosion is likely to occur where paint had been lost. This had already occurred on various parts of the nacelle and is likely to be caused by the high flow conditions or human error during maintenance.
- The high flow conditions had caused the Xylan paint coating to be removed from bolts on the nacelle. This will lead to corrosion of bolts and possible loss of integrity.
- Grease and plastic caps used on studs on the blades had not protected against water ingress, which is likely to lead to localised corrosion.
- Silt settlement had occurred in the skirt region. This may lead to corrosion due to abrasion and wear and serve as an environment for bacteria.
- Gasketed joints in the skirt may leak which will lead to further corrosion.
- Several areas of corrosion have been observed in the skirt region, with some galvanic corrosion occurring. The anodes used in the region had been significantly used.
- Barnacles need to be in an area where there is sufficient seawater flow as they filter feed. However, there is an optimum flow speed as, if too fast, it is difficult for them to settle and adhere to the surface. If there is no flow, the barnacles will eventually die as they will not be able to get food. Although barnacle fouling is important in these deployments, it is noted that research has found that barnacle growth is only important in the first 1-2 years of submersion and of little importance once mussel communities are formed (Picken and Grier, 1984).
- Bolts and fixings have been observed to both have been corroded and settled by biofouling. These will be important components in the future of the device, especially where they need to be removed for inspection and maintenance. If bolts and fixing are extensively corroded it is probable that it will not be possible for them to be removed and as such cause problems with the overall operation of the device.

This investigation leads to the development of experienced-based risk identification and analysis (Chapter 9) to highlight all potential threats associated with corrosion and biofouling of the various parts on the device. The evidence base will also be used to aid the development of risk treatment methodologies outlined in Chapters 9 and 10.

Chapter 5

Developing the Evidence Base (iii) - *In Situ* Testing and Monitoring of Carbon Steel

5.1 Introduction

In order to validate, or otherwise, the use of existing literature and case studies, data should be gathered relating directly to tidal power devices. Ideally this should be done by observation of, and sampling from, a working device, as in Chapter 4. However, such direct data gathering is not straightforward because of the limited number of such devices, access issues, and a lack of control over sampling times and exposure periods. Chapter 4 provided an insight into the corrosion and biofouling developing on an example tidal device. However, data was only obtainable when the device was retrieved for maintenance, with only minimal data available for the tripod based on one remotely operated vehicle (ROV) survey. In order to improve understanding of the types and succession settlement of fouling organisms and associated corrosion a controlled series of *in situ* experiments was devised. Carbon steel being the main material of construction was analysed. *In situ* tests were carried out to investigate the level of biofouling and corrosion over one year on plates submerged next to the quayside in Kirkwall, Orkney. While these experiments were not at the site of a working device they were in the same body of water and within 15 miles of the deployment area. In addition, during initial risk assessment discussions with the company it was possible that the deployment of a device may be delayed due to adverse weather conditions. This would mean that a device may be left in the water next to the quayside for a period of time before or on return from deployment, especially when operating arrays of a large number of devices. While it is thought that this exposure would not normally exceed 3 months, such “storage” may be extended due to continuation of adverse weather conditions, lack of a deployment vessel or backlog of devices awaiting deployment. Experiments were thus conducted to determine possible corrosion and biofouling issues that may occur on the nacelle, especially in areas where the paint coating has been compromised, either during operation or damage incurred due to retrieval or deployment back into the water at the quayside.

5.2 Panel Dunk Tests – Deployment and Methodology

5.2.1 Panel Holder Design and Placement

A panel holder (Figure 5.1) was obtained from Plymouth Marine Laboratory (PML), Plymouth, UK (PML are currently conducting tests on tidal devices to assess types of antifouling coatings). These panel holders were constructed by PML following discussions on some aspects of the design criteria with the group in Chemical and Biological Engineering, University of Sheffield, Sheffield, UK. The structure can hold 10 square panels (in this case of S355 carbon steel, Table 5.1 shows the chemical composition of carbon steel S355 in accordance with BS EN 10225:2009) separated by plastic spacers from each other and from the metal structure itself.

Table 5.1. S355 10225 G8+N typical specified composition

S355 G8+N	C max	Si	Mn	P max	S max	Cr max	Mo max	Ni max	Al (total)	Cu max	N max	Nb max	Ti max	V max
	0.14	0.15 to 0.55	1.00 to 1.65	0.020	0.007	0.25	0.08	0.50	0.015 to 0.055	0.30	0.010	0.040	0.025	0.060

The panel design is shown in Figure 5.2. The ten panels were deployed from the quayside on 22nd May 2012. At this time, the water temperature was 8.0 ^{o}C, salinity 35.0 ppt and dissolved oxygen 8.19 ml/l. Flow rate was not measured due to difficulty in determining an average flow rate over the period of immersion. However, flow rate was observed as minimal in the sheltered location except during periods of inclement weather. Figure 5.3 shows the panel holder prior to deployment, whilst Figure 5.4 shows the location of the panel holder once deployed. The panels were first removed for inspection after three months, in August 2012, and every three months subsequently until May 2013.

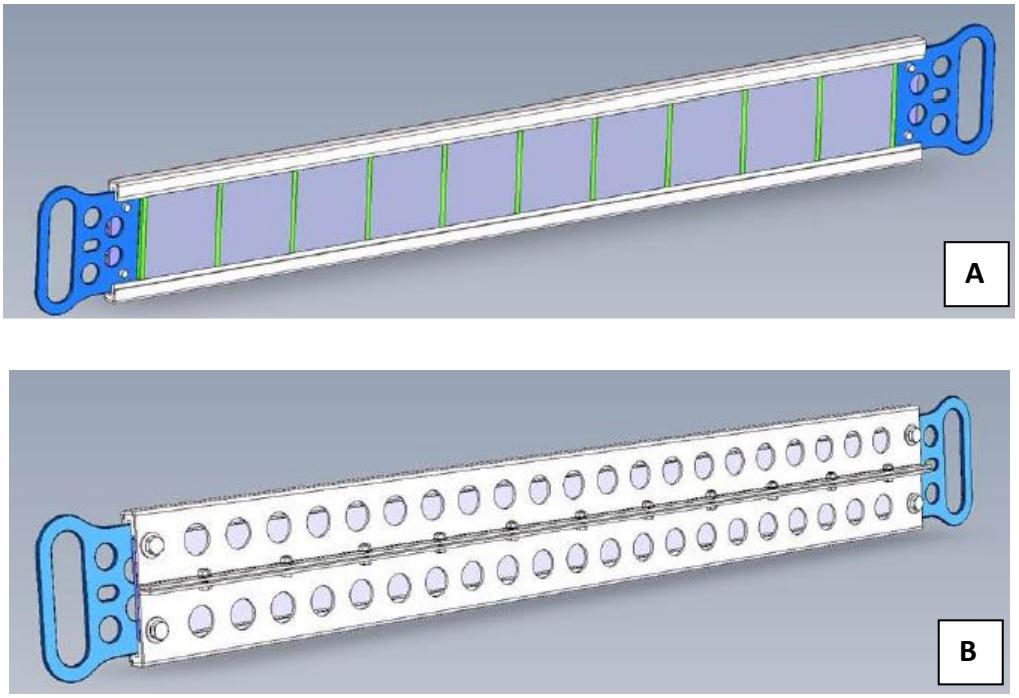

Figure 5.1. Panel holder schematic, (A) front and (B) back of the device

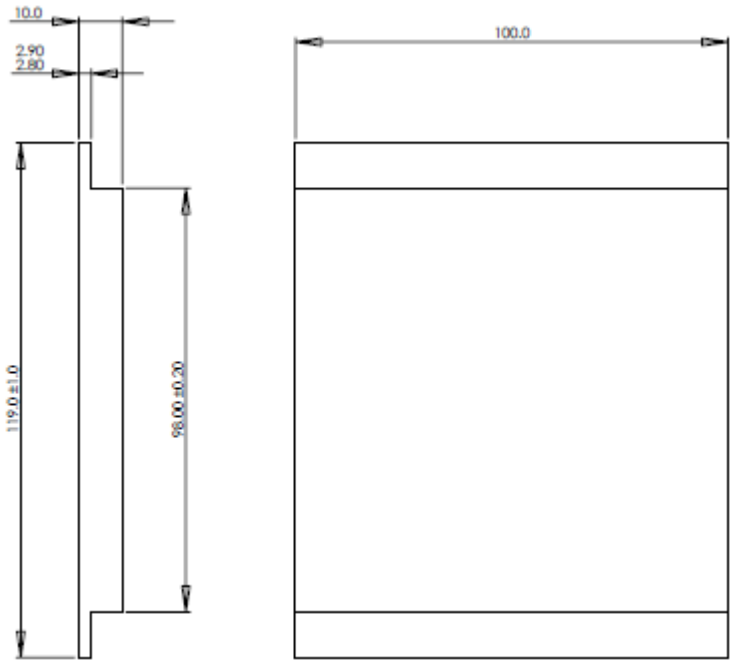

Figure 5.2. Schematic of panels including dimensions (units in mm)

The panels were designed as shown in Figure 5.2 so that they could slot easily into the holder between the plastic spacers. This design ensures that the panels will not fall out of the holder but that, when required, the panels can be slid out of the end of the holder and new panels installed.

The carbon steel panels were immersed in an 'as-rolled' condition to replicate the conditions of the metal used on the device itself. Previous work has shown that this surface finish is likely to have only a short term, temporary effect on the corrosion rate (Evans, 1960), and so should not effect this longer-term study.

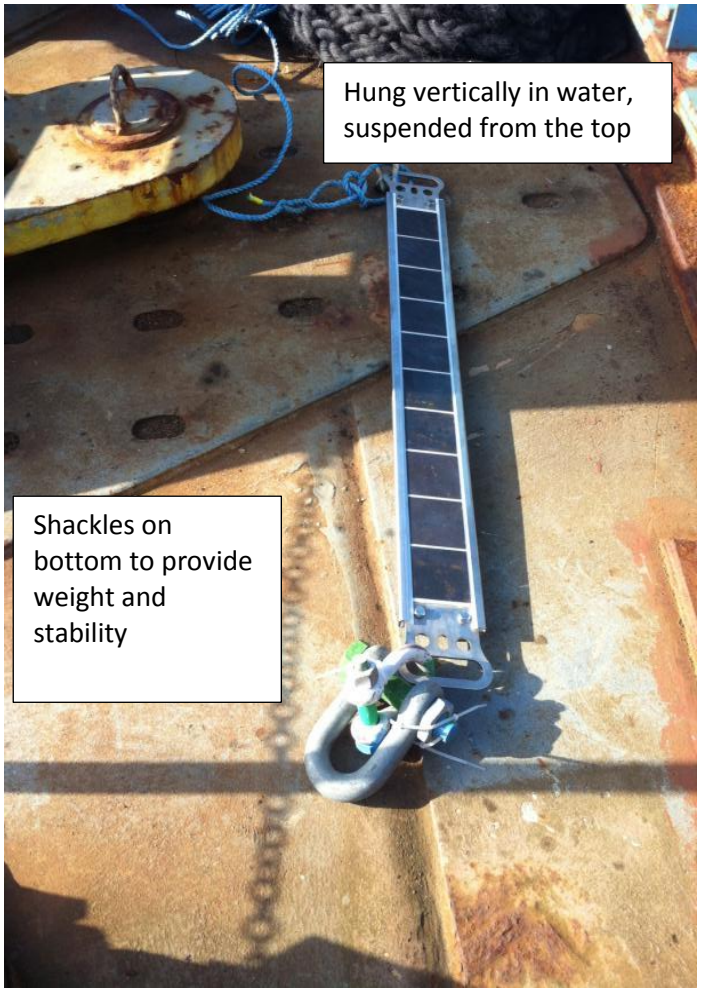

Figure 5.3. Panel holder prior to deployment May 2012

On initial deployment in May 2012, it was recognised that a weight (shackle) of approximately 6-8 kg was required on the bottom of the panel holder to ensure that the equipment would remain in a vertical position (Figure 5.3). The holder was attached to the side of the crane barge using rope so that it was suspended vertically in the water at a mean depth of 2.5 m.

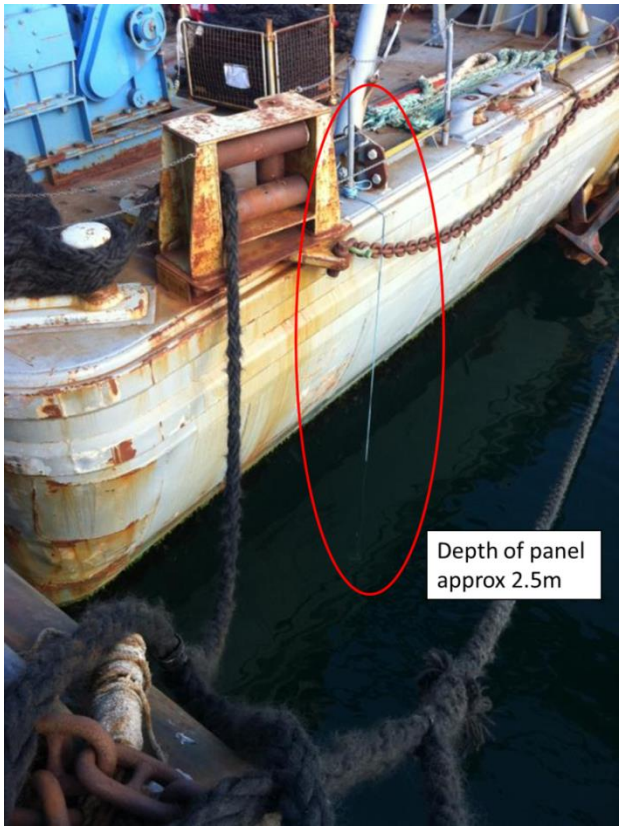

Figure 5.4. Deployment location

5.2.2 Inspection Methodology

At each retrieval the panel was examined and photographed and three of the panels were removed for further analysis and replaced with new panels. Panels were transported to Sheffield, immersed in seawater, in sealed insulated containers. The panels remained in a refrigerator until analysis. Each panel was analysed for the type and percentage cover of fouling. Corrosion rates were determined by a gravimetric method. At the time of panel removal, the temperature, salinity and dissolved oxygen levels were noted using an Orion 5-Star water meter.

5.2.3 Corrosion Analysis

All coupons were analysed for corrosion type and rate in the Department of Chemical and Biological Engineering, University of Sheffield, UK. The panels were cleaned with a 50/50 water/acetone mix to ensure that the any dirt, oil or grease was removed from the surface in accordance with procedures described in ASTM G1-03 (ASTM, 2011).

The coupons were then reweighed and the original weight of the panel less the weight after exposure was used to determine an overall average corrosion rate of the sample using Equation 5.1 (ASTM, 2011).

$$Corrosion\ Rate\ (CR) = \frac{Weight\ Loss\ (g) \times K}{Density\ \left(^{g}/_{cm^3}\right) \times Exposed\ Area\ (mm^2) \times Exposure\ time\ (hr)} \qquad [5.1]$$

Where K is a conversion factor for a corrosion rate in millimetres/year (mm/yr) equal to 8.76×10^4.

Placing three new panels at each three month retrieval allowed differences between different seasons and exposure durations to be assessed. Figure 5.5 shows the sampling procedure used for these tests.

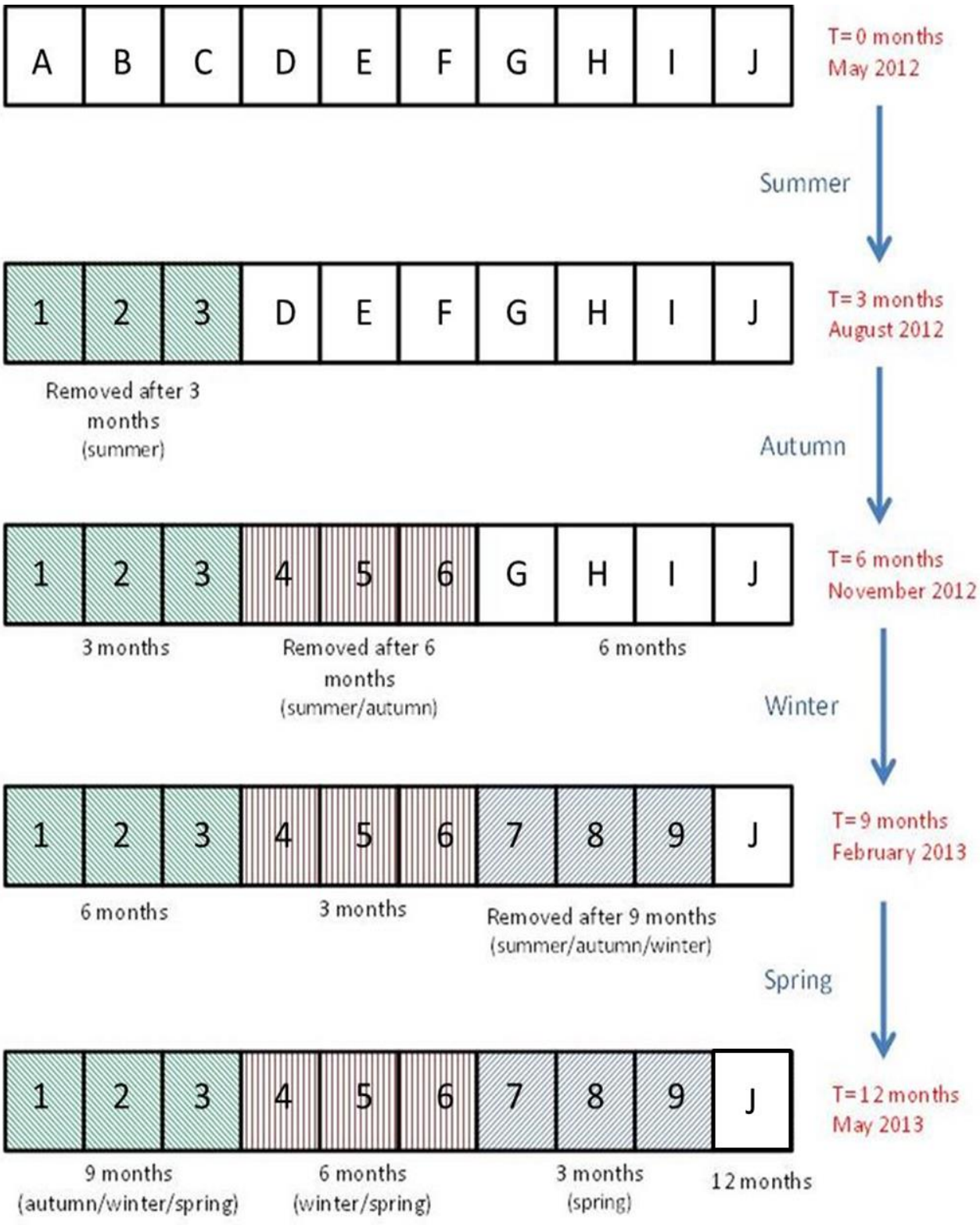

Figure 5.5. Process for panel testing

At the end of the testing the following panels were available for analysis:

- 3 x 3 months over summer
- 3 x 6 months over summer and autumn
- 3 x 9 months over summer, autumn and winter
- 3 x 9 months over autumn winter spring
- 3 x 6 months over winter and spring
- 3 x 3 months over spring
- 1 x 12 months

5.3 Results and Discussion - Biofouling

5.3.1 August 2012 – three months over summer

The panel holder was retrieved on 20th August 2012 and the first three panels removed. The panel holder and rope used for suspension were both covered in seaweed. Three panels were removed, and the plastic underneath these was cleaned of corrosion product before new panels were placed in the panel holder. Photographs were taken of all panels and the biofouling that had occurred over the period of May 2012 to August 2012 (Figures 5.6 to 5.16).

Temperature, salinity and dissolved oxygen levels recorded in August 2012 are given in Table 5.2.

Table 5.2. Water conditions August 2012

Factor	Value
Temperature (°C)	14.8
Salinity (ppt)	35.0
Dissolved Oxygen (ml/l)	6.64

Figure 5.6. All panels on retrieval in August 2012

All panels showed signs of corrosion product. The panels were evenly rust coloured over the surface but corrosion product was thicker and flakier around the edges of the panels at joints between the metal panels and the plastic holder. All panels had been fouled, covered in a thin "slime layer" and some sea squirt growth.

Figure 5.7. Corrosion and biofouling observed on panel A

Figure 5.7 shows a tube worm (*Pomatocerous triqueter*) that had settled on the panel. The same was found on panels D and F (Figure 5.10 and Figure 5.12). This is quite common on the lower shore in the North Sea region and is a fast growing colonising species. It has a small diamond-shaped tube, and can grow to 5 cm in length (Wood, 2008).

Figure 5.8. Corrosion and biofouling on panel B

Figure 5.9. Corrosion and biofouling on panel C

Figure 5.10. Corrosion and biofouling on panel D

Figure 5.11. Corrosion and biofouling on panel E

Figure 5.12. Corrosion and biofouling on panel F

Figure 5.13. Corrosion and biofouling on panel G

Figure 5.14. Corrosion and biofouling on panel H

Figure 5.15. Corrosion and biofouling on panel I

Figure 5.16. Corrosion and biofouling observed on panel J

The majority of the fouling observed for this period was soft fouling with only limited hard fouling in the form of tube worms. A small amount of hydroid growth was also observed on the panels and on the outer edge of the panel holder.

A 100 x 100 mm grid was used to examine the panels after each immersion. This allowed determination of fouling coverage (percentage). The results and description of the fouling type are presented in Table 5.3.

Table 5.3 Fouling coverage assessment August 2012

Panel	Percentage Cover ±0.25%	Description of Fouling
A	35%	New soft growth with minimal profile. Tube worm.
B	66%	New soft growth with minimal profile.
C	50%	New soft growth with minimal profile.
D	29.75%	New soft growth with minimal profile.
E	24.5%	New soft growth with minimal profile.
F	33%	New soft growth with minimal profile. Tube worm.
G	54%	New soft growth with minimal profile.
H	25.5%	New soft growth with minimal profile.
I	54.5%	New soft growth with minimal profile.
J	46.5%	New soft growth with minimal profile.

5.3.2 November 2012 - six months over summer/autumn

Panels D, E, F were removed from the panel holder for analysis on 29th November 2012. These were replaced with new panels (4, 5 and 6).

Temperature, salinity and dissolved oxygen levels are given in Table 5.4. In comparison to August 2012, the temperature of the water had dropped significantly, with an increase in dissolved oxygen level as expected with a lower temperature. The salinity remained unchanged.

Table 5.4. Water Conditions November 2012

Factor	Value
Temperature (°C)	10.2
Salinity (ppt)	35.0
Dissolved Oxygen (ml/l)	8.23

Figure 5.17 shows the whole panel holder. Fouling was observed on all but the top three (new) panels (1, 2 and 3). Fouling had also settled on the suspension rope and on the panel holder itself (stainless steel). No fouling was observed on the shackle weight at the bottom of the panel holder.

Figure 5.17. Panel holder on removal from the sea in November 2012

Fouling was observed on the back of the panel holder, although not in such a high concentration (Figure 5.18). The back of the panel holder was against the crane barge, and therefore more sheltered from light than the front of the holder.

Figure 5.18. Back of panel holder in November 2012

The three panels that were immersed in August 2012 (now three months exposure) exhibited no fouling and had only loose corrosion product that was easily wiped off (Figure 5.19). This shows that the amount of fouling organisms settling during the period between August 2012 and November 2012 was minimal relative to the extent of fouling between May 2012 and August 2012.

On the panels subject to 6 months of immersion the soft fouling observed previously had increased markedly (Figure 5.17).

Figure 5.19. Panels 1, 2, 3 exhibiting no fouling

No fouling was observed on Panels 1, 2 and 3 which had been in place 3 months (Figure 5.19). The difference between these and the remaining panels in place since May 2012 was very marked (Table 5.5). This showed that the fouling vectors (spat and spores) settled on the submerged surfaces in the summer months. The fouling that was observed in August 2012 had grown rapidly from approximately 1.5 cm in diameter with a low profile to 6-8 cm diameter on all other panels (Figures 5.20 to 5.22).

Figure 5.20. Panels D, E and F exhibiting significant fouling growth

The fouling observed on the three panels to be removed, (D, E, and F, Figure 5.20) had grown and developed in the months between August and November 2012, indicating (in comparison to panels 1,2,and 3) that this fouling had settled prior to August. The majority of the fouling on these panels was soft fouling, mainly sea squirts (see Table 5.5).

Figure 5.21. Panels E, F and G fouling growth

Figure 5.22. Panels H, I and J fouling growth

All other original panels also exhibited soft fouling, including sea squirts, sponges and hydroids. This fouling was less dense towards the bottom of the panel holder (see Table 5.5), (Compare panels D, E and F in Figure 5.20 with lower panels in Figures 5.21 and 5.22).

Figure 5.23. Fouling along edge of panel holder

Figure 5.24. Sea squirts on the back of panel holder (a Star Ascidian (*Botryllus* schlosseri) is circled

Fouling was not limited to the carbon steel. The stainless steel outer casing of the panel holder was also fouled by soft fouling, including sea squirts, sponges and hydroids (Figure 5.23). No fouling was actually attached to the visible white plastic spacers, although the fouling had grown over this in areas.

Sea squirts and sponges (*Sycon ciliatum*) had also settled and developed on the back of the panel holder (Figure 5.24 – 5.26).

Figure 5.25. Tube worm

Figure 5.26. Sponges (back of panel holder)

Several tube worms were also observed around the holder. One such organism is circled in Figure 5.25. Another tube can be seen above the circle.

Figure 5.27. Hydroids and tube worms

Figure 5.28. Algae growth

Hydroid and algae growth can be seen in Figures 5.27 and 5.28.

Panels D, E and F were analysed further under controlled conditions at The University of Sheffield. The soft fouling was removed, and on panel D a small tube worm was observed on the metal surface. This was underneath the soft fouling and so was not evident until this was removed. Panel F also had been fouled by a tube worm, as well as hydroids and sea squirts. The soft fouling was coloured red on this coupon. An analysis of the percentage

cover of all panels in November 2013 was carried out to allow comparison throughout the experiment. The results and description of the fouling type are presented in Table 5.5.

Table 5.5 Fouling coverage assessment November 2012

Panel	Percentage Cover ±0.25%	Description of Fouling
1	0%	No fouling observed
2	0%	No fouling observed
3	0%	No fouling observed
D	100%	Soft growth including sea squirts and hydroids
E	100%	Soft growth including sea squirts and hydroids
F	88%	Soft growth including sea squirts and hydroids
G	57.5%	Soft growth including sea squirts and hydroids
H	79%	Soft growth including sea squirts and hydroids
I	86.5%	Soft growth including sea squirts and hydroids
J	89.25%	Soft growth including sea squirts and hydroids

5.3.3 February 2013- three months, six months and nine months exposure

The panel holder was taken out of the water on 20th February 2013 for removal of panels G, H and I. Unfortunately in January 2013 the Orkney Islands were subjected to a significantly stormy period, with up to 100 mph gusts reported. In this time the panel holder suffered impact with the quayside and the barge from which it was suspended. This caused large amounts of the fouling to be removed from one side of the holder. Photographs were taken of all panels, and of the fouling that had remained on the back of the panel holder (Figures 5.29 to 5.36). Panels G, H and I were removed and replaced with Panels 7, 8 and 9. The water conditions recorded in February 2013 are given in Table 5.6.

Table 5.6. Water Conditions February 2013

Factor	Value
Temperature (°C)	6.0
Salinity (ppt)	34.9
Dissolved Oxygen (ml/l)	8.56

An analysis of the percentage cover of all panels in February 2013 was carried out. The results and description of the fouling type are presented in Table 5.5.

Table 5.7 Fouling coverage assessment February 2013

Panel	Percentage Cover ±0.25%	Description of Fouling
1	85.25%	Hydroids
2	90%	Hydroids and sea squirt
3	85%	Hydroids and sea squirts
4	0%	None
5	0%	None
6	0%	None
G	41.25%	Hydroids and sea squirts
H	75%	Hydroids and sea squirts
I	85.25%	Hydroids and sea squirts
J	89%	Hydroids and sea squirts

Figure 5.29. Panels on removal in February 2013

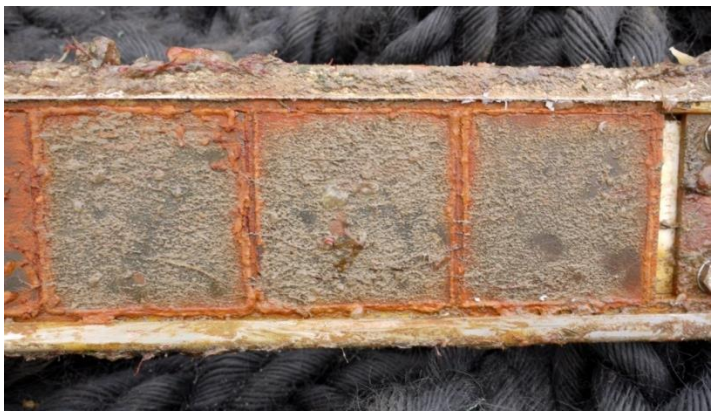

Figure 5.30. Panels 1, 2 and 3 February 2013

Figure 5.31. Panels 4, 5 and 6 February 2013

Figure 5.32. Panels G, H and I February 2013

Figure 5.33. Panel J February 2013

Minimal fouling was observed on all panels (Figures 5.29 to 5.33). However, fouling, dominated by Sponges and sea squirts (Figure 5.34 and 5.35) remained on the back of the panel holder on the stainless steel casing (Figure 5.34).

Figure 5.34. Fouling on the back of the panel holder February 2013

Figure 5.35. Urn sponges and Sea squirts

Figure 5.36. Red algae February 2013

This area was potentially shielded from the extensive wave action during the adverse weather conditions and provided crevices which might have been a more attractive surface for settlement of organisms.

5.3.4 May 2013 - three, six, nine and twelve months exposure

All panels (including panel J which had been in place for 12 months) were removed on 23rd May for final analysis. The panels that remained at this stage were panels 1 to 9 and J. The panels removed had been submerged for different length intervals and the analysis of corrosion is documented in Section 5.4. Table 5.8 provides an overview of the water conditions in May 2013 and Table 5.9 shows the fouling coverage for all panels. The temperature in May 2013 had increased in the 3 months from February 2013, and was closer to the levels reported in November 2012.

Table 5.8. Water Conditions May 2013

Factor	Value
Temperature (°C)	9.8
Salinity (ppt)	35.0
Dissolved Oxygen (ml/l)	8.23

On removal of the panel holder in May 2013, significant corrosion product was observed on all ten panels. Only limited fouling had developed on the front of the carbon steel panels (Figure 5.37), indicating that little settlement had taken place, although there was more than that recorded in February 2013. The back of the panel holder remained extensively fouled (Figure 5.38).

Table 5.9 Fouling coverage assessment May 2013

Panel	Percentage Cover ±0.25%	Description of Fouling
1	86.25%	Hydroids and sea squirt
2	91.5%	Hydroids and sea squirt
3	85%	Hydroids
4	28%	Hydroids
5	15%	Hydroids
6	12.5%	Hydroids
7	7.25%	Hydroids
8	7.75%	Hydroids
9	9%	Hydroids
J	89%	Hydroids

Figure 5.37. Panel holder on final retrieval in May 2013

Figure 5.38. Back of panel holder on final retrieval in May 2013

5.3.5 Biofouling Discussion

Fouling settled over spring and summer months, growing in the autumn and winter. It was found that the weather conditions in Orkney in the winter 2012/2013 when high winds caused significant wave action, led to substantial removal of biofouling that had settled and developed on the surface of the test coupons. While a tidal device will not experience the buffeting that these specimens did, it is likely that rougher winter conditions would sweep abrasive materials over the device, detaching fouling organisms. However, in a stable and deeper environment the fouling on the device may take slightly longer to establish and grow (Jenkins and Martins, 2010), but are less likely to be removed. In Chapter 4, a device submerged at a depth of 40 m below sea level for approximately 18 months showed minimal fouling on surfaces.

Table 5.10 Comparison of fouling coverage on removal

Panel	Aug 2012	% Change	Nov 2012	% Change	Feb 2013	% Change	May 2012	% Change
A	35%	**+35%**	-	**-**	-	**-**	-	**-**
B	66%	**+66%**	-	**-**	-	**-**	-	**-**
C	50%	**+50%**	-	**-**	-	**-**	-	**-**
D	30%	**+30%**	100%	**+70%**	-	**-**	-	**-**
E	25%	**+25%**	100%	**+76%**	-	**-**	-	**-**
F	33%	**+33%**	88%	**+55%**	-	**-**	-	**-**
G	54%	**+54%**	58%	**+3.5%**	41%	**-16%**	-	**-**
H	26%	**+26%**	79%	**+54%**	75%	**-4%**	-	**-**
I	55%	**+55%**	87%	**+61%**	85%	**-1.3%**	-	**-**
J	47%	**+47%**	89%	**+43%**	89%	**-0.25%**	89%	**0%**
1	-		0%	**0%**	85%	**+85%**	86%	**+1%**
2	-		0%	**0%**	90%	**+90%**	92%	**+1.5%**
3	-		0%	**0%**	85%	**+85%**	85%	**0%**
4	-		-	**-**	0%	**0%**	28%	**+28%**
5	-		-	**-**	0%	**0%**	15%	**+15%**
6	-		-	**-**	0%	**0%**	13%	**+13%**
7	-		-	**-**	-		7.3%	**+7.3%**
8	-		-	**-**	-		7.8%	**+7.8%**
9	-		-	**-**	-		9.0%	**+9.0%**

The season in which the metal surface is placed in the seawater will have a significant impact on the succession of the substrata due to the seasonality of organisms' reproductive pattern, growth and development as well as seasonal variation in environmental conditions (local temperature, dissolved oxygen level) (Jenkins and Martins, 2010). From Table 5.10 it can be seen that no fouling grew in the first three months of immersion when this was over autumn and winter (low temperature). The highest percentage increases in fouling coverage were on panels that were immersed for three months in spring or summer (higher temperature). The highest percentage coverage was seen in November 2012 on panels immersed for six months over summer and autumn. During this period, the fouling had settled and grown on the surface.

The panels were immersed at a depth where light was still able to penetrate. The availability of light is a strong factor in determining the volume of photosynthetic algae

within biofouling communities developing on a surface (Cowie, 2010). As depth increases, the volume of algae is much less significant. At the depth tested here it would be expected that algae would grow on the panels, as observed. However, less algae are expected to grow when the device is operational *in situ* due to the greater depth of operation. These tests have highlighted the potential biofouling that may occur if devices are stored in a location such as this prior to maintenance or prior to deployment.

5.4 Corrosion Results and Discussion

The results of the weight loss measurements to determine corrosion rate are given in Table 5.11.

Table 5.11. Corrosion Weight Loss Results

Panel	Deployment date	Starting Weight (±0.2 g)	Retrieval Date	End Weight (±0.2 g)	Weight Loss (g)
A	22nd May 2012	823.4	20th August 2012	815.8	7.6
B	22nd May 2012	808.4	20th August 2012	801.0	7.4
C	22nd May 2012	825.6	20th August 2012	818.6	7.0
D	22nd May 2012	825.2	29th November 2012	812.0	13.2
E	22nd May 2012	832.6	29th November 2012	820.0	12.6
F	22nd May 2012	825.8	29th November 2012	811.0	14.8
G	22nd May 2012	814.8	20th February 2013	798.4	16.4
H	22nd May 2012	829.4	20th February 2013	810.2	19.2
I	22nd May 2012	829.0	20th February 2013	811.2	17.8
J	22nd May 2012	830.4	23rd May 2013	807.6	22.8
1	20th August 2012	800.2	23rd May 2013	782.6	17.6
2	20th August 2012	811.8	23rd May 2013	794.6	17.2
3	20th August 2012	813.0	23rd May 2013	797.6	15.4
4	29th November 2012	816.0	23rd May 2013	804.8	11.2
5	29th November 2012	824.2	23rd May 2013	813.2	11.0
6	29th November 2012	819.8	23rd May 2013	810.4	9.4
7	20th February 2013	819.6	23rd May 2013	813.4	6.2
8	20th February 2013	814.2	23rd May 2013	807.2	7.0

9	20th February 2013	813.4	23rd May 2013	806.8	6.6

5.4.1 Corrosion Analysis

The results of the corrosion analysis are given in Table 5.12.

Table 5.12. Calculated Corrosion Rates for all Panels ('*' represents panels that exhibited localised corrosion)

Panel	Season	Exposure time (hr)	Weight loss (g)	Corrosion Rate (mm/yr)
A	Summer	2160	7.6	0.16
B	Summer	2160	7.4	0.15
C	Summer	2160	7.0	0.14
D	Summer/Autumn	4560	13.2	0.13
E	Summer/Autumn	4560	12.6	0.12
F	Summer/Autumn	4560	14.8	0.14
G	Summer/Autumn/Winter	6576	16.4	0.11*
H	Summer/Autumn/Winter	6576	19.2	0.13*
I	Summer/Autumn/Winter	6576	17.8	0.12*
J	Summer/Autumn/Winter/ Spring	8784	22.8	0.12*
1	Autumn/Winter/Spring	6624	17.6	0.12*
2	Autumn/Winter/Spring	6624	17.2	0.12*
3	Autumn/Winter/Spring	6624	15.4	0.10*
4	Winter/Spring	4224	11.2	0.12
5	Winter/Spring	4224	11.0	0.12
6	Winter/Spring	4224	9.4	0.10
7	Spring	2211	6.2	0.12
8	Spring	2211	4.8	0.14
9	Spring	2211	4.6	0.13

Table 5.12 shows the average corrosion rates calculated for the different seasons and also durations of immersion. Figure 5.39 shows the average corrosion rates calculated against duration of immersion (months) and the season over which they were tested (Su indicates Summer; Au Autumn; Wi Winter; Sp Spring). All panels immersed over a summer exhibited the highest corrosion rates compared with the same duration over different seasons. In the summer the water was warmer and more biofouling settled on the panels. Seven of the panels at the end of the testing period had exhibited localised corrosion. These had all

been immersed for nine months or longer (see Table 5.9). Panels that had been immersed for 6 months or less did not exhibit any localised corrosion.

Table 5.13 shows the average corrosion rates determined over immersion duration dependent on season. Table 5.14 shows the analysis of the average corrosion rates in terms of season and average temperature. An increase in temperature increases the corrosion rate for the same period of immersion.

Table 5.13. Average corrosion rates duration and season

Duration	Season	Average Corrosion Rate (mm/yr)
3 Months	Spring	0.13
	Summer	0.15
6 Months	Winter/Spring	0.11
	Summer/Autumn	0.13
9 Months	Autumn/Winter/Spring	0.11
	Summer/Autumn/Winter	0.12
12 Months	Summer/Autumn/Winter/ Spring	0.12

Table 5.14. Significance of season and temperature in determining corrosion rate

Duration	Immersion Period 1 (Average Temperature)	Immersion Period 2 (Average Temperature)	Average Corrosion Rate % Difference
3 Months	Spring (9.8^{o}C)	Summer (14.8^{o}C)	+15.4%
6 Months	Winter/Spring (7.8^{o}C)	Summer/Autumn (12.4^{o}C)	+18.2%
9 Months	Autumn/Winter/Spring (8.7^{o}C)	Summer/Autumn/Winter (10.3^{o}C)	+9.1%

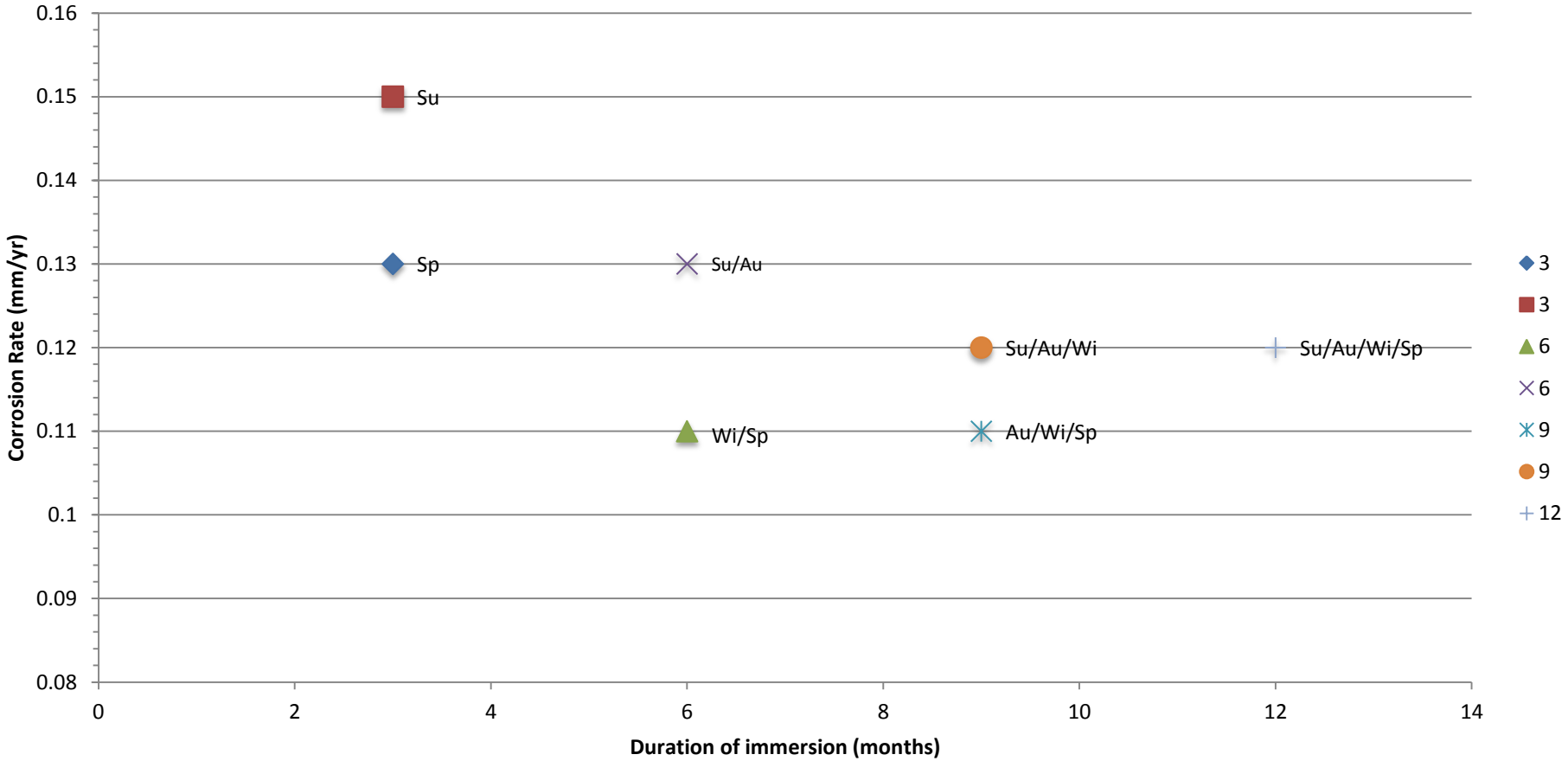

Figure 5.39. Corrosion rates observed relative to immersion duration and season

5.4.2 Localised Corrosion

The three panels removed (G, H and I) in February 2013 after 9 months exposure were analysed. A development in the three months since the removal of panels at the 6 month stage was the onset of localised corrosion on the panels. This was observed on both the front and back of the panels. The corrosion damage was also much more extensive around the exposed edges of the carbon steel near the crevices formed between the panel and the plastic spacers. To document this corrosion damage, microscopic images were taken of the collected panels (Figures 5.40 to 5.45). The red scale in the bottom right of the images represents 500 µm. The localised corrosion was all found to be greater than 1 mm in diameter.

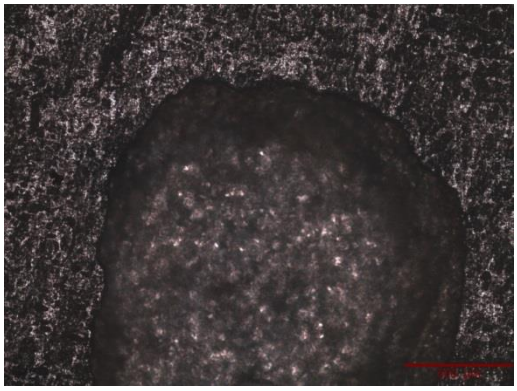

Figure 5.40. Localised corrosion on panel G

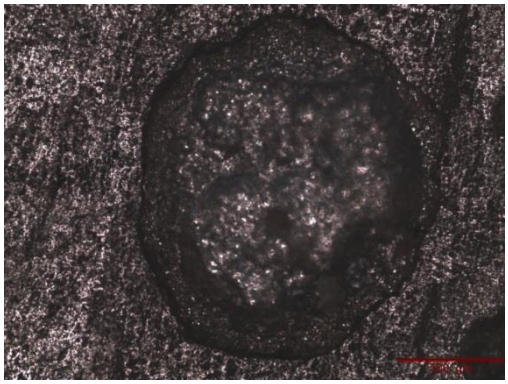

Figure 5.41. Localised corrosion on panel G

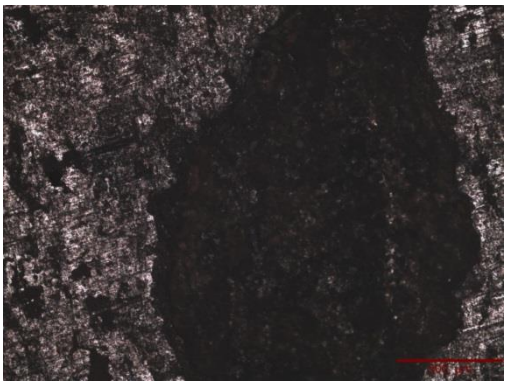

Figure 5.42. Localised corrosion on panel H

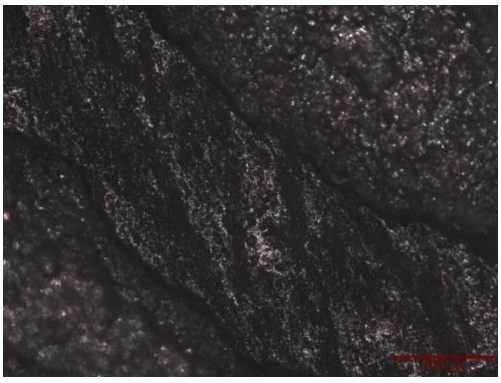

Figure 5.43. Localised corrosion on panel H

Figure 5.44. Localised corrosion on panel H

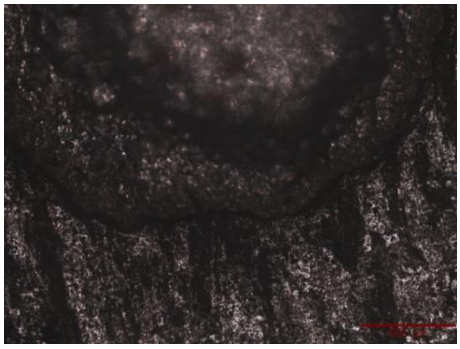

Figure 5.45. Localised corrosion on panel I

At the end of the trials in May 2013 the panels were analysed. Once cleaned, the panels that had been submerged for 9 months or longer showed extensive localised corrosion (Figures 5.46 to 5.49). These panels, along with the panels that had been immersed for 6 months, showed signs of more extensive corrosion around the joint between the panel and the plastic spacers. The red scale in the bottom right of the images represents 500 µm.

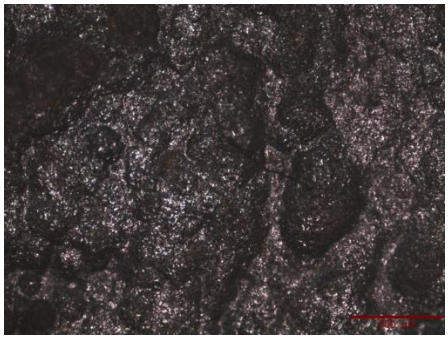

Figure 5.46. Localised corrosion on panel J

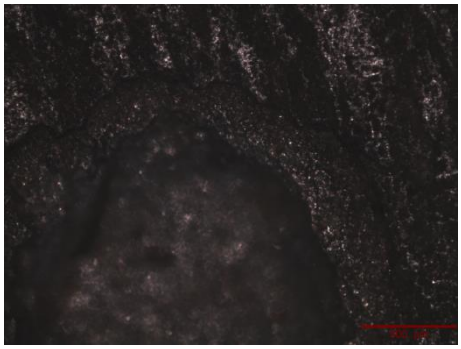

Figure 5.47. Localised corrosion on panel 1

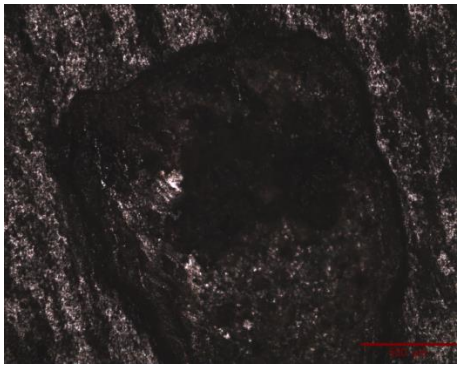

Figure 5.48. Localised corrosion on panel 2

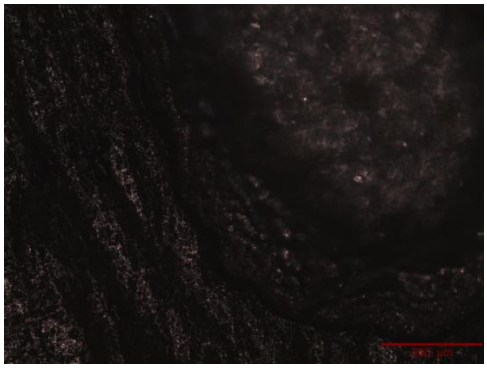

Figure 5.49. Localised corrosion on panel 3

5.4.3 Corrosion Discussion

The storage location (such as tested here) for devices between periods of maintenance and operation has been of practical interest for many years for shipping and also for vertical steel piling (Jeffrey and Melchers, 2009a), though much of the past research has focussed on the differences in corrosion rates between above and below the waterline (Evans, 1960; Jeffrey and Melchers, 2009b).

This corrosion varied between the different seasons, with panels that were immersed over a summer exhibiting higher corrosion rates than over similar durations over different seasons. Previous work has found that specimens immersed in seawater in autumn tend to show less corrosion than specimens immersed in spring for the same period of exposure (Schumacher, 1979; Melchers, 2002). To what extent this is due to the interaction with the fouling organisms and what may be due to temperature effects is examined in Chapter 6 and Chapter 7.

The corrosion rates observed for the carbon steel panels agree with what was expected from evidence previously documented in trials in different locations (Melchers and Jeffrey, 2005; Jeffrey and Melchers, 2009a), where carbon steel coupons were tested using gravimetric assessment to determine the corrosion rate dependence with time (see Table 5.15).

Table 5.15 Comparison of results with published data

Source	Exposure Period	Average Corrosion Rate (mm/yr)
Orkney 2012-2013 Trials (6-14^{o}C)	3 Months	0.14
Orkney 2012-2013 Trials (6-14^{o}C)	6 Months	0.12
Orkney 2012-2013 Trials (6-14^{o}C)	9 Months	0.12
Orkney 2012-2013 Trials (6-14^{o}C)	12 Months	0.12
Melchers and Jeffrey, 2005 Taylors Beach (20^{o}C)	12 Months	0.14
Jeffrey and Melchers, 2009a Jervis Bay (19^{o}C)	12 Months	0.15-0.25

A higher corrosion rate was observed over the shortest period of immersion, 3 months, where initial high corrosion rates were measured. The corrosion rates between immersion durations do not alter dramatically in these tests. It has been found in previous work that there exists only a very short period (less than 5 days) where there is initially a very high corrosion rate before the rate steadily declines over time (Melchers and Jeffrey, 2005) as corrosion product formation begins to control the corrosion process. Therefore, even after 3 months, it is likely that the corrosion rate has reached a steady state with a linear relationship between corrosion loss and time and only the changing environmental factors (temperature, dissolved oxygen and flow) affecting the corrosion rate.

The panels were situated approximately 2.5 m below the waterline. It is postulated that the high corrosion rates that are observed on or just below the waterline are related to the effect of differential aeration between metal that is in the highly aerated waterline region (becomes cathode) and the metal that is further below (anode, therefore greater Fe^{+} loss here). Equally, high corrosion rates observed in this location could be related to the high level of biological activity, including bacteria in this region due to good aeration, nutrients and also light. See Figure 5.50 for typical seawater corrosion profile.

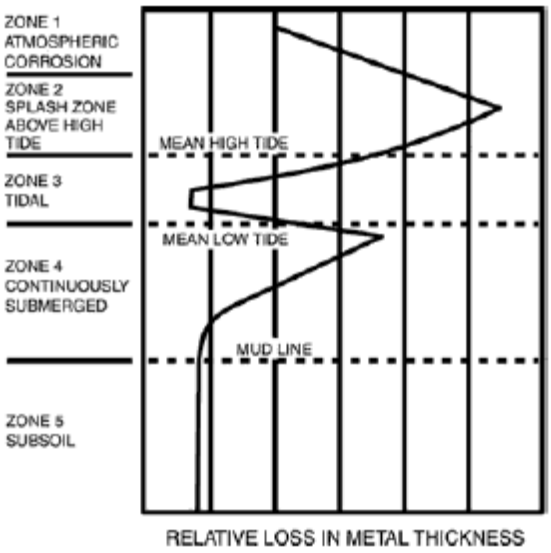

Figure 5.50. Seawater zones and relative loss in steel thickness for unprotected steel structures (Michels and Powell, 2012)

Edge corrosion was observed in November 2012 on all three samples removed at this time (6 months immersion). This was also observed on panels removed in February 2013 (9 month immersion) and May 2013 (on panels immersed for 6, 9 and 12 months). This was not apparent on panels immersed for only 3 months. Other localised corrosion was

observed on all panels that were retrieved after 6 months or longer. This is an indication that devices should not be left in conditions which may encourage localised corrosion (floating at the quayside for example) for any length of time (certainly no more than three months).

5.5 Relevance to Risk Management Development

In terms of managing risk, these tests have shown that tidal devices that are constructed mainly from carbon steel will experience corrosion and biofouling on external surfaces. Panel testing in locations near potential sites provides a good indication of potential levels of corrosion and fouling cover. This is useful to know when evaluating new sites for deployment. However, attention must be paid to even the local variables of flow and depth. The tests also indicate that published data on the type, succession and nature of the fouling can be used to predict longer term fouling of these devices.

Key conclusions from this study are that even over short durations of exposure no more than one year, there is a clear increase in corrosion rates in warmer temperatures; biofouling is dependent on “spat” settlement; and where biofouling is settled, localised corrosion is likely to occur, even after short immersion durations compared to the expected lifetime of these devices.

Increased corrosion rates are observed for test periods that have spanned a summer due to either the warmer water or an increase in biofouling coverage or both (see Tables 5.11 and 5.12). Localised corrosion was observed to have occurred on all coupons removed after 6 month immersion or longer.

The corrosion rates found in these tests are similar to that reported in the literature (see Table 5.13). This gives confidence that, certainly for carbon steel, and probably for other metals, rates reported in the literature can be used for design and risk management purposes. Such literature is site specific, and data from the North of Scotland should not be applied to a site elsewhere in the world. Specific data should be found (or generated) for a particular geographic area (such an area may be quite tightly confined).

The overall corrosion rate (at 0.124mm/yr) should be within any design limits for a reasonable design life (this equates to 3.1mm over a 25 year deployment. However, there are a number of factors highlighted by these tests that need to be considered further.

These are the effects of temperature (there is a considerable greater range of temperature worldwide, and in the operation of the device than is found between seasons at this site); the effect of flow; and the effect of fouling on localising corrosion (as seen beginning in the longer exposure tests. Any, or a combination of these has the potential to considerably increase the corrosion rate, particularly in a localised area. Fouling such as this can cause crevices to form and accelerate the onset of localised corrosion. Hard and soft fouling was observed on several locations on the example device analysed in Chapter 4.

As an additional point, The results also show that, to reduce the level of the risk, these devices should not be left submerged just below waterline near the quayside for longer than is absolutely necessary, especially in spring and summer when higher corrosion rates were observed and biofouling more likely to settle.

5.6 Conclusions

Several different variables have to be considered when interpreting the findings presented in this chapter. These include period of immersion and seasons over which immersion occurred (and hence temperature and flow effects). The following key findings have been observed:

- Fouling mainly settled during spring/summer months, with significant growth over summer and autumn
- A considerable amount of fouling can be detached in winter storms
- Coupons that were immersed over summer showed higher corrosion rates compared to the same durations over different seasons
- Coupons immersed for the shortest duration (3 months) had the highest average corrosion rate of 0.14 mm/yr. However, during these tests the 3 month durations were over spring and summer where the temperature was the highest
- Corrosion rate reduced to an average of 0.12 mm/yr for the longer lengths of immersion (9-12 months)
- Panels were visibly corroded around the edges close to the plastic spacers
- Localised corrosion was observed underneath fouling settlement on panels that had been immersed for longer than 6 months. This was not observed on panels that had been immersed for 6 months or less

Over the course of a year immersion in seawater by the quayside in Kirkwall, Orkney all carbon steel panels tested exhibited both fouling and corrosion.

These experiments have supplied evidence for the corrosion and biofouling that will occur *in situ* which will aid a risk assessment and provides key risk factors for the development of a management strategy of the associated risks.

Chapter 6

Developing the Evidence Base (iv) - Laboratory Based Investigation of the Effect of Local Conditions and their Interactions on Corrosion

6.1 Introduction

An investigation of a tidal device in Chapter 4 and *in situ* testing of carbon steel panels in Chapter 5 provided information regarding the potential threats to the operation of tidal devices associated with corrosion and biofouling.

Building on this information there are two environmental factors where additional information would further develop the evidence base. These are temperature and flow rate. Temperature is known to exert a strong influence over corrosion rate (Evans, 1960; Melchers, 2002). In the case of tidal devices, this is not only the temperature of the bulk surrounding water (which will change with season, as shown in Chapter 5, and geographical location) but also localised heating of parts of the device due to internal operation. A high tidal flow is a requirement for the devices to operate so the effects of flow need to be understood. Also valuable, is an understanding of the interaction between key environmental factors (temperature, flow, salinity and dissolved oxygen) as it is known that there will be a synergistic effect between them (Chapter 3). This synergistic effect is not yet known for the conditions that will be experienced by tidal stream devices.

Laboratory based experiments were devised to investigate these factors. This provides a comparison between *in situ* testing and controlled laboratory experiments. As well as determining the effect of varying abiotic conditions on the corrosion rates of different metal alloys, the results will allow comparison between these laboratory-based tests using an essentially abiotic environment and field samples, where both biotic and abiotic factors are involved (Chapter 5). These experiments build on the knowledge gained in the review of literature (Chapter 3) to satisfy the risk identification stage of the risk management process in Figure 2.2 in Chapter 2.

6.2 Experimental Design and Methodology

The design of the experiments was developed from the corrosion testing guidelines provided by ASTM (formally known as the American Society for Testing and Materials) (ASTM, 2004), including the environmental factors chosen and assessed as well as the methodology for experimental set up and calculation of corrosion rate. The benefit of conducting laboratory experiments is that conditions are well characterised and can be carefully controlled. Therefore it is possible to identify the effects of different factors on the corrosion rates of metals – including the separate and interactive effects of each factor in a systematic manner. Laboratory based testing also allows for comparison between the relative corrosion behaviour of different metals or alloys (McIntyre and Mercer, 2010).

6.2.1 Determining the Limits of the Environmental Variables using a World Oceanographic Database

A search of environmental data was conducted using the National Oceanographic Data Centre's (National Oceanographic and Atmospheric Administration) World Ocean Database (WOD) 2009 (Boyer et al., 2009). The database contains thousands of data sets that have been collected using a variety of methods from around the world. The 2009 database is the current version, although for some data points the sampling dates back several decades. Only the most recent data was used in this study. This database was chosen over the British Oceanographic Data Centre and MEDIN (Marine Environmental Data & Information Network, 2013) as it provides more information on global sites.

Data from a variety of global locations, chosen to represent potential tidal sites around the world, was analysed using search criteria to ensure only suitable sites were chosen. These criteria were flow rate, a seabed depth of 100 m or less and distance from shore. (Locations relatively close to land would facilitate grid connection and ease of operation and maintenance.)

The data was interrogated using Ocean Data View 4 (ODV), a visualisation and analysis software package (Schlitzer, 2011). This allows the data sets from the WOD to be displayed in an accessible format. The different global locations chosen are listed in Table 6.1, along with the sampling values for the required environmental parameters.

The data used at each site was taken from a sample depth of 50 m to ensure continuity amongst the samples and to correspond to likely depths for placement of devices in the

tidal stream for ease of deployment and retrieval. Maximum and minimum values (Table 6.2) were then used in a two factorial design of the experiments.

Table 6.1.Global locations selected for variation of environmental factors affecting corrosion (Data obtained from Boyer et al., 2009)

Area	Gulf of Alaska				South-western Central America (Panama)							North-eastern South America (Brazil)				
Station Number	76206		76203	76195	8310		8274		8316	8319	8835	2468	2472	2508	2573	2638
Depth (m)	50	100	50	50	106	53	50	80	48	54	50	49	44	60	50	48
Temperature (^{o}C)	6.61	5.72	7.75	6.68	13.76	16.28	19.17	15.14	17.54	16.83	26.73	25.92	25.54	26.13	27.51	26.69
Salinity (psu)	32.12	32.54	31.94	32.83	34.926	34.935	34.252	34.945	34.815	34.839	35.63	36.244	36.092	36.184	35.924	36.446
Oxygen Level (ml/l)	5.74	5.61	5.64	5.86	0.75	1.74	2.21	1.35	1.57	1.17	5.02	4.57	4.47	4.63	4.43	4.95
pH	8.19	8.15	8.16	8.15	7.83	7.9	7.98	7.83	7.84	7.78	8.35	8.4	8.3	8.4	8.3	8.19

Area	North-western Australia					Western France		UK		Sea of Okhotsk, Russia	
Station Number	73483	73484	73473	73471	66391	73178		69986	11902	87488	87486
Depth (m)	50	50	50	50	50	50	95	50	49	47	48
Temperature (^{o}C)	27.34	26.96	27.19	24.84	26.21	10.16	10.12	7.21	6.42	5.72	0.58
Salinity (psu)	34.79	35.1	35.12	34.67	35.17	35.17	35.19	34.85	34.7	32.670	33.18
Oxygen Level (ml/l)	4.43	4.01	4.35	4.39	4.54	5.08	4.91	4.89	6.53	7.30	6.96
pH	8.11	8.16	8.11	8.16	8.3	8.19	8.19	8.36	8	8.28	8.12

Table 6.2.Minimum and maximum values for chosen environmental factors (Data obtained from Boyer et al., 2009)

At 50 m depth	Minimum	Maximum
Temperature (^{o}C)	0.58	27.19
Salinity (psu)	31.94	36.446
Oxygen Level (ml/l)	0.75	7.30
pH	7.78	8.36

One company, Alstom Ocean Energy (AOE), has recently identified a number of potential sites for deployment of tidal devices (Table 6.3) (Newman, 2011). These sites are known to have suitable conditions of flow rate, distance to shore and depth. The values for the environmental variables at these locations lie within the minimum and maximum regimes chosen for this study (Table 6.1 and Table 6.2).

Table 6.3.Sites assessed by Alstom Ocean Energy as potential placement of tidal turbines

Country	Location
Alaska	Cook Inlet
Chile	Straits of Magallanes
Chile	Chacao Channel
Canada	Bay of Fundy
China	Guishan Channel
New Zealand	Cook Strait
Tazmania	Banks Strait
India	Gulf of Kutch
UK	Islay
UK	Pentland Firth

6.2.2 Materials

Materials were chosen to represent the main alloys used in general and critical areas of an example device (Chapter 4) and from discussions with representatives of AOE who then arranged the supply of the alloys. The alloys selected were carbon steel, spheroidal graphite cast iron and Nickel Aluminium bronze.

Carbon Steel, S355 10255 G8+N

S355 G8+N is used as a general constructional steel (e.g. to fabricate the nacelle (which houses the bulk of the working parts)), cartridge plate and tripod of the AOE tidal device (Figure 4.1, Chapter 4). Carbon steel has a relatively limited corrosion resistance; but it is widely used in marine applications due to its relatively low cost and ease of fabrication. The minimum specified yield strength of this steel is 255 MPa (British Standards Institute, 2009). The '+N' at the end of the alloy designation signifies that the alloy is supplied in furnace normalised condition (normalising is used to ensure uniform grain size and composition throughout the alloy).

Table 6.4 shows the chemical composition of S355 in accordance with BS EN 10225:2009.

Table 6.4. S355 10225 G8+N typical specified composition (%)

S355 G8+N	C max	Si	Mn	P max	S max	Cr max	Mo max	Ni max	Al (total)	Cu max	N max	Nb max	Ti max	V max
	0.14	0.15 to 0.55	1.00 to 1.65	0.020	0.007	0.25	0.08	0.50	0.015 to 0.055	0.30	0.010	0.040	0.025	0.060

Using the data in Table 6.5, the equivalent weight of the carbon steel was calculated to be 27.9 g with a density of 7.8 gcm^{-3}.

Table 6.5. Composition of S355 with atomic weights and densities

Element	Composition (%)	Atomic Weight (g/mol)	Density (g/cm^3)
Carbon	0.14	12.011	2.62
Silicon	0.35	28.086	2.33
Manganese	1.325	54.938	7.43
Phosphorous	0.02	30.974	1.82
Sulphur	0.007	32.066	2.07
Chromium	0.25	51.996	7.19
Molybdenum	0.08	95.94	10.2
Nickel	0.5	58.6934	8.9
Aluminium	0.035	26.982	2.702
Copper	0.3	63.546	8.96
Nitrogen	0.01	14.007	0.00125
Niobium	0.04	92.906	8.57
Titanium	0.025	47.88	4.5
Vanadium	0.06	50.941	5.8
Iron	96.858	55.847	7.86

Spheroidal Graphite Cast Iron (SG Iron) – Ductile Iron

SG Iron, a cast iron (internationally known as ductile iron), is used for its ductility, good wear resistance and toughness as well as low cost of manufacture (Reynaud, 2010). This type of cast iron contains nodular (spherical) graphite inclusions which allow the alloy to be more elastic (Jenkins and Forrest, 1990). It is used for the bulk hub and blade root fitting (Section 4.2.5, Chapter 4). Table 6.6 shows a typical composition of ductile iron (British Standards Institute, 1997). Two different designations of ductile iron are used by AOE, EN-GJS-400-18 (for blade root fittings) and EN-GJS-500-7U (for the blade hub). The differences between these are the minimum tensile strength in N/mm^2 (400 and 500, respectively), and the elongation (%) (18 and 7, respectively). Both specifications were tested.

Table 6.6. Ductile iron typical composition (%) (Data obtained from Jenkins and Forrest, 1990)

SG Iron	C	Mn	Si	Cr	Ni	Mo	Cu	P	S	Mg
	3.6 to 3.8	0.15 to 1.0	1.8 to 2.8	0.03 to 0.07	0.05 to 0.2	0.01 to 0.1	0.15 to 1.0	0.03 max	0.002 max	0.03 to 0.06

Using the data in Table 6.7, the equivalent weight of the SG Iron was calculated to be 26.5 g with a density of 7.52 gcm^{-3}.

Table 6.7. Composition of SG Iron with atomic weights and densities

Element	Composition (%)	Atomic Weight (g/gmol)	Density (g/cm^3)
Carbon	3.5	12.011	2.62
Manganese	0.3	54.938	7.43
Silicon	2.6	28.086	2.33
Sulphur	0.015	32.066	2.07
Phosphorus	0.05	30.974	1.82
Magnesium	0.05	24.305	1.738
Iron	93.485	55.847	7.86

Nickel Aluminium Bronze

Nickel aluminium bronzes are widely used for marine applications (Wharton et al., 2005; Schüssler and Exner, 1993b), mainly for valves, fittings, propellers, pump castings and heat exchanger water boxes. These alloys exhibits good corrosion resistance, even at high flow rates and, due to their high copper content, they are also able to resist both micro and macro fouling (Al-Hashem and Riad, 2002). They exhibit the highest resistance to cavitation damage compared to all other copper alloys (Schüssler and Exner, 1993b). Aluminium bronzes with 9-12% aluminium and ≤6% iron and nickel represent one of the most important groups of commercial bronzes. The inclusion of nickel to aluminium bronze increases the corrosion resistance and the yield strength of the alloy. The corrosion resistance of aluminium bronze is attributed to the alumina protective layer produced containing aluminium and copper oxides. Like many other copper alloys, nickel aluminium bronze has good resistance to biofouling. AOE use Nickel aluminium bronze on the blade hub at the interface between the hub and the blades and for some connectors in the skirt area (Section 4.2.5 and Section 4.2.6, Chapter 4).

Table 6.8. Nickel Aluminium Bronze EN-SS5716-15 (CuAl10Ni5Fe4) typical composition (%) (Lagermetall, 2011)

Ni-Al-Bronze	Al	Cu	Fe	Sn max	Pb max	Zn max	Mn max	Ni	Si max	Mg max	Bi max	Cr max
	8.5-10.5	76-83	4.0-5.5	0.1	0.03	0.50	3.0	4-6	0.1	0.05	0.01	0.05

Using the data in Table 6.9, the equivalent weight of the aluminium bronze was calculated to be 53.6 g with a density of 8.24 gcm^{-3}.

Table 6.9. Composition of aluminium bronze with atomic weights and densities

Element	Composition (%)	Atomic Weight (g/gmol)	Density (g/cm^3)
Aluminium	9.5	26.982	2.702
Iron	4.75	55.847	7.86
Tin	0.1	118.71	7.3
Lead	0.03	207.2	11.34
Zinc	0.5	65.39	7.14
Manganese	3	54.938	7.43
Nickel	5	58.6934	8.9
Silicon	0.1	28.086	2.33
Magnesium	0.05	24.305	1.738
Bismuth	0.01	208.98	9.8
Chromium	0.05	51.996	7.19
Copper	76.91	63.546	8.96

6.2.3 Experimental Design

The laboratory tests were carried out in black plastic tanks systems specifically built for the purpose that allowed the variables to be changed and monitored (Figure 6.2 and 6.3). The black tanks ensured that dark uniform conditions could be maintained throughout. The tanks, (Ferham-Titan PC4R) with a capacity of 18 litres (422 x 296 x 305 mm) allowed ease of maintenance of temperature, salinity and dissolved oxygen. Each experimental unit used two tanks, one holding the specimens and the other used as a balancing tank to ensure that water level and environmental factors were maintained to the specified levels. The metals were tested separately to avoid potential contamination of samples.

One set of 2 units was installed in a laboratory and maintained at 13-18^{o}C during testing using a heating system. The other units were located in a cold room held at 2^{o}C for the experiments at the minimum temperature. Pumps located in the holding tank provided a flow of 6 $lmin^{-1}$, which equated to 3 cms^{-1} across the metal samples. Although this represents only a small proportion of the flow experienced by a device in the tidal stream, it does provide a steady flow that can then be compared to stagnant conditions. Higher flow rates cause a higher margin of error and impair the electrochemical testing results.

Metal samples were obtained from the suppliers to ensure that the alloys were the same in terms of specification and fabrication as those used on an actual device. A Sheffield based engineering firm, (Special Steels Ltd.) was employed to cut and finish the samples to the required size and uniform finish. The samples were approximately 50 mm x 25 mm x 6 mm with a 5 mm diameter drilled hole to allow suspension of the sample in the electrolyte.

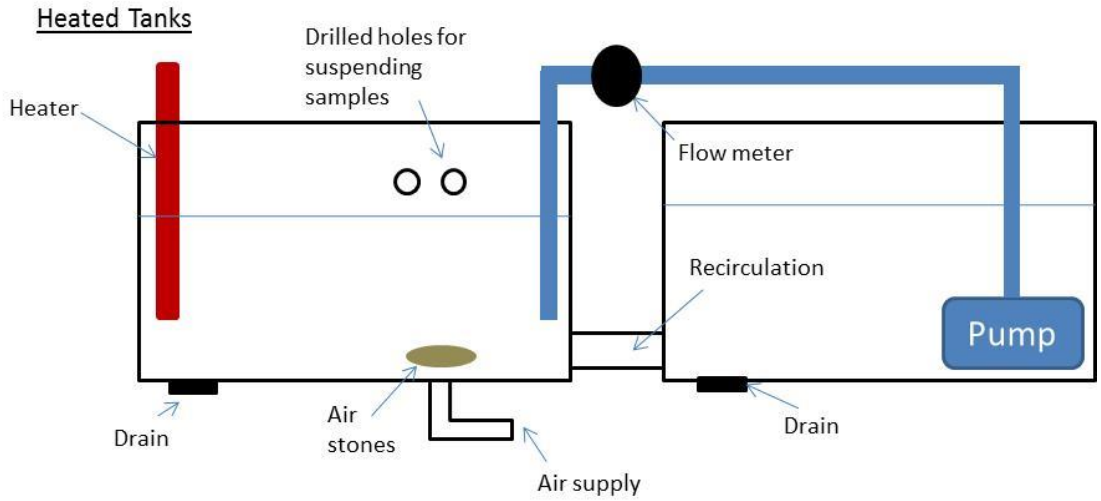

Figure 6.1.Heated tank design for electrochemical and gravimetric corrosion experiments

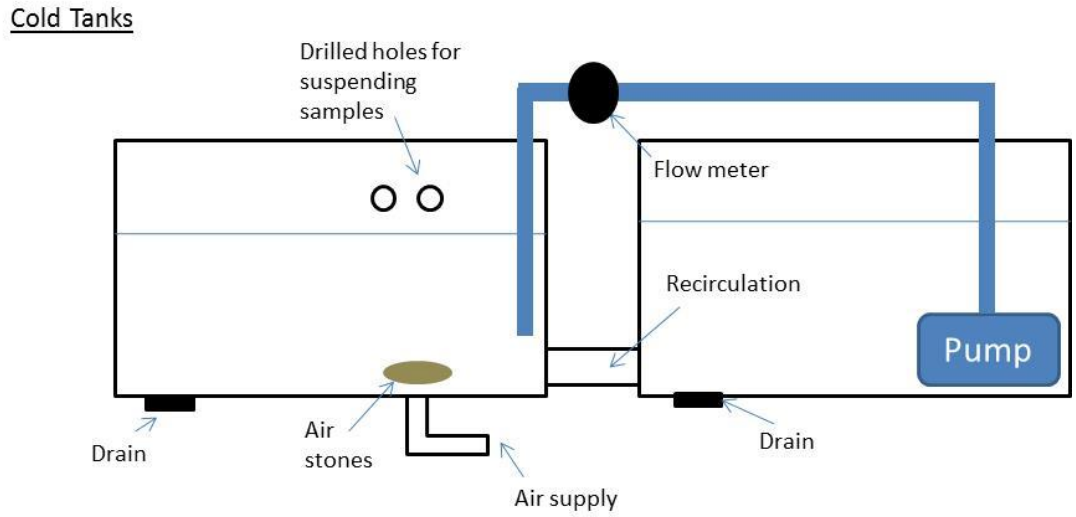

Figure 6.2.Cold tank design for electrochemical and gravimetric corrosion experiments

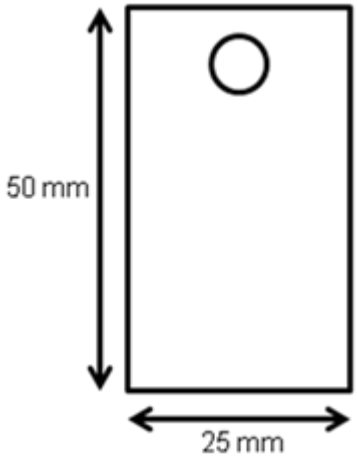

Figure 6.3. Aspect and dimensions of test samples

6.2.4 Experimental Methodology

Sample Preparation

Although the sample surface will differ from that used in service, the best practical procedure for laboratory testing is to use a standard surface condition for all samples. Using a single method of surface preparation also ensures that relative effects of the environmental conditions can be analysed without compromising effects from material preparation and therefore ensures reproducibility of results between tests.

The samples were prepared for the tests by polishing and cleaning as defined in ASTM G31 (ASTM, 2004). Samples were polished to 120 grit and cleaned with a 50/50 water/acetone mix to ensure that the any dirt, oil or grease was removed from the surface. The samples were then air dried and stored in a desiccator to ensure that the surfaces remained clean until required.

Before use the surface area of the specimens were measured to an accuracy of ± 0.5 mm.

Variation of Temperature

For the maximum temperature experiments, water in the test tanks was maintained at temperature with an accuracy of ± 0.5 ^{o}C. For the minimum temperature experiments, the tanks were placed in a cold room set to a temperature of 2 ^{o}C ± 0.5 ^{o}C.

Variation of Salinity

Salinity was varied by changing the amount of salt mix in the water. The salt mix used was Instant Ocean®, a common artificial seawater mix used for a wide range of controlled experiments (Grimes and Colwell, 1986; Saoud et al., 2003; Lewandowski et al., 1989; Mansfeld and Little, 1992b). A salinity probe was used to monitor the salinity to ensure that the system was at equilibrium prior to testing.

Variation of Dissolved Oxygen

Oxygen was provided via airstones (as used in aquariums) in conjunction with a pressurised air supply. The test rig was designed to ensure that air bubbles did not impinge directly on the samples. The amount of oxygen dissolving into the seawater could be varied by using different numbers of stones, or by controlling the air entering via the pump. The dissolved oxygen levels in the test tanks were monitored using an oxidation reduction potential (ORP) dissolved oxygen monitor, which takes a conductivity measurement automatically to correct for salinity.

Monitoring of Variables

Environmental variables were monitored throughout the experiments. The temperature in the heated tanks was stabilised at the required value. A Thermo Scientific Orion 5 Star water meter, calibrated prior to each test, was used to monitor salinity, dissolved oxygen and temperature to ensure that the readings were consistent throughout the tests. Flow was controlled by the tank pump system and measured using a rotameter.

Measures were taken to ensure that the dissolved oxygen levels were kept to those required for each trial condition. This especially was the case in trials that required a low temperature and low dissolved oxygen (nitrogen was used to purge the water of oxygen in these cases) and in trials that required a high temperature and a high dissolved oxygen concentration (an oxygen pump was used in these cases). These methods to overcome the problems also had to take the flow into consideration, as the flow level also had an effect on the oxygen level. The variables were continuously monitored throughout each test.

Artificial Seawater

Laboratory tests were carried out using artificial seawater using Instant Ocean®, mixed with distilled water. The salts were mixed vigorously with the water at a ratio of 400 g to 12 litres, which corresponds to a salinity of 35 ppt. Salinity was monitored and further salt, or more distilled water added as necessary to achieve the desired salinity.

Electrochemical Polarisation Tests for Corrosion Rate

Corrosion rates were measured using Tafel Extrapolation from electrochemical polarisation. (The background to this method and its application in laboratory based corrosion experimentation is discussed in Chapter 3.)

The potentiostat used was a PG580 Potentiostat-Galvanostat with an Ag/AgCl reference electrode and platinum counter electrode, supplied by UniScan Instruments, used in potentiodynamic polarization mode. The polarisation scan was performed at the ASTM standard scan rate (0.1667 mVs^{-1}).

The samples and electrodes were placed in the test tanks and connected to the potentiostat. Once the corrosion potential stabilised (monitored using the UiECorr software provided with the device), the potentiostat was set to scan through a ±200 mV over-potential first in the cathodic direction starting from the corrosion potential, and then in the anodic direction to produce a potential vs log current (logI-E) plot. The length of time to stabilisation prior to testing was approximately 1 hour. The experiment was controlled using the UiECorr Version 3.05 software supplied by UniScan Instruments. This also

provided the analysis tools to allow extrapolation of the Tafel slopes obtained to calculate corrosion rates.

This method is "destructive" due to the application of the large over-potential affecting the metal surface, and hence each of the metal samples could only be used once.

High flow levels cause a greater margin of error on the Tafel plot due to the turbulence caused by the flow in the test tanks. This was reduced as much as possible by ensuring that the coupon was situated in the tanks away from the pump and higher turbulence. The potentiostat was also earthed for all experiments to reduce noise.

Determination of Corrosion Rate from Corrosion Current

Once Tafel plots were obtained for three replicates of each metal under each trial condition and the corrosion current calculated, it was converted into a corrosion rate using Faraday's law (See Chapter 3).

$$Corrosion\ Rate\ (mm/yr) = \frac{I_{corr} kEW}{\rho A} \qquad [6.1]$$

Where k is equal to 3272 mm/Acmyr for corrosion rate in mm/yr, I_{corr} is the corrosion current ($mAcm^{-2}$), EW is the equivalent weight (g), ρ is the density (gcm^{-3}) and A is the exposed surface area (cm^2).

6.3 Analysis Methodology

A two factorial design was used for the experiments which enabled the influence of the controlled variables, and possible interactive effects, on the corrosion rate to be assessed. The advantage of this method of experimental design over a design that studies one factor at a time is not only a reduction in time and resources, but also the ability to assess a potential additive response for all factors (Box et al., 2005). Although individual factors affect corrosion rates of metals, they can also work together to cause synergistic effects. A two factorial experimental design allows the interactions between the environmental variables as well as their individual direct effects to be studied (Meng et al., 2007; Atashin et al., 2011b). Conversely, if factors do not act additively, this method will allow the detection and estimation of interactions that measure the non-additivity (Box et al., 2005). The minimum and maximum values for each parameter are listed in Table 6.10 (derived from Table 6.3).

Table 6.10. Maximum and Minimum values for environmental variables tested

Variable	Minimum	Maximum
Temperature (^{o}C)	2	28
Flow (l/min)	0	6
Salinity (ppt)	31.9	36.5
Dissolved Oxygen (ml/l)	1	7

Four environmental parameters were considered in this study: temperature, water flow, salinity, and dissolved oxygen concentration. Therefore, using the two-factorial design, 2 x 2 x 2 x 2 = 16 trials were conducted to satisfy all permutations (Meng et al., 2007). For each condition three sample replicates were used to ensure reproducibility of results. The design matrix is given in Table 6.11. For example, trial 6 represents a high temperature condition along with high flow and salinity but low dissolved oxygen levels.

Table 6.11. Design matrix for experimental trials (four environmental factors)

Trial	Random Order	Temperature (T)	Flow (F)	Salinity (S)	Dissolved Oxygen (O)	Corrosion rate
1	14	+	-	-	-	C_1
2	2	+	-	+	-	C_2
3	10	+	-	-	+	C_3
4	7	+	-	+	+	C_4
5	13	+	+	-	-	C_5
6	9	+	+	+	-	C_6
7	1	+	+	-	+	C_7
8	6	+	+	+	+	C_8
9	16	-	-	-	-	C_9
10	5	-	-	+	-	C_{10}
11	11	-	-	-	+	C_{11}
12	3	-	-	+	+	C_{12}
13	12	-	+	-	-	C_{13}
14	15	-	+	+	-	C_{14}
15	4	-	+	-	+	C_{15}
16	8	-	+	+	+	C_{16}

In Table 6.11, a '+' denotes the high level and a '–' denotes the low level given in Table 6.10.

The tests were not run in the order shown in the "Trial" column in Table 6.11 but randomised as in column 2 ("Random Order") to eliminate, so far as possible, extraneous effects.

From averaged corrosion rates obtained from each trial (3 replicates for each), the effects of each level of each factor can be calculated.

The method of analysis applies a 'Table of Contrast' (Table 6.12), constructed for each metal using the design matrix. This includes all possible interactions between the factors.

The columns for the interactions are obtained directly from multiplying the signs of the respective factors (Box et al., 2005).

Table 6.12. Table of possible interactions for statistical assessment (T= temperature, F= flow, S= salinity, O= oxygen)

Trial	T	F	S	O	TF	TS	TO	FS	FO	SO	TFS	TFO	TSO	FSO	TFSO	Corrosion rate
1	+	-	-	-	-	-	-	+	+	+	+	+	+	-	-	C_1
2	+	-	+	-	-	+	-	-	+	-	-	+	-	+	+	C_2
3	+	-	-	+	-	-	+	+	-	-	+	-	-	+	+	C_3
4	+	-	+	+	-	+	+	-	-	+	-	-	+	-	-	C_4
5	+	+	-	-	+	-	-	-	-	+	-	-	+	+	+	C_5
6	+	+	+	-	+	+	-	+	-	-	+	-	-	-	-	C_6
7	+	+	-	+	+	-	+	-	+	-	-	+	-	-	-	C_7
8	+	+	+	+	+	+	+	+	+	+	+	+	+	+	+	C_8
9	-	-	-	-	+	+	+	+	+	+	-	-	-	-	+	C_9
10	-	-	+	-	+	-	+	-	+	-	+	-	+	+	-	C_{10}
11	-	-	-	+	+	+	-	+	-	-	-	+	+	+	-	C_{11}
12	-	-	+	+	+	-	-	-	-	+	+	+	-	-	+	C_{12}
13	-	+	-	-	-	+	+	-	-	+	+	-	-	+	-	C_{13}
14	-	+	+	-	-	-	+	+	-	-	-	+	+	-	+	C_{14}
15	-	+	-	+	-	+	-	-	+	-	+	-	+	-	+	C_{15}
16	-	+	+	+	-	-	-	+	+	+	-	+	-	+	-	C_{16}
16	8	8	8	8	8	8	8	8	8	8	8	8	8	8	8	

The main effects of each factor and interactions (columns in Table 6.12) are the differences between two averages:

$$Main\ effect = \bar{y}_+ - \bar{y}_- \qquad [6.1]$$

Where $\bar{y}_+$ is the average response (i.e. corrosion rate) corresponding to the plus level factor of the interaction (e.g. high temperature) and $\bar{y}_-$ is the average response corresponding to the minus level of the factor (e.g. low temperature).

The effects estimated from the table of contrasts can be analysed to determine which are real and which can be explained by chance variation. The effects of the factors tested can be assessed using an internal reference set. It can be assumed that the five highest order interactions, (TFS, TFO, TSO, FSO and TFSO) represent a margin of error, and therefore these can be used to provide a reference set for the remaining effects (Box et al., 2005). The following equation can be used to determine the standard error (SE):

$$(SE\ effect)^2 = {}^1/_5\{(TFS)^2 + (TFO)^2 + (TSO)^2 + (FSO)^2 + (TFSO)^2\} \qquad [6.2]$$

$$SE_{effect} = \sqrt{(SE\ effect)^2} \qquad [6.3]$$

Effects that are greater than 2 or 3 times the standard error are not explained by chance (Box et al., 2005) and are therefore statistically significant in determining the rate of corrosion. This rule was applied to the results.

6.4 Results

The results of the experiments are in the form of Tafel Plots which are then used to determine corrosion rates under varying environmental conditions for four different metals using Tafel Extrapolation. An overview of the Tafel plots obtained is shown here. Further plots can be found in Appendix 1.

6.4.1 Example Tafel Plots for Trial 1

Shown here are the Tafel plot obtained for trial 1 for each metal. Further Tafel plots can be seen in Appendix 1.

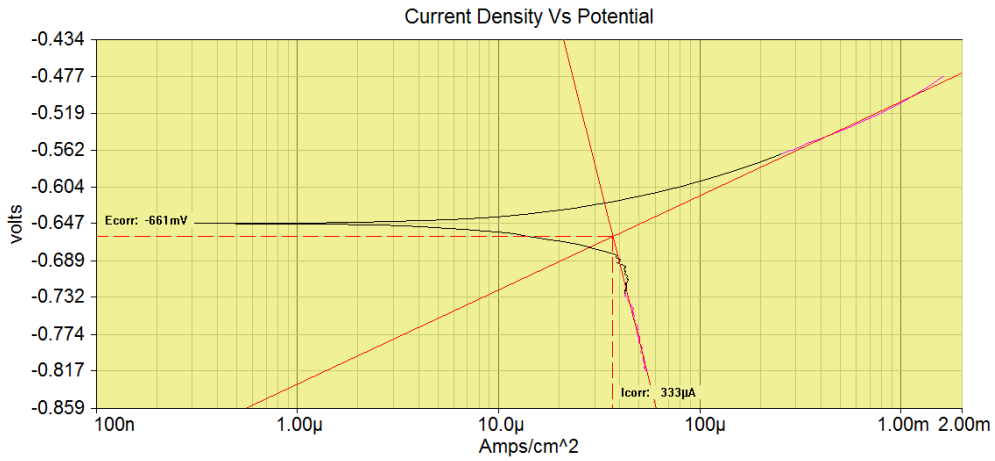

Figure 6.4. Tafel plot for carbon steel, trial 1 (high temperature, low flow, low salinity, low dissolved oxygen)

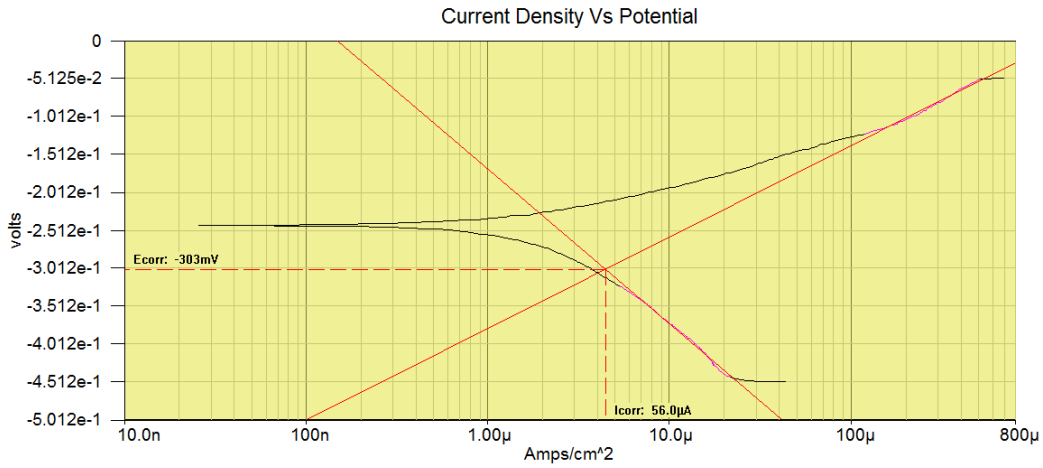

Figure 6.5. Tafel plot for aluminium bronze, trial 1 (high temperature, low flow, low salinity, low dissolved oxygen)

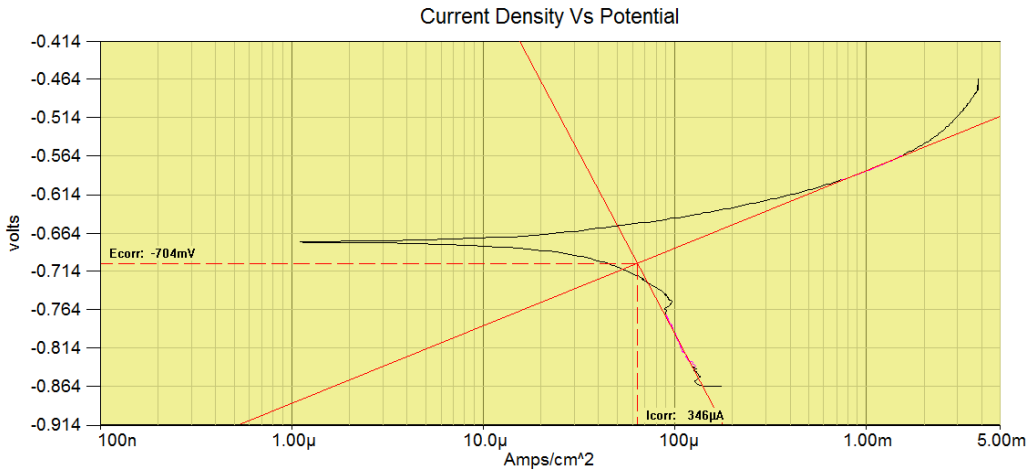

Figure 6.6. Tafel plot for SG Iron 400, trial 1 (high temperature, low flow, low salinity, low dissolved oxygen)

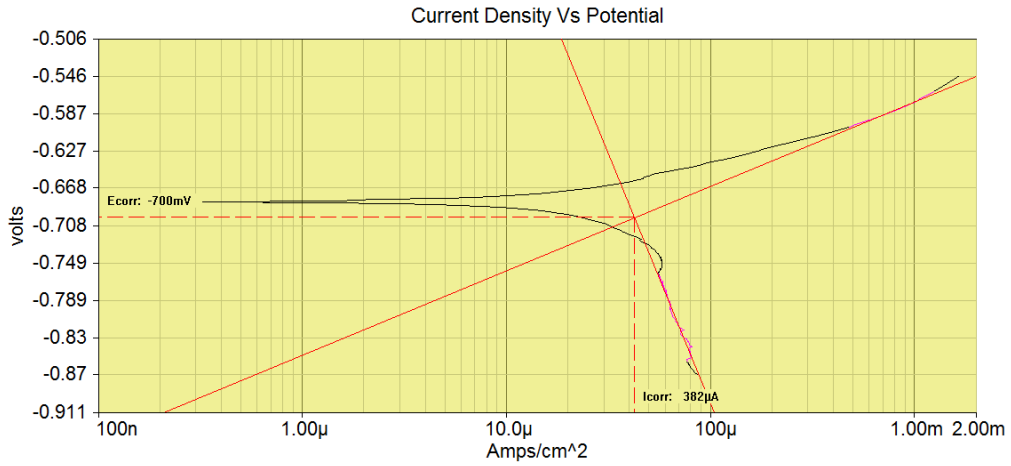

Figure 6.7. Tafel plot for SG Iron 500, trial 1 (high temperature, low flow, low salinity, low dissolved oxygen)

6.4.2 Corrosion Rates

Table 6.13 gives the results from all the experiments Standard error was calculated for the average results using the following equations (Box et al., 2005):

$$\text{Standard Deviation } (\sigma) = \sqrt{\frac{\sum(x-\bar{x})^2}{(n-1)}} \qquad [6.4]$$

$$\text{Standard Error } SE = \frac{\sigma}{\sqrt{n}} \qquad [6.5]$$

The standard errors indicate that the results are reproducible. Figure 6.8 compares results between different metals and also shows the large dependence of corrosion rate on temperature. There is a clear trend under all trial conditions with SG Iron (both 400 and 500) displaying much higher corrosion rates than both carbon steel and aluminium bronze. This order (aluminium bronze with the lowest corrosion rates observed and SG Iron with highest rates observed) is as expected from the galvanic series (Atlas Steels, 2010). However, these tests were required to show the relationship of the individual metals to the

changing relevant environmental conditions and whether this differs amongst the metals tested as well as determining the ranking of environmental influence.

Table 6.13. Corrosion Rates obtained for all metals tested (mm/yr)

	Trial 1					Trial 2					Trial 3					Trial 4				
	High T, Low F, Low S, Low DO			Average	S. Error	High T, Low F, High S, Low DO			Average	S. Error	High T, Low F, Low S, High DO			Average	S. Error	High T, Low F, High S, High DO			Average	S. Error
Carbon Steel	0.44	0.39	0.37	**0.40**	0.022	0.46	0.46	0.46	**0.46**	0.003	0.54	0.48	0.52	**0.51**	0.017	0.73	0.78	0.78	**0.76**	0.017
Al-bronze	0.08	0.06	0.07	**0.07**	0.005	0.14	0.14	0.13	**0.13**	0.002	0.22	0.23	0.22	**0.22**	0.004	0.12	0.13	0.13	**0.12**	0.005
SG400	0.74	0.64	0.60	**0.66**	0.041	1.69	1.58	1.71	**1.66**	0.040	1.96	1.96	1.91	**1.95**	0.018	2.26	2.30	2.36	**2.31**	0.030
SG500	0.48	0.55	0.56	**0.53**	0.025	1.54	1.54	1.50	**1.53**	0.014	1.93	1.79	1.79	**1.84**	0.046	1.99	1.96	1.97	**1.98**	0.010

	Trial 5					Trial 6					Trial 7					Trial 8				
	High T, High F, Low S, Low DO			Average	S. Error	High T, High F, High S, Low DO			Average	S. Error	High T, High F, Low S, High DO			Average	S. Error	High T, High F, High S, High DO			Average	S. Error
Carbon Steel	1.06	1.06	0.95	**1.02**	0.039	1.04	0.95	1.00	**1.00**	0.026	0.95	0.99	0.90	**0.95**	0.027	1.17	1.05	1.15	**1.12**	0.036
Al-bronze	0.16	0.18	0.17	**0.17**	0.007	0.25	0.26	0.28	**0.27**	0.008	0.35	0.33	0.33	**0.34**	0.006	0.36	0.42	0.34	**0.37**	0.024
SG400	1.96	1.86	1.95	**1.92**	0.031	1.94	1.92	1.94	**1.93**	0.007	1.89	1.92	1.89	**1.90**	0.010	2.26	2.28	2.21	**2.25**	0.023
SG500	1.48	1.48	1.49	**1.48**	0.005	2.07	2.11	2.12	**2.10**	0.015	1.82	1.81	1.78	**1.81**	0.012	2.02	2.02	1.95	**1.99**	0.024

	Trial 9					Trial 10					Trial 11					Trial 12				
	Low T, Low F, Low S, Low DO			Average	S. Error	Low T, Low F, High S, Low DO			Average	S. Error	Low T, Low F, Low S, High DO			Average	S. Error	Low T, Low F, High S, High DO			Average	S. Error
Carbon Steel	0.05	0.05	0.05	**0.05**	0.0003	0.07	0.07	0.07	**0.07**	0.0008	0.13	0.16	0.12	**0.14**	0.012	0.13	0.15	0.13	**0.14**	0.006
Al-bronze	0.01	0.01	0.01	**0.01**	0.0003	0.01	0.01	0.01	**0.01**	0.0002	0.02	0.02	0.02	**0.02**	0.001	0.02	0.02	0.01	**0.02**	0.003
SG400	0.22	0.19	0.22	**0.21**	0.010	0.30	0.28	0.31	**0.29**	0.009	0.70	0.60	0.69	**0.66**	0.032	0.51	0.65	0.50	**0.55**	0.048
SG500	0.26	0.24	0.25	**0.25**	0.007	0.37	0.36	0.34	**0.36**	0.010	0.84	0.72	0.89	**0.82**	0.051	0.57	0.60	0.49	**0.55**	0.034

	Trial 13					Trial 14					Trial 15					Trial 16				
	Low T, High F, Low S, Low DO			Average	S. Error	Low T, High F, High S, Low DO			Average	S. Error	Low T, High F, Low S, High DO			Average	S. Error	Low T, High F, High S, High DO			Average	S. Error
Carbon Steel	0.13	0.13	0.11	**0.12**	0.006	0.14	0.14	0.15	**0.14**	0.001	0.06	0.07	0.08	**0.07**	0.007	0.09	0.09	0.11	**0.09**	0.008
Al-bronze	0.02	0.02	0.02	**0.02**	0.0005	0.03	0.03	0.03	**0.03**	0.0002	0.02	0.02	0.02	**0.02**	0.0007	0.02	0.03	0.03	**0.03**	0.004
SG400	0.64	0.70	0.69	**0.67**	0.019	0.70	0.64	0.67	**0.67**	0.016	0.64	0.73	0.71	**0.69**	0.028	0.77	0.60	0.71	**0.69**	0.048
SG500	0.68	0.67	0.68	**0.67**	0.004	0.51	0.50	0.52	**0.51**	0.007	0.52	0.62	0.61	**0.58**	0.003	0.73	0.66	0.74	**0.71**	0.026

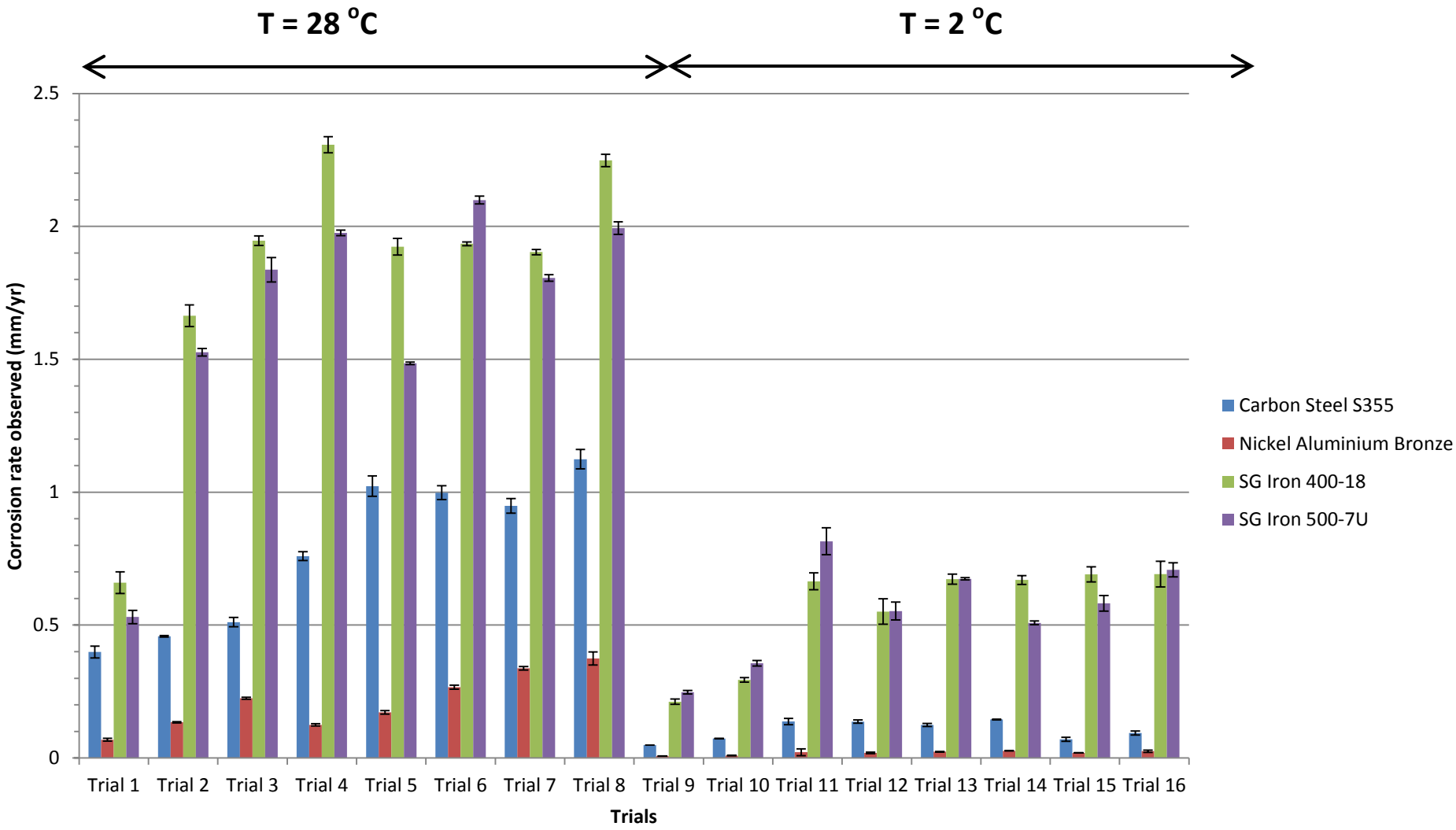

Figure 6.8. Corrosion rates obtained for the four metals tested for all trials (see Table 6.11 for environmental conditions relating to each trial). Bars = ±Standard Error

Table 6.14. The potential degradation (reduction in metal thickness) for each trial condition over a predicted device lifetime of 25 years (mm)

	Potential Degradation (mm)															
	Trial 1	Trial 2	Trial 3	Trial 4	Trial 5	Trial 6	Trial 7	Trial 8	Trial 9	Trial 10	Trial 11	Trial 12	Trial 13	Trial 14	Trial 15	Trial 16
Carbon Steel	9.97	11.45	12.78	18.99	25.57	24.96	23.72	28.11	1.22	1.83	3.43	3.42	3.11	3.62	1.76	2.34
Al-Bronze	1.72	3.36	5.61	3.12	4.30	6.65	8.44	9.36	0.19	0.23	0.54	0.48	0.59	0.68	0.49	0.63
SG440	16.49	41.60	48.65	57.68	48.10	48.37	47.58	56.21	5.30	7.35	16.62	13.77	16.82	16.74	17.27	17.29
SG500	13.26	38.16	45.93	49.39	37.12	52.48	45.14	49.84	6.19	8.90	20.38	13.82	16.85	12.71	14.54	17.70

Table 6.15. Percentage of thickness degraded in worst case scenarios for thicknesses of carbon steel likely to be used for tidal devices after predicted device lifetime of 25 years (%)

Original thickness of metal	Thickness Degraded (%)															
	Trial 1	Trial 2	Trial 3	Trial 4	Trial 5	Trial 6	Trial 7	Trial 8	Trial 9	Trial 10	Trial 11	Trial 12	Trial 13	Trial 14	Trial 15	Trial 16
20 mm	49.85	57.25	63.90	94.95	100	100	100	100	6.1	9.15	17.15	17.1	15.55	18.1	8.8	11.7
25 mm	39.88	45.8	51.12	75.96	100	100	100	100	4.88	7.32	13.72	13.68	12.44	14.48	7.04	9.36
30 mm	33.23	38.17	42.60	63.30	85.23	83.20	79.07	93.70	4.07	6.10	11.43	11.40	10.37	12.07	5.87	7.80
40 mm	24.93	28.63	31.95	47.48	63.93	62.40	59.30	70.28	3.05	4.58	8.58	8.55	7.78	9.05	4.40	5.85

6.5 Analysis and Comparison of Factors

Table 6.13 and Figure 6.9 show the results obtained in tabular and graphical form. The standard error was less than 10% in all cases indicating that these were genuine replicates of the experiment and as such the average values can be used for further statistical analysis as outlined in Section 6.3.

Using statistical analysis of the two-factorial design, the significance of the factors can be compared between metals.

Table 6.16. Contrast coefficients for carbon steel (CS), Nickel Aluminium Bronze (NAB), Ductile Iron SG400-18 (SG400) and SG500-7U (SG500) (T= temperature, F= flow, S= salinity, O= oxygen). Corrosion Rates shown in mm/yr

Trial	T	F	S	O	TF	TS	TO	FS	FO	SO	TFS	TFO	TSO	FSO	TFSO	Carbon Steel	Nickel Aluminium Bronze	Ductile Iron SG400-18	Ductile Iron SG500-7U
1	+	-	-	-	-	-	-	+	+	+	+	+	+	-	-	0.40	0.07	0.66	0.53
2	+	-	+	-	-	+	-	-	+	-	-	+	-	+	+	0.46	0.13	1.66	1.53
3	+	-	-	+	-	-	+	+	-	-	+	-	-	+	+	0.51	0.22	2.31	1.84
4	+	-	+	+	-	+	+	-	-	+	-	-	+	-	-	0.76	0.12	1.92	1.98
5	+	+	-	-	+	-	-	-	-	+	-	-	+	+	+	1.02	0.17	1.94	1.49
6	+	+	+	-	+	+	-	+	-	-	+	-	-	-	-	1.00	0.27	1.90	2.10
7	+	+	-	+	+	-	+	-	+	-	-	+	-	-	-	0.95	0.34	2.25	1.80
8	+	+	+	+	+	+	+	+	+	+	+	+	+	+	+	1.12	0.37	0.21	1.99
9	-	-	-	-	+	+	+	+	+	+	-	-	-	-	+	0.05	0.01	0.29	0.25
10	-	-	+	-	+	-	+	-	+	-	+	-	+	+	-	0.07	0.01	0.67	0.36
11	-	-	-	+	+	+	-	+	-	-	-	+	+	+	-	0.14	0.02	0.55	0.82
12	-	-	+	+	+	-	-	-	-	+	+	+	-	-	+	0.14	0.02	0.67	0.55
13	-	+	-	-	-	+	+	-	-	+	+	-	-	+	-	0.12	0.02	0.67	0.67
14	-	+	+	-	-	-	+	+	-	-	-	+	+	-	+	0.14	0.03	0.69	0.51
15	-	+	-	+	-	+	-	-	+	-	+	-	+	-	+	0.07	0.02	0.69	0.58
16	-	+	+	+	-	-	-	+	+	+	-	+	-	+	-	0.09	0.03	1.19	0.71
	8	8	8	8	8	8	8	8	8	8	8	8	8	8	8				

6.5.1 Carbon Steel

The results obtained for carbon steel (Table 6.13) were input into a table of contrast coefficients (Table 6.16) (as described in Section 6.3). The corrosion rates obtained for carbon steel are consistently higher than those found for the aluminium bronze, but less than those found for both SG irons.

From the table of contrasts the main effects of each factor and interactions between these were calculated using Equation 6.4. The results for carbon steel can be seen in Table 6.17.

Table 6.17. Carbon steel estimated effects (dimensionless)

Effects	Estimated Effects ± SE
Average	0.441
T	**0.674 ± 0.027**
F	**0.251 ± 0.027**
S	0.066 ± 0.027
O	0.064 ± 0.027
TF	**0.241 ± 0.027**
TS	0.049 ± 0.027
TO	0.052 ± 0.027
FS	-0.017 ± 0.027
FO	-0.077 ± 0.027
SO	0.046 ± 0.027
TFS	-0.022
TFO	-0.021
TSO	0.052
FSO	0.005
TFSO	-0.002

The calculation of standard error average corrosion rate can be carried out using an internal reference set made up from higher order interactions as discussed in Section 6.3.

$$(SE\ effect)^2 = {}^1/_5\{(-0.02225)^2 + (-0.02075)^2 + (0.0515)^2 + (0.0045)^2 + (-0.002)^2\}$$

$(SE\ effect)^2 = 0.00072$

SE effect = 0.027

Highlighted in bold in Table 6.17 are the factor and the interaction effects that are significantly greater than their standard error, and therefore cannot be explained by chance alone. The effects of temperature, flow and the interaction effect of temperature and flow on the corrosion rate are thus statistically important for carbon steel.

Comparison of Factors

Factorial plots are a further method to verify the results and to examine the interactions between the various environmental factors. These plots compare effects between various factors and the most significant factor, temperature, on corrosion rates. Parallel plots indicate no interaction, whereas the greater the difference between gradients the greater the interaction between factors. In the following factorial plots, an '0' represents the minimum level tested and a '1' represents the maximum level tested.

The greatest interaction is between temperature and flow (Figure 6.9). As the temperature increases from minimum to maximum for high flow conditions there is a steeper gradient than for stagnant conditions. The primary influence of velocity is to increase corrosion rates by the electrochemical processes in the reaction that are controlled by diffusion mechanisms, affecting the flow of available oxygen to the metal surface. When flow is high it is likely that dissolved oxygen concentration is higher than in stagnant flow conditions. At high temperatures higher corrosion rates would be expected despite a low oxygen concentration (as is indicated by the no-flow plot), so by increasing the flow as well as temperature, there is likely to be more oxygen available at the corrosion site which is known to further increase corrosion, (even though water holds less oxygen at higher temperatures).

The graphs of temperature and salinity (Figure 6.10) and temperature and oxygen (Figure 6.11) show very similar gradients and so there is no significant interaction between these factors. 'Mean Crate' is the mean corrosion rates obtained in mm/yr. None of the plots overlap and as such there is no significant interaction between the factors shown between the levels tested.

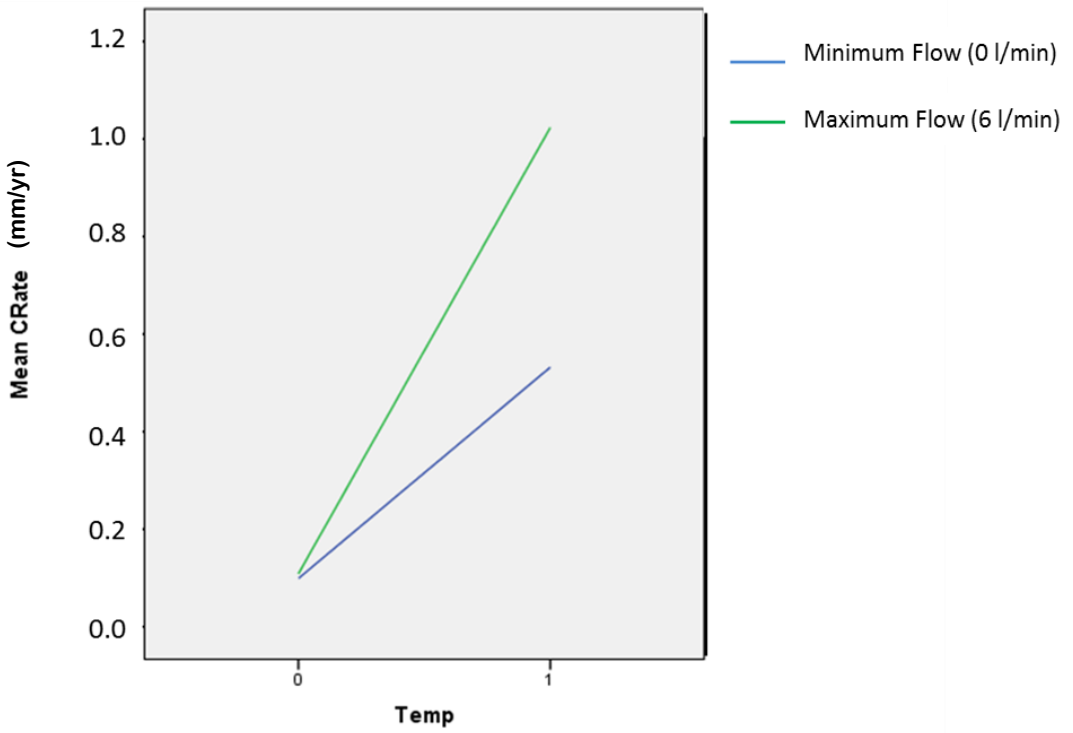

Figure 6.9. Plot comparing the mean corrosion rate (mm/yr) for a maximum (28°C) and minimum (2°C) temperature and flow for carbon steel to understand their interactive effects

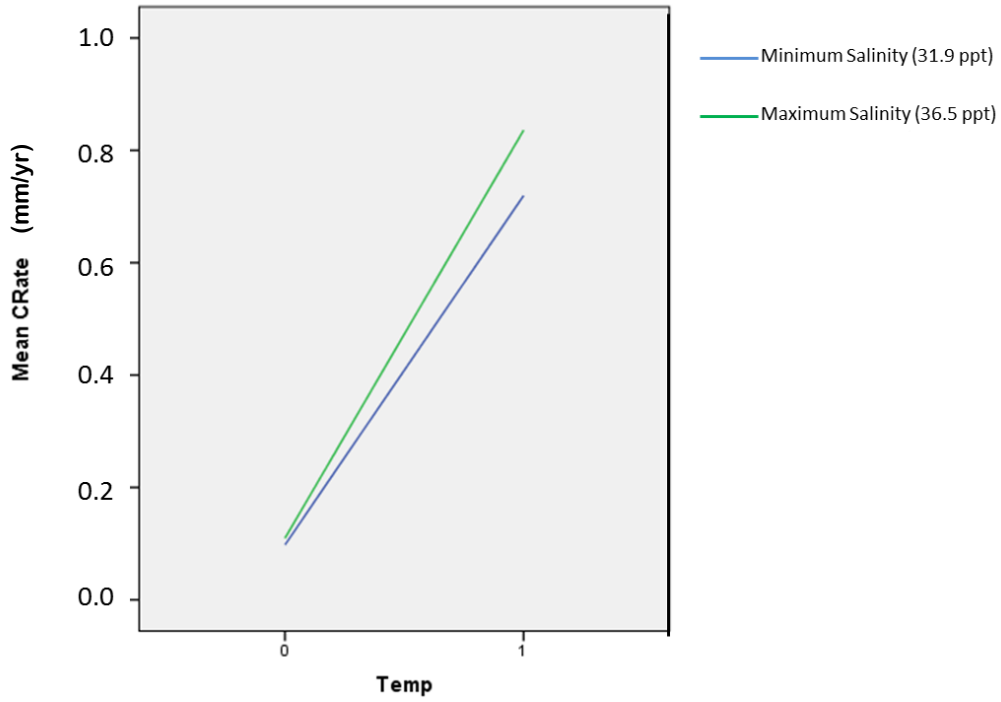

Figure 6.10. Plot comparing the mean corrosion rate (mm/yr) for a maximum (28°C) and minimum (2°C) temperature and salinity for carbon steel to understand their interactive effects

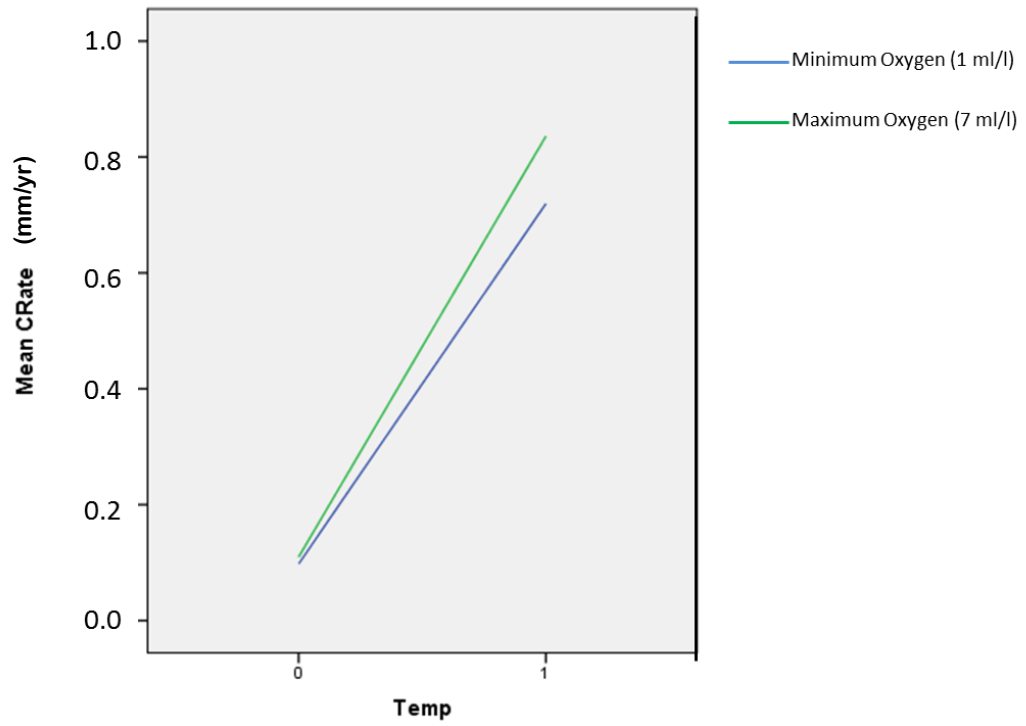

Figure 6.11. Plot comparing the mean corrosion rate (mm/yr) for a maximum (28°C) and minimum (2°C) temperature and dissolved oxygen for carbon steel to understand their interactive effects

A plot of flow and oxygen can be seen in Figure 6.12. This interaction is included as the estimated effect between flow and oxygen was observed to be of greater magnitude than that between temperature and salinity and temperature and oxygen.

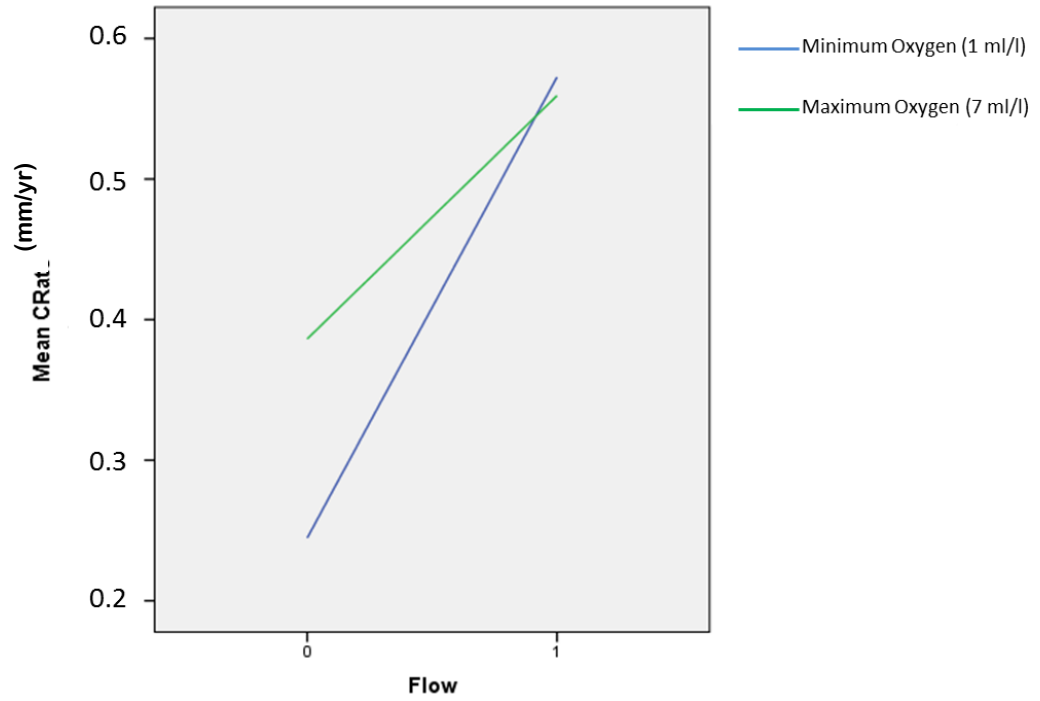

Figure 6.12. Plot comparing the mean corrosion rate (mm/yr) for a maximum (6l/min) and minimum (0 l/min) flow and oxygen for carbon steel to understand their interactive effects

6.5.2 Nickel Aluminium Bronze

The results for nickel aluminium bronze were input into a table of contrast coefficients (Table 6.16). Aluminium Bronze exhibits the lowest corrosion rates of all the alloys tested in every trial condition. It exhibits good corrosion resistance under a range of conditions. It is for this reason that it is often used on critical parts of devices operating in seawater (Schüssler and Exner, 1993a).

Using Equation 6.1, the main effects for nickel aluminium bronze were calculated from the table of contrasts (Table 6.18).

Table 6.18. Nickel aluminium bronze estimated effects (dimensionless)

Effects	Estimated Effects ± SE
Average	0.116
T	**0.194 ± 0.020**
F	**0.079 ± 0.020**
S	0.013 ± 0.020
O	0.055 ± 0.020
TF	**0.070 ± 0.020**
TS	0.009 ± 0.020
TO	0.050 ± 0.020
FS	0.022 ± 0.020
FO	0.012 ± 0.020
SO	-0.028 ± 0.020
TFS	0.019 ± 0.020
TFO	0.020
TSO	-0.027
FSO	0.014
TFSO	0.013

The calculation of standard error can be carried out in the same manner as used for carbon steel (using Equations 6.2 and 6.3).

$$(SE\ effect)^2 = {}^1/_5\{(0.01933)^2 + (0.02017)^2 + (-0.0277)^2 + (0.0144)^2 + (0.0127)^2\}$$

$(SE\ effect)^2 = 0.00038$

SE effect = 0.020

Highlighted in bold in Table 6.18 are the factor and the interaction effects that are greater than their standard error, and therefore cannot be explained by chance alone.

Comparison of Factors

Factorial plots were produced to analyse the interaction between the factors for nickel aluminium bronze. The comparison between temperature and flow (Figure 6.13) shows the greatest difference in gradient between the high and low flow conditions. This again is likely to be the effect that flow has on transporting dissolved oxygen to the surface. This was also observed in the estimation of effects of the factors, and was observed to be significant as it had an effect on corrosion rate greater than that that might be expected by chance.

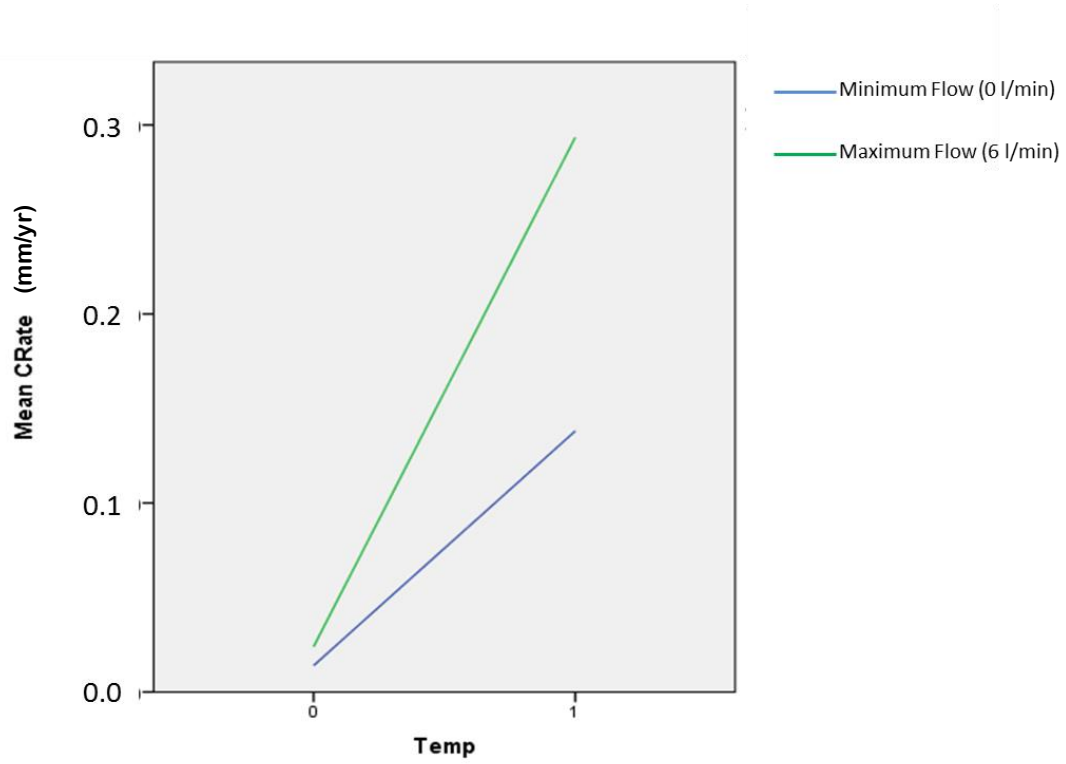

Figure 6.13. Plot comparing the mean corrosion rate (mm/yr) for a maximum (28°C) and minimum (2°C) temperature and flow for nickel aluminium bronze to understand their interactive effects

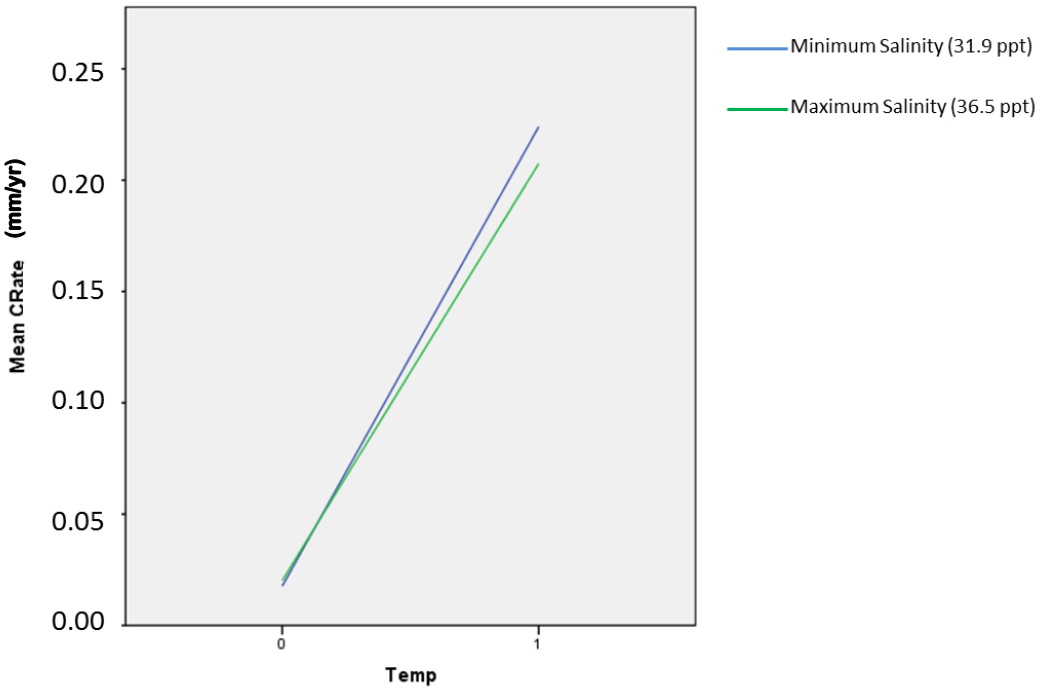

Figure 6.14. Plot comparing the mean corrosion rate (mm/yr) for a maximum (28°C) and minimum (2°C) temperature and salinity for nickel aluminium bronze to understand their interactive effects

The comparison between temperature and salinity (Figure 6.14) for aluminium bronze shows an intersection between the two levels. This implies that there is an interaction between the two factors when determining the corrosion rate for this metal. When salinity is at a maximum level and temperature is low, the rate is slightly greater that that obtained for minimum salinity level and low temperature. Conversely, at high temperature, it is higher with minimum salinity and less with maximum salinity. This may be due to changes in the breakdown potential of the nickel aluminium bronze or the formation of the protective film which provides the alloy with its good corrosion resistant properties.

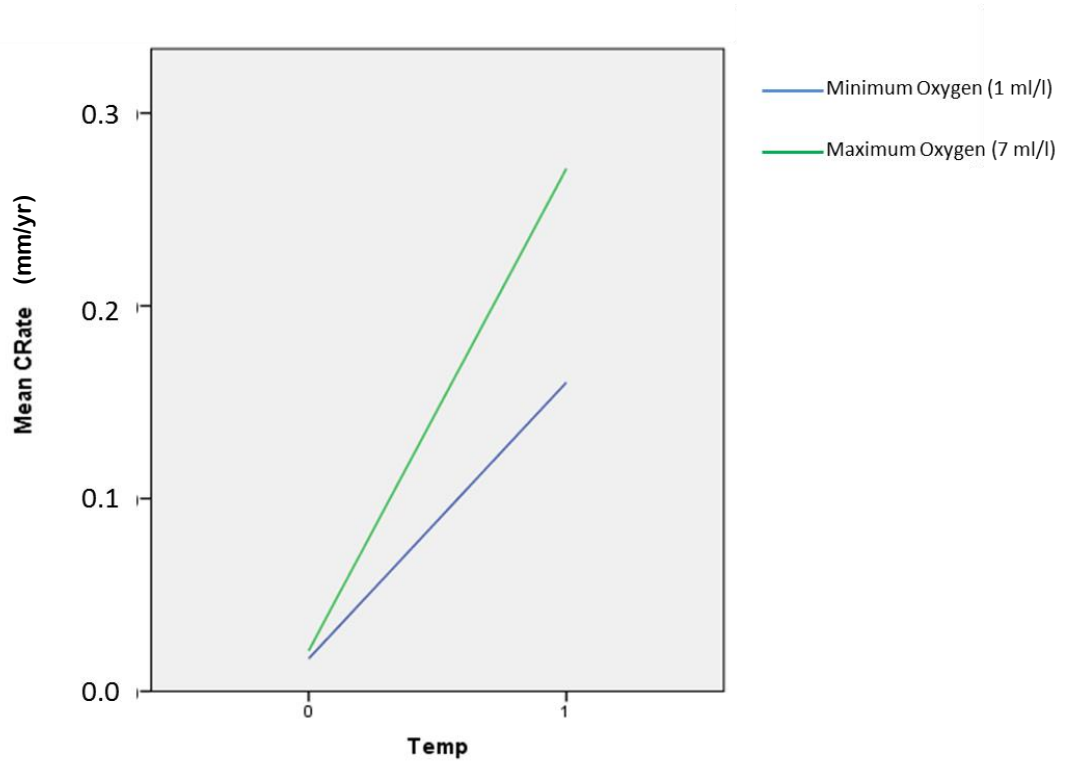

Figure 6.15. Plot comparing the mean corrosion rate (mm/yr) for a maximum (28°C) and minimum (2°C) temperature and oxygen for nickel aluminium bronze to understand their interactive effects

The plot of comparison between temperature and oxygen (Figure 6.15) for aluminium bronze shows no interaction, but a steeper gradient for the high level oxygen. This implies that the oxygen and temperature change have a combined effect, such that at high temperature level there is a greater difference between the corrosion rate obtained for the two levels of oxygen than at the lower level.

The effects between factors observed for the nickel aluminium bronze samples may be more apparent due to the very small corrosion rates observed for this metal under all trial conditions.

6.5.3 SG Iron 400-18

The results obtained for SG iron 400-18 were input into a table of contrast coefficients (Table 6.16). The SG irons tested in these experiments exhibit the highest corrosion rates under all trial conditions. In the majority of tests SG 400-18 displays the highest corrosion rate (9 out of 16 trials).

From the table of contrasts, the effects were calculated using Equation 6.1. These are shown in Table 6.19.

Table 6.19. SG iron 400-18 estimated effects (dimensionless)

Effects	Estimated Effects ± SE
Average	1.190
T	**1.268 ± 0.111**
F	0.305 ± 0.111
S	0.211 ± 0.111
O	0.372 ± 0.111
TF	0.054 ± 0.111
TS	0.219 ± 0.111
TO	0.184 ± 0.111
FS	-0.123 ± 0.111
FO	-0.288 ± 0.111
SO	-0.063 ± 0.111
TFS	-0.130 ± 0.111
TFO	-0.116 ± 0.111
TSO	-0.015 ± 0.111
FSO	0.147 ± 0.111
TFSO	0.097 ± 0.111

The calculation of standard error was carried out in the same manner as used for the previous alloys (Equations 6.2 and 6.3).

$$(SE\ effect)^2 = {}^1/_5\{(-0.1299)^2 + (-0.1161)^2 + (-0.0146)^2 + (0.0172)^2 + (0.0972)^2\}$$

$(\text{SE effect})^2 = 0.0123$

SE effect = 0.111

Highlighted in bold in Table 6.19 is the factor effects significantly greater than their standard error, and therefore cannot be explained by chance alone. Temperature is thus the only factor with a significant effect on the corrosion rate for SG iron 400-18 samples.

Comparison of Factors

All of the factors have been plotted in factorial plots for comparison with the significant factor temperature. The plots for SG iron 400-18 are different to those obtained for carbon steel and aluminium bronze. The comparison between temperature and flow (Figure 6.16) shows that an interaction between the two factors does exist for this alloy as the lines are not parallel, but intersect between the values chosen for temperature and flow.

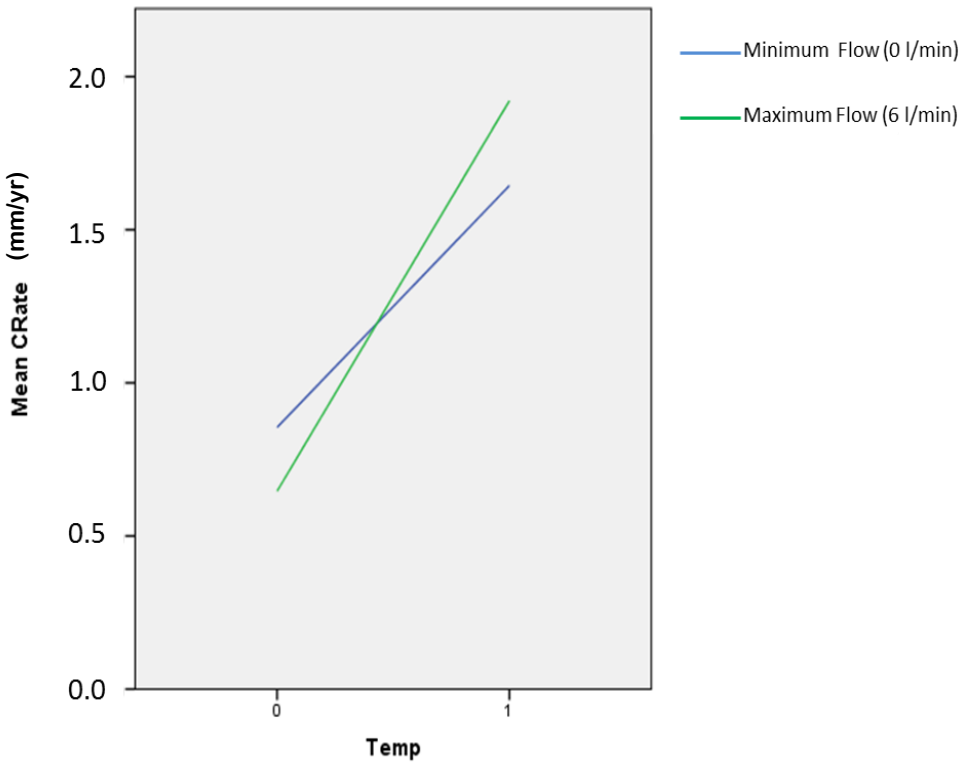

Figure 6.16. Plot comparing the mean corrosion rate (mm/yr) for a maximum (28°C) and minimum (2°C) temperature and flow for SG 400 to understand their interactive effects

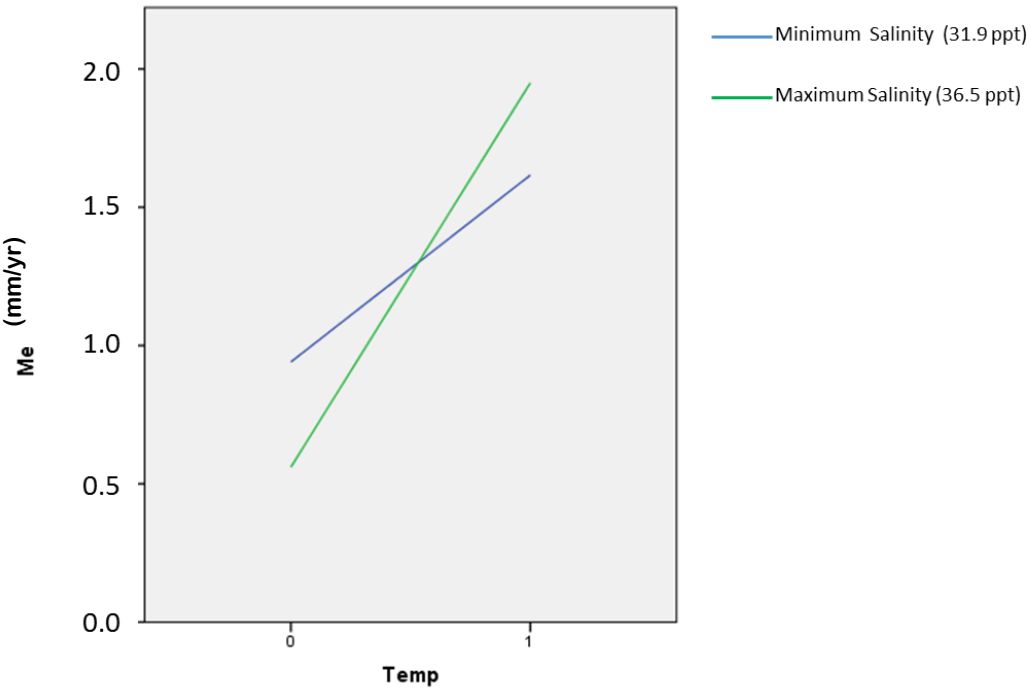

Figure 6.17. Plot comparing the mean corrosion rate (mm/yr) for a maximum (28°C) and minimum (2°C) temperature and salinity for SG 400 to understand their interactive effects

As well as an interaction between temperature and flow, there is also evidence of interaction between temperature and salinity and temperature and oxygen (Figures 6.17 and 6.18).

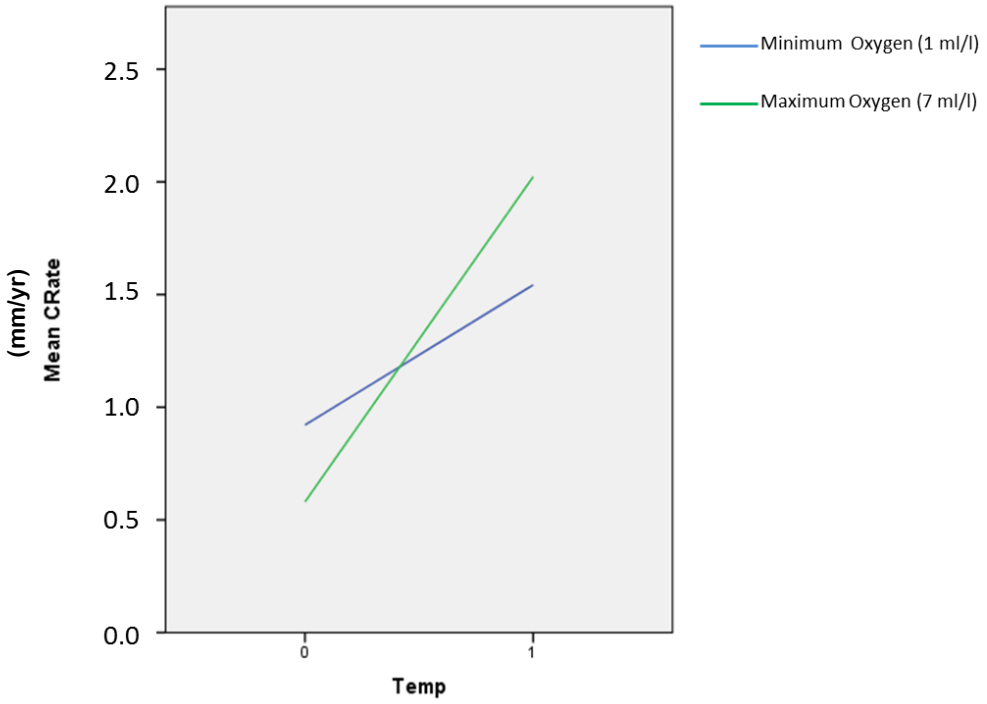

Figure 6.18. Plot comparing the mean corrosion rate (mm/yr) for a maximum (28°C) and minimum (2°C) temperature and dissolved oxygen for SG 400 to understand their interactive effects

However, it can be seen that these interactions are not as influential in determining the overall corrosion rate in comparison to the effect of temperature for SG iron 400-18.

6.5.4 SG Iron 500-7U

The results obtained for SG iron 500-7U were input into a table of contrast coefficients (Table 6.16). As with SG 400-18, the corrosion rates observed under all trial conditions for SG 500-7U are higher than the other two alloys. SG 500-7U gave the highest corrosion rate in seven out of the sixteen trials.

The effects of the factors and their interactions were calculated using Equation 6.1. These results are shown in Table 6.20.

Table 6.20. SG iron 500-7U estimated effects (dimensionless)

Effects	Estimated Effects ± SE
Average	1.106
T	**1.101 ± 0.106**
F	0.252 ± 0.106
S	0.218 ± 0.106
O	0.355 ± 0.106
TF	0.127 ± 0.106
TS	0.266 ± 0.106
TO	0.137 ± 0.106
FS	-0.027 ± 0.106
FO	-0.275 ± 0.106
SO	-0.170 ± 0.106
TFS	-0.056 ± 0.106
TFO	-0.102 ± 0.106
TSO	-0.151 ± 0.106
FSO	0.137 ± 0.106
TFSO	-0.029 ± 0.106

The standard error was calculated as below.

$$(SE\ effect)^2 = {}^1/_5\{(-0.0558)^2 + (-0.1020)^2 + (-0.1506)^2 + (0.1367)^2 + (-0.0289)^2\}$$

$(\text{SE effect})^2 = 0.0111$

SE effect = 0.106

Temperature is the only factor clearly distinguished from the margin of error (Standard Error) for SG iron 500-7U.

Comparison of Factors

The factors have been plotted as factorial plots against the significant factor, temperature. The plots for SG iron 500-7U show interaction between temperature and flow (Figure 6.19) and temperature and salinity (Figure 6.20), where the gradients of the plots are not parallel, but intersect between the values.

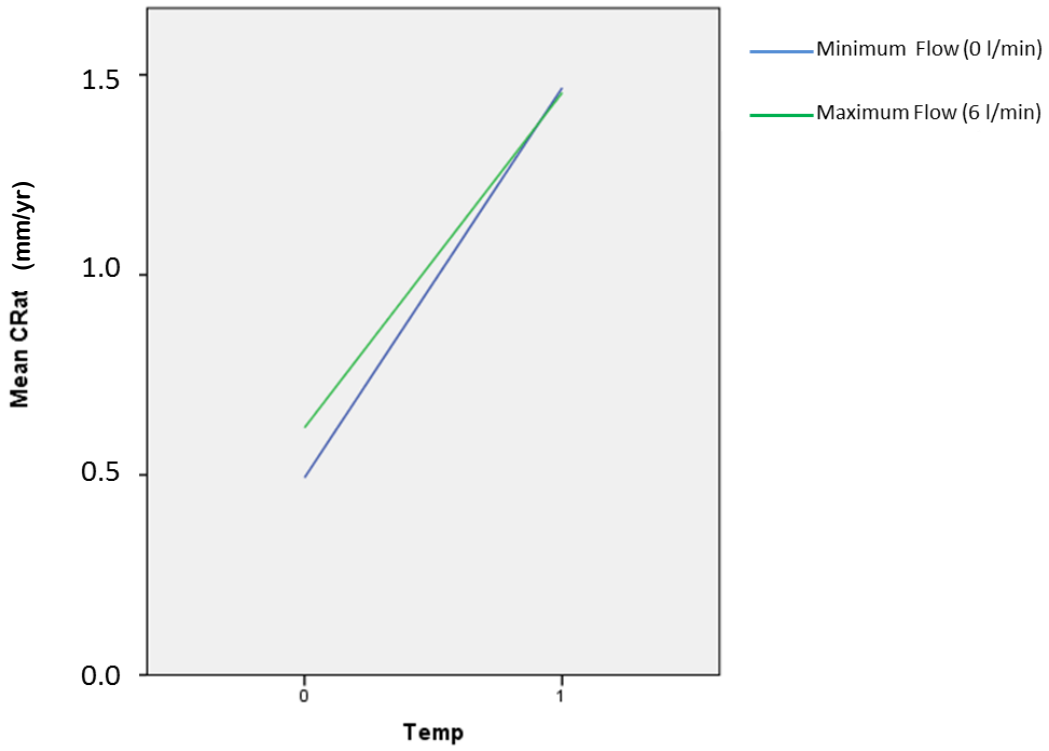

Figure 6.19. Plot comparing the mean corrosion rate (mm/yr) for a maximum (28°C) and minimum (2°C) temperature and flow for SG 500 to understand their interactive effects

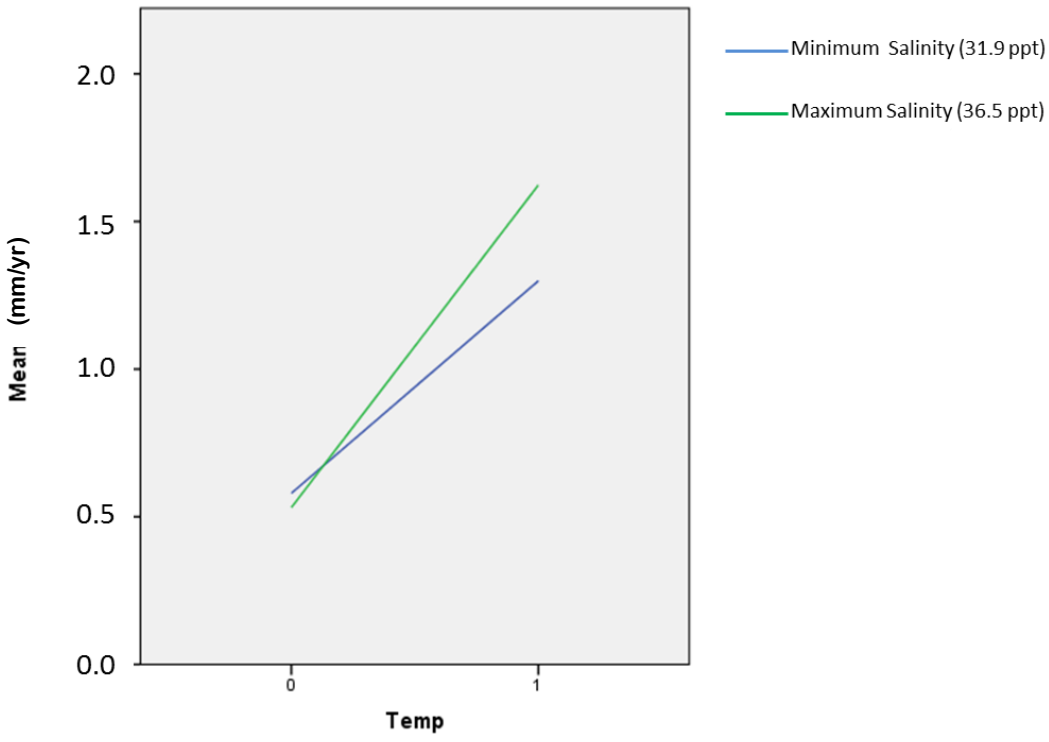

Figure 6.20. Plot comparing the mean corrosion rate (mm/yr) for a maximum (28°C) and minimum (2°C) temperature and salinity for SG 500 to understand their interactive effects

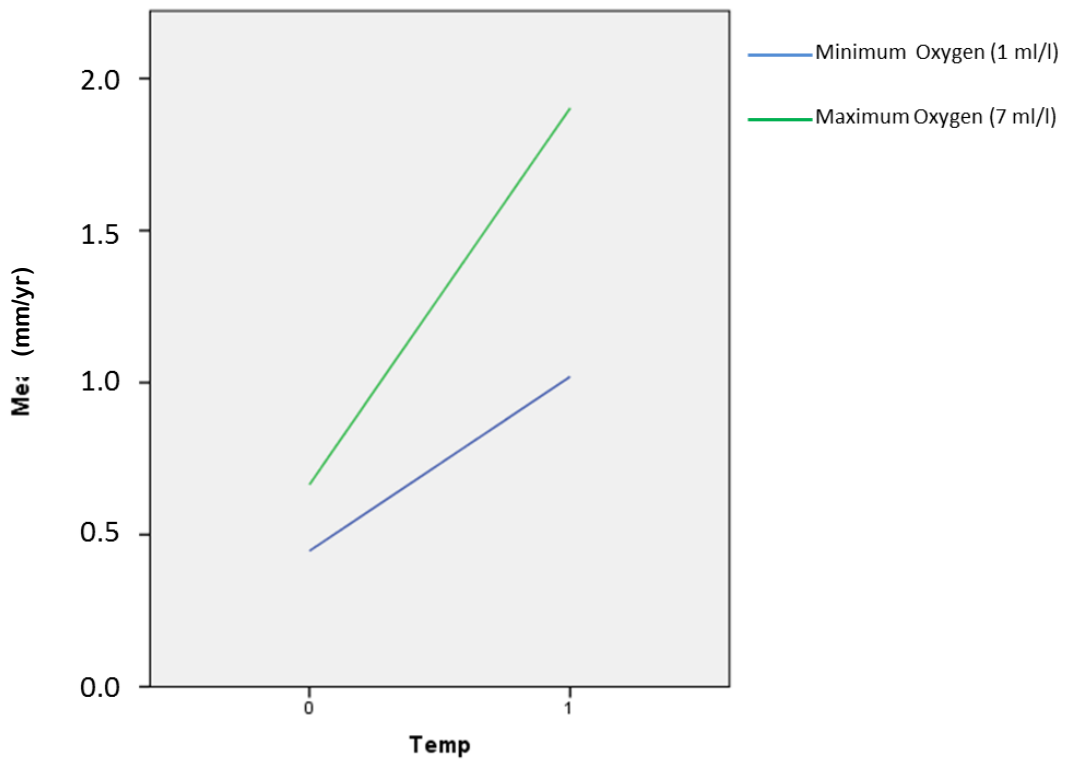

Figure 6.21. Plot comparing the mean corrosion rate (mm/yr) for a maximum (28°C) and minimum (2°C) temperature and oxygen for SG 500 to understand their interactive effects

Figure 6.21, the comparison between temperature and oxygen for SG 500 shows negative interaction between the two factors. The gradient of the plot for maximum oxygen level is greater than that for the minimum level of oxygen. Therefore the corrosion rate obtained is higher when oxygen and temperature are both at maximum levels, the two factors working together to create a more corrosive environment. However, it can be seen in Table 6.25 that the results of interactions of oxygen and temperature are not significant in their effect on corrosion rate. Only temperature has a significant effect on the corrosion rate of the SG 500-7U.

6.6 Discussion

The experiments here have shown that temperature and flow are the most significant factors when determining corrosion rate. The interaction between these and the dissolved oxygen has also been highlighted. There is a well defined relationship between temperature and dissolved oxygen concentration. When the temperature increases, dissolved oxygen concentration decreases (Shifler, 2005b). This was evident in these trials.

Corrosion rates obtained in these tests are approximately twice those reported for general seawater corrosion. These alloys, under these conditions in the range likely to be experienced by tidal devices, give a corrosion rate more than shown in previous literature and therefore are showing a high risk to the operation of tidal devices. Corrosion rates for metals in seawater have been reported as follows (Baboian, 2002) (average results obtained in the current experiments shown in brackets for comparison):

- Carbon steel: 0.127 – 0.254 mm/yr (0.44 mm/yr)
- Nickel-Aluminium Bronze: 0.0254-0.0508 mm/yr (0.11 mm/yr)
- SG Iron: 0.0508-0.508 mm/yr (SG400 – 1.18 mm/yr, SG500 – 1.10 mm/yr)

The figures quoted are documented for quiescent seawater (these experiments have testing both quiet and flowing conditions), with an average salinity of 35 ppt and at an average temperature of 12^{o}C, so it is likely that with higher salinity, dissolved oxygen levels and temperature corrosion rates will be higher, as shown in these experiments. Longer term (18 months) steady-state corrosion rates for nickel aluminium bronzes are in the range 0.01 and 0.025 mm/yr (Tuthill, 1987). These are lower than recorded in these experiments. However, it was also stated that the initial unfilmed corrosion rate of these alloys in seawater decreases significantly with time These tests were carried out after only a short exposure (approximately 2 hours prior to the potential stabilising) and so it is expected that corrosion rates will be higher than those observed for much longer exposure and can thus be taken as “worst case” scenarios.

Carbon steel and cast iron are close together in the galvanic series, with some high nickel cast irons actually more cathodic than carbon steel. However, the analysis has shown that individual effects on the corrosion rates for the cast irons are more interlinked and interaction between them is apparent. This can affect the relative positions of alloys in a metallic couple given different environmental conditions.

Overall, it was found that the corrosion rate was more dependent on temperature than the other three environmental factors tested. This has also been observed elsewhere for different alloys, for example various stainless steels (Atashin et al., 2011a; Atashin et al., 2011b). However, Meng (2007) found that water velocity was the most significant factor in determining weight loss over the ranges of temperature and sand-loading (scouring of the surface) tested. Therefore, it does depend on the ranges chosen for environmental factors as to which will have the most significant effect on corrosion rate.

The experimental data show an approximate doubling of corrosion rate with a 10 ^{o}C temperature rise. This relationship, following the Arrhenius relationship (Ijsseling, 1989), is often stated in literature but it is difficult to find proof of such a relationship. Melchers (2003a; 2003b) also attributed scatter in corrosion rate data analysed to temperature differences, agreeing with the data obtained here.

The corrosion rates observed in these tests are not exceptionally fast. However, they do highlight the care required when using these metals on a tidal device (required design life of 25-30 years). The device is situated in an extreme tidal regime where the water flow and suspended solids may affect protective coatings and indeed the potentially protective nature of corrosion products formed, hence exacerbating the corrosion rate. The potential 25 year degradation for each trial condition is shown in Table 6.14. These figures assume that the corrosion rate found in this work will continue over the duration of the operational lifetime. These results represent the worst case scenario but are likely to reduce over time with the formation of a protective rust layer. Therefore there are no standard conditions during the corrosion process - a factor which has to be built into the risk management process.

The thickness of the carbon steel used on the main nacelle body and buoyant nose varies between 20 mm and 40 mm. The data in Table 6.15 shows the percentage of thickness that would be lost in the above worst case scenarios of corrosion.

6.7 Relevance to Risk Management Development

These experiments have added to the evidence base of corrosion of the metals used on tidal devices under the conditions likely to be found in tidal locations around the world. The experiments confirm that temperature and water flow rate are key factors affecting corrosion rate and have shown that the environment in which these devices are likely to operate will exacerbate corrosion. It was found that temperature contributes most to corrosion rates in the range likely to be experienced by tidal devices (2 to 28 ^{o}C).

The corrosion rates obtained for the metals are low, with aluminium bronze exhibiting the lowest corrosion rate and SG iron the highest. However, when taking the potential operational lifetime of these devices (25-30 years), and the harsh tidal regime, into consideration the rates show that these factors must be taken into account to ensure that the device is effectively designed, protected and maintained to minimise the potential risks

associated with corrosion. In addition, these rates are for uniform corrosion and take no account of localising factors which may concentrate the corrosion in a small area.

The results of this work show that a new industry, that of tidal generation, can take much of the existing literature data of both biofouling and corrosion and apply this with confidence in its risk analysis. However there are areas that can potentially increase the risk over published predictions. There are aspects which are particularly important, and the results indicate that water flow rate and temperature, both well known influences on corrosion, need special consideration in relation to the alloys used, and likely to be used, in the construction of tidal devices. Flow and temperature must be key corrosion influencing parameters in the risk analysis. Oxygen and salinity are also contributory factors; however, these experiments have shown that these environmental factors are less significant than temperature and flow.

6.8 Conclusions

The experiments here have shown that temperature and flow are the most significant factors when determining corrosion rate. The interaction between these and the dissolved oxygen has also been highlighted. This was evident in these trials. Overall, it was found that temperature was the most significant factor in determining the corrosion rate under the conditions tested.

The experimental data prove an approximate doubling of corrosion rate with a 10 ^{o}C temperature rise. This relationship follows the Arrhenius relationship. This experimental proof of this theoretical relationship is worthy of note, as it is difficult to find experimental substantiation in published literature.

Having identified temperature as the main risk factor, further tests were developed to investigate this further and the results are described in Chapter 7. Flow also has a noticeable influence on the rate of corrosion, especially with carbon steel and nickel aluminium bronze. These tests were only carried out at a low circulating flow over the coupons compared with stagnant conditions. Therefore, it was also decided to carry out experiments at a higher flow rate to add to the evidence base (Chapter 8).

These experiments have supplied evidence for the corrosion that will be likely to occur in the environments in which tidal devices will be operating which will aid a risk assessment

and provides key risk factors for the development of a management strategy of the associated risks.

Chapter 7

Developing the Evidence Base (v) - Analysis of the Effect of Temperature on Corrosion Rates

7.1 Introduction

Previous experiments (Chapter 6) highlighted the significance of water temperature in influencing corrosion rates on the four different materials being tested. Therefore, a more detailed analysis of the effect of temperature on the corrosion rates of metals likely to be used on tidal devices was conducted.

These laboratory tests were carried out in an abiotic environment, using artificial seawater. Temperatures were chosen using the limits found for potential tidal sites around the world in the National Oceanographic Data Centre's (National Oceanographic and Atmospheric Administration) World Ocean Database 2009 (Boyer et al., 2009). (See Chapter 6 for more detail).

The metals used for these tests were the same as used in the experiments described in Chapter 6.

7.2 Experimental Design and Methodology

7.2.1 Experimental Design

The experimental protocol for these experiments was the same as used in previous laboratory experiments (See Chapter 6).

The heaters used to control the temperature used a feedback system to ensure that the water was maintained at the desired temperature for the duration of the test, with an accuracy of ±0.5 ^{o}C.

The salinity of the water was set at the average salinity of seawater of 35 ppt (Team, 1995). This was the salinity measured at the quayside in Orkney on a number of site visits throughout this thesis. The correct salinity was achieved by mixing Instant Ocean® with distilled water, and was continuously monitored throughout the testing using a Thermo Scientific Orion 5 Star water meter. The flow in the tanks was set to circulate at 6 l/min

through the pumps to ensure no stagnation. Dissolved oxygen was monitored, but not controlled, at each temperature.

Salinity, temperature and dissolved oxygen were monitored continuously using a Thermo Scientific Orion 5 Star water meter.

The experiments were randomized with respect to time to avoid any bias.

7.2.2 Methodology

Experiments were conducted between 4 ^{o}C and 30 ^{o}C, at intervals of 1.5-3.5 ^{o}C (Tables 7.1-7.4). At each level three replicates of each metal were tested to allow an assessment of reproducibility.

Corrosion rates were determined by Tafel Extrapolation (methodology given in Chapter 3, Section 3.2.3 and discussed further in Chapter 6). The Tafel extrapolation plots obtained are given in Appendix 2. The exposed surface area of the metal was determined for each sample and input into the UiECorr software as used in previous experiments (Chapter 6). The equivalent weights and densities for all the metals tested were calculated in Section 6.2.2 in Chapter 6.

Three replicates of each metal at each temperature were tested. Standard deviation and standard error were calculated for all trials with two significant figures using the following relationship:

$$Standard\ deviation\ (\sigma) = \sqrt{\frac{\sum(x-\bar{x})^2}{(n-1)}} \quad [7.2]$$

$$Standard\ Error\ (SE) = \frac{\sigma}{\sqrt{n}} \quad [7.3]$$

Where x is the value of the corrosion rate for a particular trial, $\bar{x}$ is the mean value, and *n* is the number of trials.

7.3 Results

7.3.1 Carbon Steel Results

The corrosion rates (in mm/yr) obtained for carbon steel are shown in Table 7.1.

Table 7.1. Corrosion rates for carbon steel (mm/yr)

Temperature (°C)	Sample 1 (mm/yr)	Sample 2 (mm/yr)	Sample 3 (mm/yr)	Average Corrosion Rate (mm/yr)	St. DEV	St. Error
4	0.111	0.125	0.117	0.118	0.0068	0.0039
6	0.223	0.191	0.199	0.204	0.017	0.0096
8	0.282	0.275	0.277	0.278	0.0040	0.0023
11	0.381	0.362	0.361	0.368	0.011	0.0064
12.5	0.433	0.435	0.434	0.434	0.00061	0.00035
16	0.574	0.545	0.574	0.564	0.017	0.0097
18.5	0.652	0.649	0.646	0.649	0.0030	0.0018
20	0.694	0.687	0.669	0.684	0.013	0.0074
22	0.746	0.764	0.739	0.750	0.013	0.0075
25	0.807	0.799	0.829	0.812	0.015	0.0087
28	0.880	0.899	0.885	0.888	0.0097	0.0056
30	0.937	0.952	0.934	0.941	0.010	0.0055

The average corrosion rates for carbon steel are plotted against temperature in Figure 7.1.

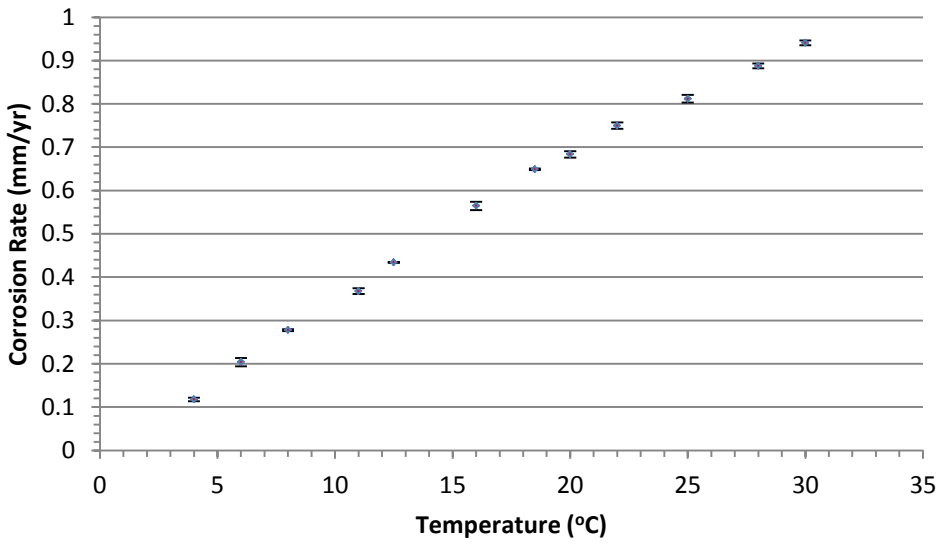

Figure 7.1. Corrosion rate vs temperature for carbon steel (black bars = ±SE)

7.3.2 SG Iron 400 (EN-GJS-400-18) Results

The corrosion rates (in mm/yr) obtained for the SG iron 400-18 samples are detailed in Table 7.2.

Table 7.2. Corrosion rates obtained for SG iron 400-18 (mm/yr)

Temperature (°C)	Sample 1 (mm/yr)	Sample 2 (mm/yr)	Sample 3 (mm/yr)	Average Corrosion Rate (mm/yr)	St. DEV	St Error
3.5	0.697	0.700	0.697	0.698	0.0017	0.00096
5.5	0.841	0.845	0.843	0.843	0.0021	0.0012
8.5	0.975	0.981	0.981	0.979	0.0037	0.0021
10.5	1.133	1.123	1.133	1.130	0.0056	0.0032
12.5	1.215	1.218	1.216	1.216	0.0015	0.00086
15	1.316	1.31446	1.311	1.314	0.0021	0.0012
17	1.392	1.406	1.403	1.400	0.0070	0.0041
20	1.509	1.512	1.509	1.510	0.0020	0.0011
23	1.673	1.673	1.678	1.674	0.0027	0.0016
25	1.793	1.770	1.772	1.778	0.013	0.0073
27	1.895	1.888	1.897	1.893	0.0045	0.0026
30	1.996	1.989	1.983	1.989	0.0063	0.0036

The average corrosion rates obtained for SG iron 400-18 are plotted against temperature in Figure 7.2.

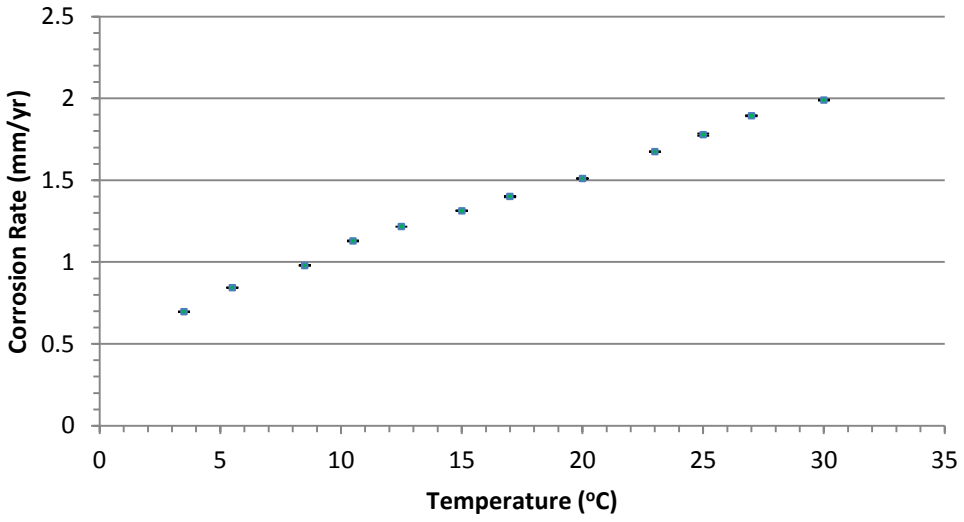

Figure 7.2. Corrosion rate vs temperature for SG iron 400-18. (black bars = ±SE)

7.3.3 SG Iron 500 (EN-GJS-500-7U) Results

The corrosion rates (in mm/yr) obtained for the SG iron 500-7U samples are detailed in Table 7.3.

Table 7.3. Corrosion rates for SG iron 500-7U (mm/yr)

Temperature (°C)	Sample 1 (mm/yr)	Sample 2 (mm/yr)	Sample 3 (mm/yr)	Average Corrosion Rate (mm/yr)	St. DEV	St. Error
4	0.805	0.783	0.785	0.791	0.012	0.0071
6	0.839	0.868	0.887	0.865	0.025	0.014
8.5	0.904	0.923	0.934	0.920	0.015	0.0088
11	1.016	0.993	1.004	1.004	0.012	0.0068
13	1.060	1.063	1.062	1.062	0.0018	0.0010
15	1.125	1.126	1.155	1.135	0.017	0.0099
16.5	1.208	1.190	1.191	1.197	0.010	0.0058
20	1.421	1.439	1.422	1.427	0.0098	0.0057
23	1.596	1.590	1.590	1.592	0.0034	0.0020
25	1.680	1.694	1.694	1.689	0.0078	0.0045
27	1.779	1.779	1.777	1.778	0.0012	0.00072
30	1.904	1.905	1.922	1.910	0.010	0.0058

The average corrosion rates for SG iron 500-7U are plotted against temperature in Figure 7.3.

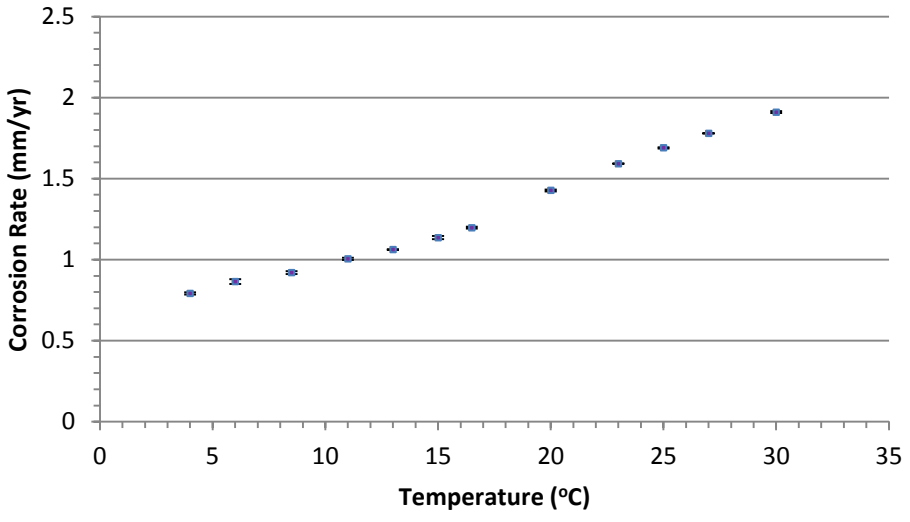

Figure 7.3. Corrosion rate vs temperature for SG iron 500-7U. (black bars = ±SE)

7.3.4 Nickel Aluminium Bronze Results

The corrosion rates (in mm/yr) obtained and standard error for the nickel aluminium bronze samples are shown in Table 7.4.

Table 7.4. Corrosion rates for nickel aluminium bronze (mm/yr)

Temperature (°C)	Sample 1 (mm/yr)	Sample 2 (mm/yr)	Sample 3 (mm/yr)	Average Corrosion Rate (mm/yr)	St. DEV	St. Error
4	0.013	0.013	0.013	0.013	0.00023	0.00013
6	0.017	0.019	0.017	0.018	0.00084	0.00048
8	0.023	0.022	0.023	0.023	0.00017	9.6E-05
10	0.029	0.028	0.028	0.028	0.00075	0.00043
13	0.033	0.034	0.034	0.034	$8.5x10^{-5}$	4.9E-05
15	0.044	0.045	0.044	0.044	0.00022	0.00013
18	0.065	0.065	0.065	0.065	0.00012	7.1E-05
20	0.071	0.079	0.072	0.074	0.0043	0.0025
22.5	0.100	0.095	0.091	0.095	0.0044	0.0025
24.5	0.162	0.155	0.159	0.159	0.0035	0.0020
26	0.204	0.203	0.195	0.201	0.0047	0.0027
28	0.302	0.285	0.307	0.298	0.011	0.0064
30	0.411	0.429	0.417	0.419	0.0092	0.0053

The average corrosion rates for nickel aluminium bronze are plotted against temperature in Figure 7.4.

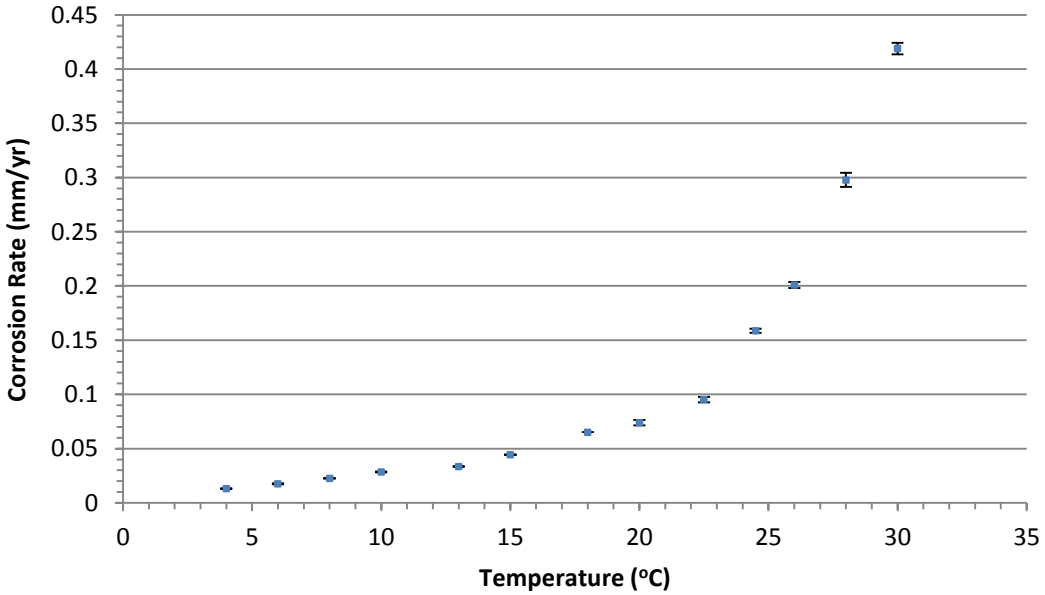

Figure 7.4. Corrosion rate vs temperature for nickel aluminium bronze (black bars = ±SE)

7.3.5 Comparison of Metal Corrosion Rates

It can be seen from the standard errors in the figures above that the results are highly reproducible.

Corrosion rates for the four metals are compared in Figure 7.5. All metals except for nickel aluminium bronze follow a linear trend, with an increase in corrosion rate with increasing temperature. However, there is a slight change in gradient as temperature increases (best seen in Figures 7.1, 7.3 and 7.4 and discussed in Section 7.4 below). Unlike the others, the corrosion rate of nickel aluminium bronze increases markedly after 22 °C, although the overall corrosion rate is much less than for the other alloys.

The most corrodible of the metals was SG iron 400-18, with SG iron 500-7U only slightly lower. At the lowest temperatures SG iron 500-7U actually exhibited slightly higher corrosion rates than the 400-18 alloy. This may be because the two alloys have a different reaction to the synergistic effects of temperature, dissolved oxygen, flow and salinity (see Chapter 6).

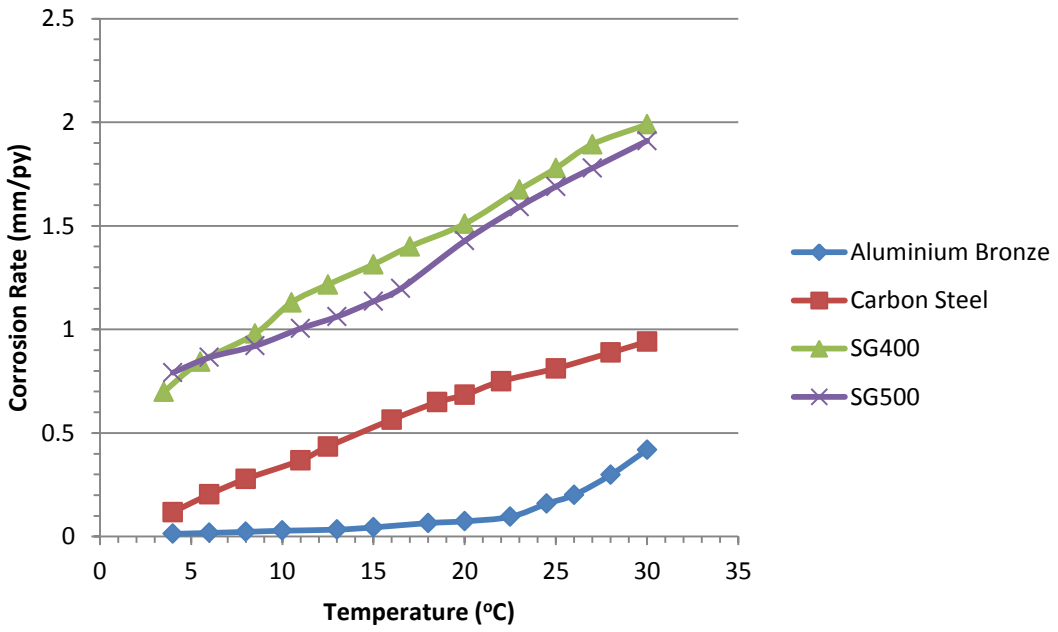

Figure 7.5. Corrosion rate vs temperature for all metals tested

7.3.6 Variation in Dissolved Oxygen with Temperature

The relationship between dissolved oxygen and temperature is given in Figure 7.6.

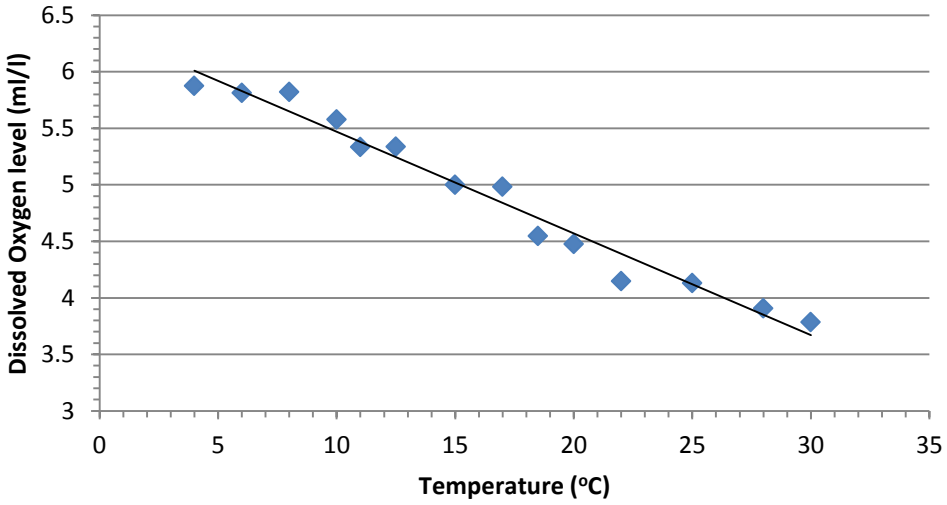

Figure 7.6. Variation of dissolved oxygen with temperature during the experiments

As water temperature increases the concentration of dissolved oxygen decreases. This is a well known effect widely reported in the literature (Shifler, 2005b).

7.4 The Effects of Temperature and Oxygen Concentration on Corrosion Rates

The results for the cast irons and carbon steel show an almost linear increase in corrosion rate with increasing temperature. The theory states that that a doubling in the corrosion rate will occur for every 10 ^{o}C rise in temperature (Tomashov et al., 1966) (see Chapter 3). This is derived from the Arrhenius relationship, although, surprisingly, while it is widely stated, there is little reported experimental observation of the effect. Carbon steel can be used to demonstrate the theory here. At 10 ^{o}C the corrosion rate is approximately 0.3 mm/yr, while at 20 ^{o}C it is approximately 0.6 mm/yr. However, the relationship becomes less direct at higher temperatures where there is some sign that the corrosion rate begins to level off. This could be due to the lower oxygen content at higher temperatures beginning to limit the cathodic reaction. To test if this oxygen effect could be shown as a specific non linear relationship, a polynomial curve fit was performed to see if this would fit the data more closely than a linear relationship. This was carried out for each metal. Sigma Plot was used to perform the curve fitting using non-linear regression analysis.

7.4.1 Carbon Steel

The equation obtained for the carbon steel curve is a 3rd order polynomial in the form shown in Equation 7.4.

$$f = y0 + a * x + b * x^2 + c * x^3 \qquad [7.4]$$

The coefficients are shown in Table 7.5.

Table 7.5. Polynomial curve fit coefficients obtained for carbon steel

Coefficient	Value
y0	-0.0347
a	0.0389
b	6.482E-6
c	-7.534E-6

The R^2 value obtained when carrying out a regression of the data (the coefficient of determination) measures how closely the regression model for the curve fit describes the actual data obtained, and how well the model would work to predict future outcomes. The closer the value of R^2 is to unity, the better the independent variables predict the dependent variable (in this case, the independent variable is temperature, and the dependent variable is corrosion rate). Equation 7.5 shows the relationship for calculating the value of R^2.

$$R^2 = 1 - \frac{SS_{err}}{SS_{tot}} \qquad [7.5]$$

Where SS_{err} is the sum of squares of residuals and SS_{tot} is the total sum of squares.

For carbon steel the R^2 value is 0.9996. This is very close to unity, and therefore shows that the curve produced describes the data obtained sufficiently well and can be used as a model to describe that data.

As part of the investigation, further non-linear regressions were also carried out for carbon steel. However, none of these modelled the data as closely as the 3rd order polynomial. The R^2 value for the straight line has been calculated as 0.9910. Therefore, a linear fit is not quite as close a fit as the calculated polynomial and so it can be concluded that an effect of oxygen depletion is occurring at higher temperatures.

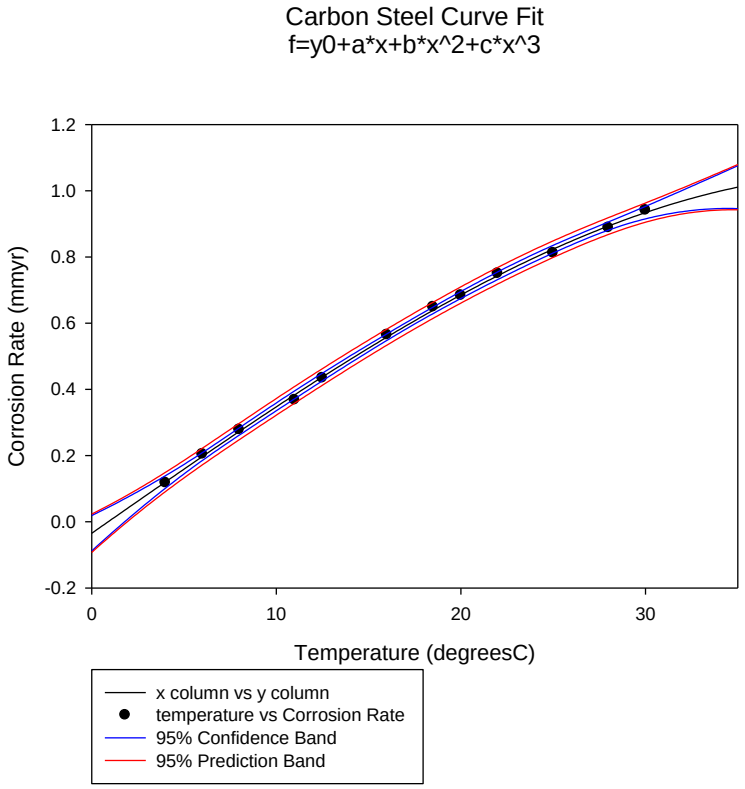

Figure 7.7. Polynomial curve fit for carbon steel including confidence and prediction bands

7.4.2 SG Iron 400 (EN-GJS-400-18)

As with the carbon steel, a non-linear regression was used to obtain a polynomial curve fit for SG iron 400-18 (Equation 7.4). The coefficients are shown in Table 7.6.

Table 7.6. Polynomial curve fit coefficients obtained for SG iron 400-18

Coefficient	Value
y0	0.4653
a	0.0741
b	-0.0015
c	2.6083E-5

The coefficient of determination (R^2) was calculated as 0.9977 for SG iron 400-18. Since this is very close to unity, it is a good model for the data obtained. The data is plotted in Figure 7.8. The R^2 value for the straight line has been calculated as 0.9956. Therefore, a linear fit is not quite as close a fit as the calculated polynomial. Therefore, it can be concluded that an effect of oxygen depletion is occurring at higher temperatures.

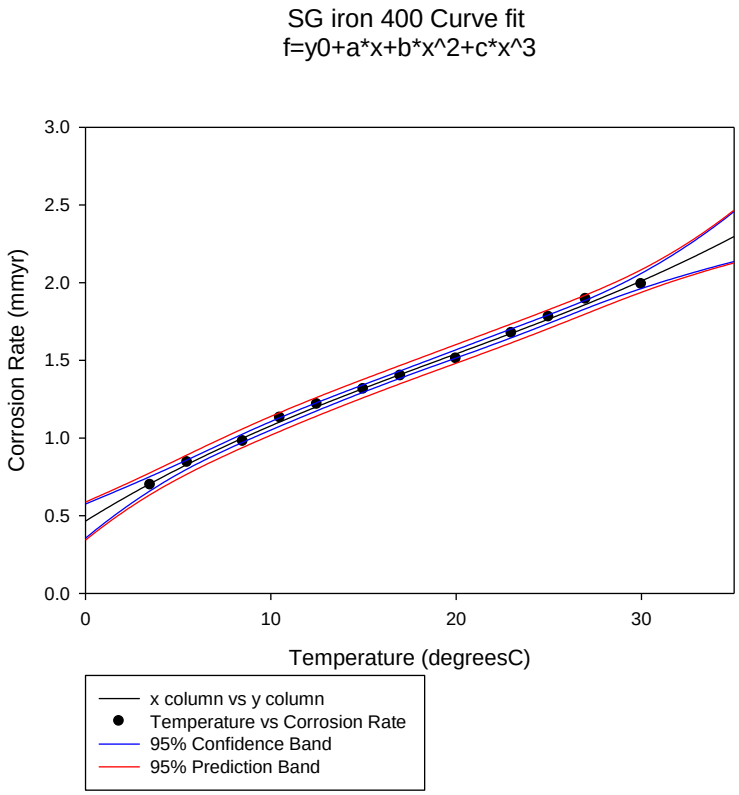

Figure 7.8. Polynomial curve fit for SG iron 400-18 including confidence and prediction bands

For SG Iron 400-18, the 3rd order polynomial fits well to the data obtained in the experiments. This means that the corrosion rate increase is slowing down as the temperature increases. This could be due to the reduction in dissolved oxygen at the metal surface at higher temperatures. The same can be said for carbon steel as this was also modelled by a 3rd order polynomial.

7.4.3 SG Iron 500 (EN-GJS-500-7U)

As with carbon steel and SG iron 400-18, the corrosion rate for SG iron 500-7U appears to be a general linear relationship with temperature. However, a polynomial curve fit (Equation 7.5) gives a coefficient of determination (R^2) of 0.9975 indicating that this is a good model for the data obtained. The coefficients are shown in Table 7.7 and the data and polynomial curve fit in Figure 7.9. The R^2 value for the straight line has been calculated as 0.99254. Therefore, a linear fit is not quite as close a fit as the calculated polynomial and so it can be concluded that an effect of oxygen depletion is occurring at higher temperatures.

Table 7.7. Polynomial curve fit coefficients obtained for SG iron 500-7U

Coefficient	Value
y0	0.8262
a	-0.0146
b	0.0032
c	-4.9916E-5

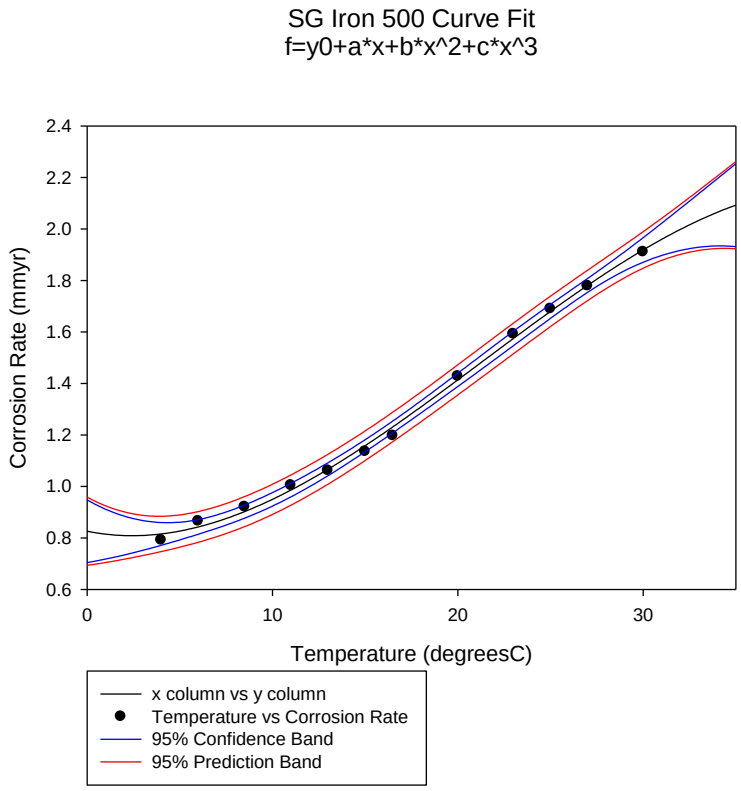

Figure 7.9. Polynomial curve fit for SG iron 500-7U including confidence and prediction bands

The 95% confidence band appears to deviate from the obtained results for SG iron 500 at the low and high temperatures in the range. Therefore a further non-linear regression was carried out to determine if there was a better fit to the data that would describe it over the whole range. A sigmoidal curve (described by Equation 7.8) was found to give an R^2 value of 0.9985, which is closer to unity than the value obtained using either of the polynomial expressions

$$f = y0 + \frac{a}{1+exp^{-\frac{x-x0}{b}}} \qquad [7.7]$$

The coefficients for the SG iron 500-7U sigmoidal curve fit are shown in Table 7.8 and the curve plotted in Figure 7.10.

Table 7.8. Sigmoidal curve fit coefficients obtained for SG iron 500-7U

Coefficient	Value
a	1.5195
b	6.7173
y0	0.6996
x0	20.8224

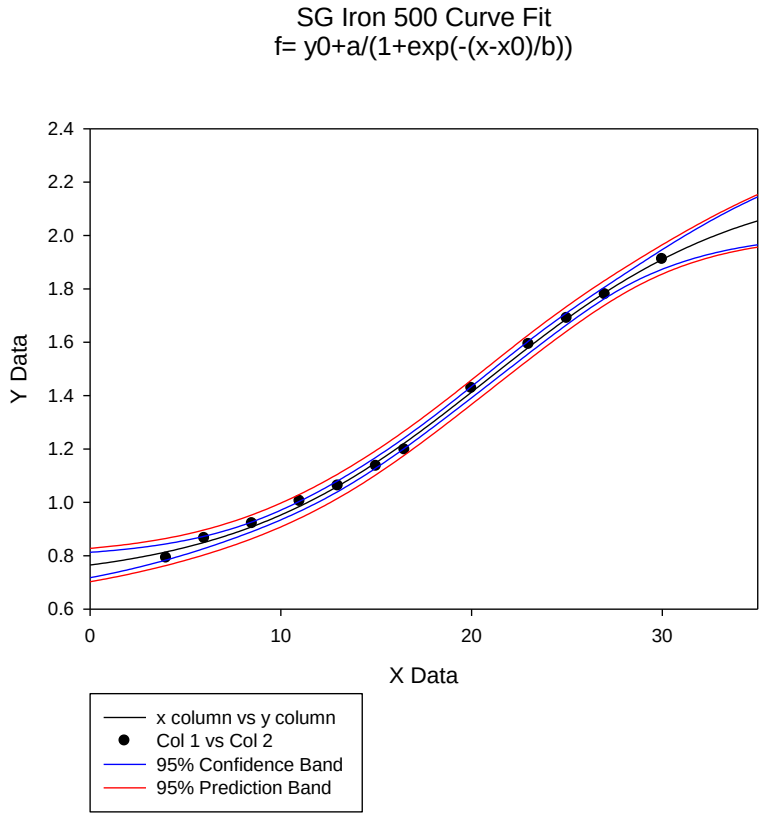

Figure 7.10. Sigmoidal curve fit for SG iron 500-7U including confidence and prediction bands

7.4.4 Nickel Aluminium Bronze

The corrosion rates observed for nickel aluminium bronze increase rapidly above 22 ^{o}C. A cubic polynomial curve fit, as fitted to the carbon steel results, (Equation 6.4) was performed to determine if this would provide a sufficiently accurate fit for the data obtained. The coefficients and are shown in Table 7.11.

Table 7.9. Polynomial curve fit coefficients obtained for nickel aluminium bronze

Coefficient	Value
y0	-0.0753
A	0.0280
B	-0.0023
C	6.502E-5

The coefficient of determination, R^2, was 0.9947. The graph of the data is given in Figure 7.11.

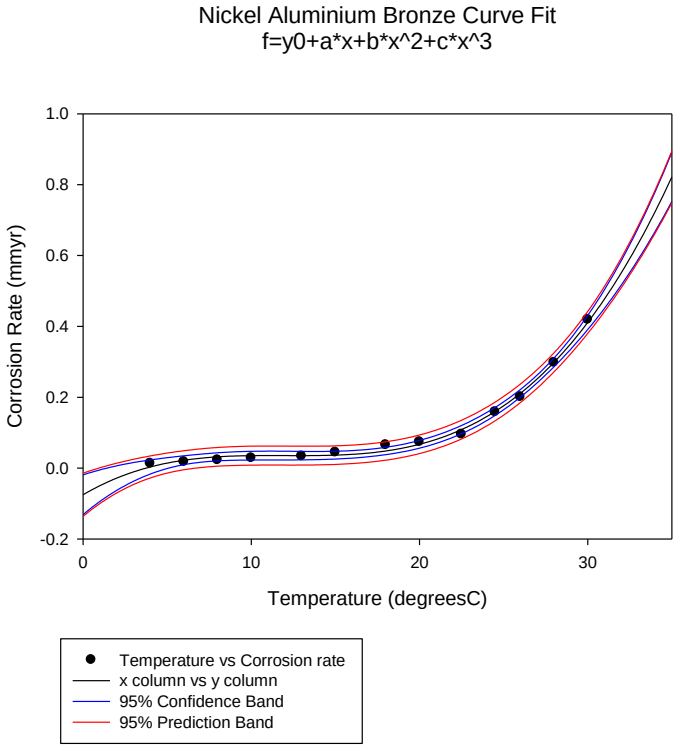

Figure 7.11. Polynomial curve fit for nickel aluminium bronze including confidence and prediction bands

The polynomial expression fits well with the data and predicts that the corrosion rate would continue to increase with increasing temperature. However, this model predicts a negative corrosion below 4 ^{o}C which is not possible. Therefore, a better model is required to fully describe the trend.

An exponential curve was next tried (Equation 7.6).

$$f = y0 + a * \exp(b * x) \qquad [7.6]$$

The coefficients are shown in Table 7.10.

Table 7.10. Exponential curve fit coefficients obtained for nickel aluminium bronze

Coefficient	Value
y0	0.0169
A	0.0012
B	0.1948

The coefficient of determination (R^2) for the exponential fit is 0.9974, suggesting that this is a better fit to the data. Throughout the region where data has been obtained, the confidence and prediction bands are much closer to the actual data than with the polynomial fit. The exponential curve fit also ensures that the y-intercept does not fall below zero as with the polynomial fit. This exponential fit is good for explaining corrosion

rates of nickel aluminium bronze in this temperature region. However, it is unlikely that the corrosion rate will continue to follow an exponential curve at higher temperatures as other factors will alter the effect, such as salinity and dissolved oxygen.

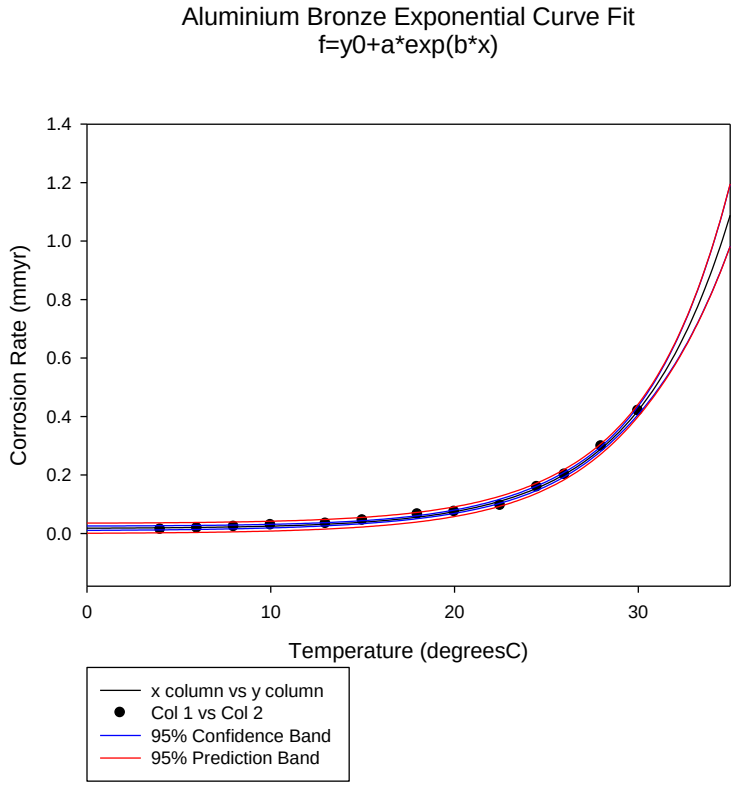

Figure 7.12. Exponential curve fit for nickel aluminium bronze including confidence and prediction bands

Nickel aluminium bronze exhibits very good corrosion resistance in seawater, hence its use for propellers and other important parts of devices and structures operating in the marine environment. This corrosion resistance is due to the formation of a thin but tough adherent aluminium oxide self-healing film that protects the metal surface (Callcut, 2002). It is possible that above 22 ^{o}C, film development or repair is not as fast due to the decrease in oxygen availability and so the corrosion rate increases. These results are similar to those obtained by Schüssler and Exner (1993b), who found that exposure of nickel aluminium bronze to a higher temperature (40 ^{o}C) initially leads to an increased dissolution rate compared to lower temperature (20 ^{o}C).

The equations for the trend lines fitted to each of the four metals' results can be seen in Table 7.11.

Table 7.11. Trend lines fitted to metal data

Metal	Fitted expression	R^2
Carbon steel	$y = -0.0347 + 0.0389x + 6.482 \times 10^{-6}x^2 - 7.534 \times 10^{-6}x^3$	0.9996
Nickel aluminium bronze	$y = 0.0169 + 0.0012exp^{0.1948x}$	0.9947
SG Iron 400-18	$y = 0.4653 + 0.0741x - 0.0015x^2 + 2.6083 \times 10^{-5}x^3$	0.9977
SG Iron 500-7U	$y = 0.6996 + \frac{1.5195}{1 + exp^{\frac{x-20.8224}{6.7173}}}$	0.9975

All of the fitted trend lines, except for nickel aluminium bronze, are polynomials of some degree. Carbon steel and SG iron 500-7U have a negative leading coefficient. This means that the rate of increase of the corrosion rate with temperature is decreasing for these metals.

7.5 Discussion

The corrosion rates in the experiments described in this chapter were obtained after the alloys had been immersed in artificial seawater for approximately one hour, until the open circuit potential stabilised. All four metals exhibited an increase in corrosion rate with increasing temperature over the range of temperature tested. The temperature values for each metal vary slightly due to randomising the experiments with respect to time. However, it was ensured that the interval between each temperature did not exceed 3.5 ^{o}C.

SG iron 400-18 (EN-GJS-400-18) exhibited the highest corrosion rates, as expected from the results in Chapter 6. The corrosion rates obtained for SG 500-7U (EN-GJS-500-7U) were slightly lower. Nickel aluminium bronze exhibited the lowest corrosion rate, although this metal showed a significant change in the rate of increase with temperature at approximately 22 ^{o}C. Carbon steel and SG iron 400-18 follow a 3rd order polynomial trend and SG iron 500-7U was found to fit more closely with a sigmoidal curve. Using the values of the coefficient of determination (R^2), it was observed that the polynomial trend for carbon steel, SG iron 400-18, the sigmoidal curve for SG iron 500-7U and the exponential trend for aluminium bronze could model the data obtained well, with all R^2 values close to unity. The 3rd order polynomial and the sigmoidal curve suggest that the rate of increase in corrosion rate will decrease as the temperature increases. A sigmoidal plot also infers that the gradient of the corrosion rate curve is smaller at low temperatures and high temperatures, with a larger gradient in between. These experiments have looked at bulk water temperature effects. If the temperature of the reacting surface of the metal is due to internal heating and that surface is therefore exposed to a flowing, cooler, water with

higher oxygen content then there may be no effect due to a lowering of dissolved oxygen with temperature. And the straight line relationship would be the “worst case” scenario.

While it is difficult to compare these results to those obtained through weight loss experiments where the corrosion rate is averaged over a much longer duration, they are of the same order of magnitude as previous tests (Chapter 5 and 6). The results, both the actual data points obtained and the overall trend, agree with previous work carried out in the field investigating temperature effects on the corrosion rate of mild steels over various periods of immersion (Melchers, 2002). The corrosion rates obtained agree with results obtained for five year exposure of the mild steel, suggesting that in these experiments the corrosion rate is controlled by mainly kinetic processes, as would be expected (Melchers, 2002). The results for corrosion rates for both SG irons tested agree with previous experimental data that has been obtained for ductile iron alloys under different seawater temperatures shown below (Davis and Committee, 1996):

- 10 ^{o}C – 0.6 mm/yr
- 20 ^{o}C – 1.0 mm/yr
- 30 ^{o}C – 1.5 mm/yr

The previous results are slightly lower than obtained in these tests as these were obtained from trials with a 60 day duration and, therefore, corrosion rates will reduce over time from the initial rate.

It is widely stated that the corrosion rate of steel can be estimated to double for every 10 ^{o}C rise in temperature when the corrosion is kinetically controlled (Melchers, 2002) due to the relationship set out in the Arrhenius relationship (Equation 6.1). However, if the corrosion rate is diffusion controlled, then a 30 ^{o}C rise is required to double the corrosion rate (Ijsseling, 1989; Fink, 1960). The Arrhenius relationship has been found to be approximately true for the carbon steel tested here with a steady, almost linear, rate of increase in corrosion rate as temperature increases. Nickel aluminium bronze could be said to follow this general trend until 20 ^{o}C, when the corrosion rate increases at a much faster rate with increasing temperature.

Both the SG iron 400-18 and SG iron 500-7U samples exhibited a slower rate of increase in corrosion as temperature increases compared to the Arrhenius relationship and carbon

steel, although, throughout the tests, the corrosion rates are higher than those on carbon steel and aluminium bronze samples.

The solubility of oxygen decreases with increasing temperature (Craig et al., 1995), as shown in these experiments. This effect can begin to counteract the temperature effect, with the rate of increase in corrosion rate slowing at higher temperatures as the cathodic reaction can no longer be sustained at the same level. Conversely, with some alloys (e.g. nickel aluminium bronze) the lower oxygen availability may prevent repair of protective oxide films and lead to higher corrosion rates.

This work could be continued by investigating a larger temperature range. However, for this study the range of temperature was sufficient as it is highly unlikely that tidal devices will operate anywhere outside this range. An investigation of the metal surface temperature of devices when operating would be worthwhile. This may change the maximum operating temperature that should be investigated.

The experiments were carried out in the range of temperatures found in potential tidal generation sites around the world. The metals tested show a clear increase in rate of corrosion as temperature increases. However, the trend between temperature and corrosion rate is not completely linear. An increase in temperature is likely to be associated with a decrease in dissolved oxygen which will reduce the cathodic reaction. This suggests that further testing should be carried out if temperatures are likely to exceed the range tested here (>30 ^{o}C) during operation to determine the likely corrosion rate. However, this is highly unlikely in the potential tidal locations for deployment in the foreseeable future.

One implication of the effect of temperature on corrosion of tidal devices is in the case of temperature generation within the device and hence at the metal surface and water flow around the device. If a temperature differential exists, this could not only result in a general increase in corrosion but also establish a corrosion cell between two areas on the device, where the hot area is more likely to corrode in preference to a colder one (Trethewey and Chamberlain, 1995).

As heat is transferred from the inside of the device to the surrounding water it is likely the outer wall surface will be at a different temperature to that of the bulk fluid. This difference and its effect on corrosion depend on the corrosion mechanism of the metal or alloy. If corrosion is under activation control (Arrhenius) the corrosion rate in the presence of heat transfer might be similar to that expected for corrosion at the same wall

temperature in the absence of heat transfer. However, if the corrosion rate is diffusion controlled (mass transfer of O_2 through the seawater to the metal surface), then heat transfer may greatly change the corrosion rate of the metal or alloy (Silverman, 2003). Heat transfer from the internal heating of the nacelle may also increase turbulence near wall, or increased diffusion/mass transfer. In stagnant areas heat transfer can cause convection currents that can enhance mass transfer and hence increase corrosion rates. This could be the reason that the aluminium bronze connectors used on the 500 kW device examined (Chapter 4) exhibited significantly more corrosion degradation than expected. The temperature at which the connectors operate needs confirmation to understand whether it is the temperature that is causing the increased corrosion. As seen in these tests the aluminium bronze corrosion rate increased dramatically above 22 ^{o}C.

7.6 Relevance to Risk Management Development

The key outcomes of this investigation for the risk register relate to the future operation of tidal devices in different locations around the world. The materials used on the devices have been shown to exhibit increased corrosion at the higher temperatures in the range in which they are likely to operate. These results can be taken forward to inform decisions at both design and operation stages of these devices. Temperature effects should be included in design stage discussions in relation to corrosion protection and increased maintenance requirements in warmer water. As operational experience increases, more information will be obtained regarding the surface temperature of these devices when operating. It is advisable that this data is collected throughout operation to determine the potential effect of increased surface temperatures.

7.7 Conclusions

These experiments were carried out after an investigation into the key environmental factors that will affect corrosion rate of tidal stream devices (Chapter 5 and 6). Temperature is the most significant rate determining variable and these experiments here have provided trends for corrosion rates of four metals tested over expected temperatures likely to be experienced in global tidal stream locations. All four metals exhibited an increase in corrosion rate with increasing temperature over the range of temperature tested. However, analysis of the trends has provided further information regarding how the corrosion rate of the four metals changes with respect to water temperature.

These experiments have supplied evidence for the corrosion rates that will be likely to occur in different global environments in which tidal devices will be operating which will aid a risk assessment and provides key risk factors for the development of a management strategy of the associated risks.

Chapter 8

Developing the Evidence Base (vi) - Analysis of the Effect of Flow on Corrosion Rate

8.1 Introduction

High flow rates can have several detrimental effects on a structure. They can increase effects that involve the removal of any passive coating on the surface of the metal. Such effects could be chemical or physical (e.g. damage by suspended solids, a higher dissolved oxygen concentration at the surface of the metal, etc.). Following on from Chapter 6, this chapter investigates further the effect of a higher seawater flows on the corrosion of the alloys used in the construction of tidal devices.

Samples were immersed in two flow regimes, a low flow environment of less than 0.001 ms^{-1} and a flow of 3.39 ms^{-1}. A comparison between the samples has been made in terms of weight loss and surface effects.

8.2 Experimental Design and Methodology

The experiments used the same system as described in Chapters 6 and 7. However, the pumping system was altered to provide a higher, more focused impingement jet flow on to the metal coupons to achieve the flow rates required and simulate a tidal regime. This was achieved by adapting the pipe attached to the pump so that it provided a water velocity of 3.39 ms^{-1} at the surface of the coupons. Low flow conditions were produced by pumping water from the holding tank at a rate of 1 l/min which allowed mixing and maintenance of the correct environmental conditions throughout the experiments without localised flow effects on the metal surface.

The water was periodically refreshed during each experiment, ensuring that the salinity remained constant at the average seawater salinity of 35 ppt.

On removal of the coupons their appearance and formation of corrosion product was recorded. The samples were then cleaned and mass loss recorded. The corrosion rate was determined using the same relationship as used in Chapter 5, Equation [5.1] (ASTM, 2011).

After weighing, the samples were examined for evidence of pitting corrosion using a Nikon Eclipse LV150 microscope. Pits observed were recorded using the Buehler Omnimet software.

Experimental design was based on guidelines published in the Standard Practice for Laboratory Immersion Corrosion Testing of Metals (G31-72) (ASTM, 2004) as was used in previous experiments (Chapters 6 and 7). Samples were cleaned and prepared following the Standard Practice for Preparing, Cleaning and Evaluating Corrosion Test specimens (G1-03) (ASTM, 2011). Weight loss measurements were used to determine corrosion rates. Although it is known that weight loss is not always a satisfactory indicator of total corrosion damage, as it ignores any localised effects (Melchers, 2002), it allows uniform corrosion rates to be assessed under high flow conditions. A reference coupon was also cleaned using the same method to determine, and correct for, weight loss from the cleaning process.

The duration of each test was 504 hours (21 days). This was sufficient to ensure that greater corrosion rates at the start of immersion did not lead to misleadingly high results. It also ensured that a corrosion rate could be determined from sufficient weight loss.

8.3 Results

8.3.1 Carbon Steel

Carbon steel coupons developed red/brown corrosion product after 18 hours of immersion. After 312 hours the coupons showed significant corrosion product on their surface. Samples in the high flow showed a red/brown corrosion product that was loosely bound to the metal surface. The coupons in the low flow quiescent conditions exhibited a darker corrosion product that appeared more tightly bound to the surface.

On removal of the coupons after 504 hours of immersion, a much thicker dark red corrosion product had formed on the surface of all coupons. This was easily wiped off the surface using a cloth. Underneath this was a thin dark film that was harder to remove from the surface, and required mechanical scrubbing.

Figure 8.1. Carbon steel coupons on removal from the test tanks. (Coupons 1-6 from left-right)

On removal from the water, the coupons were cleaned and reweighed. The overall weight losses are recorded in Table 8.1.

Table 8.1. Weight loss measurements for carbon steel

Sample	Original Weight (g)	Final Weight (g)	Time of exposure (hours)	Weight Loss (g)	% weight loss
1 – FLOW	61.0721	60.6390	504	0.4331	0.53
2 – FLOW	60.2876	59.8261	504	0.4615	0.57
3 – FLOW	59.7658	59.3496	504	0.4162	0.52
4 – NO FLOW	60.8197	60.5284	504	0.2913	0.36
5 – NO FLOW	61.2834	61.0067	504	0.2767	0.34
6 – NO FLOW	60.7156	60.4358	504	0.2798	0.35

Using Equation 8.1 the corrosion rate for each coupon could be determined using weight loss, time of exposure, surface area and material density. The density of the carbon steel is 7.8303 gcm^{-3} (Chapter 6). The corrosion rates are shown in Table 8.2.

Table 8.2. Calculated corrosion rates for carbon steel

Sample	Weight Loss (g)	Time of exposure (hours)	Exposed Area (cm^2)	Corrosion Rate (mm/yr)
1 – FLOW	0.4331	504	42.59	0.23
2 – FLOW	0.4615	504	42.59	0.24
3 – FLOW	0.4162	504	42.59	0.22
4 – NO FLOW	0.2913	504	42.59	0.15
5 – NO FLOW	0.2767	504	43.91	0.14
6 – NO FLOW	0.2798	504	42.59	0.15

Carbon Steel Surface Analysis

The carbon steel samples in the high flow showed clear corrosion damage on the surface facing the oncoming flow (Figures 8.2 and 8.3).

Figure 8.2 Surface damage on carbon steel coupon 1

Figure 8.3 Surface damage on carbon steel coupon 2

Microscopic images were taken after the test period to investigate the surface effects of the high flow rate. These can be seen in Appendix 3.

8.3.2 Nickel Aluminium Bronze

Nickel aluminium bronzes are known to have good resistance to corrosion, especially to flow-enhanced corrosion (Kear et al., 2004a; Al-Hashem et al., 1995). Hence, the alloys are often used for ship's propellers, impellers and heat exchanger systems. The corrosion protection is attributed to an adherent layer of alumina (aluminium oxide) that forms on the surface of the metal on exposure to a corrosive environment (Kear et al., 2004b). However, they can suffer surface damage when subject to high flow conditions or fluid disturbance (Kear et al., 2004a).

Within 96 hours of immersion the surfaces of all the aluminium bronze coupons, were observed to be grey in colour.

The coupons were removed from the water after 480 hours exposure. The corrosion film was dark grey in colour and uniform across the surface. This was more firmly attached than the corrosion product on the carbon steel coupons. The corrosion film was easier to remove on the side that faced the flow compared to the back of the coupons, and on coupons in the quiescent conditions. After cleaning, the coupons were reweighed and the weight loss for each sample is shown in Table 8.3.

Table 8.3. Weight loss measurements for nickel aluminium bronze

Sample	Original Weight (g)	Final Weight (g)	Time of exposure (hours)	Weight Loss (g)	% weight loss
1 – FLOW	68.0692	67.9779	480	0.0913	0.13
2 – FLOW	66.6848	66.6014	480	0.0834	0.13
3 – FLOW	67.3436	67.2484	480	0.0952	0.14
4 – NO FLOW	65.1280	65.0581	480	0.0699	0.11
5 – NO FLOW	68.5024	68.4326	480	0.0698	0.10
6 – NO FLOW	67.5794	67.5111	480	0.0683	0.10

The corrosion rates were calculated for all nickel aluminium bronze coupons using Equation 8.1 (Table 8.4). The density of the alloy used is 8.2433 gcm^{-3}.

Table 8.4. Calculated corrosion rates for nickel aluminium bronze

Sample	Weight Loss (g)	Time of Exposure (hours)	Exposed Area (cm^2)	Corrosion Rate (mm/yr)
1 – FLOW	0.0913	480	42.91	0.05
2 – FLOW	0.0834	480	43.61	0.04
3 – FLOW	0.0952	480	42.91	0.05
4 – NO FLOW	0.0699	480	42.91	0.04
5 – NO FLOW	0.0698	480	44.26	0.03
6 – NO FLOW	0.0683	480	42.91	0.03

Nickel Aluminium Bronze Surface Analysis

Nickel aluminium bronze coupons were analysed in the same way as for carbon steel. Images of surface condition of the metal after immersion are given in Appendix 3.

The nickel aluminium bronze showed no surface damage apart from two small areas of localised corrosion observed on Coupon 2 (under high flow conditions).

8.3.3 SG Iron 400-18 (EN-GJS-400-18)

After 19 hours immersion SG Iron 400-18 coupons exhibited a dark red loose corrosion product under high flow but a darker and more adherent corrosion product under low flow.

The coupons were removed after 500 hours immersion. Coupons 1-3 (left to right in Figure 8.4) were subject to high flow and the corrosion product was more loosely bound to the surface of the metal. There are also large patches where corrosion product has been removed by the flow.

Figure 8.4. SG Iron 400-18 coupons on removal after 500 hours. Coupons 1-3 (reading from the left) were subject to high flow while 4-6 were subject to low flow

Coupon 2 is shown in Figure 8.5. The extent of the corrosion product formed in the high flow conditions is shown.

Figure 8.5. SG Iron 400-18 coupon 2 on removal after 500 hours

Figure 8.6. SG Iron 400-18 coupon 3 on removal after 500 hours

Figure 8.7. SG Iron 400-18 coupon 6 on removal after 500 hours

The difference between the corrosion product formed in high flow and in the quiescent conditions can be seen in Figures 8.5-8.7.

Table 8.5. Weight loss measurements for SG Iron 400-18

Sample	Original Weight (g)	Final Weight (g)	Time of exposure (hours)	Weight Loss (g)	% weight loss
1 – FLOW	61.0483	60.5896	500	0.4587	0.75
2 – FLOW	61.5434	61.0901	500	0.4633	0.75
3 – FLOW	60.4007	59.9443	500	0.4564	0.76
4 – NO FLOW	63.4800	63.2155	500	0.3345	0.53
5 – NO FLOW	60.4029	60.1526	500	0.3403	0.56
6 – NO FLOW	63.7433	63.4749	500	0.3484	0.55

The weight losses are given in Table 8.5 and the corrosion rates, using a density of 7.5246 gcm^{-3} in equation 7.1 are given in Table 8.6. Images of the surface condition are given in Appendix 3.

Table 8.6. Calculated corrosion rates for SG iron 400-18

Sample	Weight Loss (g)	Time of exposure (hours)	Exposed Area (cm^2)	Corrosion Rate
1 – FLOW	0.4587	500	44.19	0.24
2 – FLOW	0.4633	500	44.83	0.24
3 – FLOW	0.4564	500	44.10	0.24
4 – NO FLOW	0.3345	500	44.73	0.17
5 – NO FLOW	0.3403	500	44.10	0.18
6 – NO FLOW	0.3484	500	45.38	0.18

SG Iron 400-18 Surface Analysis

SG Iron 400-18 coupons were analysed in the same way as for carbon steel. Images of surface condition of the metal after immersion are given in Appendix 3.

8.3.4 SG Iron 500-7U (EN-GJS-500-7U)

SG Iron 500-7U coupons already showed a red/brown corrosion product on the surface of all samples after 6 hours.

On removal of the coupons form the water after 504 hours, the corrosion product formed on the surface was similar to that of SG Iron 400-18.

Figure 8.8. SG iron 500-7U coupons 1-3 (high flow conditions) on removal after 504 hours.

Figure 8.9. SG iron 500-7U coupons 4-6 (low flow conditions) on removal after 504 hours.

Weight loss data is given in Table 8.7 and the corrosion rates were calculated using a specific gravity of 7.5246 gcm^{-3} in equation 8.1 and are given in Table 8.8.

Table 8.7. Weight loss measurements for SG Iron 500-7U

Sample	Original Weight (g)	Final Weight (g)	Time of exposure (hours)	Weight Loss (g)	% weight loss
1 – FLOW	64.2954	63.8637	504	0.4317	0.67
2 – FLOW	63.9482	63.5215	504	0.4267	0.67
3 – FLOW	64.3502	63.9138	504	0.4364	0.68
4 – NO FLOW	63.2232	62.8789	504	0.3343	0.53
5 – NO FLOW	64.9121	64.5911	504	0.3414	0.53
6 – NO FLOW	61.9541	61.6199	504	0.3342	0.54

Table 8.8. Calculated corrosion rates for SG iron 500-7U

Sample	Weight Loss (g)	Time of exposure (hours)	Exposed Area (cm^2)	Corrosion Rate
1 – FLOW	0.4317	504	44.38	0.23
2 – FLOW	0.4267	504	44.38	0.22
3 – FLOW	0.4364	504	44.38	0.23
4 – NO FLOW	0.3343	504	43.47	0.18
5 – NO FLOW	0.3414	504	45.65	0.17
6 – NO FLOW	0.3342	504	44.38	0.17

SG Iron 500-7U Surface Analysis

Figure 7.10 shows visible surface damage on coupon 1 in the high flow after removal of corrosion product and other micrographs age given in Appendix 3.

Figure 8.10. SG iron 500-7U coupon 1 (high flow) after corrosion product removal showing surface damage

8.4 Comparison of Metals

Figure 8.11 gives a comparison of corrosion rates for the different alloys under the two flow regimes tested while Table 8.9 gives the percentage increase in corrosion with higher flow.

It was found from the initial experiments in Chapter 6 that ductile iron is not as affected by flow as carbon steel. This is verified here with corrosion rates of both ductile irons tested exhibiting a smaller percentage increase than that observed for the carbon steel coupons (Table 8.9).

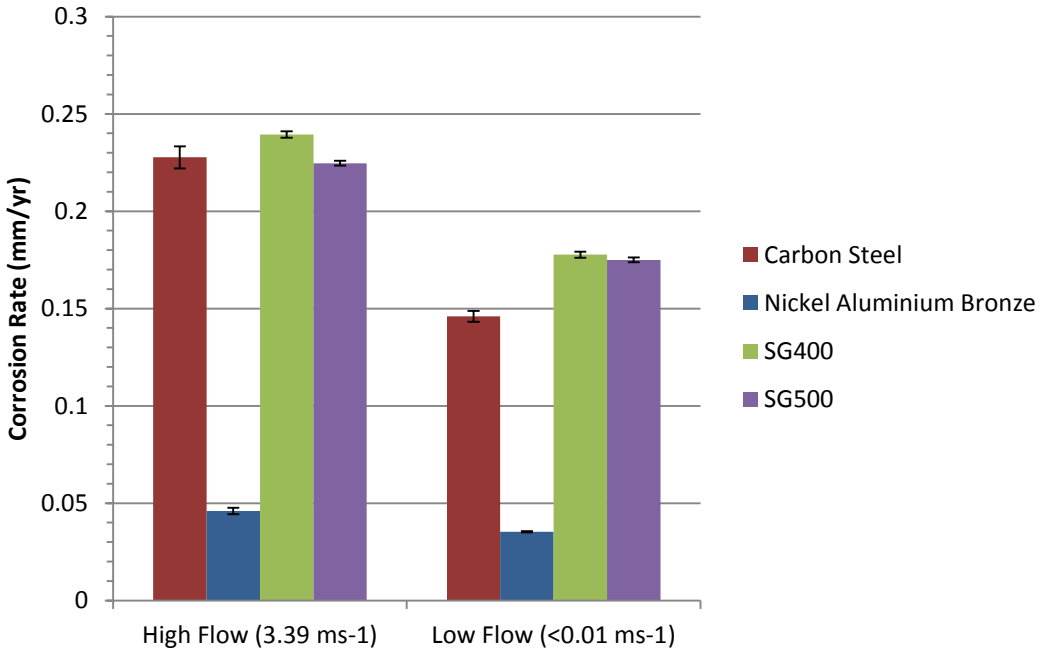

Figure 8.11. Comparison of flow effects on all metals tested

Table 8.9. Percentage increase with increased flow for all metals tested

Metal	Average Corrosion Rate (mm/yr) – LOW FLOW (<0.01 ms^{-1})	Average Corrosion Rate (mm/yr) – HIGH FLOW (3.39 ms^{-1})	Percentage Increase
Carbon Steel	0.146	0.228	56%
Aluminium Bronze	0.035	0.046	30%
Ductile Iron EN-GJS-400-18	0.178	0.241	35%
Ductile Iron EN-GJS-500-7U	0.175	0.225	28%

8.5 Discussion

Water flow rate has an impact to the corrosion rate of all the alloys tested. The least difference between the high and low flow environments was found on nickel aluminium bronze. This is to be expected since this alloy relies on a strong adherent protective film for its good corrosion resistance and its resistance is well reported in the literature. The other alloys do not produce such an adherent film under high flow conditions.

8.5.1 Carbon steel

Carbon steel coupons exhibited higher corrosion rates (0.23 mm/yr) under high flow than under low flow conditions (0.15 mm/yr). Under high flow the coupons also exhibited surface damage at both the macroscopic and microscopic level. Pitting was observed on coupons at both flow regimes but was more severe on coupons exposed to the high flow rate (Appendix 3).

Data presented in Lyon (2010) obtained from an earlier publication (Hudson, 1950) of average general penetration rates (0.136-0.158 mm/yr) for carbon steels in quiescent conditions compares well with the corrosion rate found in the present study for low flow. The corrosion rates are also in the same order of magnitude as stated in a dataset in *Copper-Nickel Alloys, Properties and Applications* (Copper Development Association, 1982).

There is little documentation on corrosion rates of carbon steel under the high velocity conditions tested here. However, some work has been carried out to model the effect of flow (Jingjun Liu. et al., 2008), and studies have shown that the corrosion of carbon steel in flowing seawater is controlled mainly by diffusion of dissolved oxygen to the metal surface (Ellermaa, 1993; Lyon, 2010), which explains the increase in corrosion under higher flow. Jingjun Liu et al. (2008) found that flow-induced corrosion rates of carbon steel increased with an increase in wall shear stress acting on the alloy, with corrosion rates rising sharply at the transition between laminar and turbulent flow (a Reynolds number of approximately 3.5×10^5).

8.5.2 Nickel Aluminium Bronze

Nickel aluminium bronze coupons show a higher average corrosion rate in high flow (0.05 mm/yr) compared to low flow (0.03 mm/yr). This is the lowest of the alloys tested. This was expected as nickel aluminium bronzes form strongly adherent protective films in seawater. These films decrease both the anodic and cathodic reactions on the alloy surface

(Schüssler and Exner, 1993a). Such passivation is due to the formation of an aluminium oxide phase, which hampers ionic transport across the corrosion product.

General weight loss derived corrosion rates of nickel aluminium bronze in seawater pipe flow can range from 0.05 mm/yr under static conditions to 1 mm/yr within turbulent and impinging fluid regimes (Kear et al., 2004b). This is the same order of magnitude as the experiments reported here.

There is no discernible difference in surface appearance between coupons in high flow (1, 2 and 3) and those in static conditions (4, 5 and 6). It has been found that, provided the relative water velocity remains below 1 ms^{-1}, nickel aluminium bronze exhibits excellent corrosion resistance and even under high flow it is known to have good resistance and to show little susceptibility to pitting corrosion (Schüssler and Exner, 1993a; Wharton et al., 2005). At very high flow rates (over 5 ms^{-1}) associated with use on ships propellers, pumps and pipe fittings cavitation erosion can occur (Wood et al., 1990; Kear et al., 2004a).

8.5.3 Ductile Irons (SG 400-18 and SG 500-7U)

The ductile irons exhibit corrosion in both high flow and quiescent conditions but this was greater under the higher flow conditions (0.241 mm/yr for SG iron 400-18 and 0.0225 mm/yr for SG iron 500-7U) compared to low flow conditions (0.178 mm/yr for SG iron 400-18 and 0.175 mm/yr for SG iron 500-7U). Localised corrosion in the form of pits was observed on both alloys. However, this was not limited to the high flow conditions; surface damage that was visible to the naked eye was found in the high flow conditions (Figure 7.10).

Seawater velocities over 3.7 ms^{-1} are reported to cause significant problems with the retention of the corrosion inhibiting protective film on the surface of ductile iron surface and this can cause severe localised corrosion and premature failure of the structure (Davis and Committee, 1996). The flow rate was close to this value at 3.36 ms^{-1}, simulating the potential environment in which these metals will be used on a tidal device. Indeed, there was a significant difference between the adherence of the corrosion product film on the high flow coupons and those under low flow conditions. The protective films that are formed on ductile irons are known to take some time to establish on the surface, resulting in higher corrosion rates for the first few hours or days of exposure and then a decline for longer exposures (Davis and Committee, 1996). This may explain the discrepancy between

higher corrosion rates results obtained in the electrochemical testing carried out previously (Chapters 6 and 7) and in these longer weight loss tests.

8.6 Relevance to Risk Management Development

These experiments have shown that tidal turbine developers will need to consider the effect of flow when making design decisions such as material selection and maintenance schedules. Not only will the high flow rate and any potential suspended solids cause erosion-corrosion (seen here where the high flow rate has removed the protective corrosion product film), it has also increased general corrosion rates by approximately a third for the ductile irons and the nickel aluminium bronze (albeit from a low starting rate), and by half for the carbon steel.

Previous investigations have shown that corrosion failures are likely to occur in areas where steady state flow patterns are disturbed (Efird, 2000). These locations include downstream of weld beads; downstream of hard fouling; bends and elbows; and threaded joints. Electrochemical investigations have revealed that corrosion cells are formed in disturbed turbulent flows (Heitz et al., 1996). Ferrous materials develop anodic regions under stagnant conditions or under conditions of non-disturbed flow, and stainless steel 316 is likely to pit in quiescent water but not in moving seawater (Silverman, 2003). Carbon steel and ductile iron tested here exhibited localised corrosion, more so on coupons under the high flow conditions, but also on those under quiescent conditions. It is recommended that the flow characteristics at the metal surface of a tidal device should be investigated. This should identify areas of the device where the wall shear stress on the metal surface is high enough to lead to turbulent flow next to the surface and hence increased flow induced corrosion.

The type of flow induced corrosion (mass transport controlled; phase transport controlled; erosion-corrosion; and cavitation (Heitz et al., 1996)) dictates the type of prevention strategy that should be used. For example, in situations where there is likely to be high erosion-corrosion, the material selected should have high strength to withstand this type of corrosion. It is likely that coatings would not withstand this regime for long periods of time so a cathodic protection system should be used, or more regular maintenance will be required.

Flow does not only affect corrosion, it is also known to affect biofouling. Fouling has been observed to be more significant in dynamic flow rather than turbulent or static conditions (Faille et al., 1999).

Observations (reported in Chapter 4) show that protective paint used on the bulk of a tidal device can be easily removed in areas. This is probably due to impact of suspended solids entrained in the fast flowing seawater. These areas become anodic in relation to the rest of the metal still coated and are likely to corrode at a faster rate than expected, especially with the higher flow.

Using a secondary line of protection, such as a sacrificial anode system will ensure that areas that become exposed to the seawater are protected. However, in high flow conditions sacrificial anodes will work harder and become spent faster than expected. As such it is likely that these will need replacing more often than the original design life if it did not take water velocity into consideration. It is recommended that if the water velocities exceed 3.5 ms^{-1} then a manufacturer of a tidal device should consider using a different alloy to SG iron, or ensuring that sufficient protection is provided in the form of coatings and cathodic protection.

8.7 Conclusions

An increase in water flow rate has been found to increase the corrosion rate of all the alloys tested. The least difference between the high and low flow environments was found on nickel aluminium bronze. Carbon steel was found to be the most affected by an increase in above the other three alloys tested. Evidence of the surface condition of the metals under both flow rates has also been documented. On all metals the corrosion product formed was less adherent in the high flow conditions than the low flow conditions. This was least apparent on nickel aluminium bronze which exhibited an even corrosion product under both conditions. Nickel aluminium bronze is known to form a protective oxide layer quickly in seawater.

Overall, both flow, and temperature (investigated in Chapter 7) have been found to be critical environmental parameters when understanding the risks associated with corrosion under conditions likely to be experienced by tidal devices. Therefore, the development of an evidence base, of both experimental data and device inspection data is a critical part of

developing a risk management system and developing a risk based inspection regime when deploying devices around the world.

Chapter 9

Developing a Risk Management System – Risk Analysis of the Alstom Ocean Energy Device as a Case Study

9.1 Introduction

This chapter draws on the knowledge gained from previous chapters to develop the principle of implementing a risk based management system and a risk-based inspection regime for tidal stream turbines relating to corrosion and biofouling, and demonstrates the third stage - "Risk Analysis" - of the five-stage process established by DNV, and identified in Chapter 2 (Figure 2.2) as ideal for tidal stream devices. The use of a real tidal device, the Alstom Ocean Energy (AOE) DeepGen III prototype (described in Chapter 4 and shown in Figure 9.1) as a case study enables understanding of how such a system could work in practice.

A Failure Modes and Effects Analysis (FMEA) was carried out with the AOE tidal device and the analysis of the risks identified was used to develop a risk management strategy for the threats to operation associated with corrosion and biofouling.

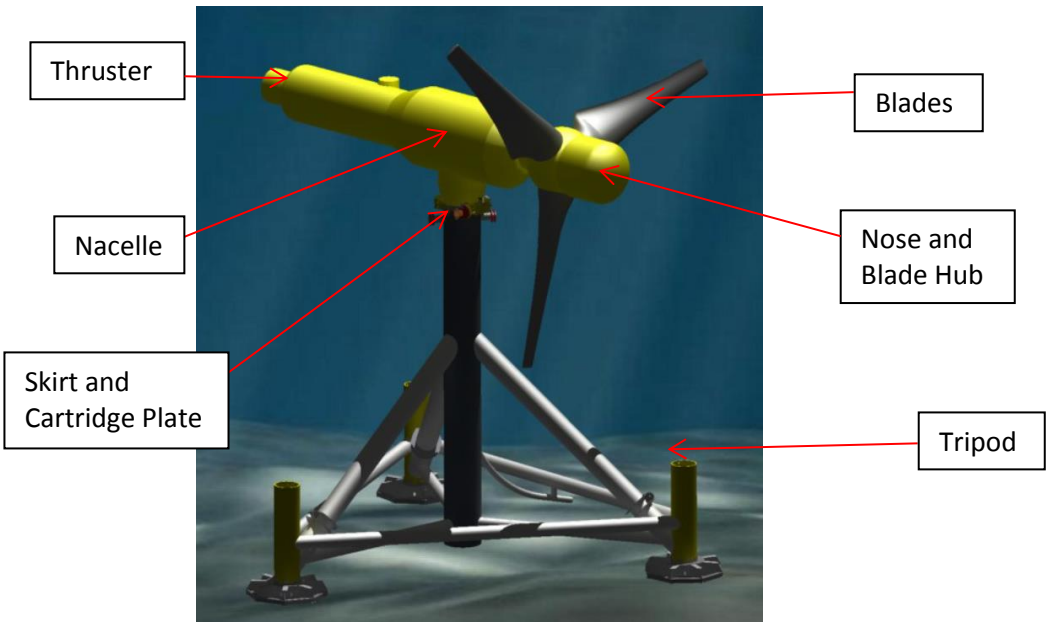

Figure 9.1. Schematic of the Alstom Ocean Energy tidal stream device (Alstom, 2013)

9.2 Risk Identification and Analysis - Failure Modes and Effects Analysis (FMEA)

To assess the risks associated with corrosion and biofouling on the AOE tidal device, a FMEA process was implemented as this was identified in the review of risk management (Chapter 2) as an ideal, well established methodology. The objective of an FMEA is to determine the criticality and the priority for mitigation of each "failure mode".

The preliminary stage of an FMEA as discussed in Chapter 2, Section 2.2.2, is the identification of the risks associated with corrosion and biofouling and their potential consequences. This chapter investigates these in relation to the prototype tidal device (DeepGen III).

Key themes for consequence analysis were identified as Economic/Cost; Environmental and Design and Operation. Using these as discussion points, all areas of the DeepGen III were analysed to identify consequence and the likelihood of each risk occurring. These qualitative assessments can be turned into a quantitative analysis by assigning both the consequence and likelihood a value between 1 and 5, using the knowledge of suitably qualified and experienced personnel (AOE). This can be analysed to determine the risk ranking. A ranking of high (red in Table 9.1), medium (orange) and low (green) is applied to the risks using the risk matrix discussed in Chapter 2.

From the literature review (Chapter 3) and discussions with the tidal turbine developers, it can be assumed that many of the risks identified here can be extrapolated to other devices experiencing the same environmental conditions, cost limitations and design requirements. For example a life cycle assessment of the Seagen tidal device (Douglas et al., 2008) highlights material similarities.

The threats identified are shown in the FMEA worksheet in Table 9.1. For this assessment it is assumed that operators are suitably qualified at all stages of the design and operation of these devices so as to allow only consideration of the device itself.

Also identified are the strategies currently employed by AOE (Table 9.2).

The FMEA worksheet for the preliminary assessment (Table 9.1) was carried out in October 2010 and formed the basis of all future risk assessments. The worksheet includes the feature discussed; the identified threat to the feature; the conditions in which it operates; the potential type of corrosion and biofouling assessed as likely to occur; the qualitative

assessment of consequences; the quantitative assignment of consequence and likelihood; the overall risk ranking and the priority. This preliminary assessment was based on the DeepGen III prototype tidal energy device that was deployed at this time. Reviews of the risk assessment were carried out on an annual basis throughout the thesis (Appendix 4). By the end of this thesis, AOE had deployed DeepGen IV, a newer, larger capacity (1 MW) device in the Fall of Warness, in the same location as that used for DeepGen III. Design changes have meant that some risks can be reduced, or indeed removed from this assessment in the future, demonstrating the evolving nature of any risk analysis. All risk assessments are included as part of the Management System Database in Appendix 5.

9.2.1 FMEA Methodology

The FMEA was carried out to provide a semi-quantitative assessment, using experimental data to support the risk matrix used as dictated by standard good practice (Table 2.1) (British Standards Institute, 2006a). A fully quantitative risk assessment process is complex, and is practically impossible for an industry with limited operational experience (OPEX) and data collected and recorded.

The FMEA was carried out on an annual basis with members of AOE, including managers, work package owners, research & development engineers, design engineers and site engineers. All members of the risk assessment process team were deemed to be suitably qualified and experienced personnel (SQEP), who could bring expert knowledge of the device and the operating conditions to the assessment. The process of an FMEA relies upon the engagement of relevant staff and non-desire to participate could have a great impact on the suitability and relevance of the analysis to the device.

The first stage of the process was to assign the consequences and likelihood values (Table 2.1) to a real-world situation to provide analysis criteria. This process was carried out using the expertise of AOE engineers and an understanding of the industry. Following this process, the FMEA was carried out, first by dividing the device into work packages. Using drawings of the device, each component was assessed in terms of the environment in which it was placed and the design features that may promote corrosion and biofouling. The potential consequences of each threat, and the likelihood of the threat occurring was then analysed using knowledge of the device, knowledge of corrosion and biofouling that had already occurred on the device (Chapter 4) and knowledge of the potential implications of operating in a tidal regime (Chapters 5-8). Current strategies were also captured as part of the process to aid understanding of the level of awareness amongst developers.

Table 9.1. Preliminary risk assessment for Alstom Ocean Energy tidal stream device, DeepGen III

Ref	Work Package	Biofouling	Corrosion	Feature	Threat	Definition	Flow Conditions	Type of Corrosion or biofouling likely to occur	Potential Consequences (themes)			Consequence (1-5)	Likelihood (1-5)	Overall Risk (1-25)	Priority (1-3)
									Economic/cost	Environmental	Design and Operation				
1	Tripod	x		External surface	Settlement and Growth of fouling organisms on external surface of tripod	Open water	High tidal flow	Hard macrofouling (barnacles, mussels) and macro algae	Problems and further costs associated with decommissioning of structure	Development of mature breeding community releasing further fouling	Increased drag on structure Corrosion underneath deposits	3	5	15	HIGH
2	Tripod	x	x	Internal structure	Growth and subsequent death leading to increased corrosion	semi-enclosed	Low flow/ stagnant	Soft fouling (sea squirts) and biofilm formation	Increased maintenance schedule Costs associated with diving/ROVs/retrieval Decommissioning costs	Corrosion products	Corrosion causing failure of Structure and support for nacelle Decreased operational time	4	3	12	HIGH
3	Tripod		x	FO connector	Accelerated corrosion	semi-enclosed	Low flow/ stagnant	Stray current corrosion (similar to galvanic corrosion)	Corrosion mitigation costs Repair/replacement of parts Increased maintenance schedule		Decreased operational time	3	3	9	HIGH
4	Tripod	x		Cartridge Plate	Barnacles form around winch rope and shell bitt	semi-enclosed	Low flow/ stagnant	Hard macrofouling (barnacles, mussels) and macro algae			ROV unable to remove rope from shell bitt during retrieval, failure to retrieve nacelle for maintenance and inspection	3	3	9	MED
5	Tripod	x		Cartridge Plate	Barnacles form on shell bitt of cartridge plate if no turbine installed	semi-enclosed	Low flow/ stagnant	Hard macrofouling (barnacles, mussels) and macro algae	Unable to deploy turbine		Macrofouling growth prevents rope attachment or creates rope wear Unable to attach nacelle to tripod correctly	3	4	12	MED

Ref	Work Package	Biofouling	Corrosion	Feature	Threat	Definition	Flow Conditions	Type of Corrosion or biofouling likely to occur	Potential Consequences (themes)			Consequence (1-5)	Likelihood (1-5)	Overall Risk (1-25)	Priority (1-3)
									Economic/cost	Environmental	Design and Operation				
6	Tripod	x		High friction surface	Fouling during turbine removal	occasionally open	Intermittent low flow	Hard macrofouling (barnacles, mussels) and macro algae	Unable to deploy turbine	Corrosion products	Unable to attach nacelle to tripod correctly due to fouling on surface Erosion of surface causing corrosion	4	4	16	MED
7	Tripod	x		Low friction surface	Fouling during turbine removal	occasionally open	Intermittent low flow	Hard macrofouling (barnacles, mussels) and macro algae	Unable to deploy turbine	Corrosion products	Unable to attach nacelle to tripod correctly due to fouling on surface Erosion of surface causing corrosion	4	4	16	MED
8	Tripod	x		Connector buckets in cartridge plate	Fouling prevents connector engagement	semi-enclosed	Low flow/ stagnant	Soft fouling (sea squirts) and biofilm formation Hard macrofouling (barnacles, mussels) and macro algae	Electrical connection failure so unable to export electricity Costly in situ maintenance/removal of barnacles using divers/ROV			5	4	20	HIGH
9	Tripod	x	x	Connectors in cartridge plate	Fouling causes corrosion of connections	semi-enclosed	Low flow/ stagnant	Soft or hard fouling crevice or pitting corrosion under deposits or in anaerobic environment created under deposit	Electrical connection failure so unable to export electricity Costly in situ maintenance/removal of barnacles using divers/ROV			5	3	15	HIGH
10	Tripod	x		Connectors in cartridge plate	Fouling prevent signal function	semi-enclosed	Low flow/ stagnant	Soft or hard fouling crevice or pitting corrosion under deposits or in	Repair/replacement of parts		Signal failure	4	3	12	MED

Ref	Work Package	Biofouling	Corrosion	Feature	Threat	Definition	Flow Conditions	Type of Corrosion or biofouling likely to occur	Potential Consequences (themes)			Consequence (1-5)	Likelihood (1-5)	Overall Risk (1-25)	Priority (1-3)
									Economic/cost	Environmental	Design and Operation				
								anaerobic environment created under deposit							
11	Power train	x		Blade	Biofouling results in efficiency reduction	Open water	High tidal flow	Hard macrofouling (barnacles, mussels) and macro algae	Electrical generation potential reducedIncreased maintenance periods for removal and decreased operational time		Decreased operational time	4	2	8	LOW
12	Power train	x	x	Blade	Exposure to air for extended periods results in coating deterioration	Air	N/A	Hard macrofouling (barnacles, mussels) and macro algae Crevice corrosion, pitting corrosion, galvanic corrosion	Electrical generation potential reduced Increased maintenance periods and schedule Increase in costs associated with recoating		Coating deterioration leading to biofouling and corrosion Decreased operational time	3	4	12	LOW
13	Power train	x		Blade	Turbine shutdown for extended period in water results in barnacle growth (water flow less than 4 knots??)	Open water	Low flow	Biofilm formation Hard macrofouling (barnacles, mussels) and macro algae	Electrical generation potential reduced Increased maintenance periods and schedule Increase in costs associated with removal of fouling	Attachment of biofouling	Biofouling of blades results in reduced efficiency Decreased operational time	3	2	6	LOW
14	Power train		x	Blade	Galvanic corrosion cell between hub, root fitting,	Open water	High tidal flow	Galvanic corrosion	Loss of electrical generation capacity	Corrosion products	Corrosion causing failure of blades	4	3	12	MED

Ref	Work Package	Biofouling	Corrosion	Feature	Threat	Definition	Flow Conditions	Type of Corrosion or biofouling likely to occur	Potential Consequences (themes)			Consequence (1-5)	Likelihood (1-5)	Overall Risk (1-25)	Priority (1-3)
									Economic/cost	Environmental	Design and Operation				
					and coppercoat (if used)										
15	Power train		x	Blade	Interaction between anodes and coppercoat on blade if copper coat not isolated	Open water	High tidal flow	Galvanic corrosion	Loss of electrical generation capacity	Corrosion products	Galvanic corrosion may occur on blades causing failure	4	3	12	MED
16	Power train	x		Blade	Water saturation of fibreglass results in coating delamination	Open water	High tidal flow	Hard macrofouling (barnacles, mussels) and macro algae Crevice corrosion, pitting corrosion, galvanic corrosion	Reduced efficiency and electrical generation potential is reduced Increased maintenance periods and schedule for removal of biofouling	Attachment of biofouling	Coating delamination allows biofouling to attach to blades resulting in reduced efficiency Decreased operational time	4	1	4	LOW
17	Power train	x	x	Blade	Water saturation of fibreglass results in inability to re-coat damaged blades	Open water	High tidal flow	Hard macrofouling (barnacles, mussels) and macro algae Crevice corrosion, pitting corrosion, galvanic corrosion	Loss of electrical generation capacity	Attachment of biofouling	Inability to re-coat blades allows biofouling to attach to surface resulting in reduced efficiency	4	1	4	LOW
18	Power train	x	x	Blade	Lifting features provide location for biofouling	Open water	High tidal flow	Hard macrofouling (barnacles, mussels) and macro algae Crevice corrosion,		Attachment of biofouling	Increased drag Increased likelihood of corrosion	3	1	3	LOW

Ref	Work Package	Biofouling	Corrosion	Feature	Threat	Definition	Flow Conditions	Type of Corrosion or biofouling likely to occur	Potential Consequences (themes)			Consequence (1-5)	Likelihood (1-5)	Overall Risk (1-25)	Priority (1-3)
									Economic/cost	Environmental	Design and Operation				
								pitting corrosion, galvanic corrosion							
19	Power train	x	x	Blade	Impact with debris (including in suspension) removes coating	Open water	High tidal flow	Hard macrofouling (barnacles, mussels) and macro algae Crevice corrosion, pitting corrosion, galvanic corrosion	Reduced efficiency and electrical generation capacity Increased maintenance periods for removal	Attachment of biofouling Corrosion products	Impact causes loss of coating leading to attachment of biofouling and corrosion Reduction in efficiency Decreased operational time	4	4	16	MED
20	Nacelle	x	x	Nacelle body	Poor painting application leads to paint loss	Open water	High tidal flow	Hard macrofouling (barnacles, mussels) and macro algaeCrevice corrosion, pitting corrosion, galvanic corrosion	Increased maintenance periods and schedule for removalCosts associated with removal and corrosion mitigation	Development of mature breeding community releasing further fouling	Loss of paint coating leads to corrosion and biofouling of nacelleDecreased drag on structureDecreased operational time	4	5	20	HIGH
21	Nacelle		x	Nacelle body	Impact with debris (including in suspension) removes coating	Open water	High tidal flow	Hard macrofouling (barnacles, mussels) and macro algae Crevice corrosion, pitting corrosion, galvanic corrosion	Increased maintenance periods and schedule for removal Costs associated with removal and corrosion mitigation	Development of mature breeding community releasing further fouling	Loss of paint coating leads to corrosion and biofouling of nacelle Increased drag on structure Decreased operational time	4	4	16	MED

Ref	Work Package	Biofouling	Corrosion	Feature	Threat	Definition	Flow Conditions	Type of Corrosion or biofouling likely to occur	Potential Consequences (themes)			Consequence (1-5)	Likelihood (1-5)	Overall Risk (1-25)	Priority (1-3)
									Economic/cost	Environmental	Design and Operation				
22	Nacelle		x	Nacelle body	Impact damage due to maintenance (tools, equipment etc.)	Air	N/A	Hard macrofouling (barnacles, mussels) and macro algae Crevice corrosion, pitting corrosion, galvanic corrosion	Loss of electricity generation Increased maintenance periods and schedule Replacement of failed equipment	Attachment of biofouling and corrosion potential, development of mature breeding community releasing further fouling	Equipment failure Decreased operational time	4	1	4	LOW
23	Nacelle	x		Rope tube	Biofouling inside rope tube prevents rope from passing during retrieval (only able to apply 5 tonnes load)	semi-enclosed	Low flow/ stagnant	Soft fouling (sea squirts) and biofilm formation Hard macrofouling (barnacles, mussels) and macro algae	Costly in situ maintenance/removal of barnacles using divers/ROVs	Build-up of fouling on structure if not removed	Inability to retrieve nacelle for maintenance/inspection	3	2	6	LOW
24	Nacelle		x	Nacelle body	Inadequate Anodic protection	Open water	High tidal flow	General corrosion, crevice or pitting corrosion, galvanic corrosion	Increase maintenance periods and schedule and increased costs associated with replacement of anodes	Corrosion products	Inadequate protection leads to corrosion Decreased operational time	3	3	9	HIGH
25	Nacelle		x	Nacelle body	Inadequate life of anodes (or galvanic cell stronger than expected)	Open water	High tidal flow	General corrosion, crevice or pitting corrosion, galvanic corrosion	Increase maintenance periods and schedule and increased costs associated with replacement of anodes	Corrosion products	Inadequate protection leads to corrosion Decreased operational time	3	2	6	MED

Ref	Work Package	Biofouling	Corrosion	Feature	Threat	Definition	Flow Conditions	Type of Corrosion or biofouling likely to occur	Potential Consequences (themes)			Consequence (1-5)	Likelihood (1-5)	Overall Risk (1-25)	Priority (1-3)
									Economic/cost	Environmental	Design and Operation				
26	Nacelle	x		Heat Exchanger	Biofouling reduces efficiency of heat exchanger	semi-enclosed	Low flow/ stagnant	Soft fouling (sea squirts) and biofilm formation Hard macrofouling (barnacles, mussels) and macro algae	Efficiency reduction resulting in overheating of internal systems and failure to generate electricity Increase maintenance periods and schedule and increased costs associated with replacement /repair of parts		Overheating of internal systems Decreased operational time	4	2	8	LOW
27	Nacelle		x	Penetrator plates	Stainless penetrator with stainless or bronze connectors results in galvanic corrosion	occasionally open	Intermittent low flow	Galvanic corrosion	Increased maintenance periods and schedule Costs associated with corrosion mitigation		Galvanic corrosion of penetrator plates Decreased operational time	3	3	9	LOW
28	Nacelle		x	External surface	Impact at interface between stands and nacelle during maintenance periods	Air	N/A	General corrosion, crevice or pitting corrosion, galvanic corrosion	Increased maintenance and cost associated with recoating	Corrosion products	Impact with stands removes protective coating leaving metal exposed, increasing potential for corrosion to occur	4	4	16	LOW
29	External Systems	x		Thruster	Biofouling of thruster	Open water	High tidal flow	Biofilm formationHard macrofouling (barnacles, mussels) and macro algae	Efficiency reduction results in more energy required to run thrusterIncreased maintenance periods and scheduleIncreased costs associated with energy		Decreased operational time	3	2	6	MED

Ref	Work Package	Biofouling	Corrosion	Feature	Threat	Definition	Flow Conditions	Type of Corrosion or biofouling likely to occur	Potential Consequences (themes)			Consequence (1-5)	Likelihood (1-5)	Overall Risk (1-25)	Priority (1-3)
									Economic/cost	Environmental	Design and Operation				
									requirement and removal of biofouling						
30	External Systems	x	x	Thruster	Decay of biofouling products in wet void cavity	semi-enclosed	Low flow/ stagnant	General corrosion, crevice or pitting corrosion, galvanic corrosion	Cost associated with repair of corroded parts	Corrosion products	Corrosion in wet void	2	3	6	MED
31	External Systems		x	Thruster	Slow leakage of water into wet void cavity	semi-enclosed	Low flow/ stagnant	General corrosion, crevice or pitting corrosion, galvanic corrosion	Cost associated with repair of corroded parts	Corrosion products	Corrosion in wet void	2	3	6	MED
32	External Systems	x		Thruster	Biofouling of grill results in efficiency reduction	Open water	High tidal flow	Hard macrofouling (barnacles, mussels) and macro algae	Efficiency reduction results in more energy required to run thruster Increased maintenance periods and schedule Increased costs associated with energy requirement and removal of biofouling		Decreased operational time	3	2	6	LOW

Ref	Work Package	Biofouling	Corrosion	Feature	Threat	Definition	Flow Conditions	Type of Corrosion or biofouling likely to occur	Potential Consequences (themes)			Consequence (1-5)	Likelihood (1-5)	Overall Risk (1-25)	Priority (1-3)
									Economic/cost	Environmental	Design and Operation				
33	External Systems	x		Thruster	Biofouling of grill results in failure through cavitation	Open water	High tidal flow	Hard macrofouling (barnacles, mussels) and macro algae	Electricity generation potential reduced due to nacelle not facing both tide directions		Cavitation causes failure of thruster so nacelle unable to yaw during slack tides	3	2	6	LOW
34	External Systems	x		Clamp	Biofouling inside torque bucket prevents operation	Open water	High tidal flow	Hard macrofouling (barnacles, mussels)	Electricity generation potential reduced due to nacelle not facing both tide directions		Clamp fails stopping movement or correct attachment of nacelle and tripod	2	2	4	LOW
35	External Systems	x		Clamp	Barnacles in clamp slots prevent clamp fully opening for retrieval	Open water	High tidal flow	Hard macrofouling (barnacles, mussels)	Costly in situ maintenance/removal of barnacles using divers/ROV	Build-up of fouling on structure if not removed	Inability to retrieve nacelle for maintenance/inspection	3	2	6	LOW
36	External Systems	x		Clamp	Barnacles in clamp slots are crushed but debris prevents full movement during retrieval	Open water	High tidal flow	Hard macrofouling (barnacles, mussels)	Costly in situ maintenance/removal of barnacles using divers/ROV		Inability to retrieve nacelle for maintenance/inspection Build-up of debris causing abrasion	4	2	8	MED
37	External Systems	x		Clamp	If turbine stored in water, off tripod for several months then barnacles could attach to high friction surface	Open water	High tidal flow	Hard macrofouling (barnacles, mussels)			Barnacles cause accelerated wear and corrosion on surface	4	4	16	HIGH

Ref	Work Package	Biofouling	Corrosion	Feature	Threat	Definition	Flow Conditions	Type of Corrosion or biofouling likely to occur	Potential Consequences (themes)			Consequence (1-5)	Likelihood (1-5)	Overall Risk (1-25)	Priority (1-3)
									Economic/cost	Environmental	Design and Operation				
38	External Systems		x	Clamp	Wear of clamp mechanism removes coating	Open water	High tidal flow	General corrosion, crevice or pitting corrosion, galvanic corrosion	Potential costly in situ maintenance if unable to retrieve nacelle.		Removal of coating exposes surface metal and corrosion occurs.	4	3	12	HIGH
39	External Systems	x		Skirt	Stab mechanism unable to retract after 2 years due to biofouling	semi-enclosed	Low intermittent flow/ stagnant	Hard macrofouling (barnacles, mussels) and macro algae	costly in situ maintenance/removal of biofouling using divers/ROVs		Inability to retrieve nacelle for maintenance/inspection	4	3	12	MED
40	External Systems	x		Skirt	Wear of cable insulation within Iges Chain due to biofouling	semi-enclosed	Low intermittent flow/stagnant	Hard macrofouling (barnacles, mussels)	Electricity generation potential reduced due to nacelle not facing both tide directions Costs associated with repair/replacement of cable Increased maintenance requirements		Insulation fails causing damage to cables Loss of cable and hence movement of turbine	4	2	8	MED
41	External Systems	x		Skirt	Wear of chain lower surface due to biofouling on cable tray	semi-enclosed	Low intermittent flow/stagnant	Hard macrofouling (barnacles, mussels)	Electricity generation potential reduced due to nacelle not facing both tide directions Costs associated with repair/replacement of cable Increased maintenance requirements		Insulation fails causing damage to cables Loss of cable and hence movement of turbine	4	2	8	MED

Ref	Work Package	Biofouling	Corrosion	Feature	Threat	Definition	Flow Conditions	Type of Corrosion or biofouling likely to occur	Potential Consequences (themes)			Consequence (1-5)	Likelihood (1-5)	Overall Risk (1-25)	Priority (1-3)
									Economic/cost	Environmental	Design and Operation				
42	External Systems	x		Skirt	Increased friction within chain wrap guard leads to chain buckling and jamming	semi-enclosed	Low intermittent flow/stagnant	Hard macrofouling (barnacles, mussels) and macro algae	Electricity generation potential reduced due to nacelle not facing both tide directions Costs associated with repair/replacement of cable Increased maintenance requirements		Inability to move chain due to fouling build up and failure to move turbine to face tide	4	2	8	MED
43	External Systems	x		Skirt	Camera lighting invalidates biofouling experience from 1MW machine	semi-enclosed	Low intermittent flow/stagnant	Soft fouling (sea squirts) and biofilm formation Hard macrofouling (barnacles, mussels) and macro algae			Lighting increases biofouling attachment to surfaces inside skirt area	2	2	4	LOW
44	External Systems	x		Skirt	Hard biofouling of stab gear wheel over tooth not regularly engaged during yawing	semi-enclosed	Low intermittent flow/stagnant	Hard macrofouling (barnacles, mussels)	Electricity generation potential reduced due to nacelle not facing both tide directions Costs associated with repair/replacement of parts Increased maintenance requirements		Biofouling jams encoder when tooth occasionally engaged, turbine not moved to correct location	3	2	6	MED

Ref	Work Package	Biofouling	Corrosion	Feature	Threat	Definition	Flow Conditions	Type of Corrosion or biofouling likely to occur	Potential Consequences (themes)			Consequence (1-5)	Likelihood (1-5)	Overall Risk (1-25)	Priority (1-3)
									Economic/cost	Environmental	Design and Operation				
45	External Systems	x		Skirt	Backup yaw sensor (swash plate within skirt) susceptible to biofouling	semi-enclosed	Low intermittent flow/stagnant	Soft fouling (sea squirts) and biofilm formation Hard macrofouling (barnacles, mussels) and macro algae	Electricity generation potential reduced due to nacelle not facing both tide directions Costs associated with repair/replacement of Sensor parts Increased maintenance requirements		Sensor compromised and turbine not moved to correct location	3	2	6	MED
46	External Systems	x		Winch	Nacelle connection to winch fails after 2 years due to biofouling	Open water	High tidal flow	Soft fouling (sea squirts) and biofilm formationHard macrofouling (barnacles, mussels) and macro algae	Costly in situ maintenance/removal for fouling using divers/ROVs		Inability to retrieval nacelle for maintenance/inspectionBuild up of fouling on structure if not removed	3	2	6	LOW
47	External Systems	x		Winch	Winch rope coupling device fails to re-attach due to biofouling	Open water	High tidal flow	Soft fouling (sea squirts) and biofilm formation Hard macrofouling (barnacles, mussels) and macro algae	Costly in situ maintenance/removal for fouling using divers/ROVs		Inability to retrieval nacelle for maintenance/inspection Build up of fouling on structure if not removed	3	2	6	LOW
48	External Systems		x	Winch	Stainless / Stainless joints result in crevice corrosion	Open water	High tidal flow/stagnation in crevice	Crevice corrosion	Costly retrieval using divers/ROVs		Crevice corrosion causes winch to fail and failure to retrieve turbine	3	3	9	MED

Ref	Work Package	Biofouling	Corrosion	Feature	Threat	Definition	Flow Conditions	Type of Corrosion or biofouling likely to occur	Potential Consequences (themes)			Consequence (1-5)	Likelihood (1-5)	Overall Risk (1-25)	Priority (1-3)
									Economic/cost	Environmental	Design and Operation				
49	Power train Nacelle External Systems		x	External surfaces	Impact with boat during deployment	Open water	High tidal flow	General corrosion, crevice or pitting corrosion, galvanic corrosion	Costly in situ maintenance Returning of nacelle to quayside for paint application		protective coating removed by impact during deployment leaving exposed metal to locally corrode during device operation over use of CP system due to exposed metal Damage to blades causing crevices to form, possible cavitation corrosion issues	4	4	16	HIGH
50	Power train Nacelle External Systems		x	Exposed surfaces	Atmospheric corrosion during periods where turbine exposed on Quayside	Atmosphere	N/A	Atmospheric corrosion			Corrosion of all surfaces exposed during periods of maintenance on quayside due to proximity to seawater and windy weather conditions	2	3	6	LOW

The development of a "Current Strategies" table (Table 9.2) from the preliminary risk assessment has shown that many of the current strategies are inadequate for managing corrosion and biofouling threats over time in the conditions found (see "Issues with Current Strategy" column in Table 9.2). This demonstrates how a risk assessment process feeds back into current design and operational strategies to improve the management of the threats posed by operating a tidal device. Such a "feedback" loop is essential in developing and updating procedures and communicating them to all relevant personnel. The feedback/updating and communication processes have to be imbedded into current strategies and should not be a stand-alone afterthought.

Table 9.2. Current strategies for identified threats

Reference from Risk Assessment (Table 9.1)	Threat	Current strategy	Issue with current strategy
1	Settlement and Growth of fouling organisms on external surface of tripod	Live with bio fouling	Need method of monitoring corrosion under fouling deposits
2	Growth and subsequent death leading to increased corrosion	Totally sealed, fully open, anodes, painting or combinations	Anodes will have limited life
3	Accelerated corrosion due to stray currents	No strategy	This has occurred on Mark 1 of the cartridge plate and Mark 2 has been installed with the same connector
4	Barnacles form around winch rope and shell bitt	Assume that clearance is adequate	Assumption may not be correct and as hard fouling settles and creates mature breeding ground may be difficult to move turbine when required
5	Barnacles form on shell bitt of cartridge plate if no turbine installed	TBD	Hard fouling may mean that it is impossible to fixed the turbine in place on the tripod during deployment
6	Fouling during turbine removal	Crush growth or cap during turbine removal	What is the debris route following crushing? How effective is the capping procedure?
7	Fouling during turbine removal	Crush growth or cap during turbine removal	What is the debris route following crushing? How effective is the capping procedure?
8	Fouling prevents connector engagement	Cap during turbine removal	Will organisms become trapped? How effective is the capping procedure?
9	Fouling causes corrosion of connections	No strategy	Corrosion may cause connections to fail, need system in place to monitor corrosion

Reference from Risk Assessment (Table 9.1)	Threat	Current strategy	Issue with current strategy
10	Fouling prevent signal function	No strategy	Need to monitor fouling and remove during maintenance
11	Biofouling results in efficiency reduction	Coating to prevent any significant biofouling	Coating must be maintained throughout lifetime
12	Exposure to air for extended periods results in coating deterioration	Specify maximum period allow in air	Ensure awareness of maximum permissible time in air
13	Turbine shutdown for extended period in water results in barnacle growth (water flow less than 4 knots)	Specify maximum period which turbine can be left shutdown or moored in water	Ensure awareness of maximum permissible time moored in water
14	Galvanic corrosion cell between hub, root fitting, and coppercoat (if used)	Anodes on hub	Anodes have limited lifetime
15	Interaction between anodes and coppercoat on blade if copper coat not isolated	Electrical isolation of coppercoat from anode. Add isolation inspection?	Inspection of isolation barrier should be carried out on a regular basis
16	Water saturation of fibreglass results in coating delamination	Assume water will not affect adherence	Investigate effect of water saturation on coating
17	Water saturation of fibreglass results in inability to re-coat damaged blades	Assume no requirement for re-coating during service	Investigate effect of water saturation on coating
18	Lifting features provide location for biofouling	Assume that blanking plug prevents growth	How effective is the blanking plug?
19	Impact with debris (including in suspension) removes coating	Assume coating remains intact	Effectiveness of coating to withstand impact
20	Poor painting application leads to paint loss	Proper procedure	Ensure awareness of proper procedure with all relevant personnel
21	Impact with debris (including in suspension) removes coating	Assume no damage	A paint touch-up procedure is required for quayside maintenance
22	Impact damage due to maintenance (tools, equipment etc.)	Assume no damage	A paint touch-up procedure is required for quayside maintenance
23	Biofouling inside rope tube prevents rope from passing during retrieval (only able to apply 5 tonnes load)	Assume biofouling does not close gap between funnel and rope	Need method for monitoring biofouling level
24	Inadequate Anodic protection	Assume adequate protection provided	Anodes have limited life
25	Inadequate life of anodes (or galvanic cell stronger than expected)	Assume adequate lifetime of anodes	Anodes have limited life
26	Biofouling reduces efficiency of heat exchanger	Build in margin based on boat experience. Monitor efficiency	Is experience relevant? Is there potential for instrument failure?

Reference from Risk Assessment (Table 9.1)	Threat	Current strategy	Issue with current strategy
		through instrumentation	
27	Stainless penetrator with stainless or bronze connectors results in galvanic corrosion	Cathodic protection	Anodes have limited life Ensure enough anodes to provide sufficient protection
28	Impact at interface between stands and nacelle during maintenance periods	No strategy	Need effective barrier to minimise damage
29	Biofouling of thruster	Build in margin based on boat experience. Monitor efficiency through instrumentation	How will periodic running of the thruster affect the biofouling? Can the thruster be run more frequently to remove biofouling effectively?
30	Decay of biofouling products in wet void cavity	No strategy	Need corrosion monitoring strategy
31	Slow leakage of water into wet void cavity	No strategy	Need corrosion monitoring strategy
32	Biofouling of grill results in efficiency reduction	No strategy	Need to monitor fouling and remove during maintenance
33	Biofouling of grill results in failure through cavitation	No strategy	Need to monitor fouling and remove during maintenance
34	Biofouling inside torque bucket prevents operation	No strategy	What is the mechanical strength of hard fouling? Need to monitor fouling and remove any in torque bucket during maintenance
35	Barnacles in clamp slots prevent clamp fully opening for retrieval	Assume clamp will crush all barnacles even if all slots are fully fouled	What is the mechanical strength of hard fouling? Need to monitor fouling and remove any in clamp slots during maintenance
36	Barnacles in clamp slots are crushed but debris prevents full movement during retrieval	Include extra slot length for barnacle debris	What is the debris route following crushing? Need to monitor fouling and remove any in clamp slots during maintenance
37	If turbine stored in water, off tripod for several months then barnacles could attach to high friction surface	Assume no barnacles attach	Ensure awareness of maximum permissible time moored in water
38	Wear of clamp mechanism removes coating	No strategy	Need monitoring programme and maintenance schedule that includes repair of coating
39	Stab mechanism unable to retract after 2 years due to biofouling	Add margin to ram capacity	What is the mechanical strength of hard fouling? Need to monitor fouling in skirt

Reference from Risk Assessment (Table 9.1)	Threat	Current strategy	Issue with current strategy
			area
40	Wear of cable insulation within Iges Chain due to biofouling	Assume no fouling	What is the mechanical strength of hard fouling? Need to monitor fouling in skirt area
41	Wear of chain lower surface due to biofouling on cable tray	Assume no fouling	What is the mechanical strength of hard fouling? Need to monitor fouling in skirt area
42	Increased friction within chain wrap guard leads to chain buckling and jamming	Assume no growth which can increase friction	If turbine shutdown for 1-2 months then hard organisms could potentially attach
43	Camera lighting invalidates biofouling experience from 1MW machine	No strategy	No camera to be put in place on future designs?
44	Hard biofouling of stab gear wheel over tooth not regularly engaged during yawing	Assume that yaw sensor or paddle drive will engage each tooth regularly	What is the mechanical strength of hard fouling? Need to monitor fouling in skirt area
45	Backup yaw sensor (swash plate within skirt) susceptible to biofouling	No strategy	What is the mechanical strength of hard fouling? Need to monitor fouling in skirt area
46	Nacelle connection to winch fails after 2 years due to biofouling	Assume connection is possible and no fouling occurs	Organisms could potentially attach, especially if mature breeding ground formed on other areas of device
47	Winch rope coupling device fails to re-attach due to biofouling	TBD	Organisms could potentially attach, especially if mature breeding ground formed on other areas of device
48	Stainless / Stainless joints result in crevice corrosion	No strategy	Likelihood of crevice corrosion occurring in this area – flow model?
49	Impact with boat during deployment	No strategy	Evidence shows coating removal from impact with boat – need to avoid collision during deployment so paint is not removed
50	Atmospheric corrosion during periods where turbine exposed on Quayside	No strategy	Need procedure for cleaning device when retrieved from seawater

9.2.2 Risk Analysis Results

In this risk assessment, 50 threats to the successful operation of the device were identified in 2010 (Table 9.1). In updated reviews over the following three years, this increased to 58.

Using the risk matrix described in Chapter 2, of these 29 (58%) were low risk (green), 13 (26%) medium risk (yellow) and 8 (16%) high risk (red). The assessment of risk level changed in some instances over the subsequent years as more information was gathered and Figure 9.2 shows the differences in risk rankings between 2010 and 2013.

Figure 9.2 shows the differences in risk rankings throughout all risk reviews carried out in this thesis, including a review in 2012 and 2013.

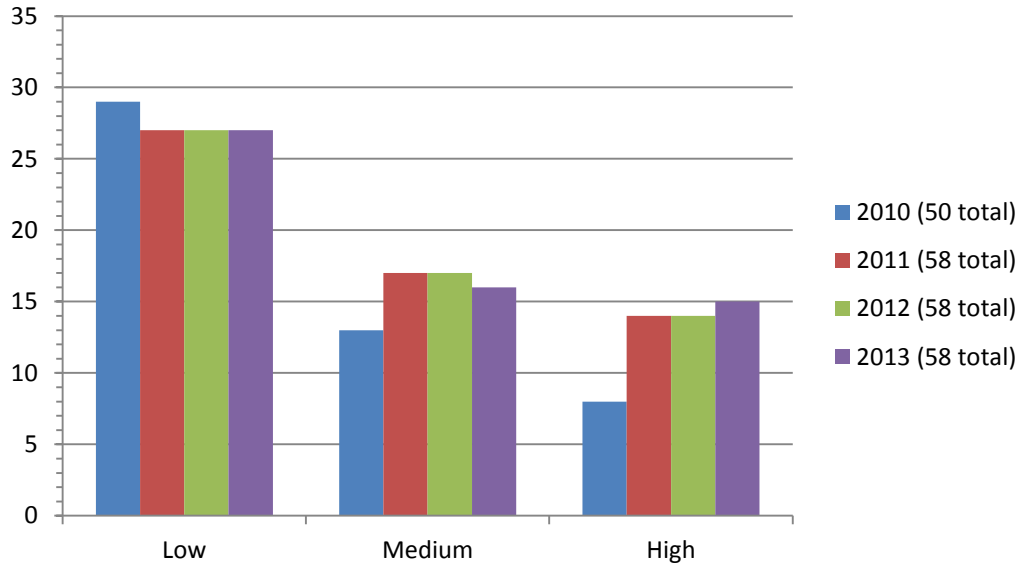

Figure 9.2. Number of threats identified at each risk level during the first two risk assessment reviews

9.2.3 Analysis of Threats Identified

Analysis of the threats identified to different parts of the structure is given below (threat numbers as in Table 9.1 and 9.2).

Tripod

The tripod used for this device has been grouted to the seabed at the test site (EMEC in the Orkney's, UK). The tripod structure is constructed from structural steel grade S355, with the outer surfaces coated in Jotamastic 87, a two pack epoxy resin for corrosion resistance. Epoxy coatings are suggested as best practice for surfaces located in the immersion zone (Det Norske Veritas, 2012). This coating will not be maintained/repainted during the lifetime of the tripod (perhaps 25 years or more) due to practical constraints and cost. The tripod has been designed to include a consideration of the expected corrosion losses (from literature) over the operating life. As well as a corrosion resistant coating, 39 anodes are attached to the tripod. Some of these have already fallen off the structure, although it is unknown whether this is due to the anodes having provided significant corrosion protection

and been consumed in the high flow rates to which the structure is subjected or whether they have been removed by impact.

Table 9.3 shows the threats identified associated specifically with the tripod.

Table 9.3. Threats identified for tripod structure

Threat	Description	Consequence	Likelihood	Risk Ranking	Notes
1	Settlement and growth of fouling organisms on the external surface of the tripod	3	5	MEDIUM	Likelihood is high as it is well established that the external surfaces of a structure will foul when immersed in seawater
2	Growth and subsequent death (inside the central member) leading to increased corrosion	4	3	MEDIUM	See Cathodic Protection System
6	Fouling of high friction surface during turbine removal	4	4	HIGH	Both consequence and likelihood are high as it is likely the surface will foul if the nacelle is removed. Fouling may cause the clamp to not work correctly
7	Fouling of low friction surface during turbine removal	4	4	HIGH	Both consequence and likelihood are high as it is likely the surface will foul if the nacelle is removed. Fouling may cause the clamp to not work correctly

The effects of fouling settlement were not considered in the design of the tripod. The current strategy for the hazards associated with biofouling on the tripod is to accept the fouling and to not attempt to remove it. During 2009-2010 extensive but patchy hard fouling was observed on the tripod. The hard fouling mainly consisted of barnacles, consistent with the area and also the period of immersion in the water (over longer periods it is more likely that mussels will appear on the surface (Forteath et al., 1982)). Soft fouling (mainly sea-squirts) was observed inside the main central member (open to seawater, although with minimal water flow) and also inside the piles of the tripod legs. The biofouling is detailed in Chapter 4.

The potential consequences of fouling have been identified as follows:

i) Increased drag on the structure

Fouling will increase the drag on the structure. The diameter of the tripod members could be increased by more than 20 cm over the lifetime of the structure and the surfaces are rougher.

ii) Development of mature breeding community releasing further fouling

The settlement of fouling on the surfaces of the tripod will, over time, increase to the extent that a "climax" community is formed. The tripod then acts as an artificial reef (Guerin et al., 2007; Langhamer et al., 2009; Sheehy and Vik, 2010) and a breeding ground for new larvae and spores. Often these are not able to survive for a long period of time in the water and so have to attach to a suitable surface as soon as possible. This suitable surface could be other areas of the device, or the devices downstream in an array.

iii) Increase in likelihood of localised corrosion under hard fouling and failure of coatings.

Hard fouling can penetrate coatings and cause the steel underneath to be exposed to the seawater. Localised corrosion can be caused by differential aeration, which can occur where fouling is present (Chapter 3).

iv) Difficulty in inspection and maintenance of structure

The high tidal flow regime in which the device will be placed will cause significant stresses which will alternate between periods of high and slack tides. Regular inspection using divers and ROVs is required to ensure that the structure is not damaged in any way. However, both of these options are costly, and biofouling will have to be removed to inspect the metal surface underneath for visible signs of corrosion, including localised corrosion as well as stress-induced cracking. This will mean that inspection will take longer than anticipated and involve higher costs.

v) Problems associated with decommissioning of structure

After the operational life of the device, the structure will be decommissioned. The decommissioning programme should ensure that biofouling and corrosion are taken into account.

There are several risks associated with the tripod. These are made more significant by the inability to retrieve the tripod during its operational lifetime, therefore increasing the cost of any repair or maintenance. However, it is likely that failure of the tripod will be a low risk to the overall operation of the device and capacity for electricity generation. The key issue for this structure is the maintenance of the cathodic protection system to ensure that corrosion is limited to as low as reasonably practicable.

As part of lowering the risk it should be made possible for new anodes to be attached to the tripod over time, which will provide corrosion protection. Anodes should be assessed during diver or ROV operations and new anodes fitted if old ones have disappeared or have reduced to half size.

Anti-fouling or fouling deterrent coatings should be investigated for use on the tripod surfaces. Features on the tripod structure should be as smooth as possible with no sharp edges. This means that protective coatings are easier to apply to the surface with better coating performance.

Cartridge Plate and Connectors

Design features which promote corrosion are those which alter the local conditions at the metal surface (Chandler, 1985). These design features may entrap moisture and salts due to static water conditions or the settlement of biofouling. Located on the cartridge plate are many features which may trap water and form crevices as well as providing attractive places for the settlement of biofouling (sheltered but with sufficient nutrient flow). The threats associated with the cartridge plate and connectors can be seen in Table 9.4.

Table 9.4. Threats identified for cartridge plate and connectors

Threat	Description	Consequence	Likelihood	Risk Ranking	Notes
3	Accelerated corrosion on the fibre optic (FO) connector	3	3	MEDIUM	It is still unknown whether the Fibre Optic connector corroded due to galvanic action, temperature effects or stray currents
4	Barnacle settlement around winch rope and shell bitt on cartridge plate	3	3	MEDIUM	Medium risk ranking given as it is thought that barnacle settlement shouldn't affect winch rope significantly and stop retrieval
5	Barnacle settlement on	3	4	MEDIUM	Medium risk ranking given as it is thought that barnacle settlement

Threat	Description	Consequence	Likelihood	Risk Ranking	Notes
	the shell bit when no turbine installed				shouldn't affect winch rope significantly and stop retrieval, likelihood is high as it is known that barnacles more likely to settle on horizontal surfaces
6	Fouling settlement on high friction surface during turbine removal	4	4	HIGH	See Tripod
7	Fouling settlement on low friction surface during turbine removal	4	4	HIGH	See Tripod
8	Fouling in connector buckets in cartridge plate prevents connector engagement	5	4	HIGH	Both consequence and likelihood high as electrical connections may be lost. Fouling has already been observed to settle in these locations
9	Fouling on connectors in cartridge plate causing corrosion of connectors	5	3	HIGH	Both consequence and likelihood high as electrical connections may be lost. Fouling has already been observed to settle in these locations
10	Fouling of connectors in cartridge plate preventing signal function	4	3	MEDIUM	Consequence not so high as previous as this will not stop the device from working, but will incur maintenance and repair

The risk assessment (Table 9.1) identified the fibre optic dry-mate connectors as a significant and urgent corrosion hazard. A 4-way "dry-mate" fibre optic connector (manufactured by Seacon) is located on the back of the cartridge plate at the top of the tripod main central member. It is in a semi-enclosed area open to seawater but with low flow. During inspection in 2010, the fibre optic connector was found to be severely corroded on one side of the outer metal surface of the engaging nut having been submerged for less than one year (Figure 9.3). The second connector exhibited less corrosion but significant sulphation.

Figure 9.3. Corrosion of outer ring of FO connector

The corroded connector underneath the cartridge plate forms part of the communication system for the turbine, a system which includes two “dry-mate” connectors (one above the stab plate and one underneath the cartridge plate) and a Seacon Hydralight connector located on the cartridge plate (oil filled connector). The Hydralight connector has a design life of 25 years and a minimum of 100 mate/de-mate cycles (Seacon 2010). The corrosion of the outer ring of the connector could result in disruption of communication with the tidal device as well as increased maintenance and decreased operational time and increased cost.

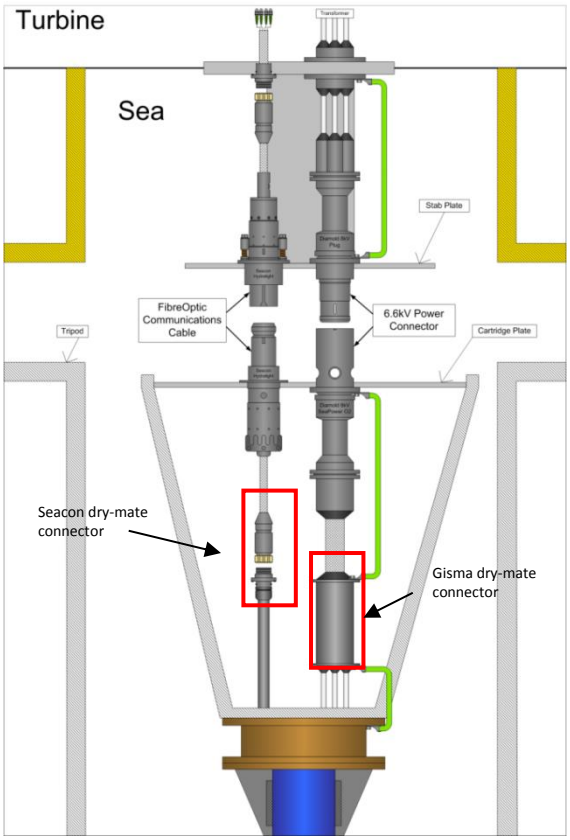

Figure 9.4. Location of FO connector and electrical cables

By identifying the construction materials, and the surrounding environment the cause of the corrosion can be assessed. The connector is made up of a variety of parts. The coupling collar which has shown corrosion and sulphation is manufactured from a high strength aluminium bronze alloy (63000, ASTM B 150 (CA105 per B.S)), (Table 9.5). The nickel content results in a higher corrosion resistance than many aluminium bronze alloys since there is usually no γ2 phase present in the structure of the alloy, only α and κ phases (Copper Development Association, 1981). However, the corrosion is limited to this alloy only on the connector. The stainless steel parts have not corroded on either connector (Figure 9.3).

Table 9.5. Composition of nickel aluminium bronze used for the engaging nut of fibre optic connector

%	Cu (incl. Ag)	Al	Fe	Mn	Ni (incl. Co)	Si	Sn	Zn
Min-Max	Remaining	9.0 – 11.0	2.0 – 4.0	1.5	4.0 – 5.5	0.25	0.20	0.30
Nominal	82.0	10.0	3.0	-	5.0	-	-	-

Galvanic corrosion of nickel aluminium bronze will occur if a large area of a more noble metal is in electrical contact with the alloy. Monel, stainless steel and titanium are examples of metals which are more noble than aluminium bronzes in flowing seawater (see the galvanic table in Chapter 3). A large proportion of the connector is made from stainless steel (Figure 9.5) and this has not corroded. As the stainless steel is electrically coupled with the aluminium bronze this may have caused the accelerated corrosion of the nickel aluminium bronze.

The location of the connector may have influenced the corrosion; the connector is in close proximity to the power cable in the central member of the tripod (Figure 9.4). The connector had been strapped to the cartridge plate frame (S275 grade structural steel painted with yellow 2 coat marine epoxy, Interzone 954) using tie wraps. In operation, the connector was located close to a hole in the cartridge plate frame which was unpainted and also showed corrosion.

Erosion corrosion can occur on nickel aluminium bronzes in conditions of high water flow and turbulent conditions where the protective films are removed. An increase in flow velocity from 0.3 ms^{-1} to 8.2 ms^{-1} is sufficient to show destructive effects on aluminium bronzes (Davis, 2000). However, since the connector is located at the back of the cartridge plate it is sheltered from the high tidal flow conditions experienced around the tidal device.

General corrosion of copper alloys does not usually occur in unpolluted environments. Pollution, sediments and debris in regions of high flow can remove the protective layer

formed on the surface of the alloy and allow corrosion of the metal underneath. However, the turbine is located in an area free of debris and not known to be polluted.

Figure 9.5. Close-up of corrosion of coupling collar

The majority of the corrosion damage had occurred only on one side of the aluminium bronze outer-ring of the 4-way connector (Figure 9.5). This suggests that the corrosion was affected by the operating environment, with the un-corroded side of the connector against a carbon steel plate and the corroded side facing the water inside the tripod central column.

As part of a forensic examination into the electrical and communication systems of the device, two electrical faults were identified in the 6.6kV power transmission system dry-mate connector. The fibre optic connector was in close proximity to this electrical fault. If aluminium bronze is exposed to an electrical "stray" current, this will accelerate corrosive attack of the metal surface. The alloy will exhibit local corrosion in the region affected by the leakage current and usually takes the form of selective phase dealloying (Copper Development Association 1981). As stainless steel is more noble than the aluminium bronze it would be likely that the aluminium bronze would preferentially corrode.

The device temperature increases when operational. It is thought that the internal temperature may reach 40 ^{o}C. This is likely to accelerate corrosion, especially of connectors that get hot during operation. Temperature effects on corrosion rate are discussed in Chapter 7.

The cartridge plate exhibited significant fouling when it was removed in 2010 for inspection and replacement (see Chapter 4, Section 4.5 for more information). When the nacelle is removed for maintenance, the cartridge plate, left exposed, provides a perfect location for settlement of fouling species.

It is also in close proximity to the rest of the external surfaces of the tripod, which have been extensively fouled (see Chapter 4), and provide a good mature breeding ground for fouling species, the larvae of which are likely to settle on nearby surfaces. It has been found previously that biofouling is more prevalent on horizontal surfaces than vertical surfaces (Lee et al., 2004), further indicating the suitability of the cartridge plate for fouling.

When the nacelle was removed in 2010 for maintenance, the connectors in the cartridge plate were capped individually. The connectors sit in recessed 'buckets' filled with oil to reduce the likelihood of corrosion occurring on the vital parts of the connectors. When these caps were removed it was apparent that micro and macro biofouling had settled in the buckets and subsequently died in the anaerobic or nutrient free conditions formed underneath the caps. The sections of the connectors that remained under oil showed no sign of corrosion.

Operations on Quayside

The threats associated with operations on the quayside can be seen in Table 9.6.

Table 9.6. Threats identified for operations on quayside

Threat	Description	Consequence	Likelihood	Risk Ranking	Notes
12	Exposure of blade to air for extended periods resulting in coating deterioration	3	4	MEDIUM	See Blades
22	Impact damage due to maintenance (tools, equipment etc.)	4	1	LOW	Likelihood assessed as low due to correct procedures and training in place on quayside
28	Impact at interface between stands and nacelle during maintenance periods	4	4	HIGH	Observed on 500 kW device. This is high risk as exposed metal will mean a higher demand on the CP system. It is difficult to move these to repaint these areas
50	Atmospheric corrosion of all external surfaces during periods where turbine exposed on quayside	2	3	LOW	Currently assessed as low risk as little evidence available from 500 kW device. This is dependent on the time left on quayside

Threat 12 (Table 9.1 and 9.6) is ranked as medium risk and 28 is a high risk. All other threats are ranked as low risk. However, these risks are highly dependent on human error.

Atmospheric corrosion is discussed in Chapter 3. This form of corrosion is very common on metallic surfaces that are exposed to the marine atmosphere, i.e. in close proximity to the sea, such as on a quayside, where wind and spray can cause seawater droplets to form on the exposed metal surface. The amount of rain, condensation and relative humidity will also influence corrosion rate (Chandler, 1985). The corrosion of carbon steel is also influenced by any pollution in the air, deposits on the surface and the time the surface stays moist. The quayside in Kirkwall experiences high winds and the local topology is fairly flat. When removed from the sea, the device is located in open air very close to water so there is a high probability that significant amounts of salt will build up on the device during these periods. Therefore, it is recommended that devices are washed down and stored undercover in the longer term.

Paint System

The threats associated specifically with the painting coating can be seen in Table 9.7.

Table 9.7. Threats identified for paint system

Threat	Description	Consequence	Likelihood	Risk Ranking	Notes
20	Poor painting application leading to paint loss	4	5	HIGH	Observed on 500 kW device. This is high risk as exposed metal will mean a higher demand on the CP system
21	Impact with debris (including in suspension) removing coating	4	4	HIGH	Observed on 500 kW device. This is high risk as exposed metal will mean a higher demand on the CP system
22	Impact damage due to maintenance (tools, equipment etc.)	4	1	LOW	See Operations on Quayside
28	Impact at interface between stands and nacelle during maintenance periods	4	4	HIGH	See Operations on Quayside

Paint has been removed from the main body (nacelle) of the device during deployment after impact with the side of the deployment vessel (see Chapter 4 for examples of this). The risk ranking of these threats is dependent on the correct application of the paint as well as handling during maintenance.

The device is complex in nature. This makes paint application more difficult. Corners and sharp edges are difficult to coat successfully and paint is more likely to be removed in the flow from these locations. Therefore these features will place more strain on the cathodic protection system.

It is estimated that 90% + of paint removal is not due to the paint quality itself. It is often attributed to poor application, surface preparation and maintenance. The paint application conditions are often less than ideal due to humidity, dust and other factors (Keane, 2011). Manufacturer's guideline for the application of a coating should be followed.

Xylan is currently used on the 500 kW turbine on all bolts on flanges located on the nacelle. This is a fluoropolymer based coating for use on bolts and fastenings in a range of applications. Xylan contains PTFE or similar lubricant and is applied as a thin film to a surface (typically 20 µm). The Xylan coatings are primarily used to provide lubrication, wear and heat resistance and an anti-friction coating to fasteners. However, the coatings are also effective at providing corrosion protection to the surface. The coating has shown good resistance to abrasion, and due to its low friction property is also suitable for use on sliding and rotating systems/surfaces.

Blades

The threats associated with the blades can be seen in Table 9.8.

Table 9.8. Threats identified for blades

Threat	Description	Consequence	Likelihood	Risk Ranking	Notes
11	Biofouling on blades resulting in efficiency reduction	4	2	LOW	Assessed as low risk as although consequence is l=high this is unlikely due to use of anti-fouling coatings on blades
12	Coating deterioration after extended expose to air	3	4	MEDIUM	Likelihood is high as past experience shows that anti-fouling coatings will deteriorate when exposed to atmosphere. A medium risk relies on successful recoating when necessary
13	Barnacle growth on blades as a result of turbine shutdown for extended periods in water (potentially near quayside)	3	2	LOW	Assessed as low risk as it is unlikely that the device will be left for extended periods of time sufficient for extensive barnacle growth

Threat	Description	Consequence	Likelihood	Risk Ranking	Notes
14	Potential for galvanic corrosion cell formation between hub, root fitting and coppercoat (if used)	4	3	MEDIUM	Consequence is high due to potential failure of blades if galvanic corrosion occurs. Likelihood is high due to several different alloys used in close proximity
15	Interaction between anodes and coppercoat on blades if not isolated	4	3	MEDIUM	Copper coat on blades may cause anodes to be used quicker than calculated
16	Water saturation of fibreglass resulting in coating delamination	4	1	LOW	Likelihood of water saturation is low due to past experience of the fibreglass
17	Water saturation of fibreglass resulting in inability to recoat damaged blades	4	1	LOW	As above
18	Lifting features providing location for biofouling	3	1	LOW	Likelihood currently assessed as low as no evidence of fouling on 500 kW device
19	Impact with debris (including in suspension) removing coating from blades	4	4	HIGH	Likelihood is high as impact damage observed on 500 kW device. Consequence is high - damage can cause areas to become fouled and cavitation to occur

A seabed survey of the Fall of Warness in 2005 (Aurora Environmental, 2005) found that the area was made up of a rocky seabed with minimal suspended solids. Therefore it is likely that impact with suspended debris will be relatively minor. However, some evidence of impact damage to the blades has been observed (Chapter 4). The DeepGen III blades are coated in an anti-fouling coating with an anti-corrosion primer. It is important that blades on these devices do not become fouled as this will change the surface properties and hence the efficiency. Any loss of coating however small may provide an area for biofouling to settle. If a small area is settled this can slowly develop into a larger fouling community and can spread even on to the anti-fouling coating.

Cathodic Protection System

A sacrificial anode system is in use on this device. Anodes are attached to all external surfaces. They require no external current and very little maintenance (see Chapter 3). Anodes are also used in any wet voids such as the thrusters and skirt area to protect the

cartridge plate and other surfaces. The threats (numbered with reference to Table 9.1 and 9.2) associated with the cathodic protection system can be seen in Table 9.9.

Table 9.9. Threats identified for cathodic protection system

Threat	Description	Consequence	Likelihood	Risk Ranking	Notes
2	Failure of anodes on tripod internal structure to protect against increased corrosion from biofouling	4	3	MEDIUM	Consequence is high due to potential failure of tripod structure from accelerated corrosion
14	Failure of anodes on hub to protect against galvanic corrosion between hub, blade root fitting and coppercoat	4	3	MEDIUM	See Blades
15	Interaction between anodes and coppercoat on blades if not isolated	4	3	MEDIUM	See Blades
24	Inadequate anodic protection on nacelle body	3	3	MEDIUM	Consequence and likelihood high due to potential failure of nacelle and increased maintenance requirements if system fails
25	Inadequate life of anodes (or galvanic cell stronger than expected) on nacelle body	3	2	LOW	Consequence high due to potential failure of nacelle and increased maintenance requirements if system fails
29	Decay of biofouling products in thruster wet void cavity	3	2	LOW	Ranked as low due to built in margin based on boat application experience
30	Slow leakage of water into wet void cavity causing corrosion	2	3	LOW	Ranked as low as no leakage observed during testing periods of 500 kW device

Aluminium anodes (type A2.0H1, 200 x 150 x 40 mm) were welded to the steel turbine via two tabs, one located at each end of the anode (total length including the tabs was 350 mm). These have a density of 2.71 gcm^{-3}, and alloying elements, particularly indium, (Table 9.4) designed to prevent the formation of a continuous adherent protective aluminium oxide film. This would stop the anode from corroding and protecting the metal structure (Trethewey and Chamberlain, 1995).

Table 9.10. Aluminium Alloy A2.0H1 Composition (Data obtained from Deepwater Corrosion Services Inc, 2010)

Iron (Fe)	0.07 max
Silicon (Si)	0.10 max
Copper (Cu)	0.003 max
Zinc (Zn)	4.75-5.25
Indium (In)	0.015-0.025
Titanium (Ti)	0.025 max
Others (each)	0.02 max
Aluminium (Al)	remainder

Aluminium anodes were selected due to their efficiency in seawater and relatively low cost compared to zinc anodes. Both aluminium and zinc are now used extensively in marine applications (although zinc anodes were used earlier than aluminium). Aluminium has several advantages over zinc, including a higher open circuit potential (for aluminium this is 1.05 – 1.07 V and for zinc 0.95 – 1.0 V (Ag/AgCl) (Cuproban, 2009)), thus aluminium is capable of delivering more current to the protected metal, and 11.3 kg of zinc is required to produce one Ampere of current for one year (a capacity of 780 Ah/kg) but only 3.4 kg of aluminium (a capacity of 2500 Ah/kg), meaning that aluminium anodes have a longer lifetime than those made from zinc alloys.

To quantify the requirements for a cathodic protection system, the surface area needing protection must be considered as well as the current density of the metal used. The following methodology can be used to calculate the number of anodes required for a given surface area of metal (Keane, 2011).

- Calculate exposed surface area

  For the body of the device an estimate of the surface area (SA) of carbon steel can be calculated as for a simple cylinder:

  $$SA = \pi dl \qquad [9.1]$$

  For full assessment, any other areas should be calculated and added to this value

- Estimate coating integrity to determine coating breakdown factor

  The coating integrity must be estimated, e.g. 60% effective (40% damaged) to determine the coating breakdown factor (usually between 20-40% (Personal communication, Keane, 2011)), dependent on the specification of the coating. If the coating is repainted every 5 years (following the stated maintenance schedule

for these devices), it is likely that this value will not be as high as 40% (i.e. frequency of maintenance will affect the breakdown factor).

- Obtain the current densities of metals to determine current required to protect the bare metal

  DNV-RP-B401 (Det Norske Veritas, 2010) can be used to obtain the current densities of metals. (This value is approximately 100 mA/m^2 for carbon steel.)

- Calculate the weight of anodes required using the following formula:

$$wt(kg) = \frac{A \times t \times 8766}{U \times E_C} \qquad [9.2]$$

  Where A is the current required, t is the required life in years, U is the utilisation factor and E_c is the electrochemical capacity function of the material (Ahr/kg). The utilisation factor, U, is dependent on the shape of the anode used. It defines the amount wasted at the end of use (e.g. a utilisation factor of 0.9 implies 10% of anode is wasted and not used for protection of the metal).

  For aluminium anodes such as those used on this device, the electrochemical capacity is 2550 Ahr/kg.

This calculation method results in a requirement for 168 kg of anodic material to be used on the nacelle alone (based on a coating integrity of 60%). Anodes typically weigh between 5-10 kg, so if using the smaller anodes, there should be 34 attached to the nacelle on exposed surfaces.

There are various ways in which sacrificial anodes are located around a device, depending on the degree of knowledge of the current (corrosion) demand. The standard default is to evenly space the anodes and this was the case here.

Figures 9.6-9.8 show anodes working correctly because of the white aluminium hydroxide ($Al(OH)_3$) corrosion product Aluminium anodes release aluminium ions into the electrolyte (seawater) which react to form aluminium hydroxide:

At the aluminium anode surface:

$$4Al \rightarrow 4Al^{3+} + 12e^{-} \qquad [9.3]$$

At the metal surface:

$$3O_2 + 12e^- + 6H_2O \rightarrow 12OH^- \qquad [9.4]$$

This leads to the production of aluminium hydroxide at the anode surface:

$$4Al^{3+} + 12OH^- \rightarrow 4Al(OH)_3 \qquad [9.5]$$

Figure 9.6. Typical skirt anode

The anodes used in the skirt exhibited a relatively uniform and cohesive hydroxide layer on the anode. There was no evidence of blistering of paint coatings on the metal surface around the anode indicating that the anodes had been sited correctly and would not cause incorrect current flow.

Figure 9.7. Typical exposed anode

The anode in Figure 9.7 is typical of all anodes placed in exposed areas around the turbine structure. The anode had lost mass but there is only a small amount of corrosion product build up on the surface. A cohesive, compact deposit on the surface of an anode shows it is working normally, any loose aluminium hydroxide being removed by the water flow. To the bottom right of Figure 9.7 some paint has been removed from the metal surface. Paint loss

was evident on various parts of the structure and it is these exposed areas that the anodes are designed to protect.

Figure 9.8. Thruster housing anode

The anode used in the thruster housing (Figure 9.8) exhibited a slightly less cohesive white layer. The anode was still working successfully and no blistering of the paint around the anode was evident.

It is likely that over time the cathodic protection system will begin to corrode faster than when first deployed and, during maintenance, anodes which have corroded to half their original size should be replaced. The combined use of coatings and cathodic protection takes advantage of both protection systems. Initially, the main primary protection of the surface will be provided by the coating, with the anodes providing protection for any defects. Over time the coating will degrade and the anodes will provide more significant protection to the metal. During maintenance periods the coating should always be inspected to identify any flaws in the surface or areas where impact with debris has caused the coating to be removed. The coatings should be reapplied (using the correct manufacturer's guidelines) when necessary.

It was reported that several anodes deployed on the device were not exhibiting any white deposit. These anodes are likely to be in areas where the paint coating is providing sufficient protection at this time so sacrificial protection by the anodes is not required to such a great degree.

The environmental conditions of the area around the turbine will affect the efficiency of the anodes. When future devices are deployed in different global locations, the temperature of the seawater as well as the level of pollution and the salinity will need to be monitored as

these may alter the rate at which the anodes corrode and require maintenance schedules to be revised.

A galvanic anode system is superior to an impressed current system for tidal devices. At commercialisation, where whole arrays of devices will be deployed in close proximity, a galvanic system is less likely to lead to stray currents and devices in the array interacting which could cause considerably enhanced corrosion.

Further Corrosion Threats

Further threats, other than those identified in the specific cases above, associated with corrosion can be seen in Table 9.11.

Table 9.11. Further threats identified associated with Corrosion

Threat	Description	Consequence	Likelihood	Risk Ranking	Notes
27	Stainless steel penetrator plates with stainless and bronze connectors	3	3	MEDIUM	Consequence and likelihood result in medium risk of galvanic corrosion occurring between the different metals used
31	Slow leakage into wet void cavity of thruster	2	3	LOW	Ranked as low as no leakage observed during testing periods of 500 kW device
38	Wear of clamp mechanism removes coating and results in corrosion	4	3	MEDIUM	Consequence is high and likelihood medium as corrosion of clamp mechanism could result in inability to retrieve nacelle. Cathodic protection is used in area to reduce likelihood
48	Stainless/stainless joints on winch system result in crevice corrosion	3	3	MEDIUM	Risk assessed as medium as crevice corrosion may cause winch to fail resulting in inability to retrieve nacelle. No evidence of this has been observed to date
49	Impact with boat during deployment removes protective coating	4	4	HIGH	Large areas of paint removal have been observed on nacelle during deployment.

The majority of corrosion threats have been assessed as medium risk as evidence of corrosion has been observed (Chapter 4). However, AOE have two lines of corrosion

protection around the device – the majority is painted with a protective coating and cathodic anodes are used as discussed in the above section.

The risk assessment process identified risks that had previously not been recognised. Joints between metals, the use of different metals together and areas where water can collect had been used to satisfy design criteria, but no thought had been given to the potential corrosion issues in these areas. As little evidence has been collected due to the short operating time, AOE require a monitoring programme and maintenance schedule that includes the assessment of corrosion as well as assessment of the state of the protective coatings and the cathodic protection system.

Further Biofouling Threats

Further threats associated with biofouling relating to different areas of the device than discussed in previous sections can be seen in Table 9.12.

Table 9.12. Further threats identified associated with biofouling

Threat	Description	Consequence	Likelihood	Risk Ranking	Notes
23	Biofouling in winch rope tube prevents rope movement during retrieval	3	2	LOW	Only soft fouling observed in winch rope tube to date which would not impede rope movement
26	Biofouling on heat exchanger surfaces	4	2	LOW	Risk assessed as low. Large evidence base of heat exchangers used on boats allows for margin to be built in to reduce effect of biofouling settlement
32	Biofouling of grill in front of thruster reduces efficiency	3	2	LOW	No evidence of biofouling on thruster grill to date. Thruster is used every 6-7 hours so movement may remove biofouling
33	Biofouling of grill in front of thruster results in cavitation failure	3	2	LOW	See discussion of threat 32
34	Biofouling inside torque bucket of clamp prevents operation	2	2	LOW	No evidence of biofouling in torque bucket to date. Clamp movement every 6-7 hours so may remove biofouling
35	Barnacles in clamp slots prevent clamp working correctly for retrieval	3	2	LOW	See discussion of threat 34

Threat	Description	Consequence	Likelihood	Risk Ranking	Notes
36	Debris from hard fouling prevent clamp working correctly for retrieval	4	2	LOW	See discussion of threat 34. The build up of debris may also cause abrasion during use, therefore the consequence has been assessed as high
37	Barnacle settlement on high friction surface during storage in water	4	4	HIGH	In situ testing (Chapter 5) has shown the settlement of biofouling throughout a 1 year period. If turbines are stored in a similar location there is a high chance that they will become fouled.
39	Stab mechanism unable to move after 2 years of operation due to biofouling	4	3	MEDIUM	Consequence is high as may result in inability to retrieve the nacelle or costly in situ maintenance may be required. Likelihood is medium as no fouling observed in this location to date
40	Wear of cable insulation within Iges Chain due to biofouling	4	2	LOW	Consequence is high as may result in loss of electricity generation. Likelihood is low as no fouling observed to date. Chain is in a protective plastic sheath
41	Wear of chain lower surface due to biofouling on cable tray	4	2	LOW	See discussion for threat 40
42	Increased friction within chain wrap guard leads to chain buckling and jamming	4	2	LOW	See discussion for threat 40
43	Camera lighting invalidates biofouling experience from 1MW machine	2	2	LOW	Risk assessed as low. Camera light was low and little biofouling observed during use
44	Hard biofouling of stab gear wheel over tooth not regularly engaged during yawing	3	2	LOW	No hard fouling observed in enclosed skirt area to date
45	Backup yaw sensor (swash plate within skirt) susceptible to biofouling	3	2	LOW	See discussion of threat 44

Threat	Description	Consequence	Likelihood	Risk Ranking	Notes
46	Nacelle connection to winch fails after 2 years due to biofouling	3	2	LOW	Consequence assessed as medium as may result in inability to retrieve nacelle. No problems found with attaching winch rope to coupling device with some barnacles attached. Winch rope likely to crush fouling
47	Winch rope coupling device fails to re-attach due to biofouling	3	2	LOW	See discussion of threat 46

9.3 Conclusions from Risk Assessment

An FMEA based on the procedure outlined in BS EN 60812:2006 (British Standards Institute, 2006a) has been conducted on a real tidal stream device. This process provides the basis for a risk evaluation to feed into a management process as defined in the five-stage process established by DNV (Chapter 2, Figure 2.2). The risk evaluation takes risks categorised as high and assesses them in detail to highlight key threats to different areas.

The risk assessment (Table 9.1) took place in consultation with AOE and identified 50 threats to the tidal device. The original FMEA has been updated on an annual basis and should be used as the basis for future ongoing risk identification and analysis for the duration of the device lifetime. Many of the threats and consequences identified through this process are due to the complexity of the device, and the harsh operating conditions. These also have effects on the mitigation measures that can be used as well as the maintenance and inspection techniques and programmes.

Addressing the level of risks identified in the risk assessment process enables recommendations to be made to designers and operatives in terms of prevention, mitigation, monitoring, operation and maintenance (Chapter 10). Various risks can be grouped together, having similar effects, or similar prevention techniques and recommendations.

The risk assessment also aids the overall management system. This process should be incorporated in to the corporate strategies, and will guide inspection and corrosion monitoring activities in order to monitor known deterioration and detect and measure unforeseen corrosion (Energy Institute, 2008). By understanding the risks involved,

potential mitigation techniques can be included in the management system. This process has emphasised the need for enhanced policies and procedures to be put in place for the management of corrosion and biofouling on tidal turbines. The number of threats identified, the risk level and their consequences shows that this is an important factor for the industry to consider during the design, operation and maintenance of the devices.

Each annual update of the risk assessments is included in the overall management system database (Appendix 5), which allows comparison between all risk assessments and provides data for design, maintenance and inspection.

Any relevant data from inspection and monitoring activities should be fed back into the risk assessment to substantiate assumptions or to modify them if necessary. For example, the first risk assessment carried out for the AOE DeepGen III tidal device identified an issue with biofouling settlement in crevices that were exposed during operation but were required for deployment and retrieval (such as the winch hook). By highlighting this issue, designers were able to implement a new style of winch hook for the DeepGen IV device. The review process will allow further risks to be identified and analysed throughout the device lifetime as more monitoring data is collected.

Many of the current strategies (Table 9.2) are inadequate for managing the corrosion and biofouling threats over the entire lifetime of individual devices. To ensure that threats are managed effectively by all relevant personnel, suitable policies and procedures must be developed.

This process has already helped to identify areas where current strategies used by developers are not sufficient and as operational experience increases, this process should continually be carried out to review strategies to ensure that they are still appropriate and sufficient.

There are various strategies that can be applied to the different risk categories. Those chosen reflect on cost effectiveness and relevance to the device. Once categorised, the risks can be prioritised. Options are developed as part of the risk treatment phase using information gathered from the risk evaluation and review of strategies used in the past in different industries.

Low risks can be accepted as tolerable and do not require further assessment. However, these should not be ignored and should be assessed during routine maintenance

procedures as an opportunity occurs to ensure that no significant changes have occurred since the previous risk assessment.

These values are subject to change over the course of development of these devices with new evidence of fouling and corrosion collected as more devices are deployed for longer periods.

An assessment of the percentage of risks categorised as ‘high risk’ should be conducted every year to ensure that the risk assessment process is working effectively at actively reducing risk over the device lifetime.

This process of developing a risk analysis of a real tidal device shows that the data gathered from the literature and from the laboratory experimental can be applied to a real situation.

Chapter 10

Discussion of Risk-Based Management of Corrosion and Biofouling for Tidal Stream Devices

10.1 Introduction

Risk-based management systems for corrosion have already been implemented with success in a number of industries, most notably and relevant, the offshore oil and gas industry. However, with a new, emerging industry, such as tidal stream power generation, systems cannot be directly transferred without suitable adaptation and development. Tailoring for a new industry requires an understanding of the existing information (sourced from that industry if possible, from other industries and from direct experimentation and testing) and developing an approach that suits the new industry. By investigating the existing literature, studying real, albeit prototype, devices and carrying out complimentary laboratory testing this current work has enabled the development of a risk-based management system for corrosion and biofouling for tidal stream devices. This is based on the knowledge and conclusions described in previous chapters; the work that has been done reviewing risk assessment processes (Chapter 2), corrosion and biofouling literature (Chapter 3), development of an evidence base from an example device (Chapter 4), findings from field and laboratory investigations (Chapters 5-8), and undertaking a risk assessment for a real device (Chapter 9).

This chapter describes how the system that has been developed can be used by the whole industry to ensure that corrosion and biofouling risks are reduced to a level that is as low as reasonably practicable (ALARP) and thus maximise efficiency and cost effectiveness.

The overall objective of this management system is to help meet the corporate objectives of efficiently operating and maintaining a safe device, capable of generating electricity from the energy contained in the tidal stream for the expected device lifetime of 25-30 years.

10.2 Risk-Based Management Systems

The management of corrosion and biofouling must be developed as part of an overall integrity management system concerned with the development, implementation, review and maintenance of the integrity of the structure (Capcis Limited for the Health and Safety Executive, 2001), and as such needs consideration from design through to operation and decommissioning. This thesis has focused on the planning and development of a risk-based management system supported by new experimental data, as the device and industry are still in their infancy in terms of operating experience.

A management system is based on an on-going risk assessment process as outlined in Chapters 2 and 9. This should be monitored, reviewed and updated on a regular, usually annual, basis.

The management system provides a structured framework that can be used for the identification of potential threats posed to the device by corrosion and biofouling. The system also provides a basis for the development, integration and operation of risk control measures that have been investigated and found suitable for the device and the environments in which it will be operating. Procedures for identifying risks and inspecting the device during operation have been developed as part of the process.

The work contributes to the following areas:

- Reducing unplanned maintenance requirements and maintenance downtime
- Structural reliability
- Reduction in operating costs
- Increase in operational time and electricity production
- Supplying operational data to risk management policies

10.2.1 Corrosion and Biofouling Management Strategy

The high-level strategy objectives of a risk-based corrosion and biofouling management system are:

- To maintain corrosion and biofouling within predetermined acceptable limits at a minimum cost to reduce the likelihood of failure of all or part of the device

- To develop and facilitate rapid access to monitoring, inspection and maintenance records that provide the corrosion and biofouling status of different locations on the device
- To ensure corrosion and biofouling failures are rapidly identified and appropriate remedial action is implemented to minimise consequences of such a failure

10.2.2 Implementation of Risk Assessment and the Underlying Database

Section 2.3 in Chapter 2 discusses the implementation of risk assessment results. The thesis has resulted in a database (Appendix 5) that can be used to manage the corrosion and biofouling of the device. The database can also be used to provide information for use as part of a gated-review process for new devices or design features prior to implementation. A gated-review process is a methodology which allows natural stopping points during a project to determine if all requirements are being met before proceeding further. This ensures that potential failure modes associated with corrosion and biofouling are identified and considered at an early stage of development. The preliminary questionnaire developed for this purpose can be seen in Appendix 6. A prompt sheet for inspection purposes, both in the short term for further compilation of an evidence base and longer term operation of the devices has also been developed to help operatives effectively monitor and record corrosion and biofouling on the device (Appendix 7).

The database provides an effective method for storing data captured during the risk assessment process. All past risk assessments are included, meaning that management options can be used to develop strategies depending on the level of risk identified (Table 10.1).

Table 10.1 Corrosion and biofouling management options (Adapted from Ashworth, 1996)

Assessed Risk	Corrosion and Biofouling Management Options
High	Corrosion prevention or control for device lifetime Corrosion prevention or control to meet predetermined maintenance schedule and replacement
Medium	Corrosion control for device life time Corrosion control to meet predetermined maintenance schedule and replacement
Low	Take no action Replace part if required during opportunistic inspection

Key challenges with a tidal device are the different sections of the device experiencing different conditions and the selection and use of different materials. Each section or material may have various threats which have been classified according to risk level. There are two options to deal with the issues:

- Corrosion prevention of the high risk item, leaving the rest of the section unprotected
- Corrosion control provided to the whole of the local section to manage the high risk item

This must be assessed on a case-by-case basis and the information provided in this document and accompanying database will aid the decision making process.

10.2.3 Development of Corrosion Models

Experimental work conducted as part of this thesis both under laboratory conditions and in the field (Chapters 5-8) has enabled development of models of potential corrosion rates under different environmental regimes. This work has quantified the relative performance of four metals used in areas of the device identified in the risk assessment as critical as well as the effect of local environmental conditions on corrosion rate. The seasonality of biofouling and the onset of localised corrosion at a location in Orkney (the European Marine Energy Centre (EMEC)) have been investigated (Chapter 5). Temperature increase will increase the rate of corrosion of all metals tested, but the relationship is different for each (Chapters 6 and 7). The effect of the high tidal flow rate has been investigated and information on the derived relationship between this flow rate and the corrosion rate can be found in Chapter 8. The data generated from these investigations forms part of the overall corrosion and biofouling strategy and can assist in making informed decisions regarding material selection and maintenance requirements depending on local operating conditions. A case study of a real tidal stream device has been performed in Chapter 9 which uses this information. More information on the AOE tidal device can be found in Appendices 4-8.

10.3 Risk Register

The evidence base (Chapter 4) and risk identification (Chapter 9) phases of this thesis have resulted in detailed knowledge of the corrosion and biofouling likely to occur on tidal devices. High risk areas that require follow up in the form of design changes, prevention techniques, replacement, repair or mitigation have been identified (Chapter 9 and Appendix 4).

The main aim is a reduction in the probability of failure due to corrosion and biofouling, thus lowering the risk to the device (Det Norske Veritas, 2012). Risks in the high risk category (red) should be prioritised, and corrective action should be implemented depending on the severity of the impact of the risk (Table 10.1).

It is more likely that corrosion and biofouling on a device will be controlled in a cost effective manner rather than completely prevented. Using the management system to select suitable prevention techniques such as coatings and cathodic protection, and the best maintenance and monitoring it should be possible to control the risk of failure due to corrosion and biofouling in the operating periods between retrieval for planned maintenance. The aim of the management system is to highlight the key risks associated with corrosion and biofouling and to develop an understanding of the corrective actions that are available. These actions are in the form of design stage techniques and rules; prevention techniques for use during operation and monitoring and maintenance guidelines (Sections 10.3.1 – 10.3.3 and Appendices 5-7).

The costs of corrosion failure can be summarised as follows (Ashworth, 1996), and these should be considered in the management of such devices:

- Safety hazards
- Loss of asset (equipment)
- Loss of electrical production capacity
- Maintenance, repair and/or replacement costs
- Increased insurance premiums
- Loss of consumer confidence and public image

If a correct management strategy is not developed based on identifying the level of risk associated with various parts of the device, there is potential to overspend on corrosion control. This includes using expensive, corrosion resistant material unnecessarily;

monitoring and inspecting the device excessively; overdesigning antifouling and anticorrosion systems, and prematurely replacing equipment.

10.3.1 Device Design

The consequences of failure due to corrosion can be severe and require identification, assessment and good management (Ashworth, 1996). These consequences include shutdown of equipment (loss of electrical generation capacity in the case of tidal devices); replacement of corroded equipment; overdesign prior to deployment; increased material requirements; and increased maintenance and repair operations including application of preventative measures (Davis, 2000). During the design stage additional thickness is included to account for the surface wastage of metal components expected over the lifetime of the structure. The selection of materials used is also an important design factor. Many metals are not suitable for extended use in seawater, whereas others with high corrosion resistance are expensive and therefore not commercially viable. Hence design is a balance between capital expenditure and operational costs throughout the lifetime of the structure. The metals selected for use on a tidal device have to be durable under the conditions posed by a strong tidal regime at the operating depth (30-90 m below sea level).

The design parameters of a structure or device are as important as the material selection. As well as determining the required strength, electrical generation capacity, and mechanical properties of the device to enable correct functionality, an allowance should be made for corrosion. Chosen materials required for their mechanical properties must be of sufficient corrosion resistance or allowance, or able to be protected against corrosion.

For example, at the design stage, many companies use a gated-review process to assess new processes or feature development or improvement. The review process is divided into stages that are separated by ‘gates’. When a gate is reached, the continuation of the process must be decided relative to its suitability to pass through that particular gate.

The assessment of the effect of corrosion and biofouling is an important consideration as part of this process. By implementing the design stage questionnaire (Appendix 6) associated with corrosion and biofouling as part of a gated-review process relevant personnel are obliged to take this into consideration before further development and application occurs.

As shown in the experiments (Chapters 5-8), the materials common to marine structures and devices exhibit a range of corrosion rates.

These corrosion rates form a base line for design and do not take into consideration potential fouling, turbulence of flow around the device and other factors that may alter the corrosion rate in practice. However, they do give a start point from which to base decisions on design, monitoring and inspection. As good practice, the thickness of the metals used should be double that which would give the desired life of the device (in this case, 25 years) (National Corrosion Service, 2010). This allows some variation in depth of corrosion penetration into the metal rather than assuming that corrosion rate will be uniform across the surface (Wallace and Webb, 1981; Melchers, 2003b). Thickness allowances have been determined under the conditions tested in Chapter 7 and 8 (not including preliminary scoping exercise or testing near to quayside) and are given in Table 10.2 and 10.3. For reference, the thickness of carbon steel that was used on different sections of the AOE DeepGen III tidal device varied between 20-40 mm.

Table 10.2. Corrosion allowances (mm) for overall wall thickness from temperature testing in Chapter 7 for a 25 year lifetime

Metal	Temperature (°C)													
	4	6	8	10	12	14	16	18	20	22	24	26	28	30
Carbon Steel	5.90	11.2	14.1	17.4	21.7	24.5	28.7	32.6	34.7	37.3	39.9	42.5	44.0	46.9
Nickel Aluminium Bronze	0.65	0.90	1.15	1.40	1.46	1.76	2.20	3.25	3.70	4.75	7.95	10.1	14.9	21.0
SG Iron 400-18	37.0	43.1	49.0	56.5	60.8	64.0	68.7	73.3	75.5	82.4	87.0	91.8	96.8	99.5
SG Iron 500-7U	39.6	43.3	46.0	47.6	51.1	55.2	59.9	65.1	71.4	76.3	81.8	86.9	91.5	95.5

Table 10.3. Corrosion allowances (mm) for overall wall thickness from flow testing in Chapter 8 for a 25 year lifetime (at 18°C)

Metal	Low Flow Conditions (ms^{-1})	High Flow Conditions (ms^{-1})
Carbon Steel	7.30	11.4
Nickel Aluminium Bronze	1.77	2.30
SG Iron 400-18	8.88	12.1
SG Iron 500-7U	8.75	11.2

Risk Factors and Recommendations

The following is a list of recommended best practice design rules which are the result of this study:

1. *Use welds instead of rivets as rivet joints provide sites for crevice corrosion.*

   Crevice and other forms of localised corrosion such as pitting will present problems for the structural integrity of tidal devices. Through-pitting will cause ingress of water into the device which could cause damage to the equipment housed inside.

   Rivet heads or other fixings will become stressed, and therefore can become anodic to the rest of the area and corrode.

   However, the welding process does alter the material (producing a heat affected zone (HAZ)), and this can cause galvanic corrosion between the HAZ and bulk metal (Chapter 3, Section 3.2.1). Therefore, if possible, welds should be internal, especially on the nacelle. External welds will create areas that are difficult to coat effectively.

2. *If joints cannot be replaced by welds, flanges should be internal where possible to minimise external bolts and to minimise potential crevice formation.*

   This is particularly important for fixings that have to be removed for maintenance of the device. If left to corrode they may become very difficult to remove.

3. *Ensure there is no part of the device that can trap water and allow it to stagnate.*

   On any tidal device there exists potential for crevice formation with varying levels of aeration, flow and also temperature. Areas where seawater is trapped without movement can cause degradation of the metal in that area, especially where areas of stagnant water are adjacent to flowing water, causing differential aeration on the surface leading to increased corrosion.

   In the marine environment, a major source of heterogeneity is the relative motion of the metal structure and the environment (water flow rate and thermal convection on localised concentrations of salt). Potential heterogeneities and geometrical factors should be considered at the design stage to reduce turbulence and hence corrosion.

   The design should ensure that occluded regions and corners are minimised (Fontana, 1987), especially in areas of the device where the flow is shielded or in regions of turbulence. In joints where rivets or bolts are used, sealants should be

used to infill occluded regions and reduce the potential for water ingress under the bolt head, etc. However, crevices between metals and non-metals should be avoided due to the crevice gap usually being much smaller than those between two metal surfaces. The severity of crevice corrosion can be reduced by decreasing the aspect ratio between the depth of the crevice and the crevice gap (Corlett et al., 2010). The area around potential crevice sites should be painted and maintained regularly as this will reduce the potential for cathodic reactions to take place and therefore reduce the rate of corrosion attack inside the crevice. The effect of flow and temperature are discussed in detail in Chapter 3.

4. *Model the flow around a device at varying degrees of surface roughness to determine if this may have an effect on the integrity of the structure in the long term.*

   The degree of surface roughness of the structure may create a differential flow with the potential for increased corrosion. The effect of flow on corrosion is discussed in more detail in Chapter 7.

5. *Avoid the potential for galvanic corrosion between dissimilar metals by avoiding electrical contact between different metals (either use different materials in the design of the system or isolate).*

   If isolation is not possible, the more anodic (more active) metal should be larger in surface area than that of the more cathodic metal (less active) (Chapter 3). If two metals are to be in electrical contact then they should be as close as possible on the galvanic series.

6. *Avoid sharp edges and corners. Sharp edges are difficult to coat satisfactorily and as such are likely to rely heavily on the cathodic protection system for corrosion protection.*

7. *Develop a list of materials used and their specifications to help ensure that correct replacements are used during maintenance and repair.*

   A list of materials should be contained within the database and should be updated whenever new materials are specified. Using incorrect parts may result in galvanic

corrosion if two metals with a large potential difference are used together. Chapter 3 provides more information on galvanic corrosion.

8. *Specify procedures for testing, storage (whilst on quayside out of the water), maintenance and inspection of the device.*

   For example - do not let water become trapped in areas of the device once on the quayside; ensure device is washed down with freshwater to reduce salt deposits on metal surfaces; repaint as soon as possible once out of the water. As part of this thesis a process for gathering information whilst a device is being maintained (opportunity-based inspection) has been developed (Appendix 7). Information on maintenance procedures is contained within the database.

9. *Reduce any areas of the device which may get hot during operation.*

   These can be investigated further using a flow model close to the metal surface around a device. Temperature increases have been shown to increase corrosion rate. When operating in higher temperatures the corrosion allowances should be altered accordingly (Table 10.2).

10. *Overall, avoid heterogeneity. (This includes hot spots, biofouling, dissimilar metals, and differential flow.)*

11. *The results of the corrosion testing in Chapters 5-8 should be used as a guideline for thickness allowances.*

    This allows for the corrosion under different environmental conditions to be accounted for and that sufficient corrosion allowance is included in the design.

10.3.2 Prevention and Minimisation Techniques

If it is not possible to "design-out" a potential problem associated with corrosion and biofouling at the design stage either due to difficulty or increased cost, the next stage is to consider other preventative or minimisation measures.

A summary of suitable techniques is given in the database (Appendix 5). Chapter 3 also contains information on various prevention techniques for both corrosion and biofouling.

Elimination of the chance of a failure occurring due to corrosion or biofouling) in a designated high risk area is rarely possible on an existing device as these options would require significant design change. Therefore, prevention and minimisation methods should be seen as options to reduce risk to a level as low as reasonably practicable.

Coatings have been reviewed and discussed in Chapter 3 and provide one of the most important strategies to implement as a first line of defence against corrosion. The most common types of coatings used are epoxy and epoxy polyester based (Det Norske Veritas, 2012).

The importance of corrosion protection whilst the device is situated on the quayside during periods of maintenance has been highlighted during this thesis. The device will be subject to atmospheric corrosion and coating degradation due to osmotic blistering. Coatings that provide suitable protection during operation may not be suitable for protection against corrosion in the atmosphere.

Cathodic protection has been identified as a further corrosion prevention technique. This has also been discussed in Chapter 3. The cathodic protection system has the potential to reduce the corrosion rate of the metal to negligible values (Det Norske Veritas, 2012), but will only work when the device is in the water.

Risk Factors and Recommendations

The following is a list of best practice rules for coatings and protection developed from this study.

1. *Coatings should be used on all parts of a device where practical.*

   Any areas left uncoated are likely to become anodic in relation to the coated surfaces and therefore more likely to corrode faster than anticipated. The high flow rate of the tidal regime will potentially reduce the life of the coating, and hence reduce the time interval required between maintenance and reapplication.

2. *Ensure good application and adhesion of protective coatings to the surface.*

   The integrity of the coating depends significantly on the cleanliness and the pre-treatment of the metal surface prior to paint coating application. The manufacturer specifications should always be followed in detail and only

manufacturers able to demonstrate appropriate performance through test results should be considered. The most important issue with paint coatings is to ensure correct application on to a clean surface. If any microscopic bubbles exist under the coating this is likely to eventually lead to corrosion and coating failure (McMurray and Williams, 2010).

The first step in an application procedure should be to ensure that the metal surface is clean. Prior to application of paint either before deployment or recoating, any rust that has formed on the surface should be removed along with any salt deposits. On steel, $FeSO_4$ is present in the corrosion product. This is water soluble and can accelerate the corrosion of the steel underneath the paint by the formation of sulphuric acid. It is recommended that the surfaces are cleaned using high pressure freshwater prior to paint application. The presence of sulphates and chlorides at the metal/paint interface (from salt spray whilst on quayside or lack of cleaning after retrieval) is known to have a detrimental effect on the integrity and efficiency of most paint systems (Morcillo, 1999), leading to a reduced lifetime of the paint and early failure of the metal structure. Any soluble salts left on the metal surface prior to paint application can cause osmotic blistering of the paint coating, where the high salt concentration will encourage water to diffuse through the paint (Morcillo et al., 1997; British Standards Institute, 2001). The dissolution of the salts then creates a pressure build up and will blister the paint. Salt contaminants can be difficult to remove from the structure surface as they can become trapped in corrosion products, in crevices on the device or in corroded pits on the surface.

It is not sufficient to only clean the device after retrieval. If the device is to be left on the quayside for an extended duration natural atmospheric pollution may cause deposition of marine chlorides, especially where the device stands are in close proximity to the sea. It is recommended that testing for soluble salts on metal surface prior to paint application is conducted. This is required by many paint manufacturers and can be carried out by swabbing the surface or using a Bresle patch to sample soluble salts on a surface (British Standards Institute, 2006b). Any paint finishes or coatings should ideally be applied in a controlled environment but this may not always be practicable for repair work and the conditions should be recorded.

3. *Any paint system specified for use on a device should have a good corrosion resistance as well as a strong finish to mitigate any potential impact damage, either during deployment, retrieval or maintenance or with suspended solids or debris entrained in the high flow.*

4. *Coatings which have a surface finish which is unattractive for settlement of fouling species may be useful in areas identified during this thesis as having the potential to foul (Chapters 4 and 9).*

   Information on different anti-fouling coatings can be found in Chapter 3. These should be considered for sensitive areas which have a high potential to provide suitable areas for settlement.

5. *The coating must be compatible with the cathodic protection system required to protect areas that cannot be coated, or those areas where coating has been removed during deployment, operation or retrieval.*

   The cathodic protection system provides the second line of defence against corrosion. The protective paint coating should be seen as a method to reduce the area of exposed steel and thereby reduce the overall current required for protection and enhance the current distribution for the cathodic protection system used (British Standards Institute, 2000).

6. *Coatings must provide both corrosion protection and anti-fouling if required, especially for the blades, whilst being resistant to erosion caused in the tidal regime.*

   It is often the case that an anti-corrosion primer is used prior to application of an antifouling top-coat. It must be remembered that a cathodic protection system will not provide a barrier to corrosion when the device is out of the water.

7. *Anti-corrosion coatings should be a minimum thickness of 450 µm (minimum of two coats) (Corus Construction and Industrial, 2004).*

   In the tidal regime a coating thicker than this will provide more protection against potential impact and erosion issues associated with the high flow. Risks have been identified associated with coating include removal due to impact and also the difficulty in sufficient coating application on edges.

8. *Sufficient anodes must be used in correct locations to ensure that enough protection is provided for the whole device for the required duration of deployment.*

Jingjun (2008) found that over a range of velocities between 0-18 ms^{-1}, the application of cathodic protection reduced the damage rates of carbon steel substantially with a degree of protection of 95% even at high velocities. Therefore, it is likely that providing there are sufficient anodes, this type of system will provide appropriate protection to a device operating in a tidal flow regime.

9. *Anodes should be regularly inspected and their condition monitored.*

In the high flow regimes there is the potential that anodes may be physically removed before providing sufficient protection. If it is found during a survey of the device that an anode has become detached, a new anode should be installed as soon as possible to ensure the correct protection is being provided.

If during maintenance and inspection procedures there is no evidence of corrosion of the anodes it is possible the anode has passivated, and is therefore no longer providing protection to the metal structure. If this is the case, the anode should be replaced with a new anode.

10. *Inspect the size of the anodes during maintenance.*

Replace anodes when corroded by a planned amount (e.g. to half their original size). The cathodic protection anodes may corrode at different rates throughout the life of the device and replacement should not be based only on time interval.

11. *Reduce the exposure time of devices to the "waterline" as far as reasonably practicable.*

Splash-zone corrosion poses a risk to tidal devices during periods in which they are being transported or towed by ship or are left in the water but docked by the quayside.

As an example, the AOE DeepGen III device was decommissioned in 2013 and left next to the quayside for several months after which exposed bare metal surfaces exhibited corrosion. Extended periods of exposure can result in "waterline

corrosion", particularly in polluted harbours and there are other risks such as stray current corrosion.

10.3.3 Monitoring and Maintenance

There are several different techniques available for corrosion monitoring and inspection as reviewed and described during this thesis. Each technique has advantages and disadvantages, making individual techniques more or less applicable to individual situations and the circumstances that arise at a given location. These are included in the database (Appendix 5) with reference to the relevant sections in the literature review for more information (Chapter 3) and reference to the different areas of the devices that they are applicable to.

This thesis has shown that Risk-Based Inspection (Chapter 2) is appropriate to tidal stream devices, especially at the current stage of development where there is limited operational experience. High risk areas should have a detailed inspection plan. This could involve the use of coupons or probes in these critical areas. Medium risks should also be regularly inspected but may not need such a rigorous testing regime. Low risk areas should be inspected on an opportunity-based basis. Further information on monitoring can be found in Chapter 3. Monitoring can be carried out during maintenance periods, or whenever a diver or ROV is deployed, and inspection of the device surfaces will establish the amount of corrosion and biofouling that has occurred.

Losing opportunities of developing an evidence base by lack of recording at early stages has significant impact on the longer term operation of these devices. An extended evidence base will also allow easier definition of required treatment.

Risk Factors and Recommendations

The following is a list of best practice rules for monitoring and maintenance developed from this study:

1. *Development of an evidence base of corrosion and biofouling should begin at design stage and be a continuous process throughout operation of a device.*

   The monitoring at this stage should be as simple as possible to increase the likelihood that the criteria are actually met and monitoring is carried out. A corrosion and biofouling inspection log has been developed based on the work and

observations from the thesis which should be used to document evidence of both of these issues every time the device is out of the water for maintenance (Appendix 7). A prompt sheet allows operatives to carry out an inspection without impinging on valuable maintenance time (Appendix 7). Data should be captured and reviewed regularly to understand how corrosion and biofouling are affecting the devices.

It is unlikely that biofouling will be a problem for the majority of the device, as the velocity at which fouling has been found to decrease in flowing water is 0.9 ms^{-1} (Copper Development Association, 1982). However, there are areas of the device that will be under lower flow conditions, and these areas need to be identified.

However, a covering by fouling organisms will make visual inspection of the surfaces and important structural features difficult and impair identification of corrosion sites. Maintenance of surfaces and the structure as a whole will be more difficult and correct procedures must be implemented to ensure that no further damage occurs. It is noted that in practice it is difficult to conduct extensive underwater operations and maintenance procedures using divers or remotely operated vehicles (ROVs) in the locations suitable for tidal power generation (high flow velocities and short turnaround times during slack tides) (Fraenkel, 2002).

The settlement of fouling organisms will have a significant effect on the corrosion of the structure, as well as preventing visual identification of corrosion damage. Crevice and pitting corrosion are the most common and frequent types of attack in biocorrosion (Videla, 1994), occurring when biofouling species have settled on the surface of the metal. The localised corrosion is often initiated by a form of differential aeration attack at the biofilm/metal interface. Biofilms may accelerate corrosion in crevices and pits due to the depletion of oxygen by microbial respiration (Videla, 1994).

2. *Coupons should be deployed to monitor biofouling levels and types and the damage that this may have caused in terms of microbially influenced corrosion of the metal surface.*

Coupons for corrosion monitoring have been discussed in Chapter 3. Analysing coupons is the simplest form of corrosion monitoring (Det Norske Veritas, 2012), using uncoated metal coupons that are exposed to the same environment in which

the device is operating. These coupons can be attached directly to the device or on a standalone structure. The coupons should be removed over time for examination of fouling and corrosion products, and analysed for corrosion rates using gravimetric assessment. Data collected can be used to develop maintenance procedures. It is recommended that coupons are monitored for weight loss and onset of localised. It is also recommended that testing is carried out for at least two years to show likely corrosion over the period expected between scheduled maintenance.

3. *Corrosion probes should be used to monitor corrosion in situ.*

The use of coupons for corrosion monitoring is limited to the time of installation and retrieval of the coupons and as such gives an average rate of corrosion over the exposure time. If more detailed knowledge is required in critical areas then probes can be used to provide time-based assessment of corrosivity of the environment without the requirement for any human interaction (Det Norske Veritas, 2012). Corrosion probes are discussed in more detail in Chapter 3.

4. *Any structure that is not retrieved for maintenance (such as the tripod on the AOE tidal stream device) should be monitored for biofouling growth using thickness measurements when possible.*

Thickness measurements along with site surveys and pictures will give an insight into the level of fouling that has occurred on a structure. Any photographs or videos should be analysed for type of fouling, density, thickness and pattern of deposition (especially in relation to the flow regime). It will not significantly affect the overall weight of the structure, although hard fouling may alter the surface properties of the structure and this may increase drag which may cause problems with the calculated loads on the structure.

Site surveys should also be used to monitor anodes on the structure, and, if any have reduced significantly or have degraded completely, these must be replaced as soon as possible (see Chapters 3 and 9 for more information on sacrificial anodes).

5. *When retrieved for maintenance, a device should be left in the water by the quayside for as short a time as possible.*

   The field trials (Chapter 8) have shown the likely corrosion and biofouling that may occur on the device if left in the water by the quayside under very low flow conditions for some time. As shown by these experiments, coupons left in these conditions have fouled throughout one year duration. General corrosion was observed on all coupons throughout the testing, but after 9 months the coupons exhibited localised corrosion.

10.4 Data Management

To ensure that a management system is successfully delivered and utilised, an Access database design has been developed as part of this work. The relational database was created as an ideal tool to bring all learning together in a manageable format that can be used by tidal stream device manufacturers and operators. Using Access allows a collection of forms, queries and reports to be established which holds all data obtained in this study, including the previous literature (Chapter 3), evidence collected (Chapter 4) results of corrosion testing (Chapters 5-8) and risk assessments (Chapter 9). Data can then be related to provide options for managing risks throughout device operation.

A database should remain active and up-to-date throughout a device lifetime. This can be seen in Appendix 5 – a populated database for a prototype device available to this project. This database contains information on past monitoring and inspection campaigns as well as corrosion data, past risk assessments and data on techniques for monitoring, inspection, corrosion prevention and mitigation.

Data contained with this database system has been continually monitored for integrity and to ensure that up-to-date data is processed and integrated into the system throughout this study. By regular review the most recent and more developed data and techniques for corrosion prevention, mitigation, monitoring and inspection can be included into assessment campaigns.

Data was entered into the database when new evidence and results were obtained. This process should be continued as regularly as possible to maintain the integrity of the database. Two forms (Figures 10.1 and 10.2) have been developed as part of this work to

facilitate this. These are for gathering data on observations of corrosion and prevention measures. These two areas were highlighted as a key risk mitigation measures for the risk assessment process (Chapter 9) in the future operation of tidal devices. These forms should be used during maintenance, and can be completed using the inspection log data (Appendix 7) which has been created for tidal stream device operators to make capturing data a simple process. These cover corrosion, biofouling and monitoring of prevention measures and their integrity. By entering data from all inspections, an evidence base can be developed which will provide reports which can be used to inform future risk-based inspection, design and maintenance. An example report produced for the AOE tidal device assessed in Chapter 9 can be seen in Figure 10.3. This shows the biofouling and corrosion that has been observed on four work packages between 2011 and 2013 when the device was inspected.

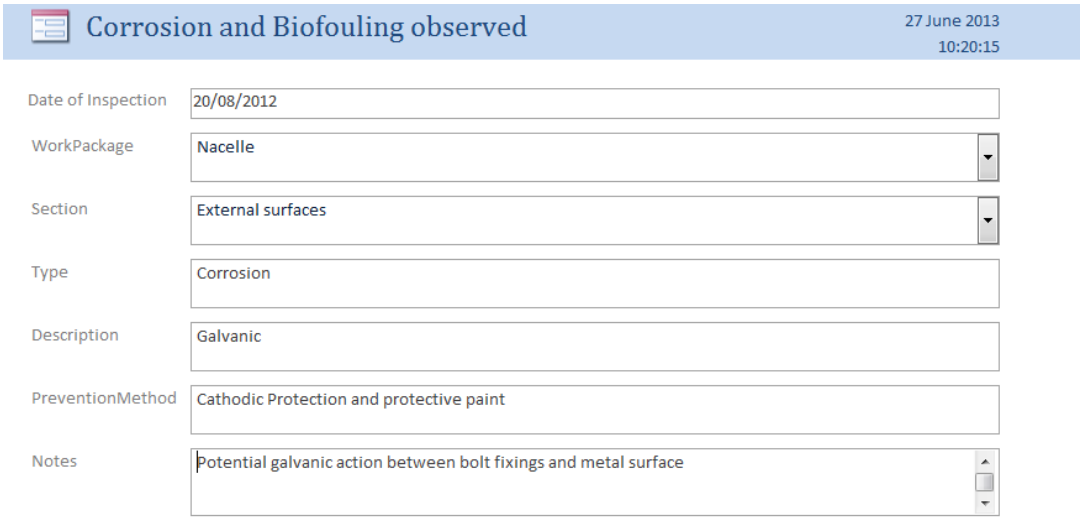

Figure 10.1. Database Form for observed corrosion and biofouling

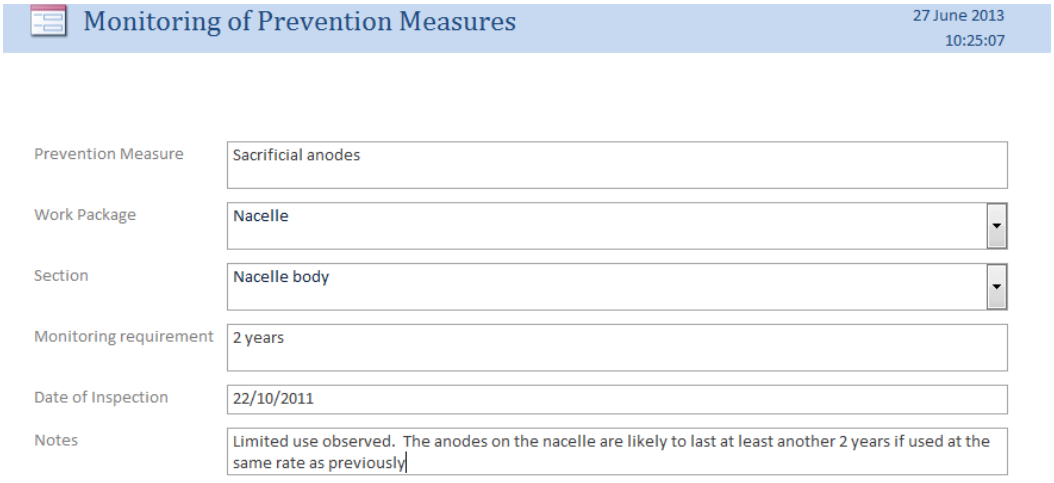

Figure 10.2. Database Form for prevention measures inspection

Corrosion and Biofouling Observed

27 June 2013
10:59:56

WorkPackage	Inspection	Section	Type	Description	PreventionMethod	Notes
External systems						
	12/04/2011	Clamp	Corrosion	Welds	Cathodic protection and protective coatings	
	12/04/2011	Thruster	Corrosion	Welds	Cathodic Protection and protective coatings	Protective coating removal from weld area can cause exposed metal to corrode
Nacelle						
	12/04/2011	External surfaces	Corrosion	Welds	Cathodic protection and protective coatings	
Powertrain						
	12/04/2011	Blades	Corrosion	Galvanic	None	Cast iron next to Al-Ni_bronze at the interface between the blades and hub
	12/04/2011	Blades	Biofouling	Hard macrofouling	Protective coatings	
Tripod						
	01/05/2011	Internal structure	Biofouling	Soft fouling	No prevention method	Soft fouling may build up in areas of stagnant or low flow
	01/05/2011	External surfaces	Corrosion	General	None	Uncoated carbon steel
	01/05/2011	Internal structure	Biofouling	Soft fouling	None	Soft fouling observed on inner surfaces of centrl tripod column in low flow
	01/05/2011	External surfaces	Biofouling	Hard macrofouling	Cathodic protection and protecive coatings	Hard hard fouling observed on outer tripod surfaces and on ADCP
	01/05/2011	Cartridge plate	Corrosion	Crevice corrosion	Cathodic protection and protective coatings	Gasketed joints on stainless steel may lead to crevice corrosion
	01/05/2011	External surfaces	Biofouling	Hard macrofouling	None	
	01/05/2011	Cartridge plate	Biofouling	Soft macrofoulingfouling	Plastic covers over bolts	if water ingress allowed into bolt holes soft fouling may settle
	01/05/2011	Exposed surfaces	Corrosion	General	Cathodic protection and protective coatings	General corrosion where paint has been removed
	01/05/2011	Cartridge plate	Corrosion	Galvanic	None	

Figure 10.3. Report of corrosion and biofouling observed to 27 June 2013

10.5 Conclusions

The documentation review and experimental work during the thesis has clearly shown the applicability suitability of a risk management process for tidal turbines.

The development of a corrosion and biofouling management system takes all the information developed in the previous chapters to produce a risk-based management system to be used by tidal device manufacturers and operators.

The database structure that has been created provides a system where data from inspection, monitoring, operational experience and the literature can be inputted to continually develop an evidence database from which decisions can be made. Prompt sheets and questionnaires have been developed to capture this data.

A risk register and recommendations have been compiled from the data, and updated to include design changes, prevention techniques and guidelines for monitoring and maintenance as these changed and developed. The risk register will aid the implementation of correct actions to mitigate the corrosion and biofouling that is likely to occur on tidal stream devices.

Chapter 11

Overall Conclusions and Recommendations to Further Research and Development

11.1 Overall Conclusions

Through review of relevant literature (Chapter 2 and 3), analysis of practical test work (Chapter 6-8) and assessment of an example tidal stream device (Chapter 4 and 5) it was found that a corrosion and biofouling strategy template could be developed for application of the process to tidal stream devices. Figure 11.1 shows the logical sequence through the process. The outcome of each stage is summarised here.

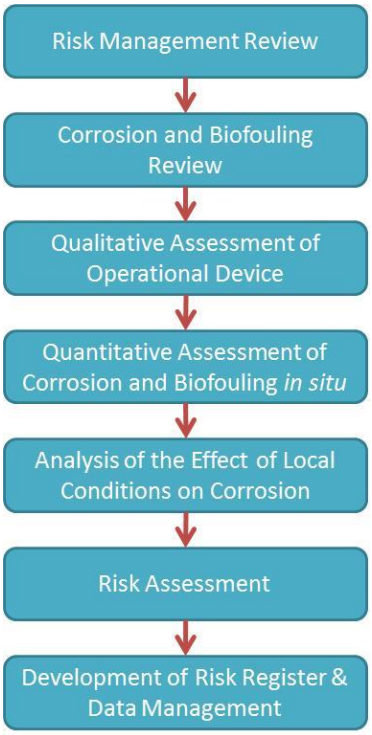

Figure 11.1. Flow chart of project process

11.1.1 Risk Management Review

Review of Risk-based management systems for corrosion and biofouling found that these have already been implemented with success in a number of industries, most notably and relevant, the offshore oil and gas industry. A detailed study of various techniques highlighted the relevance of Failure Modes and Effects Analysis and the implementation of

risk-based inspection regimes for tidal stream devices. It was considered that this would be a useful tool for the emerging marine renewables sector and therefore applied.

11.1.2 Corrosion and Biofouling Review

One of the key challenges that has been highlighted facing the sector, and tidal devices in particular, is that associated with corrosion and biofouling of the devices during operation (Mueller and Wallace, 2008). A review of relevant literature relating to corrosion and biofouling has been conducted to document evidence of the mechanisms of corrosion and biofouling and applicable historical data that has been gathered from other relevant industries, namely offshore oil and gas and shipping (Chapter 3). This literature review highlighted a gap in knowledge of corrosion and biofouling in the environmental conditions in which tidal stream devices will be operating.

11.1.3 Qualitative Assessment of an Operational Device

An example tidal device (DeepGen III developed by Alstom Ocean Energy) was used to provide a qualitative evidence base of corrosion and biofouling issues that have arisen during operation in Orkney, UK (Chapter 4). This work allowed the knowledge gained from the literature review to be applied directly to the industry to understand the risks posed to operation by corrosion and biofouling. The type and extent of corrosion and biofouling was documented using photographs taken on the device when on the quayside in Orkney.

11.1.4 Quantitative Assessment of Corrosion and Biofouling In Situ

To substantiate the qualitative assessment carried out on a prototype device, a quantitative experimental assessment of carbon steel (S355) coupons was conducted *in situ* in Orkney (Chapter 5). S355 carbon steel is commonly used for the bulk of tidal devices, especially external surfaces. These field studies identified the type, and statistically analysed the extent, of biofouling present throughout one year. Fouling was found to settle more significantly in spring and summer than autumn and winter. The study also has provided assessment of the corrosion rate of S355 carbon steel over different periods of immersion and over different seasons over the one year period. The experiments also assessed the onset of localised corrosion which occurred on coupons that had been exposed for six months and longer.

11.1.5 Analysis of the Effect of Local Conditions on Corrosion

Four metals used on tidal devices were tested in laboratory experiments, carbon steel (S355); nickel aluminium bronze (EN-SS5716-15); spheroidal graphite iron (EN-GJS-400-18) and spheroidal graphite iron (EN-GJS-500-7U). Scoping experiments were carried out in the form of a two-factorial design (Chapter 6). These identified significant environmental factors for determining corrosion rates within a range defined by potential tidal locations around the world. The experiments have highlighted and quantified the effects of the four environmental factors tested, flow rate, temperature, dissolved oxygen and salinity on corrosion rate, and provided insight into the relationship between them and the synergistic effects on corrosion rate. The spheroidal graphite irons exhibited the highest corrosion rates, with the nickel aluminium bronze the lowest in all trials. The two factorial design experiments have also provided laboratory based proof of the theoretical relationship between temperature and corrosion rate, where it has been theorised that a 10 degree rise in temperature will incur a doubling in corrosion rate. This theory has not previously been proven in published laboratory studies.

Using statistical analysis, temperature and flow were identified as the most significant environmental factors for all metals and were taken forward into more detailed laboratory testing (Chapters 7 and 8). This testing evaluated the relationship between these and potential corrosion rates. All four metals exhibited an increase in corrosion rate with increasing temperature over the range defined. The range tested, with corrosion rates analysed in 2-3 degree intervals, has not been previously studied in such fine detail. The relationship between corrosion rate and temperature was modelled for each metal. It was found that this relationship differed for each metal. A key finding of the studies was the relationship observed between temperature and the corrosion rate of the nickel aluminium bronze. The corrosion rate increased rapidly at temperatures above 20 ^{o}C, which is likely to explain the increased corrosion rate observed during assessment in Chapter 4 and 9 on connectors made from this metal used on the Alstom Ocean Energy device in this alloy. When operational, areas of the devices will become warmer than others which can increase corrosion rates in that area, exacerbated by potential temperature differentials over the exposed surfaces of the device.

The effect of a tidal flow rate was analysed for the same four metals. A change in flow between quiescent conditions and a higher impingement flow of 3 ms^{-1} (approximately that observed in a tidal flow regime) has been found to increase the corrosion rate of all four

metals tested. The carbon steel was the most affected in this flow range with a 56% increase in corrosion rate. All other metals exhibited an increase of approximately one third in corrosion rate when under the higher flow regime.

11.1.6 Risk Assessment

The data obtained from the field and laboratory studies was used to develop a Failure Modes and Effects Analysis (FMEA), as identified in Chapter 2, for the prototype device. This process was reviewed and updated on an annual basis throughout the project (Chapter 9). The risk identification process classified threats associated with corrosion and biofouling which were then be categorised with respect to consequence and likelihood. The risk analysis identified key risks to critical areas of the devices, including areas required during operation, deployment and retrieval and maintenance and allowed categorisation of the risk from its consequences and likelihood. The systematic approach of an FMEA was used to ensure that it could be practically embedded into existing company policies and processes. An annual review process proved invaluable with the categorisation of risks changing with extended operational evidence.

11.1.7 Development of Risk Register and Data Management

All knowledge gained throughout the project was brought together in a risk register for all stages of a tidal stream device lifetime including design, prevention measures and monitoring and maintenance (Chapter 10). A database (Appendix 5) has been developed to manage all information and provide an easily accessible system that can be used to access data and store further information in the future. A database approach was chosen to aid the integration of the risk-based management system into established design/maintenance processes currently used by tidal stream developers, and to ensure that the risk assessment is continually reviewed and updated. A corrosion and biofouling review has been developed to be used as part of design stage gated-review process to ensure consideration of corrosion and biofouling in the design of new features. An inspection log to capture corrosion and biofouling data throughout a device lifetime has been developed as part of the data management process to aid the assessment of associated risk in the future as operational experience increases.

11.2 Further Research and Development

The management system developed and the results obtained from field and laboratory studies can be used across the industry. Corrosion and biofouling management is a continual process and, using feedback, it should be revisited throughout a device lifetime. The risk identification and analysis process should be repeated on an annual basis to capture changes in design and also lessons learned from extended operation.

From the laboratory based and *in situ* experiments carried out, this thesis has contributed to current literature by enhancing understanding of temperature and flow effects, interactions between environmental factors, seasonality of corrosion and biofouling, and application of risk management theory to a new system. This study has shown that flow effects in a tidal regime will affect the corrosion rate and the settlement of biofouling on the surface of these devices. The complexity of the devices will cause differential flow patterns and therefore there will be areas under higher flow that will corrode faster than areas under low flow. With more operational experience as more tidal stream devices are deployed, this work can be furthered by investigation and detailed modelling of the flow regime close to the metal surface around the devices to understand localised flow effects close to the surface of the structures. Tidal devices are complex in structure and have several moving components and joints that are required for access throughout device lifetime.

Research into temperature effects in the range in which these devices are likely to operate as part of this thesis has provided models for corrosion rates throughout a device lifetime. During future risk assessments based on operating experience, it may be necessary to determine the exact positioning of hot spots on the device, and whether these are likely to be in areas of the device where potential crevices could be formed and therefore require a more substantial inspection regime with reduced periods between maintenance. From a review of literature and the assessed evidence from the Alstom Ocean Energy device, a risk factor has been documented regarding the atmospheric corrosion risk posed to the device whilst on the quayside for routine maintenance. This risk could be assessed further in long term studies using field coupons placed on the quayside and monitored for corrosion rates with exposure time.

Although it is possible to quantify an unplanned maintenance stop in production, due to limited operational experience at this time it would be difficult to perform a cost benefit

analysis for treatment methods and recommendations as detailed in this project. However, with increased operation of these devices more data will be available to enable quantification of costs and benefits and as such it is suggested that this form of analysis be carried out in the future to aid the risk assessment and treatment process.

References

A&E SYSTEMS. 2009. *Enviropeel Technical Datasheet* [Online]. Available: http://www.ae-sys.com/teksite/enviro%20data%20sheet%20170%2010-2008.pdf [Accessed June 2014].

ABP MARINE ENVIRONMENTAL RESEARCH. 2014. *Atlas of UK Marine Renewable Energy Resources* [Online]. Available: http://www.renewables-atlas.info/ [Accessed April 2014].

ABSOLOM, D. R., LAMBERTI, F. V., POLICOVA, Z., ZINGG, W., VAN OSS, C. J. & NEUMANN, A. W. 1983. Surface thermodynamics of bacterial adhesion. *Applied and environmental microbiology,* 46**,** 90-7.

AILOR, W. H. (ed.) 1971. *Handbook on Corrosion Testing and Evaluation.* John Wiley & Sons, Inc, Richmond, Virginia.

AKID, R., WANG, H., SMITH, T. J., GREENFIELD, D. & EARTHMAN, J. C. 2008. Biological Functionalization of a Sol–Gel Coating for the Mitigation of Microbial-induced Corrosion. *Advanced Functional Materials,* 18**,** 203-211.

AL-HASHEM, A., CACERES, P. G., RIAD, W. T. & SHALABY, H. M. 1995. Cavitation Corrosion Behavior of Cast Nickel-Aluminum Bronze in Seawater. *Corrosion,* 51**,** 331-342.

AL-HASHEM, A. & RIAD, W. 2002. The role of microstructure of nickel–aluminium–bronze alloy on its cavitation corrosion behavior in natural seawater. *Materials Characterization,* 48**,** 37-41.

AL-MALAHY, K. S. E. & HODGKIESS, T. 2003. Comparative studies of the seawater corrosion behaviour of a range of materials. *Desalination,* 158**,** 35-42.

ALMEIDA, E., DIAMANTINO, T. C. & DE SOUSA, O. 2007. Marine paints: The particular case of antifouling paints. *Progress in Organic Coatings,* 59**,** 2-20.

ALSTOM. 2013. *What is Tidal Energy* [Online]. Available: http://www.alstom.com/power/renewables/ocean-energy/tidal-energy/ [Accessed July 2013].

ALVAREZ, M. G. & GALVELE, J. R. 2010. 2.04 - Pitting Corrosion. *In:Shreir's Corrosion.* EDITOR-IN-CHIEF: TONY, J. A. R. (ed.). 772-800. Elsevier, Oxford.

AMIN, M. A. & IBRAHIM, M. M. 2011. Corrosion and corrosion control of mild steel in concentrated H2SO4 solutions by a newly synthesized glycine derivative. *Corrosion Science,* 53**,** 873-885.

AN, Y. H., FRIEDMAN, R. J., DRAUGHN, R. A., SMITH, E. A., NICHOLSON, J. H. & JOHN, J. F. 1995. Rapid quantification of staphylococci adhered to titanium surfaces using image analyzed epifluorescence microscopy. *Journal of Microbiological Methods,* 24**,** 29-40.

ANDERSON, C., ATLAR, M., CALLOW, M., CANDRIES, M., MILNE, A. & TOWNSIN, R. L. 2003. The development of foul-release coatings for seagoing vessels. *Journal of Marine Design and Operations,* B4**,** 11-23.

AQUARIUS MARINE COATINGS LTD. 2011. *Coppercoat multi-season anti-fouling* [Online]. Available: http://coppercoat.com/coppercoat-info [Accessed April 2011].

ARMSTRONG, E., BOYD, K. G. & BURGESS, J. G. 2000. Prevention of marine biofouling using natural compounds from marine organisms. *In:Biotechnology Annual Review.* 221-241. Elsevier.

ASHWORTH, V. 1996. Corrosion Management. *In:Industrial Corrosion and Corrosion Control Technology.* SHALABY, H. M., AL-HASHEM, A., LOWTHER, M. & AL-BESHARAH, J. (eds.). Kuwait Institute for Scientific Research.

ASTM. 2004. (G31-72). Standard Practice for Laboratory Immersion Corrosion Testing of Metals ASTM International, West Conshohocken, PA. 10.1520/G0031-72R04. www.astm.org.

ASTM. 2010. G102 - 89. Standard Practice for Calculation of Corrosion Rates and Related Information from Electrochemical Measurements. ASTM International, West Conshohocken, PA. 10.1520/G0102-89R10. www.astm.org.

ASTM. 2011. G1-03. Standard Practice for Preparing, Cleaning and Evaluating Corrosion Test specimens. ASTM International, West Conshohocken, PA. 10.1520/G0001-03R11. www.astm.org.

ASTM. 2013. G3. Standard Practice for Conventions Applicable to Electrochemical Measurements in Corrosion Testing. ASTM International, West Conshohocken, PA. 10.1520/G0003. www.astm.org.

ATASHIN, S., PAKSHIR, M. & YAZDANI, A. 2011a. Comparative studying of marine parameters' effect, via quatitative method. *Trends in Applied Sciences Research,* 6**,** 65-72.

ATASHIN, S., PAKSHIR, M. & YAZDANI, A. 2011b. Synergistic investigation into the marine parameters' effect on the corrosion rate of AISI 316 stainless steel. *Materials & Design,* 32**,** 1315-1324.

ATLANTIS RESOURCES CORPORATION. 2009. *AR Series* [Online]. Available: http://www.atlantisresourcescorporation.com/the-atlantis-advantage/atlantis-technologies/ar-series.html [Accessed October 2011].

ATLAS STEELS. 2010. *Atlas Technical Note No. 7: Galvanic Corrosion* [Online]. Available: http://www.atlassteels.com.au/documents/TN7-Galvanic_Corrosion_rev_Aug_2010.pdf [Accessed July 2010].

AURORA ENVIRONMENTAL. 2005. *EMEC Tidal Test Facility Fall of Warness, Eday, Orkney - Environmental Statement* [Online]. EMEC. Available: http://www.emec.org.uk/Fall_of_Warness_ES_Aurora_2005.pdf [Accessed January 2011].

BABOIAN, R. (ed.) 2002. *NACE Corrosion Engineer's Reference Book.* NACE International, Houston: Available: www.nace.org.

BABOIAN, R. 2005. *Corrosion tests and standards: application and interpretation, 2nd Ed.* ASTM International, West Conshohocken, PA, Available: http://dx.doi.org/10.1520/mnl20_2nd-eb.

BARCHICHE, C., DESLOUIS, C., GIL, O., REFAIT, P. & TRIBOLLET, B. 2004. Characterisation of calcareous deposits by electrochemical methods: role of sulphates, calcium concentration and temperature. *Electrochimica Acta,* 49**,** 2833-2839.

BARNES, H. & POWELL, H. T. 1950. Some observations on the effect of fibrous glass surfaces upon the settlement of certain sedentary marine organisms.

Journal of the Marine Biological Association of the United Kingdom, 29**,** 299-302.

BARTON, L. 1995. *Sulfate-reducing bacteria.* Springer Science and Business Media, New York.

BATTEN, W. M. J., BAHAJ, A. S., MOLLAND, A. F. & CHAPLIN, J. R. 2006. Hydrodynamics of marine current turbines. *Renewable Energy,* 31**,** 249-256.

BEA, R. 2001. Risk assessment and management of offshore structures. *Progress in Structural Engineering and Materials,* 3**,** 180-187.

BEECH, I. B. 2004. Corrosion of technical materials in the presence of biofilms--current understanding and state-of-the art methods of study. *International Biodeterioration & Biodegradation,* 53**,** 177-183.

BEN ELGHALI, S. E., BENBOUZID, M. E. H. & CHARPENTIER, J. F. 2007. Marine Tidal Current Electric Power Generation Technology: State of the Art and Current Status. *In:* Electric Machines & Drives Conference, 2007. IEMDC '07. IEEE International. 1407-1412.

BENNETT, T. L. & COVEY, R. 1998. Orkney (MNCR Sector 2). *In:* HISCOCK. K. (ed.) *Marine Nature Conservation Review. Benthic marine ecosystems of Great Britain and the north-east Atlantic.* Peterborough, UK: Joint Nature Conservation Committee.

BERMÚDEZ, M.-D., CARRIÓN, F. J., MARTÍNEZ-NICOLÁS, G. & LÓPEZ, R. 2005. Erosion–corrosion of stainless steels, titanium, tantalum and zirconium. *Wear,* 258**,** 693-700.

BERNTSSON, K. M., JONSSON, P. R., LEJHALL, M. & GATENHOLM, P. 2000. Analysis of behavioural rejection of micro-textured surfaces and implications for recruitment by the barnacle Balanus improvisus. *Journal of Experimental Marine Biology and Ecology,* 251**,** 59-83.

BERR. 2008. Atlas of UK Marine Renewable Energy Resources. Available: http://www.renewables-atlas.info/downloads/documents/Renewable_Atlas_Pages_A4_April08.pdf [Accessed January 2011].

BLACK AND VEATCH. 2005. Phase II UK Tidal Stream Energy Resource Assessment. Available: https://www.carbontrust.com/media/174041/phaseiitidalstreamresourcereport2005.pdf [Accessed July 2014].

BLANCHARD, D. C. & WOODCOCK, A. H. 1980. The Production, Concentration, and Vertical Distribution of the Sea-Salt Aerosol. *Annals of the New York Academy of Sciences,* 338**,** 330-347.

BÖHNI, H. & UHLIG, H. H. 1969. Environmental Factors Affecting the Critical Pitting Potential of Aluminum. *Journal of The Electrochemical Society,* 116**,** 906-910.

BOTT, T. R. 2001. Potential Physical Methods for the Control of Biofouling in Water Systems. *Chemical Engineering Research and Design,* 79**,** 484-490.

BOX, G. E. P., HUNTER, J. S. & HUNTER, W. G. 2005. *Statistics for experimenters: design, innovation, and discovery.* Wiley-Interscience, Hoboken, New Jersey.

BOYER, T. P., ANTONOV, J. I., BARANOVA, O. K., GARCIA, H. E., JOHNSON, D. R., LOCARNINI, R. A., MISHONOV, A. V., O'BRIEN, T. D., SEIDOV, D., SMOLYAR, I.

V. & ZWENG, M. M. 2009. World Ocean Database 2009. *In:* LEVITUS, S. (ed.) *NOAA Atlas NESDIS 66.* U.S. Gov. Printing Office, Wash., D.C., DVDs.

BRITISH STANDARDS INSTITUTE. 1997. Founding - Spheriodal graphite cast irons. BS EN 1563:1997. www.bsigroup.co.uk.

BRITISH STANDARDS INSTITUTE. 2000. General principles of cathodic protection in sea water. 12473:2000. www.bsigroup.co.uk.

BRITISH STANDARDS INSTITUTE. 2001. Preparation of steel substrates before application of paints and related products - Collected information on the effect of levels of water-soluble salt contamination. ISO/TR 15235:2001. www.bsigroup.co.uk.

BRITISH STANDARDS INSTITUTE. 2006a. Analysis techniques for system reliability - Procedure for failure mode and effects analysis (FMEA). BS EN 60812:2006. www.bsigroup.co.uk.

BRITISH STANDARDS INSTITUTE. 2006b. Preparation of steel substrates before application of paints and related products - Tests for the assessment of surface cleanliness. BS EN ISO 8502-6:2006. www.bsigroup.co.uk.

BRITISH STANDARDS INSTITUTE. 2009. Weldable structural steels for fixed offshore structures - Technical delivery conditions. BS EN10225:2009. www.bsigroup.co.uk.

BRITTON, C. F. 2010. 4.36 - Corrosion Monitoring and Inspection. *In:Shreir's Corrosion.* EDITOR-IN-CHIEF: TONY, J. A. R. (ed.). 3117-3166. Elsevier, Oxford.

BROEKMAN, S., POHLMANN, O., BEARDWOOD, E. S. & DE MEULENAER, E. C. 2010. Ultrasonic treatment for microbiological control of water systems. *Ultrasonics Sonochemistry,* 17**,** 1041-1048.

BUSALMEN, J. P., FRONTINI, M. A. & DE SANCHEZ, S. R. 1998. Microbial corrosion: Effect of microbial catalase on the oxygen reduction. *In:Developments in Marine Corrosion.* WALSH, F. C. & CAMPBELL, S. A. (eds.). Royal Society of Chemistry, London.

BUSSCHER, H. J. & WEERKAMP, A. H. 1987. Specific and non-specific interactions in bacterial adhesion to solid substrata. *FEMS Microbiology Letters,* 46**,** 165-173.

BWEA. 2006. *The Path to Power* [Online]. Available: http://www.bwea.com/pdf/pathtopower/PathtoPower_low.pdf [Accessed June 2014].

CALLCUT, V. 2002. Aluminium Bronzes. Available: http://www.copper.org/publications/newsletters/innovations/2002/08/aluminum2.html [Accessed June 2014].

CALLOW, M. E. & CALLOW, J. A. 2002. Marine Biofouling: a sticky problem. *Biologist,* 49**,** 5.

CANDRIES, M., ATLAR, M. & ANDERSON, C. D. 2000. Considering the use of alternative antifoulings: the advantages of foul-release systems. *In:* ENSUS 2000. 88-95.

CANNING-CLODE, J. & WAHL, M. 2010. Patterns of Fouling on a Global Scale. *In:Biofouling.* DÜRR, S. & THOMASON, J. C. (eds.). 73-86. Wiley-Blackwell, Oxford, UK.

CAPCIS LIMITED FOR THE HEALTH AND SAFETY EXECUTIVE. 2001. Review of corrosion management for offshore oil and gas processing. LONDON: STATIONARY OFFICE.

CARBON TRUST. 2006. Marine Energy Challenge. Available: http://www.carbontrust.co.uk/emerging-technologies/current-focus-areas/Pages/marine-energy-challenge.aspx [Accessed July 2014].

CATHELCO. 2010. *Seawater Pipework Anti-fouling Systems* [Online]. Available: http://www.cathelco.com/userfiles/Cathelco%20Seawater%20Pipework%20Anti-fouling.pdf [Accessed June 2013].

CHABOT, R. & BOURGET, E. 1988. Influence of substratum heterogeneity and settled barnacle density on the settlement of cypris larvae. *Marine Biology,* 97**,** 45-56.

CHAMBERS, L. D., STOKES, K. R., WALSH, F. C. & WOOD, R. J. K. 2006. Modern approaches to marine antifouling coatings. *Surface and Coatings Technology,* 201**,** 3642-3652.

CHANDLER, K. A. 1966. The influence of salts in rusts on the corrosion of the underlying steel. *British Corrosion Journal,* 1**,** 264-266.

CHANDLER, K. A. 1985. *Marine and Offshore Corrosion.* Butterworth & Co, London, UK.

CHARACKLIS, W. G. & COOKSEY, K. E. 1983. Biofilms and Microbial Fouling. *In:Advances in Applied Microbiology.* ALLEN, I. L. (ed.). 93-138. Academic Press.

CHEYNE, I. 2010. Regulation of Marine Antifouling in International and EC Law. *In:Biofouling.* DÜRR, S. & THOMASON, J. C. (eds.). 306-318. Wiley-Blackwell, Oxford, UK.

CHIU, J. M. Y., THIYAGARAJAN, V., TSOI, M. M. Y. & QIAN, P. Y. 2005. Qualitative and quantitative changes in marine biofilms as a function of temperature and salinity in summer and winter. *Biofilms,* 2**,** 183-195.

COLLAZO, A., IZQUIERDO, M., NÓVOA, X. R. & PÉREZ, C. 2007. Surface treatment of carbon steel substrates to prevent cathodic delamination. *Electrochimica Acta,* 52**,** 7513-7518.

COPPER DEVELOPMENT ASSOCIATION 1981. Aluminium bronze alloys corrosion resistance guide. Publication No. 80.

COPPER DEVELOPMENT ASSOCIATION. 1982. Copper-Nickel Alloys, Properties and Applications. TN30. Available: http://www.copperinfo.co.uk/alloys/copper-nickel/downloads/pub-30-cu-nickel-alloys.pdf [Accessed June 2014].

CORLETT, N., EISELSTEIN, L. E. & BUDIANSKY, N. 2010. 2.03 - Crevice Corrosion. *In:Shreir's Corrosion.* EDITOR-IN-CHIEF: TONY, J. A. R. (ed.). 753-771. Elsevier, Oxford.

CORUS CONSTRUCTION AND INDUSTRIAL. 2004. *A Corrosion Protection Guide* [Online]. Available: http://www.npl.co.uk/ [Accessed 15th October 2014].

COSTERTON, J. W. 1999. Introduction to biofilm. *International Journal of Antimicrobial Agents,* 11**,** 217-221.

COSTERTON, J. W., LEWANDOWSKI, Z., CALDWELL, D. E., KORBER, D. R. & LAPPIN-SCOTT, H. M. 1995. Microbial Biofilms. *Annual Review of Microbiology,* 49**,** 711-745.

COUCH, S. J. & BRYDEN, I. 2006. Tidal current energy extraction: Hydrodynamic resource characteristics. *Proceedings of the Institution of Mechanical Engineers, Part M: Journal of Engineering for the Maritime Environment,* 220**,** 185-194.

COWIE, P. R. 2010. Biofouling Patterns with Depth. *In:Biofouling.* DÜRR, S. & THOMASON, J. C. (eds.). 87-99. Wiley-Blackwell, Oxford, UK.

CRAIG, B. D., ANDERSON, D. S. & INTERNATIONAL, A. 1995. *Handbook of Corrosion Data, 2nd Ed.* Asm International.

CUPROBAN. 2009. *Sacrificial Anode Cathodic Potection System* [Online]. Available: http://www.cuproban.com/anodes.htm [Accessed April 2011].

DAVIS, J. R. 2000. *Corrosion: understanding the basics.* ASM International, Available: www.asminternational.org.

DAVIS, J. R. 2006. *Corrosion of Weldments.* ASM International, Available: www.asminternational.org.

DAVIS, J. R. & COMMITTEE, A. I. H. 1996. *Cast Irons.* Asm International, Available: www.asminternational.org.

DE MESSANO, L. V. R., SATHLER, L., REZNIK, L. Y. & COUTINHO, R. 2009. The effect of biofouling on localized corrosion of the stainless steels N08904 and UNS S32760. *International Biodeterioration & Biodegradation,* 63**,** 607-614.

DE NYS, R. & STEINBERG, P. D. 2002. Linking marine biology and biotechnology. *Current Opinion in Biotechnology,* 13**,** 244-248.

DEEPWATER CORROSION SERVICES INC. 2010. *Aluminium Anode Alloy Compositions* [Online]. Available: http://www.stoprust.com/aluminum-anodes.htm [Accessed March 2011].

DEFLORIAN, F., FEDRIZZI, L., LENTI, D. & BONORA, P. L. 1993. On the corrosion protection properties of fluoropolymer coatings. *Progress in Organic Coatings,* 22**,** 39-53.

DEPARTMENT OF ENERGY AND CLIMATE CHANGE. 2009. Renewable Energy Strategy. HM GOVERNMENT. Available: https://www.gov.uk/government/publications/the-uk-renewable-energy-strategy [Accessed August 2014].

DEPARTMENT OF ENERGY AND CLIMATE CHANGE. 2013. UK Renewable Energy Roadmap: 2013 Update. HM GOVERNMENT. Available: https://www.gov.uk/government/publications/uk-renewable-energy-roadmap-second-update [Accessed August 2014].

DET NORSKE VERITAS. 2010. Cathodic Protection Design. Recommended Practice DNV-RP-B401. www.dnvgl.com.

DET NORSKE VERITAS. 2012. Risk Based Corrosion Management. Recommended Practice DNV-RP-C302. www.dnvgl.com.

DEXTER, S. C. & LIN, S.-H. 1992. Effect of marine biofilms on cathodic protection. *International Biodeterioration & Biodegradation,* 29**,** 231-249.

DOUGLAS, C. A., HARRISON, G. P. & CHICK, J. P. 2008. Life cycle assessment of the Seagen marine current turbine. *Proceedings of the Institution of Mechanical Engineers, Part M: Journal of Engineering for the Maritime Environment,* 222**,** 1-12.

DUAN, J., WU, S., ZHANG, X., HUANG, G., DU, M. & HOU, B. 2008. Corrosion of carbon steel influenced by anaerobic biofilm in natural seawater. *Electrochimica Acta,* 54**,** 22-28.

DUBIEL, M., HSU, C. H., CHIEN, C. C., MANSFELD, F. & NEWMAN, D. K. 2002. Microbial iron respiration can protect steel from corrosion. *Applied and Environmental Microbiology,* 68**,** 1440-1445.

DUBOST, N., MASSON, G. & MORETEAU, J.-C. 1996. Temperate freshwater fouling on floating net cages: method of evaluation, model and composition. *Aquaculture,* 143**,** 303-318.

DÜRR, S. & THOMASON, J. (eds.) 2010. *Biofouling.* Wiley-Blackwell, Oxford, UK.

EDALATI, K., RASTKHAH, N., KERMANI, A., SEIEDI, M. & MOVAFEGHI, A. 2006. The use of radiography for thickness measurement and corrosion monitoring in pipes. *International Journal of Pressure Vessels and Piping,* 83**,** 736-741.

EDYVEAN, R. G. J., MAINES, A. D., HUTCHINSON, C. J., SILK, N. J. & EVANS, L. V. 1992. Interactions between Cathodic Protection and Bacterial Settlement on Steel in Seawater *International Biodeterioration & Biodegradation,* 29**,** 251-271.

EDYVEAN, R. G. J., TERRY, L. A. & PICKEN, G. B. 1983. Marine fouling and its effects on offshore structures in the North Sea. *In:Biodeteriorationn 5.* OXLEY, T. A. & BARRY, S. (eds.). 336-347. John Wiley & Sons, London.

EDYVEAN, R. G. J., TERRY, L. A. & PICKEN, G. B. 1985. Marine Fouling and Its Effects on Offshore Structures in the North-Sea - A Review. *International Biodeterioration,* 21**,** 277-284.

EDYVEAN, R. G. J., THOMAS, C. J. & BROOK, R. 1988. The Effect of Marine Fouling on Fatigue and Corrosion-Fatigue of Offshore Structures. *In:Biodeterioration 7.* HOUGHTON, D. R., SMITH, R. N. & EGGINS, H. O. W. (eds.). 385-390.

EFIRD, K. D. 2000. Jet impingement testing for flow accelerated corrosion. Paper No. 00052. *NACE CORROSION/2000* Florida, USA.

EFIRD, K. D. & ANDERSON, D. B. 1975. Sea Water Corrosion of 90-10 and 70-30 Cu-Ni: 14 Year Exposures. *Materials Performance,* 14**,** 37-40.

EGAN, F. 2007. Responsibilities in Asset Integrity Management. *TWF Best Practice Forum.* Wellington, New Zealand: Transfield Worley Services.

EL DIN, A. M. S., EL-DAHSHAN, M. E. & EL DIN, A. M. T. 2003. Bio-film formation on stainless steels Part 2. The role of seasonal changes, seawater composition and surface roughness. *Desalination,* 154**,** 267-276.

ELLERMAA, R. R. R. 1993. Erosion prediction of pure metals and carbon steels. *Wear,* 162–164, Part B**,** 1114-1122.

EMEC. 2008. *Environmental Description for the EMEC Tidal Test Facility* [Online]. Available: http://www.emec.org.uk/tidal_environmental.asp [Accessed April 2011].

EMEC. 2013. *Site Specific Projects* [Online]. Available: http://www.emec.org.uk/research/emec-site-specific-projects/ [Accessed April 2013].

EMEC. 2013. *Tidal Devices* [Online]. Available: http://www.emec.org.uk/marine-energy/tidal-devices/ [Accessed July 2013].
ENCYCLOPAEDIA BRITANNICA 2006. Tides. *In:* ENCYCLOPAEDIA BRITANNICA INC. (ed.). Chicago.
ENERGY INSTITUTE 2008. *Guidance for corrosion management in oil and gas production and processing.* Energy Institute Publications.
ENERGY TECHNOLGIES INSTITUTE (ETI). 2014. *ReDAPT* [Online]. Available: http://www.eti.co.uk/project/redapt/ [Accessed January 2014].
ENOS, D. & SCRIBNER, L. 1997. The Potentiodynamic Polarization Scan, Technical Report No.33. Solartron Analytical, Hampshire, UK.

EUROPEAN FEDERATION OF CORROSION. 1989. A Working Party report on General Guidlines for Corrosion Testing of Materials for Marine Applications. THE INSTITUTE OF METALS.

EVANS, S. M., BIRCHENOUGH, A. C. & BRANCATO, M. S. 2000. The TBT Ban: Out of the Frying Pan into the Fire? *Marine Pollution Bulletin,* 40**,** 204-211.
EVANS, U. R. 1925. Oxygen Distribution as a Factor in the Corrosion of Metals. *Industrial & Engineering Chemistry,* 17**,** 363-372.
EVANS, U. R. 1960. *The Corrosion and Oxidation of Metals: Scientific Principles and Practical Applications.* St. Martin's Press, New York.
EXXONMOBIL. 2009. Operations Integrity Management System. Available: http://www.exxonmobilsafety.com/ [Accessed May 2014].

FAILLE, C., DENNIN, L., BELLON-FONTAINE, M. N. & BENEZECH, T. 1999. Cleanability of stainless steel surfaces soiled by bacillus thuringiensis spores under various flow conditions. *Biofouling,* 14**,** 143-151.
FANG, J., KELARAKIS, A., WANG, D., GIANNELIS, E. P., FINLAY, J. A., CALLOW, M. E. & CALLOW, J. A. 2010. Fouling release nanostructured coatings based on PDMS-polyurea segmented copolymers. *Polymer,* 51**,** 2636-2642.
FINK, F. W. 1960. Corrosion of Metals in Sea Water. *In:SALINE WATER CONVERSION.* 27-39. American Chemical Society.
FINNIE, A. A. & WILLIAMS, D. N. 2010. Paint and Coatings Technology for the Control of Marine Fouling. *In:Biofouling.* DÜRR, S. & THOMASON, J. C. (eds.). 185-206. Wiley-Blackwell, Oxford, UK.
FLEMMING, H.-C. & WINGENDER, J. 2010. The biofilm matrix. *Nat Rev Micro,* 8**,** 623-633.
FLEMMING, H. C. 2002. Biofouling in water systems – cases, causes and countermeasures. *Applied Microbiology and Biotechnology,* 59**,** 629-640.
FLETCHER, M. & FLOODGATE, G. D. 1973. An Electron-microscopic Demonstration of an Acidic Polysaccharide Involved in the Adhesion of a Marine Bacterium to Solid Surfaces. *Journal of General Microbiology,* 74**,** 9.
FLORES, S. & MORCILLO, M. 1999. Anticipated levels of soluble salts remaining on rusty steel prior to painting. *Surface Coatings International Part B: Coatings Transactions,* 82**,** 19-25.
FONTANA, M. G. 1987. *Corrosion Engineering.* McGraw-Hill, New York.

FORTEATH, G. N. R., PICKEN, G. B. & RALPH, R. 1984. *Patterns of macrofouling on steel platforms in the central and northern North Sea.* Ellis Horwood Limited.

FORTEATH, G. N. R., PICKEN, G. B., RALPH, R. & WILLIAMS, J. 1982. Marine growth studies on the North Sea oil platform Montrose Alpha. *Marine Ecology Progress Series* 8**,** 8.

FRAENKEL, P. 2002. Power from marine currents. *Proceedings of the Institution of Mechanical Engineers, Part A: Journal of Power and Energy,* 216**,** 1-14.

FRANKEL, G. S. 1998. Pitting Corrosion of Metals. *Journal of The Electrochemical Society,* 145**,** 2186-2198.

FUNKE, W. 1981. Blistering of paint films and filiform corrosion. *Progress in Organic Coatings,* 9**,** 29-46.

GALVELE, J. R. 1978. Present State of Understanding of the Breakdown of Passivity and Repassivation. *In:* Passivity of metals: proceedings of the fourth International Symposium on Passivity. Electrochemical Society, 285.

GEOGHEGAN, M., ANDREWS, J. S., BIGGS, C. A., EBOIGBODIN, K. E., ELLIOTT, D. R., ROLFE, S., SCHOLES, J., OJEDA, J. J., ROMERO-GONZALEZ, M. E., EDYVEAN, R. G. J., SWANSON, L., RUTKAITE, R., FERNANDO, R., PEN, Y., ZHANG, Z. & BANWART, S. A. 2008. The polymer physics and chemistry of microbial cell attachment and adhesion. *Faraday Discussions,* 139.

GIBBONS, B. 2008. *Seashore Life of Britain and Europe.* New Holland Publishers, London, UK.

GITTENS, J. E., WANG, H., SMITH, T. J., AKID, R. & GREENFIELD, D. 2010. Biotic Sol-Gel Coating for the Inhibition of Corrosion in Seawater. *ECS Transactions,* 24**,** 211-229.

GLOBAL ENERGY NETWORK INSTITUTE. 2011. *Global Renewable Energy Resources* [Online]. Available: http://www.geni.org/globalenergy/library/renewable-energy-resources/ocean.shtml [Accessed December 2011].

GOODMAN, P. D. 1987. Effect of chlorination on materials for sea water cooling systems: a review of chemical reactions. *British Corrosion Journal,* 22**,** 56-62.

GOUDA, V. K., SHALABY, H. M. & BANAT, I. M. 1993. The effect of sulphate-reducing bacteria on the electrochemical behaviour of corrosion-resistant alloys in sea water. *Corrosion Science,* 35**,** 683-691.

GRANHAG, L., FINLAY, J., JONSSON, P., CALLOW, J. & CALLOW, M. 2004. Roughness-dependent Removal of Settled Spores of the Green Alga Ulva (syn. Enteromorpha) Exposed to Hydrodynamic Forces from a Water Jet. *Biofouling: The Journal of Bioadhesion and Biofilm Research,* 20**,** 117 - 122.

GRIMES, D. J. & COLWELL, R. R. 1986. Viability and virulence of *Escherichia coli* suspended by membrane chamber in semitropical ocean water. *FEMS Microbiology Letters,* 34**,** 161-165.

GUEDES SOARES, C., GARBATOV, Y., ZAYED, A. & WANG, G. 2009. Influence of environmental factors on corrosion of ship structures in marine atmosphere. *Corrosion Science,* 51**,** 2014-2026.

GUERIN, A. J., JENSEN, A. C. & JONES, D. 2007. Artificial reef properties of North Sea oil and gas production platforms. *In:* OCEANS 2007, Aberdeen, Scotland.

HACK, H. P. 2010. 2.07 - Galvanic Corrosion. *In:Shreir's Corrosion.* EDITOR-IN-CHIEF: TONY, J. A. R. (ed.). 828-856. Elsevier, Oxford.

HAMILTON, W. A. 1985. Sulphate-reducing bacteria and anaerobic corrosion. *Annual Review of Microbiology,* 39**,** 195-217.
HAMMERFEST STROM. 2011. *Tidal Turbines* [Online]. Available: http://www.hammerfeststrom.com/ [Accessed December 2011].
HARLAND, E. J. 2013. Faill of Warness Tidal Test Site: Additional Acoustic Characterisation. Scotland National Heritage Commissioned Report No. 563.

HEAF, N. J. 1981. The effect of marine growth on the performance of fixed offshore platforms in the North Sea. *Marine fouling of offshore structures.* London: Society for underwater technology.
HEITZ, E., FLEMMING, H. C. & SAND, W. 1996. *Microbially influenced corrosion of materials: scientific and engineering aspects.* Springer-Verlag.
HENRIKSEN, J. F. 1969. The distribution of NaCl on Fe during atmospheric corrosion. *Corrosion Science,* 9**,** 573-577.
HERMANSSON, M. 1999. The DLVO theory in microbial adhesion. *Colloids and Surfaces B: Biointerfaces,* 14**,** 105-119.
HERRERA, L. K. & VIDELA, H. A. 2009. Role of iron-reducing bacteria in corrosion and protection of carbon steel. *International Biodeterioration & Biodegradation,* 63**,** 891-895.
HILLEBRAND, H. 2004. Strength, slope and variability of marine latitudinal gradients. *Marine Ecology-Progress Series,* 273**,** 251-267.
HM GOVERNMENT. 2005. The Offshore Installations (Safety Case) Regulations 2005. London: The Stationary Office. Available: http://www.legislation.gov.uk.

HM GOVERNMENT. 2008. Climate Change Act 2008 (C.27). London: The Stationary Office. Available: www.legislation.gov.uk.

HORI, K. & MATSUMOTO, S. 2010. Bacterial adhesion: From mechanism to control. *Biochemical Engineering Journal,* 48**,** 424-434.
HOUGHTON, D. R. 1978. Marine fouling and offshore structures. *Ocean Management,* 4**,** 347-352.
HOWELL, D. & BEHRENDS, B. 2010. Consequences of Antifouling Coatings – The Chemist's Perspective. *In:Biofouling.* DÜRR, S. & THOMASON, J. C. (eds.). 226-242. Wiley-Blackwell, Oxford, UK.
HUDSON, J. C. 1950. Corrosion of Bare Iron or Steel in Sea Water. *Journal of Iron and Steel Institute,* 166**,** 123-126.
IEV GROUP. 2011. *"Ocean-Powered" Marine Growth Control* [Online]. Available: http://www.iev-group.com/index.php?p=contents-item&id=6527 [Accessed May 2011].
IJSSELING, F. P. 1989. General guidelines for corrosion testing of materials for marine applications: Literature review on sea water as test environment. *British Corrosion Journal,* 24**,** 53-78.
INSTITUTE OF PETROLEUM. 1987. Microbial Problems in the Offshore Oil Industry. *In:* HILL, E. C., SHENNAN, J. L. & WATKINSON, R. J., eds. Aberdeen. John Wiley & Sons.
INTERNATIONAL ASSOCIATION OF OIL AND GAS PRODUCERS. 2008. Asset Integrity - the key to managing major accident risks.

INTERNATIONAL ENERGY AGENCY (IEA). 2010. *World Energy Outlook* [Online]. Available: www.iea.org [Accessed November 2010].
INTERNATIONAL ENERGY AGENCY (IEA). 2011. *Key World Energy Statistics* [Online]. Available: www.iea.org [Accessed June 2011].
INTERNATIONAL ENERGY AGENCY (IEA). 2012. *World Energy Outlook* [Online]. Available: www.iea.org [Accessed May 2012].
INTERNATIONAL PAINTS. 2010. Interspeed Product Datasheet. Available: http://www.international-marine.com/Product%20Datasheets/4511+M+eng+A4.pdf [Accessed July 2014].

JEFFREY, R. & MELCHERS, R. E. 2003. Bacteriological influence in the development of iron sulphide species in marine immersion environments. *Corrosion Science,* 45**,** 693-714.
JEFFREY, R. & MELCHERS, R. E. 2009a. Corrosion of vertical mild steel strips in seawater. *Corrosion Science,* 51**,** 2291-2297.
JEFFREY, R. & MELCHERS, R. E. 2009b. Effect of Vertical Length on Corrosion of Steel in the Tidal Zone. *Corrosion,* 65**,** 695-702.
JENKINS, L. R. & FORREST, R. D. 1990. Ductile Iron. *In:ASM Handbook Volume 1, Properties and Selection: Irons, Steels and High-Performance Alloys.* ASM International.
JENKINS, S. R. & MARTINS, G. M. 2010. Succession on Hard Substrata. *In:Biofouling.* DÜRR, S. & THOMASON, J. C. (eds.). 60-72. Wiley-Blackwell, Oxford, UK.
JINGJUN LIU., YUZHEN LIN. & XIAOYU LI. 2005. Application of numerical simulation to flow-induced corrosion in flowing seawater systems. *Anti-Corrosion Methods and Materials,* 52**,** 276-279.
JINGJUN LIU., YUZHEN LIN. & XIAOYU LI. 2008. Numerical simulation for carbon steel flow-induced corrosion in high-velocity flow seawater. *Anti-Corrosion Methods and Materials,* 55**,** 66-72.
JUSOH, I. & WOLFRAM, J. 1996. Effects of marine growth and hydrodynamic loading on offshore structures. *Jurnal Mekanikal,* 1**,** 77-98.
Tables of Physical & Chemical Constants (16th Edition 1995). 2.7.9 Physical properties of sea water. Kaye & Laby Online. Version 1.0. 1995. Available: www.kayelaby.npl.co.uk [Accessed January 2013].
KEANE, R. 8th July 2011. *RE: Personal Communication regarding cathodic protection anode requirements, Ark Corrosion Services, UK.*
KEAR, G., BARKER, B. D., STOKES, K. & WALSH, F. C. 2004a. Flow influenced electrochemical corrosion of nickel aluminium bronze – Part I. Cathodic polarisation. *Journal of Applied Electrochemistry,* 34**,** 1235-1240.
KEAR, G., BARKER, B. D., STOKES, K. & WALSH, F. C. 2004b. Flow influenced electrochemical corrosion of nickel aluminium bronze – Part II. Anodic polarisation and derivation of the mixed potential. *Journal of Applied Electrochemistry,* 34**,** 1241-1248.
KHAN, F. I. & HADDARA, M. M. 2003. Risk-based maintenance (RBM): a quantitative approach for maintenance/inspection scheduling and planning. *Journal of Loss Prevention in the Process Industries,* 16**,** 561-573.

KHAN, F. I., SADIQ, R. & HADDARA, M. M. 2004. Risk-Based Inspection and Maintenance (RBIM): Multi-Attribute Decision-Making with Aggregative Risk Analysis. *Process Safety and Environmental Protection,* 82**,** 398-411.

KHUN, N. W. & FRANKEL, G. S. 2013. Effects of surface roughness, texture and polymer degradation on cathodic delamination of epoxy coated steel samples. *Corrosion Science,* 67**,** 152-160.

KINGSBURY, R. W. S. M. 1981. Marine Fouling of North sea Installations. *Marine Fouling of Offshore Structures.* London: Society for underwater technology Vol. I.

KIRKPATRICK, J. P., MCINTIRE, L. V. & CHARACKLIS, W. G. 1980. Mass and heat transfer in a circular tube with biofouling. *Water Research,* 14**,** 117-127.

KNOELL, T., SAFARIK, J., CORMACK, T., RILEY, R., LIN, S. W. & RIDGWAY, H. 1999. Biofouling potentials of microporous polysulfone membranes containing a sulfonated polyether-ethersulfone/polyethersulfone block copolymer: correlation of membrane surface properties with bacterial attachment. *Journal of Membrane Science,* 157**,** 117-138.

KOVAC, J., ALAUX, C., MARROW, T. J., GOVEKAR, E. & LEGAT, A. 2010. Correlations of electrochemical noise, acoustic emission and complementary monitoring techniques during intergranular stress-corrosion cracking of austenitic stainless steel. *Corrosion Science,* 52**,** 2015-2025.

KRISTENSEN, J. B., MEYER, R. L., LAURSEN, B. S., SHIPOVSKOV, S., BESENBACHER, F. & POULSEN, C. H. 2008. Antifouling enzymes and the biochemistry of marine settlement. *Biotechnology Advances,* 26**,** 471-481.

LAGERMETALL. 2011. *Material sheet SS 5716-15 Aluminium bronze* [Online]. Available: http://www.lagermetall.com/bronze/alubrons_5716-15.aspx [Accessed November 2011].

LANGHAMER, O., WILHELMSSON, D. & ENGSTRÖM, J. 2009. Artificial reef effect and fouling impacts on offshore wave power foundations and buoys - a pilot study. *Estuarine, Coastal and Shelf Science,* 82**,** 426-432.

LAQUE, F. L. 1975. *Marine corrosion: causes and prevention.* Wiley, CA.

LARSSON, A. I. & JONSSON, P. R. 2006. Barnacle Larvae Actively Select Flow Environments Supporting Post-Settlement Growth and Survival. *Ecology,* 87**,** 1960-1966.

LARSSON, A. I., MATTSSON-THORNGREN, L., GRANHAG, L. M. & BERGLIN, M. 2010. Fouling-release of barnacles from a boat hull with comparison to laboratory data of attachment strength. *Journal of Experimental Marine Biology and Ecology,* 392**,** 107-114.

LAWRENCE, J., KOFOED-HASEN, H. & CHEVALIER, C. 2009. High-resolution metocean modelling at EMEC's (UK) marine energy test sites. *In:* Proceedings of the 8th European Wave and Tidal Energy Conference, Uppsala, Sweden.

LEE, A. K. & NEWMAN, D. K. 2003. Microbial iron respiration: impacts on corrosion processes. *Applied Microbiology and Biotechnology,* 62**,** 134-139.

LEE, J., RAY, R., LEMIEUX, E., FALSTER, A. & LITTLE, B. 2004. An Evaluation of Carbon Steel Corrosion under Stagnant Seawater Conditions. *Biofouling,* 20**,** 237-247.

LEWANDOWSKI, Z., LEE, W. C., CHARACKLIS, W. G. & LITTLE, B. 1989. Dissolved oxygen and pH microelectrode measurements at water-immersed metal surfaces. *Corrosion,* 45**,** 92-98.

LIND, J. L., HEIMANN, K., MILLER, E. A., VAN VLIET, C., HOOGENRAAD, N. J. & WETHERBEE, R. 1997. Substratum adhesion and gliding in a diatom are mediated by extracellular proteoglycans. *Planta,* 203**,** 213-221.

LITTLE, B. & LEE, J. S. 2007. Microbiologically influenced corrosion. *Wiley Series in Corrosion.* Wiley & Sons Inc, CA.

LITTLE, B., RAY, R., WAGNER, P., LEWANDOWSKI, Z., LEE, W. C., CHARACKLIS, W. G. & MANSFELD, F. 1991a. Impact of biofouling on the electrochemical behaviour of 304 stainless steel in natural seawater. *Biofouling,* 3**,** 45-59.

LITTLE, B., WAGNER, P. & MANSFELD, F. 1991b. Microbiologically influenced corrosion of metals and alloys. *International Materials Reviews,* 36**,** 253-272.

LITTLE, B. J., LEE, J. S. & RAY, R. I. 2008. The influence of marine biofilms on corrosion: A concise review. *Electrochimica Acta,* 54**,** 2-7.

LUICKX, P. J., DELARUE, E. D. & D'HAESELEER, W. D. 2008. Considerations on the backup of wind power: Operational backup. *Applied Energy,* 85**,** 787-799.

LYON, S. B. 2010. 3.01 - Corrosion of Carbon and Low Alloy Steels. *In:Shreir's Corrosion.* EDITOR-IN-CHIEF: TONY, J. A. R. (ed.). 1693-1736. Elsevier, Oxford.

MACNAB, R. M. & KOSHLAND, D. E. 1972. The Gradient-Sensing Mechanism in Bacterial Chemotaxis. *Proceedings of the National Academy of Sciences,* 69**,** 2509-2512.

MADIGAN, M. T., BROCK, T. D., MARTINKO, J. M. & PARKER, J. 2010. *Brock Biology of Microorganisms 13th Ed.* Pearson, London.

MALIK, A. U., AHMAD, S., ANDIJANI, I. & AL-FOUZAN, S. 1999. Corrosion behavior of steels in Gulf seawater environment. *Desalination,* 123**,** 205-213.

MANSFELD, F. & LITTLE, B. 1992a. Electrochemical techniques applied to studies of microbiologically influenced corrosion (MIC). *Trends in Electrochemistry,* 1**,** 47-61.

MANSFELD, F. & LITTLE, B. 1992b. Microbiologically influenced corrosion of copper-based materials exposed to natural seawater. *Electrochimica Acta,* 37**,** 2291-2297.

MARÉCHAL, J.-P. & HELLIO, C. 2009. Challenges for the development of new non-toxic antifouling solutions. *International Journal of Molecular Sciences,* 10**,** 4623-4637.

MARGARIT, I. C. P. & MATTOS, O. R. 1998. About coatings and cathodic protection: Properties of the coatings influencing delamination and cathodic protection criteria. *Electrochimica Acta,* 44**,** 363-371.

MARINE CURRENT TURBINES. 2011. *Marine Current Turbines - Turning the Tide* [Online]. Available: http://www.marineturbines.com/ [Accessed September 2011].

MARINE ENVIRONMENTAL DATA & INFORMATION NETWORK 2013. MEDIN Data Archive Centre. Available: http://portal.oceannet.org/search/full [Accessed April 2014].

MARSHALL, K. C. 1986. Adsorption and adhesion processes in microbial growth at interfaces. *Advances in Colloid and Interface Science,* 25**,** 59-86.

MATSUNAGA, T., NAKAYAMA, T., WAKE, H., TAKAHASHI, M., OKOCHI, M. & NAKAMURA, N. 1998. Prevention of marine biofouling using a conductive paint electrode. *Biotechnology and Bioengineering,* 59**,** 374-378.

MATZ, C. & KJELLEBERG, S. 2005. Off the hook – how bacteria survive protozoan grazing. *Trends in Microbiology,* 13**,** 302-307.

MCALLISTER, E. W., CAREY, L. C., BRADY, P. G., HELLER, R. & KOVACS, S. G. 1993. The role of polymeric surface smoothness of biliary stents in bacterial adherence, biofilm deposition, and stent occlusion. *Gastrointestinal Endoscopy,* 39**,** 422-425.

MCCAFFERTY, E. 2005. Validation of corrosion rates measured by the Tafel extrapolation method. *Corrosion Science,* 47**,** 3202-3215.

MCINTYRE, P. J. & MERCER, A. D. 2010. Corrosion Testing and Determination of Corrosion Rates. *In:Shreir's Corrosion.* TONY, J. A. R. (ed.). 1443-1526. Elsevier, Oxford.

MCMURRAY, H. N. & WILLIAMS, G. 2010. 2.14 - Under Film/Coating Corrosion. *In:Shreir's Corrosion.* EDITOR-IN-CHIEF: TONY, J. A. R. (ed.). 988-1004. Elsevier, Oxford.

MCQUAID, C. D. & MILLER, K. 2010. Larval Supply and Dispersal. *In:Biofouling.* S. DÜRR. & THOMASON, J. C. (eds.). 16-29. Wiley-Blackwell, Oxford, UK.

MEARS, R. B. & EVANS, U. R. 1934. Corrosion at contact with glass. *Transactions of the Faraday Society,* 30**,** 417-423.

MELCHERS, R. 2003a. Probabilistic Model for Marine Corrosion of Steel for Structural Reliability Assessment. *Journal of Structural Engineering,* 129**,** 1484-1493.

MELCHERS, R. & JEFFREY, R. 2008. The critical involvement of anaerobic bacterial activity in modelling the corrosion behaviour of mild steel in marine environments. *Electrochimica Acta,* 54**,** 80-85.

MELCHERS, R. E. 2002. Effect of Temperature on the Marine Immersion Corrosion of Carbon Steels. *Corrosion,* 58**,** 768-782.

MELCHERS, R. E. 2003b. Probabilistic Models for Corrosion in Structural Reliability Assessment---Part 1: Empirical Models. *Journal of Offshore Mechanics and Arctic Engineering,* 125**,** 264-271.

MELCHERS, R. E. & JEFFREY, R. 2004. Influence of water velocity on marine immersion corrosion of mild steel. *Corrosion,* 60**,** 84-94.

MELCHERS, R. E. & JEFFREY, R. 2005. Early corrosion of mild steel in seawater. *Corrosion Science,* 47**,** 1678-1693.

MELCHERS, R. E. & WELLS, T. 2006. Models for the anaerobic phases of marine immersion corrosion. *Corrosion Science,* 48**,** 1791-1811.

MENG, H., HU, X. & NEVILLE, A. 2007. A systematic erosion-corrosion study of two stainless steels in marine conditions via experimental design. *Wear,* 263**,** 355-362.

MERCER, A. D. 1976. 18.2 Corrosion Inhibition: Principles and Practice. *In:Corrosion.* SHREIR, L. L. (ed.). Butterworth & Co (Publishers) Ltd, London, UK.

MET OFFICE. 2013. *Kirkwall Weather Observations* [Online]. Available: http://www.metoffice.gov.uk/public/weather/climate/kirkwall#?tab=climateTables&fcTime=1374102000 [Accessed July 2013].

METOC PLC. 2007. Tidal Power in the UK – Research Report 1: UK Tidal Resource Assessment. Sustainable Development Commission.

MICHELS, H. & POWELL, C. 2012. Alloys of Copper and Nickel for Splash Zone Sheathing of Marine Structures. *In:* COPPER DEVELOPMENT ASSOCIATION (ed.).

MÖLLER, H. 2007. The influence of Mg2+on the formation of calcareous deposits on a freely corroding low carbon steel in seawater. *Corrosion Science,* 49**,** 1992-2001.

MORCILLO, M. 1999. Soluble salts: their effect on premature degradation of anticorrosive paints. *Progress in Organic Coatings,* 36**,** 137-147.

MORCILLO, M., CHICO, B., MARIACA, L. & OTERO, E. 2000. Salinity in marine atmospheric corrosion: its dependence on the wind regime existing in the site. *Corrosion Science,* 42**,** 91-104.

MORCILLO, M., RODRíGUEZ, F. J. & BASTIDAS, J. M. 1997. The influence of chlorides, sulphates and nitrates at the coating-steel interface on underfilm corrosion. *Progress in Organic Coatings,* 31**,** 245-253.

MOTT, I. E. C., STICKLER, D. J., COAKLEY, W. T. & BOTT, T. R. 1998. The removal of bacterial biofilm from water-filled tubes using axially propagated ultrasound. *Journal of Applied Microbiology,* 84**,** 509-514.

MUELLER, M. & WALLACE, R. 2008. Enabling science and technology for marine renewable energy. *Energy Policy,* 36**,** 4376-4382.

MUYZER, G. & STAMS, A. J. M. 2008. The ecology and biotechnology of sulphate-reducing bacteria. *Nat Rev Micro,* 6**,** 441-454.

NAKASONO, S., BURGESS, J. G., TAKAHASHI, K., KOIKE, M., MURAYAMA, C., NAKAMURA, S. & MATSUNAGA, T. 1993. Electrochemical Prevention of Marine Biofouling with a Carbon-Chloroprene Sheet. *Appl. Environ. Microbiol.,* 59**,** 3757-3762.

Corrosion Control in Engineering Design. National Physical Laboratory. 2010. Available: www.npl.co.uk [Accessed June 2014].

NEUMANN, A. W., GOOD, R. J., HOPE, C. J. & SEJPAL, M. 1974. An equation-of-state approach to determine surface tensions of low-energy solids from contact angles. *Journal of Colloid and Interface Science,* 49**,** 291-304.

NEVILLE, A. & HODGKIESS, T. 2000. Corrosion of stainless steels in marine conditions containing sulphate reducing bacteria. *British Corrosion Journal,* 35**,** 60-69.

NEVILLE, A. & MORIZOT, A. P. 2002. Calcareous scales formed by cathodic protection--an assessment of characteristics and kinetics. *Journal of Crystal Growth,* 243**,** 490-502.

NEWMAN, P. 2011. *RE: Personal Communication Regading Potential Future Placement of Tidal Turbines, Alstom Ocean Energy, UK.*

NICC SYSTEMS. 2005. *Corrosion Resistant Coatings - Armawrap* [Online]. Available: http://www.armawrap.com/ [Accessed May 2011].

NICHOLLS-LEE, R. F. & TURNOCK, S. R. 2008. Tidal energy extraction: renewable, sustainable and predictable. *Science Progress,* 91**,** 81-111.

O ROURKE, F., BOYLE, F. & REYNOLDS, A. 2010. Tidal energy update 2009. *Applied Energy,* 87**,** 398-409.

OJEDA, J. J., ROMERO-GONZALEZ, M. E., BACHMANN, R. T., EDYVEAN, R. G. J. & BANWART, S. A. 2008. Characterization of the Cell Surface and Cell Wall Chemistry of Drinking Water Bacteria by Combining XPS, FTIR Spectroscopy, Modeling, and Potentiometric Titrations. *Langmuir,* 24**,** 4032-4040.

OLDFIELD, J. W. 1996. Correct Materials Selection for Desalination: The Key to Plant Reliability. *In:Industrial Corrosion and Corrosion Control Technology.* SHALABY, H. M., AL-HASHEM, A., LOWTHER, M. & AL-BESHARAH, J. (eds.). Kuwait Institute for Scientific Research.

OMAE, I. 2003. General Aspects of Tin-Free Antifouling Paints. *Chemical Reviews,* 103**,** 3431-3448.

OSPAR COMMISSION. 2010. Quality Status Report 2010. Available: http://qsr2010.ospar.org/en/index.html [Accessed February 2014].

OWEN, A. 2008. Tidal Current Energy: Origins and Challenges. *In:Future Energy: Improved, Sustainable and Clean Options for Our Planet.* LETCHER, T. M. (ed.). Elsevier.

PEDERSEN, K. 1982. Method for Studying Microbial Biofilms in Flowing-Water Systems. *Appl. Environ. Microbiol.,* 43**,** 6-13.

PHILLIPPI, A. L., O'CONNOR, N. J., LEWIS, A. F. & KIM, Y. K. 2001. Surface flocking as a possible anti-biofoulant. *Aquaculture,* 195**,** 225-238.

PICKEN, M. J. & GRIER, C. 1984. *Fouling and corrosion off the Outer Hebrides.* Ellis Horwood Limited, UK.

PIPPO, F., ELLWOOD, N., GUZZON, A., SILIATO, L., MICHELETTI, E., PHILIPPIS, R. & ALBERTANO, P. 2012. Effect of light and temperature on biomass, photosynthesis and capsular polysaccharides in cultured phototrophic biofilms. *Journal of Applied Phycology,* 24**,** 211-220.

POMERAT, C. M. & WEISS, C. M. 1946. The Influence of Texture and Composition of Surface on the Attachment of Sedentary Marine Organisms. *Biological Bulletin,* 91**,** 57-65.

PRENDERGAST, G. S. 2010. Settlement and Behaviour of Marine Fouling Organisms. *In:Biofouling.* DÜRR, S. & THOMASON, J. C. (eds.). 30-59. Wiley-Blackwell, Oxford, UK.

RAHMAN, M. & CHAKRAVARTTY, I. C. 1981. Hydrodynamic Loading Calculations for Offshore Structures. *SIAM Journal on Applied Mathematics,* 41**,** 445-458.

RALSTON, E. & SWAIN, G. 2009. Bioinspiration - the solution for biofouling control? *Bioinspiration and Biomimetics,* 4**,** 1-9.

REID, P. C., EDWARDS, M., BEAUGRAND, G., SKOGEN, M. & STEVENS, D. 2003. Periodic changes in the zooplankton of the North Sea during the twentieth century linked to oceanic inflow. *Fisheries Oceanography,* 12**,** 260-269.

RENEWABLEUK. 2010. Channeling the Energy: A Way Forward for the UK Wave and Tidal Industry Towards 2020 Available: http://www.bwea.com/pdf/marine/RenewableUK_MarineReport_Channeling-the-energy.pdf [Accessed July 2014].

RENEWABLEUK. 2011. Wave and Tidal Energy in the UK: State of the Industry Report. Available:

http://www.bwea.com/pdf/marine/Wave_Tidal_energy_UK.pdf [Accessed August 2014].

RENEWABLEUK. 2014. *Wave and Tidal Energy* [Online]. Available: http://www.renewableuk.com/en/renewable-energy/wave-and-tidal/ [Accessed 20th October 2014].

REYNAUD, A. 2010. 3.02 - Corrosion of Cast Irons. *In:Shreir's Corrosion.* EDITOR-IN-CHIEF: TONY, J. A. R. (ed.). 1737-1788. Elsevier, Oxford.

RITTSCHOF, D., BRANSCOMB, E. S. & COSTLOW, J. D. 1984. Settlement and behavior in relation to flow and surface in larval barnacles, Balanus amphitrite Darwin. *Journal of Experimental Marine Biology and Ecology,* 82**,** 131-146.

ROTHWELL, G. P. 1978. Corrosion monitoring: some techniques and applications. *NDT International,* 11**,** 108-111.

SAOUD, I. P., DAVIS, D. A. & ROUSE, D. B. 2003. Suitability studies of inland well waters for *Litopenaeus vannamei* culture. *Aquaculture,* 217**,** 373-383.

SCHLITZER, R. 2011. *Ocean Data View* [Online]. Available: http://odv.awi.de [Accessed April 2011].

SCHMITT, H. G. & BAKALLI, M. 2010. 2.13 - Flow Assisted Corrosion. *In:Shreir's Corrosion.* EDITOR-IN-CHIEF: TONY, J. A. R. (ed.). 954-987. Elsevier, Oxford.

SCHULTZ, M. P., FINLAY, J. A., CALLOW, M. E. & CALLOW, J. A. 2003. Three Models to Relate Detachment of Low Form Fouling at Laboratory and Ship Scale. *Biofouling,* 19**,** 17-26.

SCHUMACHER, M. 1979. *Seawater corrosion handbook.* Noyes Data Corp, Michigan.

SCHÜSSLER, A. & EXNER, H. E. 1993a. The corrosion of nickel-aluminium bronzes in seawater--I. Protective layer formation and the passivation mechanism. *Corrosion Science,* 34**,** 1793-1802.

SCHÜSSLER, A. & EXNER, H. E. 1993b. The corrosion of nickel-aluminium bronzes in seawater—II. The corrosion mechanism in the presence of sulphide pollution. *Corrosion Science,* 34**,** 1803-1815.

SCOTTO, V. & LAI, M. E. 1998. The ennoblement of stainless steels in seawater: a likely explanation coming from the field. *Corrosion Science,* 40**,** 1007-1018.

SHALABY, H. M., ATTARI, S., RIAD, W. T. & GOUDA, V. K. 1992. Erosion-Corrosion Behavior of Some Cast Alloys in Seawater. *Corrosion,* 48**,** 206-217.

SHEEHY, D. J. & VIK, S. F. 2010. The role of constructed reefs in non-indigenous species introductions and range expansions. *Ecological Engineering,* 36**,** 1-11.

SHIFLER, D. A. 2005a. Factors that influence corrosion of materials and how modeling may predict these effects. *2005 Tri-Service Corrosion Conference.* Orlando, Fl.

SHIFLER, D. A. 2005b. Understanding material interactions in marine environments to promote extended structural life. *Corrosion Science,* 47**,** 2335-2352.

SIGALEVICH, P. & COHEN, Y. 2000. Oxygen-Dependent Growth of the Sulfate-Reducing Bacterium Desulfovibrio oxyclinae in Coculture with Marinobacter sp. Strain MB in an Aerated Sulfate-Depleted Chemostat. *Appl. Environ. Microbiol.,* 66**,** 5019-5023.

SILVERMAN, D. C. 2003. Aqueous Corrosion. *In:ASM Handbook Volume 13A, Corrosion: Fundamentals, Testing, and Protection.* ASM International.

SNEDDON, A. D. & KIRKWOOD, D. 1989. The influence of fouling upon corrosion rates of steels and copper-nickel alloys in seawater. *Construction and Building Materials,* 3**,** 35-39.

SØRENSEN, P. A., DAM-JOHANSEN, K., WEINELL, C. E. & KIIL, S. 2010. Cathodic delamination of seawater-immersed anticorrosive coatings: Mapping of parameters affecting the rate. *Progress in Organic Coatings,* 68**,** 283-292.

SRIDHAR, N., BROSSIA, C. S., DUNN, D. S. & ANDERKO, A. 2004. Predicting localised corrosion in seawater. *Corrosion,* 60**,** 21.

STAROSVETSKY, D., ARMON, R., YAHALOM, J. & STAROSVETSKY, J. 2001. Pitting corrosion of carbon steel caused by iron bacteria. *International Biodeterioration & Biodegradation,* 47**,** 79-87.

STRAUB, D. & FABER, M. H. 2005. Risk based inspection planning for structural systems. *Structural Safety,* 27**,** 335-355.

SUBSEA INDUSTRIES 2008. Technical Information Ecospeed.

SYRETT, B. C. & WING, S. S. 1980. Effect of flow on corrosion of copper-nickel alloys in aerated sea water and in sulfide-polluted sea water. *Corrosion,* 36**,** 73-76.

SZKLARSKA-SMIALOWSKA, Z. 1999. Pitting corrosion of aluminum. *Corrosion Science,* 41**,** 1743-1767.

TEAM, O. U. O. C. 1995. *Seawater: Its Composition, Properties and Behaviour.* Butterworth-Heinemann, UK.

TEN HALLERS-TJABBES, C. C. & WALMSLEY, S. 2010. Consequences of Antifouling Systems – An Environmental Perspective. *In:Biofouling.* DÜRR, S. & THOMASON, J. C. (eds.). 243-251. Wiley-Blackwell, Oxford, UK.

TERLIZZI, A. & FAIMALI, M. 2010. Fouling on Artificial Substrata. *In:Biofouling.* 170-184. Wiley-Blackwell, UK.

THE INSTITUTE OF RISK MANAGEMENT. 2002. The Risk Management Standard. www.theirm.org.

TITTENSOR, D. P., MORA, C., JETZ, W., LOTZE, H. K., RICARD, D., VANDEN BERGHE, E. & WORM, B. 2010. Global patterns and predictors of marine biodiversity across taxa. *Nature,* 466**,** 1098-U107.

TOMASHOV, N. D., TYTELL, B. H., GELD, I. & PREISER, H. S. 1966. *Theory of corrosion and protection of metals.* The Macmillan Company, CA.

TRETHEWEY, K. R. & CHAMBERLAIN, J. 1995. *Corrosion for Science and Engineering.* Longman Scientific & Technical, Essex, England.

TUTHILL, A. H. 1987. GUIDELINES FOR THE USE OF COPPER ALLOYS IN SEAWATER. *Materials Performance,* 26**,** 12-22.

VALAND, T. 1969. The behaviour of NaCl on Fe exposed to a humid atmosphere of nitrogen and oxygen. *Corrosion Science,* 9**,** 577-584.

VAN OSS, C. J., DOCOSLIS, A., WU, W. & GIESE, R. F. 1999. Influence of macroscopic and microscopic interactions on kinetic rate constants: I. Role of the extended DLVO theory in determining the kinetic adsorption constant of proteins in aqueous media, using von Smoluchowski's approach. *Colloids and Surfaces B: Biointerfaces,* 14**,** 99-104.

VERA, R., ROSALES, B. M. & TAPIA, C. 2003. Effect of the exposure angle in the corrosion rate of plain carbon steel in a marine atmosphere. *Corrosion Science,* 45**,** 321-337.

VIDELA, H. A. 1994. Biofilms and corrosion interactions on stainless steel in seawater. *International Biodeterioration & Biodegradation,* 34**,** 245-257.
VIDELA, H. A. 1995. Biocorrosion problems in the marine environment: New perspectives. *9th Int. Congress on Marine Fouling and Corrosion,* Developments in Marine Corrosion**,** 1-25.
VIDELA, H. A. & HERRERA, L. K. 2005. Microbiologically influenced corrosion: looking to the future. *International Microbiology,* 8**,** 169-180.
WAGNER, C. & TRAUD, W. 1938. On the Interpretation of Corrosion Processes Through the Superposition of Electrochemical Partial Processes and on the Potential of Mixed Electrodes. *Zeitschrift Fur Elektrochemie und Angewandte Physikalische Chemie,* 44**,** 391-402.
WAHL, M. 1989. Marine epibiosis: I. Fouling and antifouling: some basic aspects. *Marine Ecology Progress Series,* 58**,** 175-189.
WALKINGTON, I. & BURROWS, R. 2009. Modelling tidal stream power potential. *Applied Ocean Research,* 31**,** 239-245.
WALLACE, A. E. & WEBB, W. P. 1981. Cut Costs with Realistic Corrosion Allowances. *Chemical Engineering,* 88 (17)**,** 123.
WALLÉN, B. & HENRIKSON, S. 1989. Effect of chlorination on stainless steels in seawater. *Materials and Corrosion,* 40**,** 602-615.
WALSH, F. C. 1993. *A first course in electrochemical engineering.* Electrochemical Consultancy, UK, Romsey.
WAN, Y., ZHANG, D., LIU, H., LI, Y. & HOU, B. 2010. Influence of sulphate-reducing bacteria on environmental parameters and marine corrosion behavior of Q235 steel in aerobic conditions. *Electrochimica Acta,* 55**,** 1528-1534.
WANG, W., LI, X., WANG, J., XU, H. & WU, J. 2004. Influence of biofilms growth on corrosion potential of metals immersed in seawater. *Materials and Corrosion,* 55**,** 30-35.
WATERMANN, B. T., DAEHNE, B., SIEVERS, S., DANNENBERG, R., OVERBEKE, J. C., KLIJNSTRA, J. W. & HEEMKEN, O. 2005. Bioassays and selected chemical analysis of biocide-free antifouling coatings. *Chemosphere,* 60**,** 1530-1541.
WEST, J. M. 1980. *Basic Corrosion and Oxidation.* Ellis Horwood Ltd, Chichester, England.
WHARTON, J. A., BARIK, R. C., KEAR, G., WOOD, R. J. K., STOKES, K. R. & WALSH, F. C. 2005. The corrosion of nickel-aluminium bronze in seawater. *Corrosion Science,* 47**,** 3336-3367.
WHITE, S. P., WEIR, G. J. & LAYCOCK, N. J. 2000. Calculating chemical concentrations during the initiation of crevice corrosion. *Corrosion Science,* 42**,** 605-629.
WINTLE, J. B., KENZIE, B. W., AMPHLETT, G. J. & SMALLEY, S. 2001. Best Practice for Risk Based Inspection as a part of Plant Integrity Management. Health and Safety Executive, UK. Available: www.hse.gov.uk.

WOOD, L. 2008. *Sea Fishes & Invertebrates of the North Sea & English Channel.* New Holland Publishers, London.
WOOD, R. J. K., HUTTON, S. P. & SCHIFFRIN, D. J. 1990. Mass transfer effects of non-cavitating seawater on the corrosion of Cu and 70Cu-30Ni. *Corrosion Science,* 30**,** 1177-1201.
WORLD ENERGY COUNCIL 2010. 2010 Survey of Energy Resources. London, UK.

XU, C., ZHANG, Y., CHENG, G. & ZHU, W. 2006. Corrosion and Electrochemical Behavior of 316L Stainless Steel in Sulfate-reducing and Iron-oxidizing Bacteria Solutions. *Chinese Journal of Chemical Engineering,* 14**,** 829-834.

XU, C., ZHANG, Y., CHENG, G. & ZHU, W. 2008. Pitting corrosion behavior of 316L stainless steel in the media of sulphate-reducing and iron-oxidizing bacteria. *Materials Characterization,* 59**,** 245-255.

YAN, T., YAN, W., DONG, Y., WANG, H., YAN, Y. & LIANG, G. 2006. Marine fouling of offshore installations in the northern Beibu Gulf of China. *International Biodeterioration & Biodegradation,* 58**,** 99-105.

YANG, L. (ed.) 2008. *Techniques for Corrosion Monitoring.* Woodhead Publishing Ltd, Cambridge, UK.

YEBRA, D. M., KIIL, S. & DAM-JOHANSEN, K. 2004. Antifouling technology--past, present and future steps towards efficient and environmentally friendly antifouling coatings. *Progress in Organic Coatings,* 50**,** 75-104.

ZEZZA, F. & MACRI, F. 1995. Marine aerosol and stone decay. *Science of the Total Environment,* 167**,** 123-143.

ZHANG, Z., PEN, Y., EDYVEAN, R. G., BANWART, S. A., DALGLIESH, R. M. & GEOGHEGAN, M. 2010. Adhesive and conformational behaviour of mycolic acid monolayers. *Biochimica et Biophysica Acta (BBA) - Biomembranes,* 1798**,** 1829-1839.

ZOBELL, C. E. 1943. The effect of solid surfaces upon bacterial activity. *J. Bacteriol,* 46**,** 39-56.